THE UNIVERSITY OF
WARWICK

University of Warwick institutional repository: http://go.warwick.ac.uk/wrap

A Thesis Submitted for the Degree of PhD at the University of Warwick

http://go.warwick.ac.uk/wrap/61717

This thesis is made available online and is protected by original copyright.

Please scroll down to view the document itself.

Please refer to the repository record for this item for information to help you to cite it. Our policy information is available from the repository home page.

Effect of protein glycation by methylglyoxal on pancreatic beta cell function

By

Amy Tym

A thesis submitted in partial fulfilment of the requirements for the degree of

Doctor of Philosophy in Life Sciences

School of Life Sciences and Warwick Medical School,
University of Warwick

February 2014

Contents

List of Figures

List of Tables

Acknowledgements

I am extremely grateful to my supervisors, Professor Paul Thornalley and Dr Paul Squires for all their help and support throughout the course of my PhD. Professor Thornalley's knowledge, understanding and enthusiasm for science and endless source of ideas was inspirational. Dr Squires' continued positivity, enthusiasm and support was warmly appreciated. Thanks also go to the joint group leader, Dr. Naila Rabbani.

I thank Tianrong Jin for his collaboration and working with me on the AFM-FS experiments, these experiments would not have been possible without his help and hard work. I also thank Dr Jan Kopecky and colleagues at the Institute of Physiology, Academy of Sciences of the Czech Republic for sending the pancreas and plasma samples and the accompanying data. I am extremely grateful to the many hours of hard work which must have gone into completing the study and generating these samples. I thank BBSRC for funding my PhD project and giving me this opportunity.

I am appreciative also to my current and previous colleagues in the Protein Damage and Systems Biology Research Group who have provided help, support and friendship throughout my project. The numerous questions I have been asked have certainly helped to ensure I understood the details of so many methods! Particular thanks must go to the Mass Spectrometry technicians, Dr Maqsud Anwar, Dr Derek Wilkinson and Dr Attia Anwar, for all their technical help. I am especially grateful for the expertise, support and friendship provided by Dr Fozia Shaheen, especially in the IHC analysis, confocal microscopy and running the Xevo MS. Thanks also to Dr Mingzhan Xue for his guidance with cell culture and molecular biology techniques.

Finally, I would like to thank my friends and especially my family for their continued support throughout this challenging and unique experience. I am heartily grateful to my parents for their endless support and love in helping me through all the challenges I face. I appreciate the help provided by my mum in helping to proofread what must have seemed like a foreign language to her. Finally, I thank Adam Leaney for always being there with patience and support throughout all the highs and lows of this eventful journey.

Declaration

This thesis is submitted to the University of Warwick in support of my application for the degree of Doctor of Philosophy. It has been composed by myself and has not been submitted in any previous application for any degree. The work presented (including data generated and data analysis) was carried out by the author except in the cases outlined below:

The atomic force microscopy force spectroscopy experiments were performed in collaboration with Tianrong Jin in the Department of Engineering. Initial data analysis was performed by Tianrong.

The *in vivo* HFD mouse study was performed by collaborators (Jan Kopecky and colleagues) at the Institute of Physiology, Academy of Sciences of the Czech Republic. Data was provided as to measurements of basal parameters to give indications as to glucose homeostasis and insulin resistance status. Plasma and pancreas samples were sent to the University of Warwick and all subsequent analysis was performed by the author.

Summary

Methylglyoxal is a physiological dicarbonyl metabolite and potent arginine-directed glycating agent. It often modifies proteins at functional sites producing loss of positive charge, structural distortion and inactivation. Plasma methylglyoxal is increased in hyperglycaemia associated with diabetes and is linked to the development of vascular complications of diabetes – particularly nephropathy, retinopathy and neuropathy. The effects of dicarbonyl glycation on beta cells and involvement in early stage dysfunction and development of type 2 diabetes mellitus are not known. The aim of this project was to investigate the effect of dicarbonyl protein glycation on beta cell function and related involvement in the development of diabetes. Studies were performed in an *in vitro* model of beta cell dysfunction - MIN6 insulinoma cells incubated under low and high glucose concentrations, and in a pre-clinical *in vivo* model of decline of glucose tolerance preceding development of type 2 diabetes - high fat diet-induced insulin resistant mice. Dicarbonyl metabolism and protein damage by glycation and oxidation were studied by stable isotopic dilution analysis liquid chromatography-tandem mass spectrometry. Localisation of methylglyoxal glycation adducts within the pancreas were visualised by immunostaining. Interactions between the extracellular matrix protein, collagen IV, and MIN6 cells *in vitro* were investigated and impairments in adhesion were assessed following glycation with methylglyoxal. Impairments in adhesion of MIN6 cells to methylglyoxal-glycated collagen IV were assessed using atomic force microscopy force spectroscopy.

The results show that MIN6 cells were resistant to accumulation of methylglyoxal when incubated in high glucose concentration although the flux of methylglyoxal was increased 41%. Glycation of collagen IV by methylglyoxal impairs binding to MIN6 cells *in vitro* resulting in a 91% decrease in the energy necessary to detach cells from the extracellular matrix protein. In high fat diet fed mice the concentration of methylglyoxal in the pancreas was increased. Visualisation of MG-H1 adduct residues in the pancreas showed they were predominantly on the extracellular matrix.

In conclusion, protein glycation by methylglyoxal occurs in MIN6 cells *in vitro* and in the mouse pancreas *in vivo*. Although the methylglyoxal concentration in the pancreas of high fat diet fed, insulin resistant mice was increased, the lack of a concurrent increase in methylglyoxal protein glycation adducts suggests there may be increased turnover of methylglyoxal-modified proteins. Impairment of beta cell attachment to the extracellular matrix protein, collagen IV, by methylglyoxal and increased protein turnover stimulated by an increased rate of methylglyoxal glycation may impair beta cell function in pre-diabetes *in vivo*. Glycation by methylglyoxal may contribute to beta cell glucotoxicity and dysfunction with progression to type 2 diabetes mellitus.

Abbreviations

3-DG	3-deoxyglucosone
3DG-H	structural isomers of hydroimidazolone of 3-deoxyglucosone N_{δ}-[5-(2,3,4-trihydroxybutyl)-5-hydro-4-imidazolon-2-yl]ornithine, 3DG-H1; 2-amino-5-(2-amino-5-hydro-5-(2,3,4-trihydroxybutyl) -4-imidazolon-1-yl)pentanoic acid, 3DG-H2; 2-amino-5-(2-amino-4-hydro-4-(2,3,4-trihydroxybutyl)--5-imidazolon-1-yl)pentanoic acid, 3DG-H3.
3-NT	3-nitrotyrosine
AAA	α-aminoadipic acid
AASA	α-aminoadipic semialdehyde
ADA	American Diabetes Association
ADP	adenosine diphosphate
AFM-FS	atomic force microscopy force spectroscopy
AGEs	advanced glycation end products
AKR	aldoketo reductase
Atg7	autophagy-related protein 7
ATP	adenosine triphosphate
BCAA	branched-chain amino acid
BMI	body mass index
$BrBzGSHCp_2$	S-p-bromobenzylglutathione cyclopentyl diester
BSA	bovine serum albumin
cAMP	cyclic adenosine monophosphate
CBQCA	3-(4-carboxybenzoyl)quinoline-2- carboxaldehyde
CDK	cyclin dependent kinase
cDNA	complementary deoxyribonucleic acid
CEL	(1-carboxyethyl)lysine
CMA	N_{ω}-carboxymethyl-arginine
CML	N_{ε}-carboxymethyl-lysine
CO_2	carbon dioxide
CV	coefficient of variation
CVD	cardiovascular disease
Cx36	connexin36
Cx43	connexin43
DAPI	4',6-diamidino-2-phenylindole
DETAPAC	diethylenetriaminepentaacetic acid
dG	deoxyguanosine
DHA	docosahexaenoic acid
DHAP	dihydroxyacetonephosphate
DMEM	Dulbecco's Modified Eagles Medium
DMSO	dimethyl sulphoxide
dNTP	deoxyribonucleotide triphosphate

DTNB	5,5'-dithiobis-(2-nitrobenzoic acid), Ellman's reagent
EASD	European Association for the Study of Diabetes
E-cadherin	epithelial-cadherin
ECM	extracellular matrix
EDTA	ethylenediaminetetraacetic acid
EHS	Engelbreth-Holm-Swarm
EPA	eicosapentaenoic acid
ER	endoplasmic reticulum
EURODIAB	European Epidemiology and prevention of diabetes collaborative research group established in 1988
eV	electronvolt
FBS	fetal bovine serum
FL	Nε-Fructosyl-lysine
FTO	fat-mass and obesity-related gene
G	guanine
G6P	glucose-6-phosphate
GA3P	glyceraldehyde-3-phosphate
GDM	gestational diabetes mellitus
GEEK	ε-(γ-Glutamyl)lysine
G-H1	hydroimidazolone of glyoxal, N_{δ}-(5-hydro-4-imidazolon-2-yl)-ornithine
Glo1	glyoxalase 1
Glo2	glyoxalase 2
GLUT2	glucose transporter type 2
GSA	glutamic semialdehyde
GSH	reduced glutathione
GSIS	glucose stimulated insulin secretion
GSSG	oxidised glutathione
HC	hyperplastic islet-derived cells
HCl	hydrochloric acid
HEPES	4-(2-hydroxyethyl)piperazine-1-ethanesulfonic acid
HFD	high fat diet
HIT	hamster pancreatic beta cell line
HNF	hepatocyte nuclear factor
HOMA	homeostatic model assessment
HPLC	high performance liquid chromatography
HSA	human serum albumin
ICAM-1	intercellular adhesion molecule -1
IDF	International Diabetes Federation
IGT	impaired glucose tolerance
IgG	immunoglobulin
IL-1β	interleukin-1β
IL-6	interleukin-6

Ins1	rodent insulin gene 1
Ins2	rodent insulin gene 2
IRS-1	insulin-receptor substrate 1
Itgb1	integrin beta 1
K^+_{ATP}	ATP sensitive potassium channels
KCl	potassium chloride
KCNJ15	potassium inwardly rectifying channel, subfamily J, member 15
LC-MS/MS	liquid chromatography-tandem mass spectrometry
LC-PUFA	long-chain polyunsaturated fatty acids
LDL	low-density lipoprotein
LoD	limit of detection
MafA	V-maf musculoaponeurotic fibrosarcoma oncogene homologue A
MAPK	mitogen-activated protein kinase
MC4R	melanocortin-4 receptor
MeCN	acetonitrile
MetSO	methionine sulphoxide
MG	methylglyoxal
$MgCl_2$	magnesium chloride
MG-H1	hydroimidazolone of methylglyoxal, N_δ-(5-hydro-5-methyl-4-imidazolon-2-yl)-ornithine
MGdG	Methylglyoxal derived imidazopurinone 3-(2'-deoxyribosyl)-6,7-dihydro-6,7-dihydroxy-6-methylimidazo[2,3-b]purin-9(8)one
MIN6	mouse insulinoma derived cell line-6
MODY	maturity onset diabetes of the young
MOLD	methylglyoxal derived lysine dimer
MRM	multiple reaction monitoring
mRNA	messenger ribonucleic acid
MTT	thiazolyl blue tetrazolium bromide
NA	numerical aperture
NaCl	sodium chloride
NAD+	nicotinamide adenine dinucleotide
NADH	nicotinamide adenine dinucleotide (reduced form)
NEFA	non-esterified fatty acids
NeuroD1	neurogenic differentiation 1
NFK	N-formylkynurenine
NOD	Non-obese diabetic
Nrf2	nuclear erythroid factor E2 related factor-2
ODS	octadecyl silane
PBS	phosphate buffered saline
PCA	perchloric acid
qPCR	quantitative polymerase chain reaction
Pdx-1	pancreatic duodenum homeobox-1
PFA	paraformaldehyde

RGD	L-arginylglycyl-L-aspartic acid
RIN	rat insulinoma cell line
ROS	reactive oxygen species
SAX	strong anion exchange
SPE	solid phase extraction
STZ	streptozotocin
SV40	Simian vacuolating virus 40
T1DM	type 1 diabetes mellitus
T2DM	type 2 diabetes mellitus
TBS	tris buffered saline
TCA	trichloroacetic acid
TES	N-[Tris(hydroxymethyl)methyl]-2-aminoethanesulphonic acid
TFA	trifluoroacetic acid
THF	tetrahydrofuran
TNB	2-nitro-5-thiobenzoate anion
TNF-α	tumour necrosis factor-α
TQS	triple quadrupole mass spectrometry
UKPDS	United Kingdom Prospective Diabetes Study
VGCC	voltage-gated calcium channels

1. Introduction: Diabetes Mellitus

1.1. Classification and types of diabetes mellitus

1.1.1. Prevalence of diabetes

Diabetes is a group of metabolic diseases characterised by hyperglycaemia which arises from defects in insulin secretion, insulin action, or both (American Diabetes Association, 2012). It poses a major health threat worldwide with increasing impact. The International Diabetes Federation (IDF) estimates that more than 371 million people worldwide have diabetes, of which half are undiagnosed (International Diabetes Federation, 2012). In 2008 it was estimated that the number of adults worldwide with diabetes was 248 million and that this would reach 380 million by 2025 (The Lancet, 2008). Although a number of causative factors are implicated in the development of the disease, impairment in the ability to produce, release, or respond to insulin, and hence an inability to maintain normal glucose levels underlies these causes. Maintaining normal beta cell function is of paramount importance to metabolic health. Even in healthy individuals insulin secretion declines at the rate of 0.7% per year, increasing to 1.2% per year in people with impaired glucose tolerance (Szoke, *et al.*, 2008).

1.1.2. Diagnosis of diabetes mellitus

Diabetes is diagnosed on the basis of plasma glucose criteria: - either a fasting plasma glucose concentration greater than 7.0 mM or a plasma glucose concentration greater than 11.1 mM after 2 h during an oral glucose tolerance test (American Diabetes Association, 2013). However, in 2009 an International Expert Committee composed of representatives of the American Diabetes Association (ADA), IDF and the European Association for the Study of Diabetes (EASD) recommended the use of the glycated haemoglobin HbA_{1C} or "A1C" test for diagnosis, with a threshold of greater than or equal to 6.5% and this criterion was adopted by the ADA in 2010 (American Diabetes Association, 2012; International Expert Committee, 2009). This has the advantage of giving a better indication of long-term glycaemic control (glycaemic control in 6 - 8 weeks preceding blood sampling) with a mean red blood cell age of 38 – 60 days and so not markedly influenced by short-term fluctuations in plasma glucose levels (Cohen, *et al.*, 2008).

An A1C value of between 5.7% and 6.4% has been accepted by the ADA for the diagnosis of pre-diabetes – impaired fasting glucose and impaired glucose tolerance (IGT), with individuals with A1C measurements above 6% considered at high risk of both diabetes and cardiovascular disease (CVD) (American Diabetes Association, 2013). This is still controversial and as discussed by Bergman *et al*. (2013) the World Health Organisation has not accepted A1C measurement for diagnosis of glucose intolerance, although it has been accepted for diagnosis of diabetes. The A1C measurement has limitations, such as in rapidly developing type 1 diabetes mellitus (T1DM) cases it will not be elevated as early as plasma glucose (International Expert Committee, 2009). Haemoglobinopathies such as sickle cell anaemia and conditions that affect red blood cell turnover such as malaria, haemolytic anaemia, and blood transfusions may lead to unreliable A1C results (International Expert Committee, 2009; Kilpatrick, *et al.*, 2009). It is therefore advised that diagnosis of diabetes should be on the basis of repeated analysis or on a combination of both A1C and plasma glucose criteria.

In 1985 a model was published to quantify insulin resistance and beta cell function – homeostatic model assessment, HOMA (Matthews, *et al.*, 1985). This model, based on measurements of fasting plasma glucose and insulin, has been widely utilised; the impact of this model was discussed by Nolan and Færch (2012). HOMA is used as a method to measure insulin resistance, but it has not been used extensively to assess beta cell function.

1.1.3. Gestational diabetes

Gestational diabetes mellitus (GDM) has been defined as 'any degree of glucose intolerance with onset or first recognition during pregnancy' (The Expert Committee on the Diagnosis and Classification of Diabetes Mellitus, 1997). However, recently it has been recommended that women diagnosed with diabetes at their initial prenatal visit are diagnosed with overt, and not gestational diabetes, since these women, most likely, had undiagnosed type 2 diabetes mellitus (T2DM) before pregnancy (American Diabetes Association, 2012). In GDM not enough insulin is secreted during pregnancy to meet the increased demands, and therefore there is an increase in blood glucose levels (hyperglycaemia) in both the mother and foetus. Most cases of GDM resolve post-delivery, but the hyperglycaemic environment *in utero* may have long term effects on the foetus. In addition, women diagnosed with

GDM are at heightened risk of developing T2DM and some remain diabetic after the pregnancy.

1.1.4. Type 1 diabetes mellitus

T1DM is typically diagnosis in childhood or adolescence, but it can occur at any age. It is characterised by a deficiency in insulin production, with little or no insulin being secreted, and is therefore treated by exogenous administration of insulin. The first known use of insulin as a successful treatment for T1DM was in January 1922 when Banting and Best used a pancreatic extract isolated by Collip to treat a 14 year old, Leonard Thompson. By the end of 1923, insulin was being used commercially and safely as a treatment of T1DM in Western countries (Bliss, 1993).

Autoimmune destruction of beta cells leads to this absolute insulin deficiency (Atkinson and Maclaren, 1994). There is currently no established prevention of T1DM although clinical studies are being conducted to test methods of prevention in individuals with evidence of autoimmunity (Orban, *et al.*, 2011; Pescovitz, *et al.*, 2009). Incidence of T1DM in children under the age of 15 in Europe is predicted to increase from 94,000 in 2005 to 160,000 in 2020 and evidence from the Europe and Diabetes Study (EURODIAB) register predicts that new cases in children under the age of five will double between 2005 and 2020 (Ma and Chan, 2009; Patterson, *et al.*, 2009).

1.1.5. Type 2 diabetes mellitus

T2DM is the most common form of diabetes mellitus, accounting for over 90% of cases globally (American Diabetes Association, 2012; Zimmet, *et al.*, 2001). It is characterised by a state in which tissues in the body become less responsive or resistant to insulin - insulin resistance - and/or insufficient insulin is secreted, either of which may predominate. Gerald Reaven was the first to define insulin resistance in the pathogenesis of T2DM (Nolan and Færch, 2012; Reaven, 1988). Although insulin levels may initially appear normal, or even elevated (hyperinsulinaemia), given the higher blood glucose levels observed in such patients with diabetes, there is a relative deficiency of insulin activity in comparison to that expected with normal beta cell function (American Diabetes Association, 2011). Hyperglycaemia develops gradually and T2DM is often asymptomatic; therefore it often goes undiagnosed for a number of years.

T2DM is a multi-factorial disease with both modifiable lifestyle factors - obesity and inactivity - and non-modifiable risk factors - age and genetic susceptibility - increasing the risk. Studies of diabetes in monozygotic twins has indicated that genetic susceptibility is implicated to a greater extent with age – with more discordance observed in twins diagnosed at a younger age. In addition, the concordance rate was higher in identical than non-identical twins regardless of age of onset indicating the genetic involvement (Barnett, *et al.*, 1981). Most genetic risk loci currently discovered act through changes in insulin secretion and beta cell function and not through insulin action. Abnormalities in beta cell mass and function are critical in the development of type 2 diabetes (Florez, 2008; McCarthy, 2010; Rosengren, *et al.*, 2012). Some of the known genetic variants associated with T2DM are listed in Table 1. Whilst a number of risk variants have been identified, their impact is limited as indicated by the association of the fat-mass and obesity-related (FTO) gene; it is one of the strongest known associations of genetic loci with obesity and body mass index (BMI) and accounts for less than 0.5% of overall variance in BMI. This equates to approximately a 2 - 3 kg difference between adults homozygous for the risk allele and those homozygous for the alternative allele (McCarthy, 2010).

Lifestyle intervention studies in the United States, China and Finland targeting diet and exercise have shown efficiency of these interventions in decreasing the risk of developing diabetes from IGT. Other studies, such as the United Kingdom Prospective Diabetes Study (UKPDS), indicate that these interventions would not be sufficient to prevent all cases of T2DM (UKPDS, 1995; UKPDS, 1998; Zimmet, *et al.*, 2001).

Table 1: Genetic Susceptibility factors implicated in T2DM

Genetic factor	Implication in diabetes
Hepatocyte nuclear factor (HNF)-1α	Abnormalities cause the most common form of maturity onset diabetes of the young (MODY). It is also a known risk variant for type 2 diabetes. HNF-1α is expressed in the liver, but affects the expression of insulin.
TCF7L2	A transcription factor which modulates pancreatic islet function – implicated in beta cell dysfunction. Associated with decreased glucose stimulated insulin secretion (GSIS) and decreased depolarisation evoked insulin exocytosis. Genetic variants in TCF7L2 have a 30% increase in risk per risk allele - the largest known effect on T2DM susceptibility.
Melanocortin-4 receptor (MC4R)	Low frequency coding variants implicated in 2 - 3% of severe obesity.
CDKAL1, CDKN2A and CDKN2B	Regulators of cyclin dependent kinases (CDKs). Each copy of a susceptibility allele of these loci is associated with 15 - 20% increased risk of diabetes; implicated in decreased beta cell mass and decreased insulin secretion.
Insulin-receptor substrate 1 (IRS1)	Risk variant for T2DM implicated in insulin resistance.
FTO	One of strongest associations of genetic loci with obesity risk and BMI.
KCNQ1	Encodes a voltage-gated potassium channel. Variants affect insulin granule docking and show decreased depolarisation-evoked insulin secretion – hence impaired exocytosis and declining beta cell function.
Potassium inwardly rectifying channel, subfamily J, member 15 (KCNJ15)	Associated with beta cell dysfunction. The risk allele is present at elevated levels due to increased mRNA stability. Overexpression of KCNJ15 in the beta cell line INS-1 resulted in decreased GSIS.

Data source: American Diabetes Association (2004), Mathews and Mathews (2012), McCarthy (2010), McCarthy *et al*. (2013), Rosengren *et al*. (2012), and Voight *et al*. (2010).

1.1.6. Other types of diabetes mellitus

There are other types of diabetes mellitus of low prevalence, including diabetes linked to rare genetic mutations, pre-existing pancreatic disease and endocrine disorders with diabetes as an associated complication. Approximately 1 - 2% of the total diabetes mellitus cases are monogenic (Muoio and Newgard, 2008). These cases are usually diagnosed at a young age and involve defects in GSIS. Genetic conditions, known as MODY, include mutations in HNF-1α, Neurogenic differentiation 1 (NeuroD1) and glucokinase and are inherited in an autosomal dominant pattern (American Diabetes Association, 2012). The most common form of MODY involves a mutation in the transcription factor HNF-1α and results in impaired insulin secretion. Similarly, mutation of the transcription factor NeuroD1 impairs insulin secretion through its effect on insulin gene expression. Glucokinase mutations result in defective protein production and consequently defects in glucose sensing within the beta cell; increased plasma glucose levels are therefore necessary to stimulate normal insulin secretion in the pancreas (Tinto, *et al.*, 2008; Zhang, *et al.*, 2009).

Extensive damage to the pancreas by diseases such as pancreatitis and cystic fibrosis, or by trauma, as well as endocrinopathies such as Cushing's syndrome and glucagonoma can also lead to diabetes (American Diabetes Association, 2012). In Cushing's syndrome and glucagonoma excessive amounts of cortisol and glucagon respectively, antagonise the action of insulin and can cause diabetes (American Diabetes Association, 2004). These rare forms of the disease highlight the fundamental importance of beta cell function to the maintenance of metabolic health, and highlight the complexity of its regulation.

1.1.7. Diabetes insipidus

Diabetes insipidus is a rare condition unrelated to diabetes mellitus. It is primarily a hormonal condition relating to a lack of or decreased sensitivity to anti-diuretic hormone, and therefore leads to problems in the kidney and an inability to conserve water (Spanakis, *et al.*, 2008). Diabetes insipidus is unrelated to beta cell function; any further discussion of diabetes will therefore refer to diabetes mellitus and not to diabetes insipidus.

1.2. Complications of diabetes

There is a significant increase in morbidity and mortality as well as a financial cost of patient care associated with diabetes; 4.8 million deaths were attributed to diabetes in 2012 – equivalent to a death every 7 s, half of which were of people between the ages of 20 and 60 (Guariguata, 2012; International Diabetes Federation, 2012). Additionally, treatment of diabetes accounted for 11% of global healthcare expenditure in 2011 (International Diabetes Federation, 2012). Although good diabetes management can decrease the risk of complications, some studies show at least one complication present in more than 50% of people at the time of diagnosis with diabetes and consequently life expectancy is more than 8 years lower in patients with diabetes (Franco, *et al.*, 2007; International Diabetes Federation, 2011).

Complications of diabetes include: microvascular complications – nephropathy, retinopathy and neuropathy; macrovascular complications – increased risk of CVD and cerebrovascular disease; and others – cataract and embryo malformations in pregnancy. CVD is the major cause of morbidity and mortality for patients with diabetes; 50% of diabetes-associated deaths are attributed to CVD (The Lancet, 2008). Although conditions which commonly coexist with T2DM, such as dyslipidaemia and hypertension, are also risk factors for CVD, diabetes is an independent risk factor for CVD (American Diabetes Association, 2013). The global impact of beta cell dysfunction and diabetes, and the numerous complications, highlight the importance of maintaining glycaemic control and beta cell function; hence the necessity of improving our understanding of the factors which control it.

1.3. Biology of beta cells

1.3.1. Functional role and biochemistry

The functional role of pancreatic beta cells is to secrete insulin in response to raising blood glucose levels – GSIS. Insulin is an anabolic hormone involved in: carbohydrate metabolism – increasing glucose uptake in skeletal muscle, adipose tissue and liver, increasing the activity of glycogen synthase, glycolysis and the pentose-phosphate pathway and decreasing glycogenolysis and gluconeogenesis; lipid metabolism – increasing fatty acid and triglyceride synthesis in adipose tissue

and liver and decreasing lipolysis in adipose tissue and ketone body synthesis in the liver; and protein metabolism – increasing amino acid transport and protein synthesis in muscle, adipose tissue and liver, and decreasing protein degradation in muscle (Taniguchi, *et al.*, 2006).

Glucose enters pancreatic beta cells via the glucose transporter type 2 (GLUT2). These transporters are the lowest affinity and highest capacity glucose transporters, with a K_M of 17 mM (Johnson, *et al.*, 1990a). This confers a high capacity for glucose uptake into beta cells by facilitated diffusion when plasma glucose levels increase, and therefore enables responses to subtle changes in plasma glucose concentration. However, since glucose is taken up into beta cells in far higher quantities than can be metabolised – a 75% decrease in transport has been calculated to be necessary to limit glucose usage by islets, it is thought that GLUT2 does not act directly as a glucose sensor but rather glucose transport beyond that required for sensing occurs (Efrat, 1997; Johnson, *et al.*, 1990b). It was rather suggested that phosphorylation of glucose by glucokinase to form glucose-6-phosphate (G6P) acts as the mechanism by which extracellular glucose levels are coupled to insulin secretion (Matschinsky, 1990).

The biochemical pathway by which glucose entry via GLUT2 into beta cells leads to insulin granule exocytosis is shown in Figure 1. Glucose metabolism leads to an increase in the ATP:ADP ratio and the consequential closure of ATP sensitive potassium channels (K^+_{ATP}). The subsequent membrane depolarisation activates voltage-gated calcium channels (VGCC), leading to calcium influx and hence an increase in the intracellular calcium concentration ($[Ca^{2+}]_i$) – the triggering signal for exocytosis (Muoio and Newgard, 2008). The increase in intracellular calcium also activates the slow calcium-activated potassium channel ($K_{Ca,slow}$) which removes potassium ions from the cell, helping to repolarise the beta cells and prevent continuous calcium influx and insulin release (Nunemaker, *et al.*, 2004). It has also been suggested that increases in intracellular calcium may open K^+_{ATP} channels, and thus contribute to cell repolarisation (Nunemaker, *et al.*, 2004).

Medium and long chain fatty acids and amino acids act as physiological potentiators of insulin secretion (Itoh, *et al.*, 2003; Newsholme, *et al.*, 2005). The G protein coupled receptor GPR40 functions as a receptor for free fatty acids in pancreatic islets; its expression is 17 times greater in the islets than in the total pancreas and it is non-specific for fatty acids (Briscoe, *et al.*, 2006; Itoh, *et al.*,

2003). Activation of this receptor was shown to increase intracellular calcium through release from intracellular stores, such as the endoplasmic reticulum (ER), thereby amplifying the triggering signal for GSIS. The stimulatory effects of both oleic and linoleic acids on insulin secretion were greater in high glucose conditions indicating that these fatty acids potentiate GSIS (Itoh, *et al.*, 2003). Fatty acids are necessary for insulin secretion; they function to maintain basal insulin secretion as well as 'priming' beta cells to respond to elevated glucose levels (Briscoe, *et al.*, 2006; Corkey, 2012).

The mechanisms by which amino acids enhance insulin secretion vary. Arginine, in the presence of glucose, directly depolarises the plasma membrane. Other amino acids, such as alanine, are co-transported into the beta cells with sodium and consequently lead to depolarisation as a result of the sodium transport. The metabolism of alanine also leads to an increase in the ATP:ADP ratio within the cell. Mitochondrial metabolism of glucose is crucial to the action of amino acids on insulin secretion. Amino acids increase mitochondrial metabolism by increasing substrate availability for the Krebs cycle as well as by the activation of glutamate dehydrogenase by leucine (Newsholme, *et al.*, 2005). The effects of alanine and arginine on insulin secretion are illustrated in Figure 1.

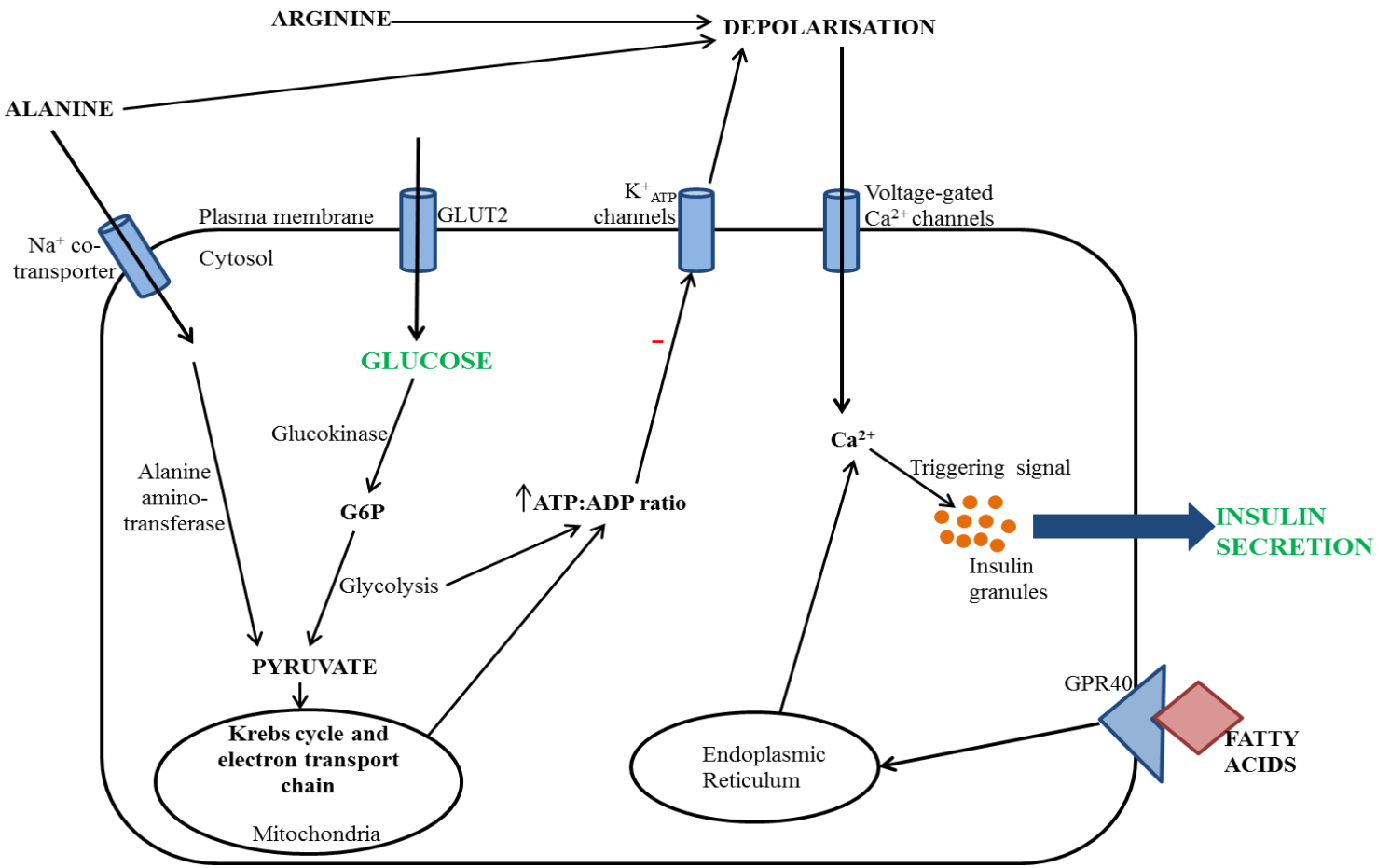

Figure 1: The biochemical pathway of GSIS in the beta cell including the role of amino acids and free fatty acids. Glucose metabolism generates an increase in the ATP:ADP ratio, which inhibits the ATP-sensitive potassium channels and leads to membrane depolarisation. The resultant calcium influx acts as the triggering signal for insulin granule exocytosis.

1.3.2. Structure of pancreatic islets

Beta cells form a central core within pancreatic islets of Langerhans in mice. Other cells, such as glucagon secreting alpha cells, form a peripheral mantle surrounding the beta cells. This differs to the architecture of human islets where beta cells are interspersed with non-beta cells (Jain and Lammert, 2009). Pancreatic islets have an extensive vascular supply ensuring that beta cells are supplied with the necessary nutrients and can regulate blood glucose levels appropriately. It has been suggested that no part of the pancreatic islets is more than a cell away from the arterial blood supply and that all cells are surrounded by the structural basement membrane – the specialised extracellular matrix (ECM) (Olsson and Carlsson, 2011; Otonkoski, *et al.*, 2008). Up to 15 - 20% of the pancreatic blood flow is received by the pancreatic islets of Langerhans despite them representing approximately 1 - 2% of the total organ mass, distributed in clusters throughout the pancreas; this indicates how highly vascularised the islets are (Ahnfelt-Rønne, *et al.*, 2012; Stendahl, *et al.*, 2009).

1.3.3. ECM and cell-cell coupling

Pancreatic beta cells function within an organ system; cell to cell coupling and interactions with other beta cells, other types of cells and with proteins of the basement membrane are vital to their integrated response to nutrient stimuli. This was indicated by the calcium response to glucose stimuli being greater when cells were cultured as three-dimensional islet-like structures than when cultured as a monolayer (Hauge-Evans, *et al.*, 1999). Other studies, such as that of Hopcroft *et al.* (1985), indicated that basal insulin secretion could be increased by re-aggregation of dispersed islets. Signalling between beta cells is therefore necessary for maintenance of normal beta cell function and insulin secretion. A more recent study by Konstantinova *et al*. (2007) showed that when the cell density of the insulinoma cell line MIN6 was increased there was a decrease in the basal insulin secretion and an increase in GSIS. This again indicates the importance of cell to cell communication to beta cells.

Gap junctions are channels between cells composed of connexins which enable the transfer of cytoplasmic ions and metabolites. They have been proposed to be involved in the coordination and synchronisation of cellular responses in beta cells (Jain and Lammert, 2009). Vozzi *et al*. (1995) showed a causal link between

loss of gap junctional communication and impairment of insulin secretion. It was demonstrated that separation of beta cells resulted in a decrease in both insulin biosynthesis and secretion, proposed to be due to connexin43 (Cx43) since insulin secreting cell lines with secretory defects often lack Cx43. However, this conclusion has been more recently disputed. Connexin36 (Cx36) has been shown to form gap junctional complexes in beta cells whilst Cx43 has not been found in either the insulin secreting cell line MIN6 or in primary beta cells (Cigliola, *et al.*, 2013; Jain and Lammert, 2009; Serre-Beinier, *et al.*, 2000). It is therefore considered that connexins have a vital role in communication between beta cells and that Cx36 underlies this communication.

The role of Epithelial-cadherin (E-cadherin) in GSIS was indicated by studies showing that down regulation of E-cadherin in MIN6 cells decreased GSIS to similar levels as found in unattached cells. This suggests that E-cadherin may be necessary for synchronisation of glucose stimulated calcium oscillations (Rogers, *et al.*, 2007). Silencing cadherins in MIN6 cells using small interfering RNA also decreased GSIS, whilst exposure to an anti-cadherin antibody blocked the elevation of intracellular calcium in response to glucose stimulation (Jaques, *et al.*, 2008; Yamagata, *et al.*, 2002).

Interactions of beta cells with ECM proteins are also necessary for optimal beta cell function (Weber, *et al.*, 2008). Interactions with collagen IV and laminin improve MIN6 cell survival and the presence of ECM proteins in the extracellular environment also increased insulin secretion (Weber, *et al.*, 2008). ECM proteins in the basement membrane surrounding beta cells promote cell survival. When cells are detached from their natural ECM environment in the pancreas they undergo apoptosis; this can be prevented *in vitro* by culturing cells on collagen IV or laminin (Pinkse, *et al.*, 2006). Beta cells interact with basement membrane proteins via integrins. Heterodimers containing the β1-integrin have been suggested to affect insulin transcription and secretion, as well as cell proliferation (Kragl and Lammert, 2010). The expression of ECM proteins such as collagen IV has been suggested to regulate insulin secretion with the specific interaction between the α1β1-integrin heterodimer and collagen IV potentiating insulin secretion (Eberhard, *et al.*, 2010; Kaido, *et al.*, 2004; Kragl and Lammert, 2010). The known components of the basement membrane surrounding pancreatic beta cells and the integrin receptors through which they interact with pancreatic beta cells are given in Table 2.

Table 2: Matrix proteins and their receptors on pancreatic beta cells

Protein	Localisation	Integrin Receptor
Collagen IV	Basement membrane	$\alpha_1\beta_1$
Laminin	Basement membrane	$\alpha_1\beta_1$, $\alpha_3\beta_1$, $\alpha_5\beta_1$, $\alpha_6\beta_1$
Collagen I	ECM	$\alpha_V\beta_3$, $\alpha_2\beta_1$
Fibrinogen	Plasma	$\alpha_V\beta_3$
Fibronectin	Plasma, ECM	$\alpha_V\beta_1$, $\alpha_V\beta_3$, $\alpha_5\beta_1$
Vitronectin	Plasma, ECM	$\alpha_V\beta_1$, $\alpha_V\beta_3$, $\alpha_V\beta_5$

Adapted from Weber *et al*. (2008).

Recently syndecan-4, a cell-surface proteoglycan, has been shown by immunostaining to be present on insulin-positive but not glucagon-positive cells. It has also been shown to be present in MIN6 cells and it was therefore suggested that beta cells form some of the basement membrane components (Cheng, *et al.*, 2012a). The cytoplasmic domain of syndecan-4 binds to phosphatidylinositol 4,5-bisphosphate and has intracellular effects through activation of protein kinase Cα in a calcium independent manner (Simons and Horowitz, 2001). Syndecans have been described as co-receptors as they frequency work alongside other receptors, particularly integrins in interactions with ECM proteins. Syndecans and integrins collaborate in mediating cell adhesion to ECM proteins and the processes these interactions regulate, including cell migration and cell spreading (Xian, *et al.*, 2010). However, syndecan-4 knockout mice showed no significant impairments in pancreatic function; this may indicate that their role is limited, or alternatively, as suggested by Cheng *et al*. (2012a) that there is isoform redundancy and other syndecan isoforms are upregulated to compensate. Whilst these proteoglycans have been suggested by Cheng *et al*. (2012a) to be the missing link to maintaining islet longevity after isolation, further work is required to fully understand their role and the interactions of syndecans with integrins in the basement membrane of the islets of Langerhans.

1.3.4. Insulin gene expression

Humans have one insulin gene designated the abbreviation INS. The primary translational product of INS is preproinsulin. The signal peptide is cleaved in the ER, leaving proinsulin which is processed further to produce insulin (Støy, *et al.*, 2007). This differs to the expression in rodents wherein insulin is expressed by two genes: Ins1 and Ins2. Ins2 has the greater structural homology to other mammalian insulin genes with conservation of nucleotide sequence in the coding region and identical arrangement of introns and exons (Wentworth, *et al.*, 1986). Ins1 contains only one of the two introns present in Ins2 and other mammalian insulin genes and is considered to be a functional retroposon – a repetitive DNA fragment inserted into the DNA following reverse transcription from RNA (Kuroda, *et al.*, 2009). Phylogenetic analysis has shown Ins1 to have originated before the separation of rat and mouse 15 million years ago and is a rodent specific retrogene (Hay and Docherty, 2006; Shiao, *et al.*, 2008).

Both Ins1 and Ins2 are expressed in mouse islets and contain homologous regulatory regions upstream of the gene itself. However, as discussed by Roderigo-Milne *et al*. (2002) this homology extends to approximately 500 base pairs upstream of the transcriptional start site; regulatory regions further upstream may contribute to differences in responsiveness of the genes. Their studies of the murine MIN6 cell line indicated that Ins1 expression, but not Ins2 expression, is altered by both glucose stimulation and cell-cell contact, thereby indicating that in this system there is differential control of the expression of these 2 genes (Roderigo-Milne, *et al.*, 2002). Previous studies using wild type and Ins1 and Ins2 knockout mice showed that the presence of either Ins1 or Ins2 is sufficient to prevent diabetes, with a similar level of pancreatic insulin observed in both single homozygous mutants and the wild type mouse. The double homozygous mutant had severe insulin deficiency and diabetes (Leroux, *et al.*, 2001). Both the human insulin gene and the mouse Ins2 gene have biallelic expression in the adult. Demethylation of the insulin gene promoter region specifically in beta cells has been suggested to be an important step in the differentiation of insulin producing cells from embryonic stem cells (Kuroda, *et al.*, 2009). The insulin gene promoter spans approximately 400 base pairs upstream of the transcriptional start site. The compact promoter region enables overlap of regulatory elements and synergistic interactions. It is highly conserved in mammals with a decline in homology observed beyond 400 base pairs upstream of

the transcriptional start site (Hay and Docherty, 2006). The regulatory sequences of the A3, C1 and E1 boxes and their flanking sequences are highly conserved between species, with 100% homology between the 5' flanking region of the A3 box in mouse Ins2 and human INS. The homology between INS and the mouse Ins1 is 87% indicating a greater degree of homology between Ins2 than Ins1 and the single INS gene of other mammalian species (Hay and Docherty, 2006). There are however differences between the promoter regions of human and rodent insulin genes, such as the spacing between the key regulatory elements, which will impact upon synergistic interactions – rodent insulin promoters contain insertions and deletions between the three regulatory domains (Hay and Docherty, 2006).

Blood glucose regulates insulin production through its modulation of three beta cell specific transcriptional regulators – Pancreatic duodenum homeobox-1 (Pdx-1), V-maf musculoaponeurotic fibrosarcoma oncogene homologue A (MafA) and NeuroD1 (Andrali, *et al.*, 2008). Pdx-1, MafA and NeuroD1 bind to the A3, C1 and E1 sites of the insulin promoter respectively to stimulate insulin gene expression synergistically in response to elevated glucose levels. It is suggested that the subcellular localisation of NeuroD1 is altered in response to changing glucose levels, being translocated from the cytoplasm to the nucleus when the glucose concentration is elevated (Andrali, *et al.*, 2008). The expression of MafA is regulated by glucose; transcription increases in response to high glucose concentrations. The DNA-binding activity of Pdx-1 and its interaction with both activators and repressors is modulated by glucose (Andrali, *et al.*, 2008). Glucose also increases the stability of the preproinsulin mRNA transcript through regulation of the binding of a binding protein to the pyrimidine-rich sequence in the 3' untranslated region as well as promoting the translation of the preproinsulin transcript in beta cells (Poitout, *et al.*, 2006; Tillmar, *et al.*, 2002; Welsh, *et al.*, 1985; Wicksteed, *et al.*, 2001). In addition, glucose upregulates mRNA translation specifically in beta cells, particularly of granule proteins such as insulin (Bensellam, *et al.*, 2012; Tillmar, *et al.*, 2002; Vander Mierde, *et al.*, 2007). This ensures that enough insulin is available to meet the higher demands.

1.3.5. Mechanisms of regulation of insulin secretion

Production and secretion of insulin are independently regulated with insulin prepared and stored in granules in beta cells awaiting secretion upon stimulus. As

well as nutritional stimuli (glucose, fatty acids and amino acids) insulin release is further modulated by a number of other factors including sympathetic and parasympathetic innervation, feedback mechanisms of insulin and glucagon and other environmental cues (interactions with other cells and the basement membrane). Parasympathetic innervation of beta cells, mediated by the action of acetylcholine through M_3 muscarinic receptors, is stimulatory to both insulin secretion and synthesis. Sympathetic innervation of beta cells, mediated by noradrenaline acting through adrenergic receptors, is inhibitory (Eberhard and Lammert, 2009; Gautam, *et al.*, 2006). The importance of this innervation was demonstrated by Gautam *et al.* (2006) who found mice lacking the M_3 muscarinic receptor specifically in beta cells displayed IGT and reduced insulin release. The same study also showed that if this receptor was overexpressed in beta cells mice displayed improved glucose tolerance and were resistant to diet-induced IGT and hyperglycaemia.

There are interactions between the cells of the islets of Langerhans – some of these are paracrine, others occur through the systemic circulation. In rodent islets, it has been shown that blood flows from beta cells to alpha and gamma cells, therefore whilst secretion from beta cells can directly affect other cell types within the islets, it is not believed that this is reciprocal. Rather, glucagon and somatostatin pass through the systemic circulation before affecting beta cells (Kanno, *et al.*, 2002). The inhibitory paracrine effect of insulin on alpha cells and glucagon production is well established and has been demonstrated in both rodents and humans. The high level of insulin receptor expression in alpha cells, similar to that of the liver, indicates the importance of this paracrine interaction (Asplin, *et al.*, 1981; Cooperberg and Cryer, 2010; Franklin, *et al.*, 2005). The negative effect of insulin secretion on glucagon production is thought to be due directly to the action of insulin and also due to zinc, which is co-released in insulin granules. Zinc and insulin together increase K^+_{ATP} channel activation and thus inhibit glucagon secretion (Franklin, *et al.*, 2005).

It has long been known that glucagon is stimulatory to insulin release (Samols, *et al.*, 1966). More recently evidence has suggested that this effect is through glucagon receptors on beta cells and intracellular cAMP increases (Huypens, *et al.*, 2000; Kanno, *et al.*, 2002). Insulin also has an autocrine effect on its own production, as well as on beta cell survival and proliferation. These effects are mediated by insulin binding to insulin receptors on beta cells (Jain and Lammert,

2009; Kulkarni, *et al.*, 1999). The study performed by Kulkarni *et al*. (1999) showed that knockout of the insulin receptor specifically in pancreatic beta cells in mice resulted in a loss of GSIS and progressive impairments in glucose tolerance – similar to observed in T2DM. Research using a beta cell specific knockout of the insulin receptor has implicated the insulin receptor in beta cell proliferation, especially the compensatory islet growth of states of insulin resistance and obesity (Okada, *et al.*, 2007). This indicates that beta cell physiology is tightly regulated. Changes in secretion of insulin, and the factors regulating it, as well as insulin resistance of the beta cells may be implicated in beta cell dysfunction.

1.4. Maintenance of beta cell mass

Beta cell number is determined by the initial number of cells formed during development and by the rate of turnover. The turnover of beta cells is determined by the rate of beta cell formation and the rate of beta cell loss by apoptosis (Taylor, 2006). Factors which affect either the rate of formation of beta cells or the rate of beta cell apoptosis will affect the beta cell mass and consequently the physiology and functionality of the endocrine pancreas.

1.4.1. Growth and regeneration

Growth of pancreatic islets could occur by either beta cell replication, neogenesis (formation from stem cells and progenitor cells) or a combination of both. In 1911 it was suggested that islet growth occurred by both replication and differentiation (Bensley, 1911). However at this early stage the function of islet cells was unknown. Genetic studies, such as that performed by Dor *et al*. (2004) have questioned the role of neogenesis in the formation of pancreatic beta cells in adults. In this study a tamoxifen-inducible Cre-lox system was used to label beta cells; the proportion of these labelled cells that remained after 4, 6, 9 and 12 months was measured. It was concluded that cells were either post-mitotic or derived from existing beta cells by self-duplication since this label was not diluted with time. However, this evidence has been disputed and the study criticised due to the low level of labelling used (approximately 30%) and that neogenesis was discounted on the basis of a lack of label dilution (Bonner-Weir, *et al.*, 2010). Indeed, these two

processes are not mutually exclusive, and it is possible, and indeed likely, that both duplication and neogenesis contribute to the maintenance of beta cell mass after birth. These processes are not fully understood due largely to experimental limitations; in humans, evidence is predominantly based on observations at autopsies and surgery. Recent studies indicate that in adult humans beta cell replication is negligible, although it may occur with significant impact on beta cell mass in children (In't Veld, *et al.*, 2010; Perl, *et al.*, 2010). This is likely due to the slow turnover of beta cells in human adults wherein only about one per cent of beta cells enter into the mitotic phase from the resting G_0 stage of mitosis (Skelin, *et al.*, 2010). Given the current evidence, both replication and neogenesis are likely involved in maintaining beta cell mass after birth. Contributions of the two factors vary depending on the conditions used and species studied.

1.4.2. Beta cell decline with age

The prevalence of both IGT and diabetes increases markedly with age from under 5% in individuals under the age of 30 to greater than 20% in individuals over the age of 70 (International Diabetes Federation, 2012; Shaw, *et al.*, 2010; Szoke, *et al.*, 2008). The study by Szoke *et al*. (2008) examining the effect of ageing on glucose homeostasis and insulin secretion concluded that in healthy individuals with normal glucose tolerance, insulin secretion declined at a rate of approximately 0.7% per year. This decline was more rapid in people with IGT at 1.2% per year. The involvement of impairments in function or decreases in beta cell mass in the cause of this decline was not determined, although it was hypothesised to be due to a decrease in beta cell mass. This is consistent with an earlier study which showed changes in both rates of apoptosis and proliferation in human pancreatic islets with ageing (Maedler, *et al.*, 2006). More recently, evidence has indicated that the age-related decrease in replication of beta cells is due to systemic circulating factors, although the identity of these factors is not known (Salpeter, *et al.*, 2013). However, it is estimated that beta cell area – the fractional beta cell area of the pancreas measured in a large representative section of the tissue removed at surgery - has declined by approximately 65% when diabetes develops. Therefore, age alone cannot account for the deterioration in beta cell mass and function leading to the development of IGT and T2DM. The decline in beta cell mass is far greater in individuals with diabetes (Meier, *et al.*, 2012). In addition, Szoke *et al*. (2008) demonstrated that

ageing has no apparent effect on insulin sensitivity – assessed using HOMA and hyperglycaemic clamp techniques, but rather has effects only on beta cell function and the ability of the islets to secrete sufficient insulin.

1.4.3. Beta cell reserve capacity

It is often assumed that anatomical and functional beta cell mass are the same. Studies such as that of Chen *et al*. (2008) have used insulin as an indirect measure of beta cell mass, whereas this actually indicates the functional mass of beta cells producing and secreting insulin. Weir and Bonner-Weir (2011) recently discussed evidence provided by Olsson and Carlsson (2011) that there may be differences between functional and actual beta cell mass. Olsson and Carlsson (2011) indicated that there is a low-oxygenated population of islets which are functionally dormant, but act as a functional reserve of endocrine cells. They showed, by means of partial pancreatectomy, that the number of low-oxygenated dormant islets could be altered and activated when demand increases. Based on this, it was hypothesised that dormant islets are activated on demand – as desired in pregnancy and insulin resistance of pre-diabetes and T2DM and also inactivated when demand decreases – such as after weight loss (Weir and Bonner-Weir, 2011). However, the plasticity and adaptability of the endocrine pancreas varies between species; for example, the beta cell mass can be increased several fold in obese rodents whereas the capacity to increase beta cell mass is only 20 - 50% in human subjects (Henquin, *et al.*, 2008). Caution should therefore be taken in extrapolating conclusions across species; although this phenomenon has been demonstrated in rodents, it is not known whether it occurs in humans (Weir and Bonner-Weir, 2011).

1.4.4. Factors promoting beta cell survival

Beta cells interact with other beta cells via processes involving E-cadherin and Cx36, as well as interacting with ECM proteins. These interactions promote beta cell survival (Parnaud, *et al.*, 2011; Pinkse, *et al.*, 2006). The protective nature of these interactions indicates the importance of not only individual beta cells, but also communication with other beta cells and between beta cells and the ECM. Damage to the ECM and associated loss of cell attachment may lead to either a decrease in insulin secretion from individual cells or a decrease in the beta cell mass.

1.5. Factors implicated in the beta cell decline of diabetes

The decrease in insulin secretion observed in diabetes is due to interplay between a loss of beta cell function and alterations in beta cell survival/growth. The latter is due to impairments in the maintenance of beta cell mass – Figure 2. It has been shown that beta cell replication is not altered in individuals with diabetes compared to healthy controls but rather that replication was low in both groups (Butler, *et al.*, 2003). Neogenesis was shown to increase in obesity, but was no different in weight match individuals with and without diabetes (Butler, *et al.*, 2003). The study showed a significant increase in apoptosis of beta cells in people with diabetes. This shift in the balance of beta cell formation and apoptosis prevents the maintenance of beta cell mass and likely contributes to the decrease in both beta cell mass and insulin secretion seen in diabetes. Other studies, such as those discussed by Taylor (2006), showed a substantial decline in beta cell mass in T2DM. Estimates of beta cell mass at the onset of diabetes vary – from a 25 - 50% decline to a 65% decline (Chang-Chen, *et al.*, 2008; Meier, *et al.*, 2012). The decrease in beta cell mass alone is not thought to be sufficient to cause T2DM – further beta cell dysfunction is involved in the deleterious effects of the pathogenesis of diabetes, of which numerous factors have been implicated, some of which are illustrated in Figure 2 (Chang-Chen, *et al.*, 2008).

The decline in functional activity of beta cells in diabetes may also be due to less effective insulin secretion. The insulin secretion pathway is well characterised (Figure 1) and mutations or environmental factors affecting components of this pathway, or associated modulators and regulators, will affect insulin secretion. Reviews such as that by Muoio and Newgard (2008) have discussed the many factors implicated in the development of insulin resistance and T2DM. These include hormonal and inflammatory factors, genetic susceptibility, nutritional overload – as occurs in obesity, ER stress and protein glycation – as given in Table 3. As can be seen from the numerous factors implicated in the pathogenesis of diabetes, there is no consensus as to a single pathway or mechanism by which chronic exposure of pancreatic islets to hyperglycaemia (and hyperlipidaemia) leads to the deleterious effects on the beta cell phenotype and consequential diabetes – the concept of glucotoxicity (or glucolipotoxicity) (Muoio and Newgard, 2008). Rather, it is thought that the numerous stresses discussed are inter-related and act at multiple

levels to cause dysfunction through alterations in gene expression, function, survival and growth (Bensellam, *et al.*, 2012; Jonas, *et al.*, 2009; Muoio and Newgard, 2008). Indeed, detrimental effects of fatty acids on beta cell function have been shown to only occur if high glucose is also present – hence the concept glucolipotoxicity to describe the beta cell impairments of the combined metabolic overload (Muoio and Newgard, 2008; van Raalte and Diamant, 2011).

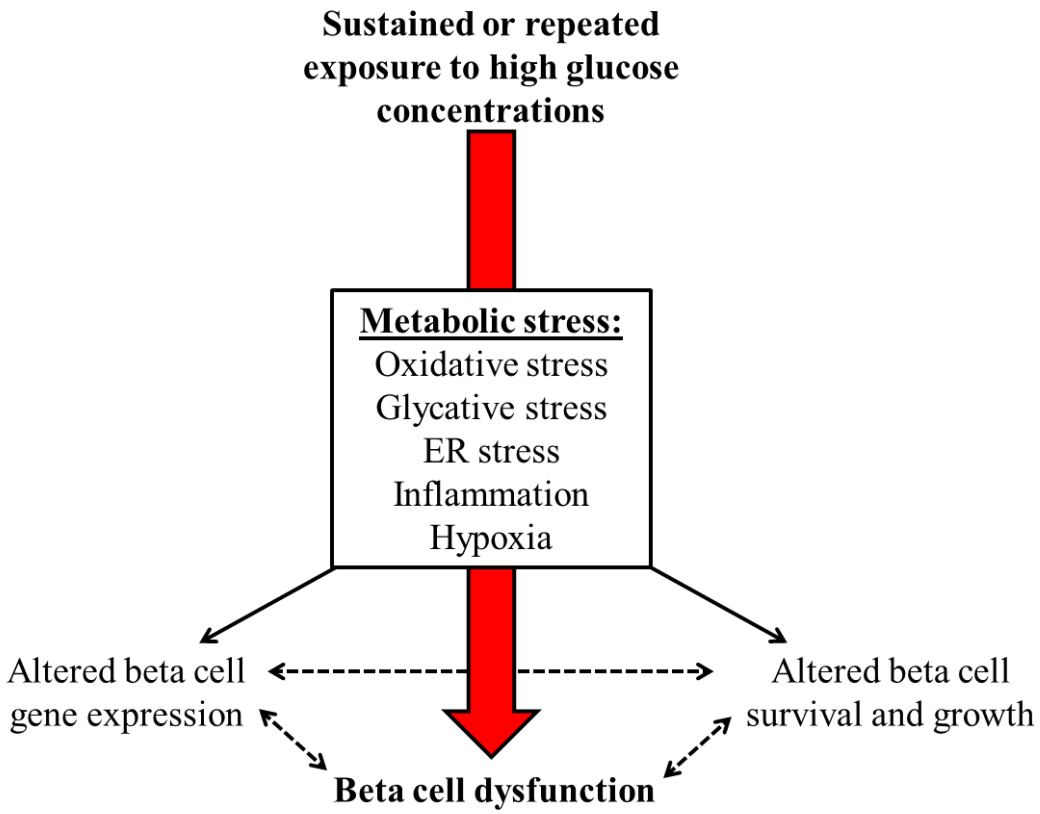

Figure 2: Possible mechanisms of beta cell dysfunction from glucotoxicity. Exposure of beta cells to a number of metabolic stresses associated with elevated glucose can cause dysfunction through effects on gene expression and functionality as well as the balance of cell production and cell death (apoptosis) – the concept of glucotoxicity. Adapted from Jonas *et al*. (2009).

Table 3: Factors implicated in development of diabetes

Factor	Implication in diabetes	References
Genetics	Susceptibility factors (Table 1) and rare monogenic inheritance forms of diabetes are implicated. Other genetic syndromes – such as Klinefelter, Turner, Down and Prader-Willi syndromes – are associated with increased incidence of diabetes.	(American Diabetes Association, 2012)
Obesity	Obesity may lead to insulin resistance in liver/skeletal muscle as well as accumulation of other factors implicated in the pathogenesis of diabetes (mitochondrial stress and increases in reactive oxygen species (ROS)) due to nutritional and metabolic overload. Central obesity and an increased BMI correlate with loss of beta cell function and greatly increase the lifetime risk of developing diabetes.	(Muoio and Newgard, 2008; Narayan, *et al.*, 2007; van Raalte and Diamant, 2011)
Age	Insulin secretion decreases at approximately 0.7% per year in healthy individuals.	(Szoke, *et al.*, 2008)
Inflammation	High doses of aspirin (a salicylate) have been shown to reverse insulin resistance and diabetes. Inflammatory markers, such as C-reactive protein, IL-6 and TNF-α, are increased in insulin resistance and are suggestive of an increased risk of diabetes, although the underlying mechanisms are not determined.	(Dandona, *et al.*, 2004; Haffner, 2006; Kim, *et al.*, 2001; Muoio and Newgard, 2008)
ER stress	An increased demand for insulin increases the workload for cellular components such as the ER. Beta cells are particularly susceptible to ER stress due to the high rate of proinsulin biosynthesis. Akita mice, a model of enhanced ER stress, have a decreased beta cell mass and increased apoptosis. Long chain saturated fatty acids have also been implicated in causing ER stress in beta cells – both	(Back, *et al.*, 2012; Bensellam, *et al.*, 2012; Muoio and Newgard, 2008; Nguidjoe, *et al.*, 2011;

	by the unfolded protein response and by altered calcium handling in the ER. Overexpression of the sodium-calcium exchanger, responsible for extruding calcium from cells is associated with ER stress through ER depletion of calcium. Activation of glucokinase has also been associated with ameliorating ER-stress induced apoptosis in beta cells.	Shirakawa, *et al.*, 2013)
Oxidative stress	Elevated levels of glucose and fatty acids are associated with increased production of ROS. ROS act as signalling intermediates in a variety of cellular processes. When present in high levels ROS cause oxidative stress which can initiate apoptosis through MAPK pathways. ROS-mediated alteration of GSIS has been suggested to relate to down regulation of glyceraldehye-3-phosphate dehydrogenase activity and increased formation of AGEs. Islets are particularly vulnerable to oxidative stress since they contain low levels of ROS-scavenging enzymes and antioxidants and also have a poor capacity of DNA repair against oxidative damage. Oxidative damage suppresses insulin gene transcription through its effects on the transcription factors Pdx-1 and MafA.	(Bensellam, *et al.*, 2012; Grankvist, *et al.*, 2012; Harmon, *et al.*, 2005; Modak, *et al.*, 2009; Pi, *et al.*, 2007; Robertson, *et al.*, 2003; Sakai, *et al.*, 2003)
Glycative stress	Protein glycation increases in hyperglycaemia and diabetes.	Investigated in this project
Infection/ Disease of exocrine pancreas	Processes which injure the pancreas can cause diabetes. This includes pancreatitis, cancers, trauma and infection. Pancreatic damage must be extensive to cause diabetes – except in the case of cancers; adrenocarcinomas involving small sections of pancreas have been associated with diabetes. Viral infections such as mumps have	(American Diabetes Association, 2012; Karjalainen, *et al.*, 1988)

	also been associated with T1DM.	
Endocrino-pathies	Hormones such as glucagon, cortisol, growth hormone and adrenaline antagonise the action of insulin. Excesses of these in conditions such as glucagonoma can lead to diabetes.	(American Diabetes Association, 2012)
Amylin fibrils	Amylin fibrils have been suggested as a mechanism by which over-nutrition and increased beta cell stimulation can lead to beta cell dysfunction. Amylin is secreted with insulin by beta cells. Overexpression of human amylin has been associated with increased apoptosis and decreased beta cell mass in rats.	(Matveyenko and Butler, 2006; Muoio and Newgard, 2008)
In utero programming	The thrifty phenotype hypothesis indicates that reduced foetal growth *in utero* is associated with metabolic conditions later in life. An increase in nutrient availability potentially leads to similar consequences as obesity.	(Hales and Barker, 1992)
Leptin	Leptin is involved in appetite regulation in the hypothalamus; deficiency is associated with severe obesity and diabetes and is treated with exogenous leptin therapy. Other studies have reported inhibitory effects of leptin on insulin secretion and insulin gene expression, indicating a more peripheral role for leptin. Disruption of the leptin receptor in the pancreas indicates a critical role of leptin signalling in the islets, with IGT and poor compensatory islet growth in obesity.	(McCarthy, 2010; Morioka, *et al.*, 2007)
Impairments in autophagy	Autophagy is known to be upregulated in beta cells in diet-induced diabetic rodents; this serves a crucial stress response to protect the cells against oxidative stress. Loss of autophagy in beta cell specific knockouts of Atg7 in mice has shown impaired glucose tolerance and decreased serum insulin levels. Impairments in autophagy could be	(Ebato, *et al.*, 2008; Fujitani, *et al.*, 2009; Jung, *et al.*, 2008; Meijer and Codogno, 2008)

	a risk factor for T2DM.	
Branched-chain amino acids (BCAAs)	BCAAs (valine, isoleucine and leucine) are among the nine essential amino acids - they cannot be synthesised *de novo* but are provided by food intake. Plasma concentrations of BCAAs are elevated in human and animal models of obesity and insulin resistance. Both an increase in protein degradation and a decrease in BCAA catabolism has been implicated in this increase. Levels of BCAAs in plasma increase in the fasting state, consistent with the suggestion of increased protein degradation. Newgard *et al.* (2009) showed that elevated BCAAs contribute to the development of obesity-related insulin resistance using a rat model and demonstrated a similar association in humans. Whilst a number of studies have associated BCAAs with insulin resistance and diabetes, the underlying mechanism is not known and their role in beta cell (dys)function has not been reported.	(Adeva, *et al.*, 2012; Lu, *et al.*, 2013; Sailer, *et al.*, 2013; She, *et al.*, 2007; Tom and Nair, 2006)

1.6. Stages of pathogenesis of diabetes

T2DM has been described as beta cell failure in the context of insulin resistance (Chang-Chen, *et al.*, 2008). In early stages of diabetes, beta cells are able to adapt to insulin resistance by increasing total beta cell mass and function. However, the associated stresses of these high nutritional demands have a negative impact on beta cell function, leading to impaired secretion and cell death. The loss in insulin secretion will result in diminished inhibition of glucagon secretion from alpha cells; the consequential increase in glucagon release exacerbates the problem, with more glucagon counteracting the action of insulin and thus increasing the insulin resistance. Indeed, both a decrease in beta cell number and an increase in the number of alpha cells have been reported in people with T2DM (Taylor, 2006). Weir and Bonner-Weir (2004) proposed a model of five stages of progressive beta cell dysfunction during the development of diabetes – these stages are summarised in

Table 4. Although this model shows progressive dysfunction, movement through stages 1 - 4 can be in either direction – for example with successful treatment individuals with T2DM can move back from stage 4 to stage 1 or 2, and likewise individuals with T1DM may move back to stage 2.

Table 4: Stages of beta cell dysfunction in diabetes

Stage	Details
1: Compensation	Insulin secretion increases to maintain normal glycaemic control in the face of decreased beta cell mass and/or insulin resistance. GSIS function is maintained.
2: Stable adaptation	This stage often remains for a number of years. Glucose concentrations start to rise; fasting glucose concentration is maintained at approximately 5.0 - 7.3 mM. GSIS is diminished and individuals have IGT.
3: Unstable early decompensation	Glucose levels rise rapidly – this is an unstable transition stage. The instability may be due to a greater decline in beta cell mass or to increases in insulin resistance.
4: Stable decompensation	Glucose levels rise again and stabilise at approximately 16 - 20 mM; diabetes is apparent. This stage usually lasts a lifetime for people with T2DM and symptoms may become more noticeable in undiagnosed cases.
5: Severe decompensation	This stage is rare in T2DM but typically occurs in people with T1DM. The loss of beta cells is so severe that patients are dependent on insulin for survival. Glucose levels can typically be greater than 22 mM.

Information from Weir and Bonner-Weir (2004).

2. Introduction: Glycation

2.1. Protein glycation – a definition

The Biochemical Nomenclature Committee of the International Union of Biochemistry and the International Union of Pure and Applied Chemistry suggested in 1985 the term glycation for "all reactions that link a sugar to a protein or peptide" (Sharon, 1988). Later, it was differentiated between enzymatic modification of proteins forming glycoproteins, by the process of glycosylation and non-enzymatic modification of proteins forming glycated proteins, by the process of glycation (Lis and Sharon, 1993). Selective use of the term glycation for non-enzymatic modification of proteins by saccharides and saccharide derivatives is now the accepted nomenclature. However, in older scientific literature, terms used to describe the glycated protein haemoglobin vary. Terminology has included glycosylated haemoglobin, non-enzymatic glycosylated haemoglobin, glycohaemoglobin and glucosylated haemoglobin.

Protein glycation involves the non-enzymatic addition of a reducing sugar or derivative to a protein. A reducing sugar has a free aldehyde or ketone group and will therefore reduce Benedict's solution to form green, yellow or red precipitates of the insoluble copper (I) oxide (Benedict, 1909). It was initially thought that glycation was limited to amino groups of lysine side chains and N-terminal amino acid residues. However, more recently glycation of arginine residues by dicarbonyls has been implicated in physiological systems, as discussed by Rabbani and Thornalley (2012b).

Glycation occurs by a series of sequential and parallel reactions known collectively as the Maillard reaction. This is named after the French chemist L.C. Maillard who pioneered work on the reactions between sugars and amino acids – he observed that brown pigments were formed when glucose was heated in the presence of proteins (Cerami, 1986; Maillard, 1912). Historically, it was thought that glycation occurred first to early stage glycation adducts, known as Amadori products (or fructosamine adducts) via a Schiff's base intermediate, before being degraded to more stable advanced glycation endproducts (AGEs), as is the case for glucose (Rabbani and Thornalley, 2012b; Thornalley, *et al.*, 1999; Ulrich and Cerami, 2001). Glucose reacts with amino groups to form glycosylamines which dehydrate to form

Schiff's bases. N-(1-deoxy-D-fructos-1-yl)amino acids, or fructosamine, are consequently formed when the Schiff's base undergoes the 'Amadori rearrangement' (Hodge and Rist, 1953). Glycosylamine, Schiff's bases and fructosamine are all known as early stage glycation adducts (Thornalley, 2008). Further degradation of fructosamine to more stable adducts is known as advanced glycation and results in the formation of AGEs. The term AGE was first used by Cerami (1986) to describe "yellow-brown fluorescent pigments that can crosslink proteins together," but at this stage AGEs were not well characterised or understood.

Reactive α-oxoaldehydes (dicarbonyls) also react directly with proteins to form AGEs, not necessarily via early stage glycation adducts (Rabbani and Thornalley, 2012b). In addition, degradation of Schiff's bases via a non-Amadori pathway (the Namiki pathway) forms dicarbonyls and subsequently leads to production of AGEs (Thornalley, 2008; Thornalley, 2005). AGEs can therefore be formed in glycation from glucose from pre- (Schiff's base) and post- Amadori product reactions as well as from processes where an Amadori product is not a precursor – as detailed in Figure 3. This has consequently led to inconsistencies in the nomenclature and classification of AGEs, since AGEs are formed in both early and advanced stages of the Maillard reaction (Rabbani and Thornalley, 2012b). The nomenclature of fructosamine and AGEs is now widely used and accepted.

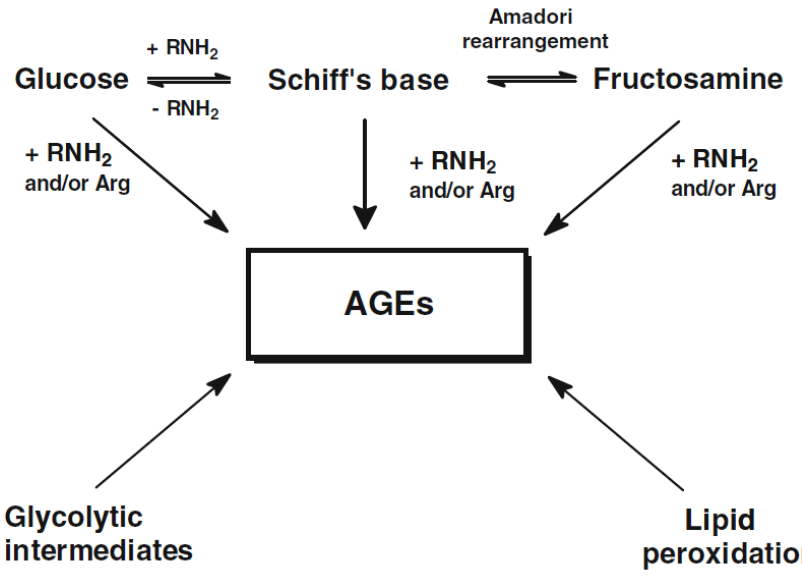

Figure 3: Formation of AGEs from glucose and physiological dicarbonyl metabolites (Rabbani and Thornalley, 2012b).

Allen *et al*. (1958) first reported evidence of a glycated protein *in vivo*. However, at the time it was not understood that the heterogeneity they observed in haemoglobin was actually due to glycation. It was characterised as glycated haemoglobin by Bookchin and Gallop (1968), whilst Rahbar (1968) described the increases observed in diabetes (Rabbani and Thornalley, 2012b). The formation of glycated haemoglobin, as well as its relevance to diabetes was further described by Bunn *et al*. (1978; 1976).

2.2. Dicarbonyls

2.2.1. Physiological formation of dicarbonyls

Dicarbonyls are compounds with two aldehyde or ketone functional groups or an aldehyde and ketone group. In this study a particular type of physiological dicarbonyl is considered: α-oxoaldehydes or α-ketoaldehydes. They are usually highly reactive and potentially toxic compounds formed endogenously as by-products of cellular metabolism. They are also present in many foods and beverages, increasing when foods and beverages are thermally processed in manufacture, pasteurisation, sterilisation and culinary processing. Three major dicarbonyls have been studied for their role in protein glycation in physiological systems: methylglyoxal, glyoxal and 3-deoxyglucosone (3-DG) – the structures of which are displayed in Figure 4.

Methylglyoxal (MG) is produced predominantly from degradation of the triose phosphate intermediates of the glycolytic pathway - glyceraldehyde-3-phosphate (GA3P) and dihydroxyacetone-phosphate (DHAP), as well as in smaller amounts from oxidation of acetone and aminoacetone in the catabolism of ketone bodies and threonine respectively and from the degradation of glycated proteins and monosaccharides (Phillips and Thornalley, 1993; Rabbani and Thornalley, 2012a; Turk, 2010). Although flux from triose phosphates is the major mechanism by which methylglyoxal is formed, formation of methylglyoxal is a minor or trace level fate of glucose metabolism – accounting for approximately 0.1% of the glucose flux. This low percentage flux increases in hyperglycaemia accounting for between 0.2% and 1% of glucose flux (Rabbani and Thornalley, 2011; Thornalley, 1988). Since the whole body rate of formation of methylglyoxal has been calculated as

approximately 3 mmol per day and the urinary excretion rate of methylglyoxal glycation adducts is approximately 10 µmol/day in healthy individuals, this indicates that only a small proportion (less than 1%) of the methylglyoxal produced physiologically acts to modify the proteome (Rabbani and Thornalley, 2012a). However, a 15-fold increase in urinary excretion of methylglyoxal-derived glycation adducts has been measured in people with diabetes with a mean A1C of 8%, when compared to levels in healthy individuals, indicating a marked increase in protein glycation by methylglyoxal in clinical diabetes (Ahmed, *et al.*, 2005a). Some methylglyoxal-derived glycation adducts are also absorbed from food (Ahmed, *et al.*, 2005b).

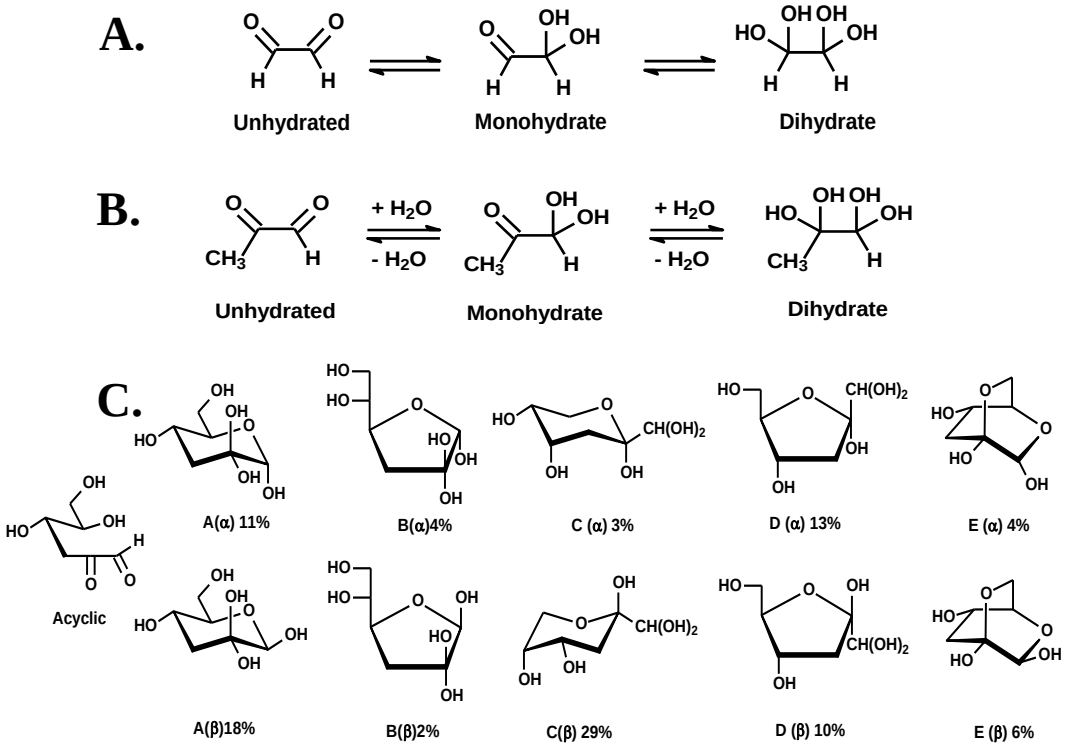

Figure 4: Structures of Glyoxal, MG and 3-DG in solution. A. Unhydrated and hydrate structures of glyoxal. B. Unhydrated and hydrate structures of MG. C. Acyclic unhydrated forms of 3-DG with related α- and β anomers. Adapted from Rabbani and Thornalley (2012c).

Glyoxal is formed under physiological conditions by the slow, non-enzymatic oxidative degradation of glucose and proteins glycated by glucose (Thornalley, *et al.*, 1999). It is also formed by the autoxidation of glycolaldehyde which is formed by oxidation of serine residues by hypochlorite in the phagocyte respiratory burst by myeloperoxidase (Rabbani and Thornalley, 2012c; Yang, *et al.*,

2011). Glyoxal is also formed by lipid peroxidation and degradation of nucleotides (Thornalley, 2005). 3-DG is formed by degradation of fructosamine-3-phosphate in the repair of early glycated proteins, degradation of fructose-3-phosphate and the slow non-enzymatic degradation of glucose and proteins glycated by glucose (Delpierre, *et al.*, 2000; Lal, *et al.*, 1997; Thornalley, *et al.*, 1999).

2.2.2. Levels of dicarbonyls in plasma of healthy people and patients with diabetes

As methods for measuring dicarbonyls in plasma have improved to control and eliminate analyte formation in pre-analytic processing, reported estimates have decreased. These lower estimates are probably closest to the true values. Plasma glyoxal is *ca*. 200 nM in healthy people and increases 2 - 3 fold in patients with diabetes. Plasma MG is 100 – 150 nM in healthy people and similarly increases 2 – 5 fold in patients with diabetes. Plasma 3-DG is 100 – 200 nM in healthy people and increases 2 – 3 fold in patients with diabetes (Agalou, *et al.*, 2002; Hamada, *et al.*, 1997).

2.2.3. Relative glycation reactivity

The relative reactivity towards protein glycation *in situ* of different saccharides and derivatives varies, due to both their different plasma concentrations and also their different reactivity towards protein. For example, the relative reactivity towards protein glycation *in situ* of methylglyoxal and glucose is similar and thus similar levels of glycation adducts are formed on proteins by glucose and methylglyoxal. This is despite the plasma concentration of methylglyoxal being approximately 50,000 times lower than that of glucose (*ca*. 100 nM as opposed to 5 mM (Beisswenger, *et al.*, 1999; Rabbani and Thornalley, 2012a)). This is explained by a much higher specific reactivity of methylglyoxal towards protein glycation than glucose: rate constants for glycation of proteins by methylglyoxal are 10,000 - 50,000 fold higher than for glycation by glucose (Rabbani and Thornalley, 2012a; Thornalley, 2005). The specific reactivity of glyoxal in glycation reactions is approximately 4-fold lower than methylglyoxal. This is perhaps surprising as the dialdehyde structure is more electronically deficient and chemically reactive than methylglyoxal but for this reason it is also more highly hydrated than methylglyoxal which decreases its reactivity for protein glycation. The specific reactivity of 3-DG

in glycation reactions is approximately 100-fold lower than methylglyoxal. This is due to the existence of 3-DG in many cyclic and hydrated forms which stabilise it towards glycation reactions (Thornalley, *et al.*, 1999).

2.2.4. Clinical implications of dicarbonyls

Dicarbonyls react with proteins to form AGE residues and also with guanyl bases of nucleotides to form nucleotide AGEs. Methylglyoxal is the precursor of the major protein and nucleotide AGEs quantitatively, methylglyoxal-derived hydroimidazolone Nδ-(5-hydro-5-methyl-4-imidazolon-2-yl)-ornithine (MG-H1) and imidazopurinone 3-(2'-deoxyribosyl)-6,7-dihydro-6,7-dihydroxy-6-methylimidazo[2,3-b]purin-9(8)one (MGdG), respectively. Formation of AGEs has been implicated in ageing and disease - including diabetes and its vascular complications, obesity, renal failure, CVD, neurological disorders such as Alzheimer's disease, Parkinson's disease and rare forms of schizophrenia, osteoarthritis, mutagenesis and multi-drug resistance in cancer chemotherapy (Brownlee, 2005; Kuhla, *et al.*, 2005; Lüth, *et al.*, 2005; Morcos, *et al.*, 2008; Rabbani, *et al.*, 2011; Sakamoto, *et al.*, 2001). MG modification of DNA increases DNA strand breaks and frameshift mutations (Murata-Kamiya, *et al.*, 2000b; Thornalley, *et al.*, 2010). Protein modification by MG is directed to functional sites where it is associated with metabolic, structural and functional abnormalities: for example, mitochondrial dysfunction with increased formation of ROS (Rosca, *et al.*, 2002), cell detachment from the ECM by decreased integrin binding to MG-modified ECM proteins and anoikis (Dobler, *et al.*, 2006; Pedchenko, *et al.*, 2005) and induction of accelerated cell senescence (Sejersen and Rattan, 2009).

2.3. Glycation by dicarbonyls

2.3.1. Formation of AGE residues on DNA

Dicarbonyls react with nucleic acids to form nucleotide AGEs (Brambilla, *et al.*, 1985; Murata-Kamiya and Kamiya, 2001; Thornalley, 2008). Deoxyguanosine (dG) is the most reactive nucleotide under physiological conditions. Glyoxal and methylglyoxal react with deoxyguanosine under physiological conditions to form mainly imidazopurinone derivatives, 3-(2'-deoxyribosyl)-6,7-dihydro-6,7-

dihydroxyimidazo[2,3-b]purin-9(8)one (dG-G) and MG-dG, respectively, – 6- and 7-methyl structural isomeric mixtures (Thornalley, 2008). Glyoxal and methylglyoxal also form N_2-carboxymethyl-deoxyguanosine (CMdG) and N^2-(1,*R/S*-carboxyethyl)-deoxyguanosine (CEdG) – the latter a stereoisomeric mixture of R/S-epimers at the N^2-1-carboxyethyl chiral centre (Li, *et al.*, 2006; Thornalley, *et al.*, 2010). The imidazopurinones are stabilised by incorporation into single and double stranded DNA. Accumulation of nucleotide AGEs is associated with an increase in both the frequency of mutagenesis and cytotoxicity. For glyoxal derived AGEs single-base substitutions primarily at C:G sites predominate, whereas for methylglyoxal multi-base deletions of 8 - 320 base pairs predominate (50%) followed by base pair substitutions (35%), tandem mutations (8%), single base additions and deletions (4%), and multi-base additions (2%) (Murata-Kamiya, *et al.*, 2000a; Thornalley, 2008). Studies have indicated that nucleotide excision repair suppresses and limits the effects of glycation damage (Murata-Kamiya, *et al.*, 1999; Murata-Kamiya, *et al.*, 1998).

2.3.2. Formation of AGE residues on proteins

Dicarbonyls are predominantly arginine directed glycating agents (Dobler, *et al.*, 2006; Queisser, *et al.*, 2010). Quantitatively the most important AGEs are the hydroimidazolones. The hydroimidazolone MG-H1 formed from the reaction of methylglyoxal with arginine residues in proteins (Figure 5) accounts for more than 90% of AGE adducts on proteins (Rabbani and Thornalley, 2012a). The reaction of arginine and lysine residues with pentose and glucose-derived dicarbonyls forms the protein crosslinks, pentosidine and glucosepane, respectively (Sell and Monnier, 2004). Ornithine residues in proteins are formed from decomposition of hydroimidazolone AGEs (Sell and Monnier, 2004). Examples and classification of glycation adducts are given in Figure 6.

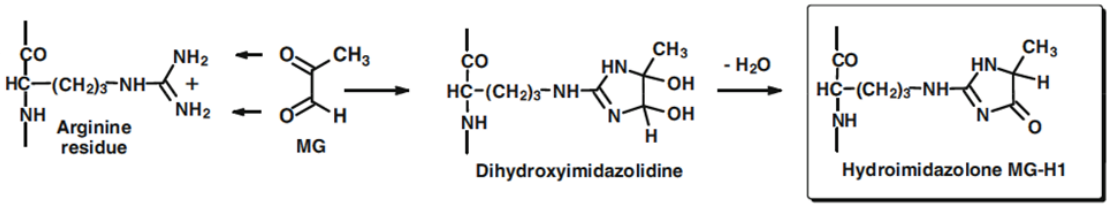

Figure 5: Formation of the major hydroimidazolone MG-H1. Glycation of arginine residues by methylglyoxal form the hydroimidazolone MG-H1 via the intermediate dihydroxyimidazolidine. Figure reproduced from Rabbani and Thornalley (2012a).

N_{ε}-Carboxymethyl-lysine (CML) is one of the most studied AGEs since being reported in the 1980s. CML is formed in physiological systems by the oxidative degradation of Nε-fructosyl-lysine (FL) (Ahmed, *et al.*, 1986; Smith and Thornalley, 1992). Other sources of CML are the oxidative degradation of L-tetrulose-lysine formed in the protein glycation by ascorbic acid and the reaction of lysine residues with glyoxal (Dunn, *et al.*, 1990). CML is also formed as a minor AGE in glycation of proteins by glucose, ribose and other saccharides by oxidative fragmentation with formation of glyoxal during the Maillard reaction. CML residues have been found in proteins of human cells in culture, cellular and ECM proteins of tissues and physiological fluids of laboratory rodents and human tissues and body fluids (Duran-Jimenez, *et al.*, 2009; Karachalias, *et al.*, 2010; Schleicher, *et al.*, 1997; Thornalley, *et al.*, 2003). CML is a chemically stable AGE and CML residue content of long-lived proteins such as lens protein and skin and cartilage collagen of human subjects increases with age (Dunn, *et al.*, 1989; Dyer, *et al.*, 1993). CML content of collagen of skin and cartilage is related to the rate of collagen turnover (Verzijl, *et al.*, 2000). CML content of protein increases in diabetes in association with an increase in the protein content of the precursor FL (Dyer, *et al.*, 1993; Karachalias, *et al.*, 2010). Proteolysis of CML modified proteins forms CML free adducts which are released into body fluids and excreted in urine. Dietary content of CML residues in proteins ingested in food contributes to urinary excretion of CML free adducts (Knecht, *et al.*, 1991; Liardon, *et al.*, 1987). Nε-Carboxymethyl-hydroxylysine is found in collagen formed from hydroxylysine (Dunn, *et al.*, 1991).

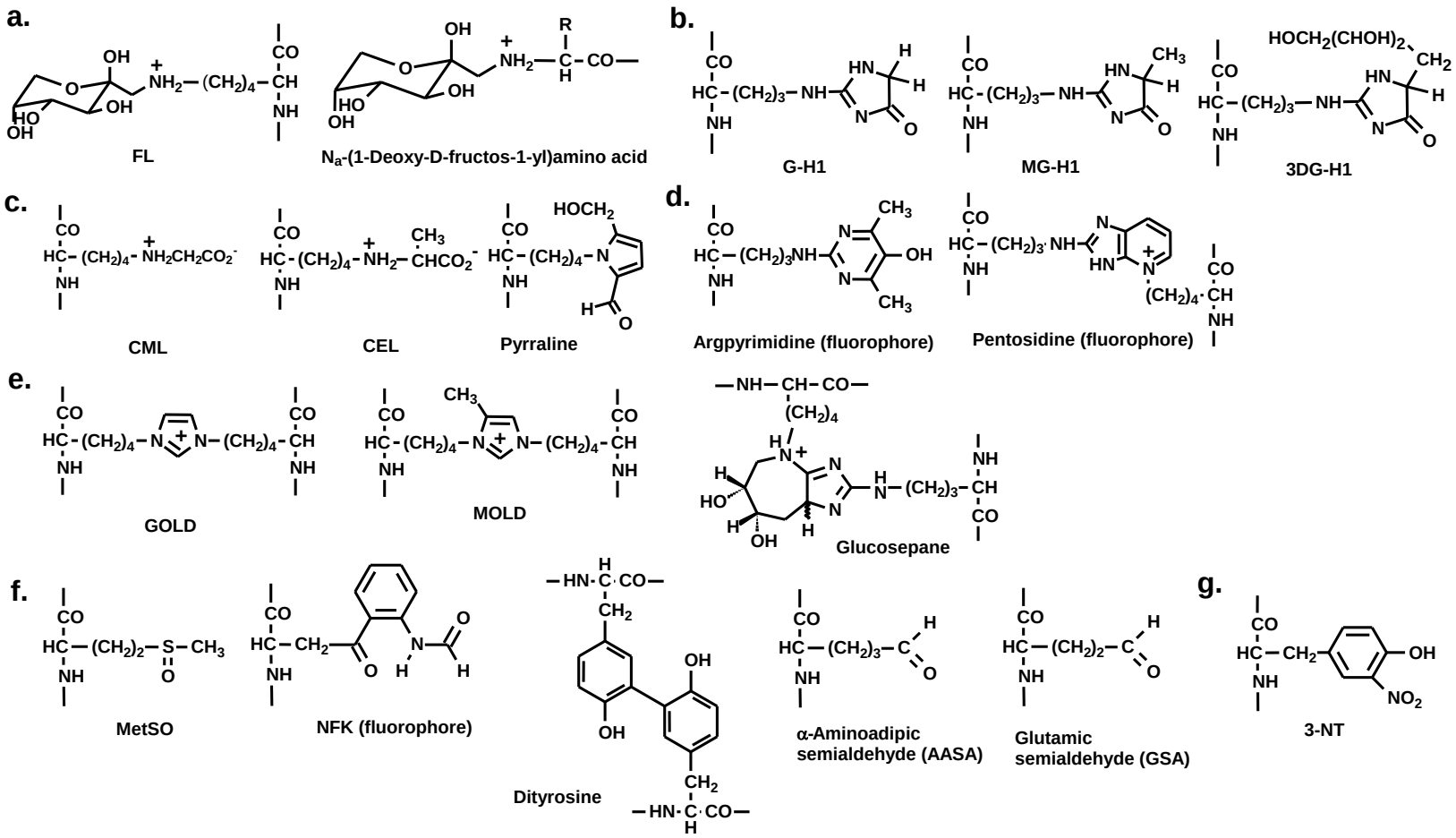

Figure 6: Protein glycation, oxidation and nitration adducts. a. Early glycation adducts. AGEs: b. Hydroimidazolones, c. Monolysyl, d. Fluorophores and e. Non-fluorescent crosslinks. f. Oxidation adducts. g. Nitration adduct. Reproduced from Thornalley and Rabbani (2013).

Formation of MG-H1 residues results in a loss of the positive charge associated with the amino acid side chain. This can lead to a loss of hydrogen bonding within parts of the protein and consequently rotation and separation of functional motifs, protein misfolding and changes in the tertiary structure of the protein (Dobler, *et al.*, 2006; Xue, *et al.*, 2011). Therefore, protein glycation can lead to a loss of protein function, and consequently lower levels of the functional protein, or alternatively it can lead to alterations in the functional activity of the modified protein. Since under 5% of a protein is typically glycated the decline in the amount of functional protein is unlikely to have severe functional effects (Rabbani and Thornalley, 2012a). However, glycation is thought to target proteins for proteolysis and decrease protein half-life. Without compensatory increases in protein expression, this may decrease the concentration of functionally active proteins significantly. It is, perhaps, more likely that damaging effects occur when the modified protein has an altered physiology and functions differently (as is the case with the modification of collagen IV by methylglyoxal) as opposed to a loss of function (Dobler, *et al.*, 2006).

The modification of proteins by methylglyoxal forming MG-H1 residues is particularly damaging because it is usually focussed on functionally important arginine residues within the active site of the protein. These arginine residues are often easily accessible for modification and have highly polarisable electronic charge (Rabbani and Thornalley, 2012a). Between 0.1% and 3% of arginine residues on cellular proteins are known to be modified by methylglyoxal, and these modifications typically increase 2 - 5 fold in diabetes (Rabbani and Thornalley, 2011; Thornalley, *et al.*, 2003). Arginine residues are frequently found in active sites of proteins – analysis of Swissprot database sequences and Protein Data Bank information has indicated that it is the most abundant amino acid residue within protein receptor binding domains, the most frequent residue within protein nucleotide binding sites and the third most frequent residue in enzyme active sites, behind histidine and aspartic acid (Bartlett, *et al.*, 2002; Chetyrkin, *et al.*, 2011; Gallet, *et al.*, 2000; Lejeune, *et al.*, 2005). Analysis of residues involved in catalysis at 178 enzyme active sites indicated that 11% of residues were arginine, despite it only representing 4.9% of the total residues; this again highlights the accessibility of arginine to glycation and that this could have severe functional consequences (Bartlett, *et al.*, 2002).

2.3.3. Repair of glycated proteins

The major early stage glycation adduct of glucose, FL, can be de-glycated. Thus glycated proteins can be repaired in a pathway catalysed by fructosamine 3-phosphokinase (Delpierre, *et al.*, 2000; Pascal, *et al.*, 2010). However, there is no known de-glycation mechanism for hydroimidazolone-modified proteins – but there is slow dynamic reversibility of MG-H1 with a half-life of approximately 12 days (Rabbani and Thornalley, 2012a). Proteins containing hydroimidazolone adducts have distorted and damaged structures and may therefore be targeted to the proteosome for proteolysis (Dobler, *et al.*, 2006; Grune, *et al.*, 1996; Hernebring, *et al.*, 2006). MG-H1 adduct residues are therefore released from proteins by cellular proteolysis. MG-H1 free adducts are then cleared from cells and tissues and consequently MG-H1 free adducts are detectable in plasma and urine in both rodents and humans (Karachalias, *et al.*, 2010; Thornalley, *et al.*, 2003).

2.3.4. Measurement of AGEs in physiological systems

Quantification of glycation adducts has proved problematic with commonly used methods, namely immunoassay and fluorescence, having major limitations, as reviewed by Ahmed and Thornalley (2007). Immunoassays have been widely used to detect AGEs (Chow, *et al.*, 2013; Jung, *et al.*, 2011; Sugimoto, *et al.*, 1997; Yamaguchi, *et al.*, 1998). Limitations include a lack of antibody specificity – an antibody for CML has been shown to cross-react with CEL, high concentrations of AGEs in solutions used to block non-specific binding and interference caused by glycation free adducts (Ahmed and Thornalley, 2007). Similarly, as discussed by Ahmed and Thornalley (2007), the use of total AGE fluorescence methods, as performed by Tajiri *et al.* (1997), has been questioned. There are multiple fluorophores present in physiological samples contributing to total fluorescence and so quantitation is not possible, the major quantitative AGEs - hydroimidazolones - are not fluorescent and there are interferences from oxidative adducts such as N-formylkynurenine (NFK). Fluorescent adducts must be separated using HPLC or other techniques.

Mass spectrometric detection and quantification of the different AGEs using stable isotopic substituted standards is the more reliable method by which to quantify both glycation adducts on proteins and free adducts (Lieuw-A-Fa, *et al.*, 2004; Niwa, 2006; Thornalley, *et al.*, 2003). This method has been developed to measure

glycation, oxidation and nitration adducts concurrently. Oxidative adducts include: methionine sulphoxide (MetSO) – formed by oxidation of methionine; NFK – formed by oxidation of tryptophan; dityrosine – formed by oxidation of tyrosine; α-aminoadipic semialdehyde (AASA) - formed by oxidative deamination of lysine; and glutamic semialdehyde (GSA) - formed by oxidation of proline and arginine residues.

2.4. Defence against dicarbonyls

The damaging effects of protein glycation by dicarbonyls on physiological systems are limited by the enzymatic defences which catalyse the metabolism of dicarbonyls. The glyoxalase system in combination with other more minor defence systems, such as aldose reductase, is responsible for metabolising over 99% of dicarbonyls to less damaging metabolites (Rabbani and Thornalley, 2012a). Dicarbonyl damage to the genome and proteome is caused by less than one per cent of the methylglyoxal produced in the body; that such a small proportion of methylglyoxal can cause this damage indicates the importance of these enzymatic defences in lowering the levels of both dicarbonyls and the consequential AGEs.

2.4.1. The glyoxalase system

The glyoxalase system is estimated to account for over 97% of methylglyoxal metabolism in most human tissues (Rabbani and Thornalley, 2011). It is a fundamental protective system found ubiquitously throughout biological life.

2.4.1.1. Historical perspectives

Since the discovery of glyoxalase activity a century ago it has been known that the glyoxalase system catalyses the conversion of methylglyoxal to lactate (Dakin and Dudley, 1913). However, this was originally thought to be L-lactate and act as a major metabolic process converting glucose to L-lactate, as discussed by Thornalley (1990). The widespread distribution of glyoxalase in all studied organisms indicated that this enzymatic system performs an important cellular function (Hopkins and Morgan, 1945). Racker identified that metabolism of methylglyoxal to lactate by the glyoxalase system occurred in a two-step process via

the intermediate S-D-lactoylglutathione (Racker, 1951). In 1977 it was discovered that methylglyoxal and related aldehydes react with arginine residues, although the physiological significance of this was not understood (Takahashi, 1977). A number of studies in the 1980s and 1990s began to implicate the glyoxalase system and dicarbonyl metabolism in diabetes. An increase in dicarbonyl formation was shown in both hyperglycaemia and in patients with diabetes as well as overexpression of glyoxalase 1 (Glo1) preventing the increase in AGE formation in hyperglycaemia (Thornalley, 1988; Thornalley, *et al.*, 1989). Methylglyoxal was shown to be a protein glycating agent and MG-H1 a significant type of proteome damage and a significant AGE occurring in diabetes (Ahmed, *et al.*, 2005a; Lo, *et al.*, 1994; Thornalley, *et al.*, 2003). Overexpression of Glo1 in endothelial cells has been shown to prevent the increases in MG and associated AGEs observed in hyperglycaemia and to correct the cell dysfunction observed in diabetes (Shinohara, *et al.*, 1998). Recent studies have continued to show the impact of metabolism by the glyoxalase system and alterations therein in diabetes – for example methylglyoxal has been shown to be decreased by the glucose lowering drug metformin, and MG-H1 modification of both collagen IV and LDL has been shown to have functional impairments significant in states of diabetes (Beisswenger, *et al.*, 1999; Dobler, *et al.*, 2006; Rabbani, *et al.*, 2011). Knockdown of Glo1 in mice, leading to a 45 - 65% decrease in the tissue Glo1 activity, resulted in an increase in proteasomal modification and impaired proteasomal activity (Queisser, *et al.*, 2010). In addition, treatment of rodents with a cell permeable fusion protein construct of Glo1 has been shown to prevent the beta cell ablation induced by Streptozotocin treatment, indicative of its protective capacity (Kim, *et al.*, 2013).

2.4.1.2. Glyoxalase pathway

The glyoxalase system consists of two cytosolic enzymes – Glo1 and glyoxalase 2 (Glo2) - which catalyse the conversion of methylglyoxal to D-lactate via the intermediate S-D-lactoylglutathione. It thereby achieves metabolism of methylglyoxal, a detoxification function. GSH binds non-enzymatically to methylglyoxal forming the methylglyoxal-glutathione hemithioacetal, and Glo1 then subsequently catalyses the isomerisation of the hemithioacetal to S-D-lactoylglutathione (Thornalley, 2003a). Glo2 is a thiolesterase which hydrolyses S-

D-lactoylglutathione to D-lactate, reforming GSH (Rabbani and Thornalley, 2012a; Thornalley, 1994). These sequential enzymatic reactions are illustrated in Figure 7.

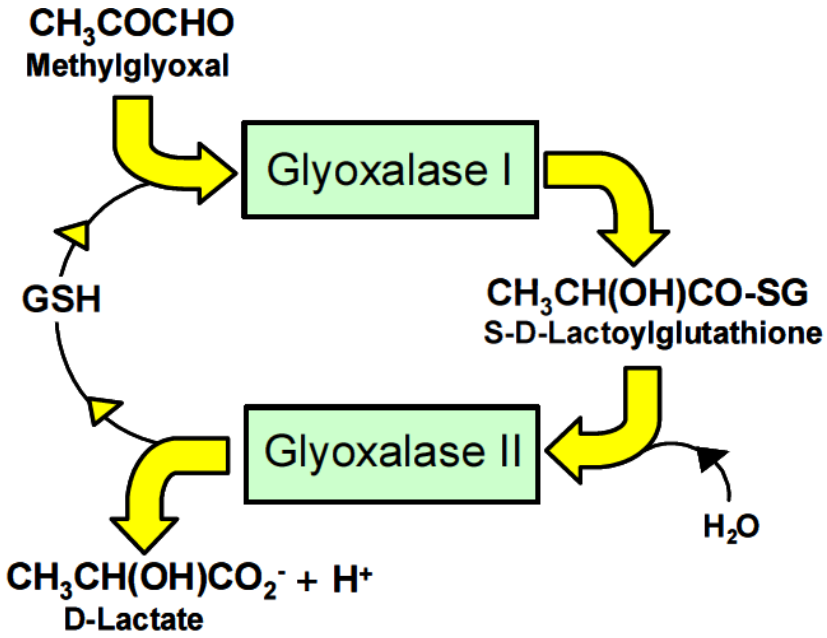

Figure 7: The glyoxalase system. Adapted from Xue, *et al.* (2011).

Glyoxalase 1

Human glyoxalase 1 is a dimeric Zn^{2+}-metalloenzyme, with one zinc ion per subunit, of molecular mass 42 kDa (Thornalley, 2003a). The translation product of the gene consists of 184 amino acids, of which the amino acid residues tryptophan, lysine, tyrosine, histidine and glutamic acid lie within the active site situated at the dimer interface (Thornalley, 1993; Thornalley, 2003a). Expression of Glo1 as a dimer has been reported in humans, other mammalian species, bacteria and plants (Xue, *et al.*, 2011). In yeast, however, Glo1 is a monomer, of size 32 and 37 kDa in *Saccharomyces cerevisae* and *Schizosaccharomyces pombe*, respectively (Xue, *et al.*, 2011).

The human gene, GLO1, has three phenotypes – GLO 1-1, GLO 1-2 and GLO 2-2, representing the homozygous and heterozygous expression of the diallelic gene (Xue, *et al.*, 2011). GLO^2 is the ancestral gene and GLO^1 is thought to have arisen through mutation (Xue, *et al.*, 2011). The two alleles differ only in the amino acid at position 111 – an alanine in one allele and glutamic acid in the alternative allele (Kim, *et al.*, 1995). The diallelic gene is located on chromosome 6 in humans

and on chromosome 17 in mice, the locus of both are closely linked to the major histocompatability complex indicating conservation of linkage groups throughout evolution (Bender and Grzeschik, 1976; Minna, *et al.*, 1978).

Glyoxalase 2

Glyoxalase 2 is a monomeric thiolesterase found in the cytosol of all eukaryotic and prokaryotic organisms (Thornalley, 1993). It molecular mass is *ca.* 29.5 and 29.0 kDa in mouse and human, respectively, estimated by SDS polyacrylamide gel electrophoresis (Oray and Norton, 1980; Thornalley, 1993). Glo2 contains a Fe(II)Zn(II) centre, with substrate hydrolysis linked to the Zn(II) site (Limphong, *et al.*, 2009). It is a basic protein which is competitively inhibited by the hemithioacetal substrate of Glo1 (Oray and Norton, 1980). Arginine, histidine and lysine residues are present in the Glo2 active site, with histidine important to the enzyme catalysed mechanism (Thornalley, 1990).

The gene for human glyoxalase 2 is hydroxyacylglutathione hydrolase, HAGH, or GLO2. It is located on human chromosome 16 and on chromosome 17 in mice (Tan and Whitney, 1993). There are no common polymorphisms for GLO2 (Thornalley, 1993). A rare polymorphism for GLO2 has been found in Micronesian and Japanese populations (Sugita and Takahama, 1983; Tan and Whitney, 1993; Thornalley, 1993).

S-D-Lactoylglutathione

S-D-Lactoylglutathione is formed from the catalytic action of Glo1 and is hydrolysed by Glo2 to form D-lactate. Addition of S-D-lactoylglutathione to cultures of HL60 cells caused growth arrest and toxicity (Thornalley and Tisdale, 1988). Its formation has been shown to be elevated in hyperglycaemia and clinical complications of diabetes correlated with maintenance of higher cellular levels of S-D-lactoylglutathione (Thornalley, *et al.*, 1989). The concentration of S-D-lactoylglutathione in human blood is *ca*. 41 nmol per mL red blood cells, increasing to *ca*. 54 nmol per mL red blood cells in diabetic patients (Thornalley, 1993). It has poor membrane permeability and therefore it is expected that it is produced and hydrolysed within the cytosol (Rae, *et al.*, 1991).

D-Lactate

D-Lactate is produced by the thiolesterase Glo2. In physiological systems it is metabolised to pyruvate by the enzyme 2-hydroxyacid dehydrogenase (Thornalley, 1993). However, it is not metabolised by red blood cells (Thornalley, 1988). Activity of this enzyme is lacking in some immortalised cell lines, and therefore D-lactate accumulates. The concentration of D-lactate is *ca*. 10 and 20 nmol per g blood in healthy controls and diabetic patients, respectively (Thornalley, 1993). Increases in plasma D-lactate concentration are also observed after a meal and after exercise (Kondoh, *et al.*, 1992; Ohmori and Iwamoto, 1988). D-Lactate is membrane permeable, crossing membranes via a specific lactate transporter, the inorganic anion exchanger and by diffusion. Approximately half the D-lactate membrane transport in human red blood cells is via the lactate transporter (Thornalley, 1993).

2.4.1.3. The glyoxalase system in diabetes

Since the *in situ* activity of Glo1 is proportional to the cellular concentration of GSH, GSH has a vital role in the glyoxalase system and cellular metabolism of methylglyoxal (and other α-oxoaldehydes) (Thornalley, 2003a). Tissue concentrations of GSH decrease with age and recently chronic methylglyoxal infusion into Sprague-Dawley rats was shown to decrease the GSH levels within the pancreas (Dhar, *et al.*, 2011; Meister, 1983). In addition, GSH is depleted in states of oxidative stress (Abordo, *et al.*, 1999). This indicates that the *in situ* activity of Glo1 may become limited by GSH availability in the pancreas, particularly so with ageing or in pathogenic states. This could intensify the problem with a decrease in cellular defences against glycation occurring in combination with an increase in glycative agents. However, it has been reported that only minor decreases in GSH occur in most tissues and plasma of streptozotocin induced diabetic rats and no changes occur in GSH concentration of red blood cells in clinical diabetes. Consequently, it is suggested that GSH and glutathionylation do not alter the *in situ* activity of Glo1 in diabetes (Rabbani and Thornalley, 2011).

Glyoxal and MG concentrations may be increased in diabetes as a consequence of impaired activity of Glo1. Renal and vascular cell activity of Glo1 may be decreased in diabetes by decreased concentration of GSH in oxidative stress, glutathionylation of Glo1 and decreased expression of Glo1 (Birkenmeier, *et al.*,

2010). Glo1 expression may be decreased by activation of the receptor for AGEs and by down regulation of signalling by transcription factor nuclear erythroid factor E2 related factor-2 (Nrf2) (Bierhaus, *et al.*, 2005; Xue, *et al.*, 2012). Signalling by Nrf2 is impaired in diabetes which may lead to decreased metabolism and increased glyoxal and MG (Tan, *et al.*, 2011).

Studies of patients with T1DM and T2DM have indicated that methylglyoxal, S-D-lactoylglutathione and D-lactate were all elevated in blood, compared to healthy controls. The activity of Glo1 was also shown to increase in red blood cells in diabetic patients, likely as a response to sensing a higher methylglyoxal concentration – exposure to dicarbonyl stress (Rabbani and Thornalley, 2011).

2.4.1.4. Chemical Inhibitors of the glyoxalase system

Chemical inhibitors of Glo1 and Glo2 have been used experimentally to examine the effects of endogenous increases in dicarbonyls. Some of the earlier studies demonstrated that S-conjugates of glutathione could be used as inhibitors of Glo1 and linked these inhibitors to potential uses as anticancer drugs (Vince and Daluge, 1971; Vince, *et al.*, 1971). Similarly, inhibitors of Glo2 were developed, but as discussed by Lo and Thornalley (1992) these still had some inhibitory activity towards Glo1 (Bush and Norton, 1985). These early studies did not appreciate that conjugates had to be diesterified to be delivered into cells and to be stable to decomposition by γ-glutamyl transferase (Lo and Thornalley, 1992). The effects of different S-conjugates of glutathione on growth and viability of cells were investigated (Lo and Thornalley, 1992). This indicated that GSH conjugate inhibitors did not enter cells. Diester derivatives were shown to be resistant to cleavage by the enzyme γ-glutamyl transferase and also permeable to cells. Inside cells, ester groups were cleaved by non-specific esterases forming the active inhibitor (Thornalley, 2003a). Consequently, the compound S-p-bromobenzyl-glutathione cyclopentyl diester ($BrBzGSHCp_2$) was shown to be a cell permeable inhibitor of Glo1, suitable for use in cell based experiments and also suggested to be of use in inhibiting tumour growth and inducing apoptosis (Thornalley, *et al.*, 1996).

2.4.2. Metabolism of dicarbonyls by aldoketo reductases and aldehyde dehydrogenase

When the glyoxalase system is impaired, aldoketo reductase (AKR) isozymes 1B1, 1B3 and 1B8 may metabolise glyoxal to glycolaldehyde and AKR isozymes 1A4, 1B1 and 1B3 may metabolise MG to mainly hydroxyacetone (Baba, *et al.*, 2009). Aldose reductase (AKR 1B1) was claimed to have an important role in MG metabolism by Baba *et al*. (2009). However, since the Glo1 activity measurement was made incorrectly - without preformation of the hemithioacetal substrate, making non-enzymatic formation of hemithioacetal rate-limiting in this study - it is likely that the Glo1 activity was underestimated, as discussed by Rabbani and Thornalley (2011). Metabolism by AKR 1B1 may be a major fate of glyoxal and MG in the renal medulla where high expression of AKR 1B1 outcompetes Glo1 (Larsen, *et al.*, 1985; Nishimura, *et al.*, 1993). AKRs 1A4, 1B1, 1B3 and 1B8 are antioxidant-response element-linked genes with expression regulated by the transcription factor Nrf2 (Kwak, *et al.*, 2003; MacLeod, *et al.*, 2009; Nishinaka and Yabe-Nishimura, 2005; Thimmulappa, *et al.*, 2002). 3-DG is metabolised to 3-deoxyfructose by AKRs 1A4, 1B1 and 1B3 (3-DG reductase activity) and to 3-deoxy-2-ketogluconate by aldehyde dehydrogenase 1A1 (3-DG dehydrogenase activity) (Baba, *et al.*, 2009; Collard, *et al.*, 2007). All genes encoding these enzymes have expression regulated by Nrf2 and hence may be down-regulated in diabetes leading to an increased 3-DG concentration (Kwak, *et al.*, 2003; MacLeod, *et al.*, 2009; Nishinaka and Yabe-Nishimura, 2005; Reisman, *et al.*, 2009).

Aldose reductase, in conjunction with sorbitol dehydrogenase, mediates the conversion of glucose to fructose – the polyol pathway (Lindstad and McKinley-McKee, 1993). Methylglyoxal is however a better substrate than glucose for human aldose reductase (aldoketo reductase isoform 1B1), as is indicated by the much lower K_M value – 8 μM compared to 70 mM (Lindstad and McKinley-McKee, 1993; Vander Jagt, *et al.*, 1992). Aldose reductase catalyses the NADPH-dependent reduction of methylglyoxal to produce hydroxyacetone (95%) and D-lactaldehyde (5%) (Thornalley, 1994). Both hydroxyacetone and L-1,2-propanediol, formed from further reduction of hydroxyacetone, are known to accumulate in states of uncontrolled diabetes (Vander Jagt, *et al.*, 1992). It is reported that these increases are due to increases in ketone body metabolism when insulin is lacking and fat is therefore used as an energy source, consistent with the ketoacidosis observed in

undiagnosed or uncontrolled diabetes (Wolfsdorf, *et al.*, 2009). An increase in the metabolism of methylglyoxal by aldose reductase could also lead to such increases. However, since aldose reductase also metabolises flux through the polyol pathway it can act to increase triose phosphate formation and thereby increase methylglyoxal formation. Indeed, the use of the aldose reductase inhibitor, Statil, has been shown to prevent some of the increases in methylglyoxal observed in diabetic rats (Phillips, *et al.*, 1993).

Methylglyoxal may also be metabolised in some mammalian tissues by aldehyde dehydrogenase. Activity of methylglyoxal dehydrogenase has been detected in the liver of sheep; it catalyses the conversion of methylglyoxal to pyruvate in a NAD^+ dependent process (Monder, 1967).

3. Project Specific Background

3.1. Implications of glycation in beta cells and diabetes

Increased protein glycation and formation of AGEs has been linked to dysfunction in T1DM and T2DM. Both concentrations of dicarbonyls in the plasma and their flux through the glyoxalase system increase in hyperglycaemia and in diabetes (Beisswenger, *et al.*, 1999; McLellan, *et al.*, 1994). Plasma concentrations of methylglyoxal and 3-DG increase in postprandial hyperglycaemia, indicating that dicarbonyl concentrations are responsive to short term hyperglycaemia *in vivo* (Beisswenger, *et al.*, 2001; Masterjohn, *et al.*, 2012). In contrast, glycation by glucose with formation of A1C and other proteins modified by fructosamine residues is relatively unresponsive to short term hyperglycaemia.

The glyoxalase system is known to be modified in diabetes, although it is not known whether these changes are implicated in causing or are a consequence of the dysfunctional state. Development of insulin resistance, impaired fasting glucose and IGT leading to T2DM likely lead to increased methylglyoxal formation which, without compensatory increased expression and activity of Glo1, will lead to increased formation of MG-derived AGEs. Moreover, insulin resistance and the metabolic syndrome are associated with increased expression of the inflammatory mediators S100 proteins (Yamaoka, *et al.*, 2013). S100 proteins are likely important activators of RAGE *in vivo* which may down-regulate expression of Glo1 (Thornalley, 2007).

Modifications of dicarbonyl metabolism in pre-diabetes and diabetes therefore likely include: increased flux of formation of methylglyoxal - proportional increase due to down-regulation of glyceraldehyde-3-phosphate dehydrogenase and increased concentrations of intermediates GA3P and DHAP; and decreased *in situ* activity of the glyoxalase system due to decreased GSH and/or down-regulation of Glo1 expression via inflammatory signalling (Rabbani and Thornalley, 2011).

An increase in protein damage by reactive dicarbonyls is associated with diabetes. Protein glycated by methylglyoxal has been reported to increase 2 - 5 fold in people with diabetes (Ahmed, *et al.*, 2005a; Hegab, *et al.*, 2012; Karachalias, *et al.*, 2010; Nicolay, *et al.*, 2006; Rabbani and Thornalley, 2011). Accumulation of AGE residues on both extracellular and intracellular proteins is a risk factor for

diabetic complications such as diabetic neuropathy and nephropathy (Duran-Jimenez, *et al.*, 2009; Matafome, *et al.*, 2013; Perkins, *et al.*, 2012; Thornalley, *et al.*, 2003). Whilst this 2 - 5 fold increase is damaging, it still represents a low extent of modification, typically 0.1 - 1% of arginine and lysine residues (Thornalley, 2008). It is therefore crucial to interpret the physiological relevance of literature showing the importance of protein glycation with caution and in context. Many articles such as Fiory *et al*. (2011) and Riboulet-Chavey *et al*. (2006) use methylglyoxal concentrations which far exceed physiological levels to show an effect, or use highly glycated proteins which would not occur physiologically. The study by Fiory *et al*. (2011) used aminoguanidine as a dicarbonyl scavenger; it reacts rapidly with dicarbonyls and thereby inhibits the actions of methylglyoxal. However, it is highly reactive and at higher concentrations will react with other physiological metabolites such as glucose and pyruvate - caution should therefore be taken in its use, and an appropriate concentration used so that it acts as a selective scavenger of dicarbonyls (Thornalley, 2003b). The 4 mM aminoguanidine used in this study was of too high a concentration to act as a selective scavenger. The reported impairments in GSIS as a result of methylglyoxal treatment cannot be reliably concluded from experiments using a scavenger at levels sufficient to scavenge other essential metabolites.

It has been known for a number of years that insulin can be glycated by glucose (Dolhofer and Wieland, 1979; Lapolla, *et al.*, 1988). These earlier studies used highly glycated insulin formed by incubation with 222 mM glucose, and whilst this glycated insulin had decreased biological activity, its physiological relevance was not known. More recently, studies have again indicated that insulin can be glycated by glucose or glucose metabolites, both *in vitro* and *in vivo*, and that this may have physiological effects (Abdel-Wahab, *et al.*, 1997; Abdel-Wahab, *et al.*, 1996; O'Harte, *et al.*, 1996). Abdel-Wahab *et al*. (1996) observed glycated insulin within pancreatic islets of both insulin-deficient and insulin-resistant rodent models of diabetes. It was suggested that G6P was the glycating agent and not glucose, since G6P is more reactive and of an elevated concentration in the ER. In addition, both proinsulin and insulin were glycated, as would be expected if this glycation occurred in the ER of beta cells (Abdel-Wahab, *et al.*, 1996). However, the specific sites of glycation and the glycating agent were not identified in this *in vivo* study. More recently the extent of glycated insulin in the pancreas and circulating plasma of ob/ob mice was shown to be decreased by vitamin C supplementation, resulting in

improvements in insulin sensitivity and glycaemic control (Abdel-Wahab, *et al.*, 2002). It was identified by O'Harte *et al.* (1996) that glycation of insulin by glucose occurs *in vitro* on the phenylalanine residue at the amino terminus of the beta chain, however it is not known if this glycation occurs physiologically. This *in vitro* glycated insulin was shown to have impaired biological activity compared to non-glycated insulin when injected by intraperitoneal injection into mice (Abdel-Wahab, *et al.*, 1997). Insulin has also been shown to be glycated on arginine-22 of the beta chain by methylglyoxal *in vitro* (Jia, *et al.*, 2006). This resulted in decreased insulin-mediated glucose uptake as well as impaired insulin secretion. However, this is unlikely to be of physiological relevance, since the half-life of insulin in plasma is approximately 4 - 6 min. Glycation of insulin by methylglyoxal is unlikely to lead to the functional impairments observed in clinical diabetes (Rabbani and Thornalley, 2011; Sherwin, *et al.*, 1974). Indeed, it was suggested that due to the short half-life of insulin, any glycation which occurs will predominantly occur during synthesis and storage of insulin within beta cells and not post secretion (Abdel-Wahab, *et al.*, 1996). However, glycation may lead to some functional impairment in synthetic long-acting insulin derivatives.

Supraphysiological concentrations of methylglyoxal (0.5 mM and 1 mM) have long been shown to have effects on pancreatic beta cells, as discussed by Rabbani and Thornalley (2011). It was shown using patch-clamping techniques that methylglyoxal caused depolarisation of isolated rat pancreatic beta cells and that in intact islets methylglyoxal increased the intracellular calcium concentration (Cook, *et al.*, 1998). This was associated with a transient stimulation of insulin secretion, followed by inhibition of GSIS. It was then reported that the depolarisation was due to activation of a volume-sensitive anion channel due to cell swelling following exposure to methylglyoxal and the formation of D-lactate (Best, *et al.*, 1999). As discussed by Cook *et al.* (1998) the concentration of methylglyoxal used in these studies far exceeds physiological or patho-physiological levels to which beta cells may be exposed, and consequently methylglyoxal is unlikely to induce depolarisation of beta cells. However, this work was indicative of the potential role of methylglyoxal in the physiology of beta cells and their dysfunction in diabetes.

Studies infusing high levels of methylglyoxal into rats indicate the significance of methylglyoxal and protein glycation in diabetes (Berlanga, *et al.*, 2005; Dhar, *et al.*, 2011). The study by Berlanga *et al.* (2005) exposed Wistar rats to

a progressively increasing continuous infusion of methylglyoxal (from 50 - 75 mg/kg of body weight/day) for a period of 7 weeks. They demonstrated the development of diabetes-like vascular damage and impaired wound healing following chronic exposure – even with the maintenance of normal glycaemic control. A more recent study (Dhar, *et al.*, 2011) continuously infused 60 mg/kg body weight/day methylglyoxal into Sprague-Dawley rats for 28 days. They showed functional effects of dicarbonyls on pancreatic beta cells *in vivo*, such as decreased insulin secretion, decreased GSH and increased apoptosis as well as increased plasma glucose. The increased plasma glucose differs to the maintenance of normal glycaemic control in the earlier study (Berlanga, *et al.*, 2005). It was suggested by Dhar *et al*. (2011) that their observed effects may be tissue specific, with effects observed in the pancreatic, skeletal and adipose tissue. However, they make no mention of which other tissues were studied wherein effects were not seen. Although these studies infused high levels of methylglyoxal, the use of continuous infusion makes them of more physiological relevance than other studies (such as Jung, *et al.*, 2011; Zhao, *et al.*, 2009) which spiked high bolus doses of dicarbonyls or AGEs into plasma, leading to a sudden increase in the plasma levels, which would not occur physiologically.

Recently, a study using a cell permeable fusion protein construct of Glo1, Tat-Glo1, showed that Glo1 protected against chemical induction of toxicity to insulinoma cells *in vitro* and diabetes *in vivo*. The expression vector contained consecutive cDNA sequences for human Glo1, Tat peptide and six histidine residues at the amino-terminus. Purified Tat-Glo1 protein protected RINm5F cells against sodium nitroprusside induced cell death and DNA fragmentation. It also protected against induction of diabetes by streptozotocin (STZ) in mice (Kim, et al., 2013). It was shown that injection of Tat-Glo1 into mice was equally effective in partially suppressing the development of diabetes when given 12 h before or 1 day after STZ injection. This was associated with increased serum insulin and decreased free fatty acids in Tat-Glo1 treated animals compared to STZ-treated animals. Although the mechanism is yet to be elucidated, the study indicates the potential role of Glo1 and dicarbonyls in pancreatic beta cell destruction by STZ and potentially other types of beta cell toxicity. However, a limitation of this study is that neither the amount of Glo1 protein reaching the beta cells nor the activity of this protein was determined. It is therefore unknown how the amount of protein providing protection to beta cells

in this study compares to physiological levels observed in beta cells. The protective nature of Tat-Glo1 reported by Kim *et al*. (2013) is in agreement with other recent publications which suggest a decrease in AGEs and oxidative stress in diabetic rats following overexpression of Glo1 (Brouwers, *et al.*, 2011). Brouwers *et al*. (2011) indicated that a 10 - 50 fold overexpression of Glo1 decreased the elevations of both dicarbonyls and AGEs observed in diabetes and this has been shown to protect against retinopathy (Berner, *et al.*, 2012). These studies further highlight the protective nature of the glyoxalase system and the importance of maintaining metabolic control – limiting the effects of damaging reactive metabolites such as the dicarbonyls.

3.2. Collagen and ECM proteins

3.2.1. Beta cell mass and ECM proteins

Decreases in beta cell mass have been repeatedly associated with the development of diabetes. Loss of beta cells by apoptosis is implicated in beta cell dysfunction and the pathogenesis of T2DM (Chang-Chen, *et al.*, 2008; Meier, *et al.*, 2012; Szoke, *et al.*, 2008; Taylor, 2006). The mechanism of apoptosis activation is not known, although potential causes have been postulated (detailed in Figure 2 and Table 3). Interaction of beta cells with ECM proteins of the basement membrane have been shown to be important in maintaining beta cell mass as well as in regulation of insulin secretion. Loss of these interactions was associated with detachment-stimulated cell death – a phenomenon termed 'anoikis' (Frisch and Francis, 1994). The loss of functional ECM interactions when islets are removed from the pancreas results in integrin-mediated anoikis unless islets are cultured on ECM proteins, such as collagen IV and laminin. This indicates the clinical significance of studies into beta cell-ECM interactions (Pinkse, *et al.*, 2006).

3.2.2. Collagen IV

Collagen IV was first discovered and isolated by Kefalides (1966). It is a trimeric protein present exclusively in the basement membrane of all tissues (Khoshnoodi, *et al.*, 2008; Kühn, 1994). Collagen IV is commonly composed of two α1 subunits and one α2 subunit; subunit structure $(\alpha1)_2(\alpha2)_1$, (Khoshnoodi, *et al.*,

2008). Whilst two other distinct collagen IV heterotrimers are known to exist, α3α4α5 and $(\alpha5)_2(\alpha6)_1$, these have specific spatial and temporal regulation and occur in specific tissues – such as the kidney, eye and skin - during development (Khoshnoodi, *et al.*, 2008).

The two genes for the α1 and α2 subunits are a bidirectional gene pair located on chromosome 13 in humans. The other four α subunits form two other bidirectional gene pairs on chromosome 2 (α3 and α4) and X (α5 and α6). These bidirectional gene pairs are arranged head-to-head and transcribed from opposite DNA strands. They share a short promoter region which separates the transcriptional start sites by 127 base pairs (Khoshnoodi, *et al.*, 2008; Pöschl, *et al.*, 1988). This shared promoter region with symmetrical arrangement of sequence elements and shared enhancers enables co-ordinated control of transcription of the two subunits of the heterotrimeric collagen IV (Burbelo, *et al.*, 1988; Pöschl, *et al.*, 1988).

Collagen IV is a 500 kDa protein with three distinct functional domains: an amino terminal signal peptide rich in cysteine and lysine, a collagenous domain and a long carboxy-terminal noncollagenous domain (NC1) (Hudson, *et al.*, 2003; Khoshnoodi, *et al.*, 2008). The structural features of the α1 and α2 chains are detailed in Table 5. The NC1 domain is important in determining chain specificity and acts as the folding origin for the triple helical assembly, and hence initiates the molecular assembly of collagen IV molecules (Khoshnoodi, *et al.*, 2008). The collagenous domain forms a supercoiled triple helical structure with glycine residues frequently repeating every third amino acid residue (Cameron, *et al.*, 1991; Dobler, *et al.*, 2006; Stendahl, *et al.*, 2009). Glycine is essential to this tightly coiled triple helix because it is the only amino acid which will fit in the centre of the triple helix. Interruptions in the collagenous triple helical structure provide molecular flexibility and enable cell-binding and interchain crosslinking (Khoshnoodi, *et al.*, 2008). Collagen IV is secreted by cells into the ECM and self-associates into a network of triple-helical molecules which provide a molecular scaffold for other ECM components such as laminin (Khoshnoodi, *et al.*, 2008). Cell attachment is mediated at specific binding sites within both the collagenous and NC1 domains, with both integrin receptors and non-integrin receptors implicated; the specific receptors involved in interactions with pancreatic beta cells are detailed in section 1.3.3.

Table 5: Structural features of α1 and α2 chains of human collagen IV

	α1	α2
Residues after translation (procollagen)	1669	1712
Residues in signal peptide	27	36
Residues in collagenous domain	1413	1449
Residues in NC1 domain	229	227
Number of interruptions to collagenous domain	21	23

Adapted from Khoshnoodi, *et al*. (2008)

3.2.3. Modification of ECM proteins

Agents that react with and modify ECM proteins and thus impair integrin-mediated binding to beta cells may prove detrimental to beta cell survival through activation of anoikis. ECM proteins are particularly susceptible to damage because protective enzymatic defence systems, such as the glyoxalase system, are located within the cell cytosol; increases in methylglyoxal are therefore larger in extracellular medium and plasma than observed within cells (Dobler, *et al.*, 2006). Furthermore, functionally important arginine residues lie within integrin binding sites in ECM proteins (Chetyrkin, *et al.*, 2011). The plasma concentration of methylglyoxal is known to increase in hyperglycaemia and diabetes, and consequently levels of AGE residues on proteins also increase. In addition, the half-life of aortal collagen – including collagen IV - is estimated to be 60 - 70 days and so modifications by glycation may accumulate (Nissen, *et al.*, 1978).

Collagen IV is susceptible to modification by methylglyoxal with functional consequences (Cameron, *et al.*, 1991; Dobler, *et al.*, 2006). Arginine residues within the integrin binding site motifs of RGD on the α2 chain and GFOGER on the α1 chain were specifically modified by methylglyoxal, leading to impairments in endothelial cell binding to collagen and subsequent cell detachment and anoikis. Dobler *et al*. (2006) additionally showed that these modifications resulted in a decrease in angiogenesis within endothelial cells *in vitro*. This study identified the specific hotspots for glycation within collagen IV and indicated in endothelial cells that this modification impaired cell-ECM interactions and subsequently resulted in anoikis. Similar effects of the modification of collagen with methylglyoxal were observed earlier by Paul and Bailey (1999), again indicative of the deleterious

changes in tissues in both ageing and disease. Since both cell-ECM interactions and the maintenance of beta cell mass are known to be vital for normal beta cell functioning, it is possible that similar modifications within the basement membrane of the islets of Langerhans may have a role in beta cell dysfunction.

3.2.4. Culture of beta cells on collagen

ECM proteins have been utilised for cell culture studies of cell-ECM interactions *in vitro* (Kleinman, *et al.*, 1987). ECM proteins regulate cell function as well as enabling survival of some cell lines and primary cultures. Indeed, primary beta cells require matrix components to survive out of their natural environment (Pinkse, *et al.*, 2006; Wang and Rosenberg, 1999). The interactions between ECM proteins and the MIN6 insulinoma cell line have been investigated by a number of *in vitro* studies. These studies have indicated that matrix proteins provide a suitable surface for cell growth (Iino, *et al.*, 2004; Nikolova, *et al.*, 2006; Weber, *et al.*, 2008). They also highlight the importance of interactions between beta cells and basement membrane proteins and suggest that interactions with collagen IV and laminin predominate for beta cells. Modifications of ECM proteins at functional sites involved in these interactions may impair cell metabolism, signalling and viability.

3.3. Experimental models of beta cells and diabetes

Beta cell function has been characterised experimentally by studying isolated mammalian beta cells *in vitro*. The difficulties in isolating and maintaining mammalian beta cells in primary culture has led to the development and use of insulinoma cell lines which exhibit some characteristics of the beta cell phenotype. Beta cell function *in vivo* has been studied in animal models of pre-diabetes, insulin resistance and diabetes. There are limitations to extrapolating conclusions from *in vitro* and *in vivo* rodent models to human physiological systems, particularly due to the differences in the arrangement of islet cells between the different species (Stendahl, *et al.*, 2009). These models are, however, useful tools in furthering understanding of both beta cells and diabetes, with similar mechanisms and molecular events underlying these processes in both humans and rodents.

3.3.1. Beta cells in culture

A number of beta cell lines have been developed for research into beta cells and diabetes. The changing characteristics that they display with continued culture and abnormal protein expression are their main limitations. The main advantage is their availability and susceptibility to genetic modification (Skelin, *et al.*, 2010). Characteristics of the commonly used beta cell lines are given in Table 6. The glucose responsiveness varies greatly and many cell lines have defects in the insulin secretion pathway. Methods used to transform beta cells and overcome replicative senescence have included induction of tumours by irradiation, viral infection and development of transgenic mice with targeted expression of a recombinant oncogene in beta cells (Skelin, *et al.*, 2010). Expression of the Simian vacuolating virus 40 (SV40) has been successful in adapting primary cells to continuous growth in culture and transforming cells into a tumourigenic condition. It is believed to suppress the tumour-suppressor p53, and so lead to uncontrolled proliferation and a tumour (Skelin, *et al.*, 2010).

The cell lines MIN6 and INS-1 are considered to provide the best models of physiological beta cell function (Skelin, *et al.*, 2010). They are both glucose responsive in the physiological range and express the glucose sensor glucokinase. The glucose responsiveness of MIN6 cells does, however, deteriorate with passage and it is therefore important to use lower passage cells for a model of healthy beta cells (Cheng, *et al.*, 2012b). Primary rodent beta cells are also grown in culture. These do not easily proliferate and are usually cultured for approximately a week (Skelin, *et al.*, 2010). The main limitation of their use is availability due to the reliance on fresh animal material. Although the rodent pancreatic beta cell lines have enabled many advances in the study of beta cell physiology, the current developments in human cell lines will provide a new, more clinically relevant source of experimental beta cells and enable testing of advances in human-derived tissue (McCluskey, *et al.*, 2011; Vasu, *et al.*, 2013).

Table 6: Insulin secreting cell lines

Cell line and origin	Characteristics
MIN6 –C57BL6 mouse insulinoma (SV40 T-antigen transgenic mouse)	Expresses GLUT-2 and glucokinase and responds to glucose within the physiological range. Developed by Miyazaki *et al*. (1990).
INS-1 – rat insulinoma (radiation induced)	Displays many of the characteristics of beta cells – glucose responsive (express GLUT-2 and glucokinase) and has a high insulin content compared to some other cell lines. Dependent on mercaptoethanol. Developed by Asfari *et al*. (1992).
Rat insulinoma cell line (RINm) (radiation induced)	Physiology differs to beta cells. Abnormal glucose metabolism, poor sensitivity to glucose insulin (Halban, *et al.*, 1983).
Hamster pancreatic beta cells (HIT) (SV40 T-antigen transformed)	GSIS similar to observed in hamster islets. Responds to known modulators of insulin release (glucose and glucagon). Insulin content 2.5 - 20 fold lower than hamster islets (Santerre, *et al.*, 1981).
Beta-tumour cells – transgenic rodents (SV40 T-antigen transgenic rodents)	Maintains the features of differentiated beta cells for approximately 50 passages in culture. Secretes insulin but with a lower threshold for maximal stimulation than normal beta cells. Developed by Efrat *et al*. (1988).
Beta-hyperplastic islet-derived cells (HC), e.g. βHC-9 from hyperplastic mice islets (SV40 T-antigen transgenic mouse)	Displays normal concentration dependent GSIS – expresses both GLUT-2 and glucokinase. Kinetics of glucose metabolism are determined by glucokinase activity (Liang, *et al.*, 1996). Developed by Radvanyi *et al*. (1993)
Human pancreatic beta cell line 1.1B4 (electrofusion of freshly isolated beta cells and the immortal human PANC-1 epithelial cell line)	Novel human cell lines were developed by McCluskey *et al.* (2011) and characterised further (Vasu, *et al.*, 2013). This cell line was shown to demonstrate glucose sensitivity and respond to known insulin modulators, such as glucose and alanine. Implantation of the 1.1B4 cell line into STZ-induced diabetic mice improved glucose tolerance.

Insulin release by MIN6 cells has been compared to that of mouse islets (Kelly, *et al.*, 2010). It was found that although islets have greater insulin content, insulin release was higher from MIN6 cells cultured as pseudo-islets than from primary mouse islets. However, the underlying functional and molecular features of MIN6 cells (glucose responsiveness and expression of adhesion molecules such as E-cadherin and Cx36) are similar to beta cells. In addition, when MIN6 cells are cultured as pseudo-islets they contain a similar number of cells to in the islets of Langerhans in mice (approximately 4,000 cells per pseudo-islet), indicating the suitability of MIN6 as a beta cell line.

3.3.2. Animal models of diabetes

3.3.2.1. Streptozotocin induced diabetes

STZ is synthesised by *Streptomycetes achromogenes* and is used to chemically induce diabetes (Szkudelski, 2001). STZ has selective toxicity to pancreatic beta cells. It induces beta cell necrosis which can be detected by electron microscopy within hours of treatment (Rossini, *et al.*, 1977; Szkudelski, 2001). STZ enters beta cells via the GLUT2 glucose transporter and induces alkylation of DNA and subsequent activation of poly ADP-ribosylation. This leads to depletion of cellular ATP as well as formation of ROS. Since STZ ablates the beta cell mass and induces diabetes it is useful for studies investigating the consequences, complications and treatments for diabetes. It is not usually of use in studying changes within the pancreas in the normal pathogenesis of T2DM. The study injecting Tat-Glo1 into STZ-induced diabetic mice and observing changes in beta cell ablation is a clear exception to this (Kim, *et al.*, 2013). In addition, a treatment combining nicotinamide with STZ has been used to induce a moderate decrease in beta cell mass as a model of T2DM (Masiello, *et al.*, 1998; Szkudelski, 2012).

3.3.2.2. Animal models of diabetes and obesity

Selective inbreeding of mice for a number of generations has led to the NOD mouse model of T1DM. Hyperglycaemia has specifically been selected for and so not all the genes and phenotypes which have become enriched will be relevant to the pathogenesis of diabetes in either rodents or humans (Rees and Alcolado, 2005). In addition, NOD mice suffer less ketoacidosis and animals can survive for weeks

without insulin administration, unlike humans with T1DM. This mouse model is useful in improving understanding of the genetic and immunological basis of T1DM.

Models of T2DM are more complex due to the heterogeneity of the disorder – the interplay of insulin resistance and aspects of beta cell dysfunction and impaired insulin secretion. Animals with single gene mutations, such as the leptin deficient and leptin resistant models of obesity, ob/ob and db/db mice respectively, have been used to gain insights into T2DM. A number of tissue specific gene deletions or "knockout" animal models have also been utilised to identify the role of genes in specific tissues. For example knockout of the insulin receptor specifically in pancreatic beta cells in mice indicated insulin resistance within beta cells (Kulkarni, *et al.*, 1999).

3.3.2.3. HFD model of insulin resistance

The HFD fed mouse is a model of impaired glucose tolerance, insulin resistance and the early stages of T2DM (Hancock, *et al.*, 2008; Souza-Mello, *et al.*, 2010; Winzell and Ahrén, 2004). It is the most clinically relevant model of T2DM. This model was introduced in 1988 with suggestions of genetic predisposition to develop diabetes in diet-induced obese mice (Surwit, *et al.*, 1988). A combination of higher dietary intake and lower metabolic efficiency increases body weight as well as plasma glucose after a week of HFD feeding in C57BL6J mice. Insulin increases more progressively with time, although insulin release in response to glucose stimuli was shown to be impaired after a week of HFD feeding (Winzell and Ahrén, 2004).

It has been shown that HFD feeding of rodents for 16 weeks leads to changes within the pancreas suggestive of changes in morphology and impairments in function – these include an increase in islet mass, insulin content and glucagon content as well as a decrease in immunodensity for GLUT2 (Souza-Mello, *et al.*, 2010). Drugs used to treat T2DM, such as metformin, were shown to prevent these changes in the pancreas, with similar levels of insulin, glucagon and GLUT2 observed in mice treated with a combination of HFD and metformin as seen in mice fed a standard chow diet (Souza-Mello, *et al.*, 2010). Another recent study demonstrated similar effects as well as indicating that HFD feeding of C57BL6J mice leads to decreased insulin secretion - due to the functional dissociation of VGCC from exocytosis in beta cells (Collins, *et al.*, 2010). This was suggested to be because calcium entry in beta cells becomes more dispersed following HFD. It is

therefore less efficient and intracellular increases in calcium occur too far from release-competent granules to trigger release. Additionally, it was reported that the inhibitory effect of prolonged non-esterified fatty acid (NEFA) treatment on GSIS involves a redistribution of VGCC such that the granule pool close to the calcium channels are lost (Hoppa, *et al.*, 2009; Rorsman and Braun, 2013). These studies are suggestive of a direct link between increased dietary lipids – a high fat diet – and pancreatic beta cell dysfunction; this indicates the importance of this model for not only studying insulin resistance, but also beta cell dysfunction during the pathogenesis of diabetes.

Further studies have replaced some of the dietary fats with n-3 long-chain polyunsaturated fatty acids (LC-PUFA), namely eicosapentaenoic acid (EPA) and docosahexaenoic acid (DHA), which are abundant in fish oils. These LC-PUFA have been shown to be hypolipidaemic in both humans and rodents and prevent obesity and insulin resistance in rodents fed a HFD (Jilkova, *et al.*, 2013; Rossmeisl, *et al.*, 2009). Plasma lipid levels were decreased, further weight gain prevented and glucose tolerance improved when these LC-PUFA were fed to dietary obese mice, the treatment did not however decrease the plasma insulin levels (Rossmeisl, *et al.*, 2012). The role of LC-PUFA in beta cell dysfunction or maintenance of healthy beta cell physiology remains to be determined.

3.4. Aims and Objectives

The aim of this investigation is to investigate the effect of protein glycation by methylglyoxal on pancreatic beta cell dysfunction and the subsequent development of diabetes. The MIN6 cell line and HFD-induced diabetic mouse model were used in this study.

Objective 1: To characterise the glyoxalase system and dicarbonyl metabolism in MIN6 cells *in vitro*

There are few publications on the glyoxalase system and the associated dicarbonyl metabolism in beta cells or relevant cell lines. It is therefore important to characterise this enzymatic system in a relevant cell type. To achieve this objective, MIN6 cells were used as a model to characterise the glyoxalase system in both basal

glucose concentration (5.5 mM) and high glucose concentration (20 mM) conditions. Activities of the glyoxalase enzymes and concentrations of the associated metabolites - dicarbonyls, D-lactate and glutathione - were determined. The glyoxalase pathway flux was determined and the glucose consumption used to calculate the proportional flux from triosephosphates in cells cultured in basal and high glucose. Cellular protein was analysed for glycation, oxidation and nitration adducts to assess whether exposure to higher concentrations of glucose has an impact on the level of cellular protein damage. A cell permeable inhibitor of Glo1, $BrBzGSHCp_2$, was utilised to induce dicarbonyl stress. In this model dicarbonyls and glutathione were measured, as well as the mRNA expression of insulin and Glo1 to characterise changes in dicarbonyl metabolism and beta cell function.

Objective 2: To study the effect of modification of collagen IV with methylglyoxal on the function and adhesion of MIN6 cells *in vitro*

The functional effect of modifying collagen IV with methylglyoxal has been previously demonstrated in endothelial cells (Dobler, *et al.*, 2006). The sites of modification were identified – specific arginine residues within integrin binding sites, necessary for cell-ECM binding in both endothelial cells and beta cells. To achieve this objective MIN6 cells were cultured on control and methylglyoxal-modified collagen IV coated plates and adhesive interactions assessed. Controls were performed using both an anti-integrin β_1 antibody and RGD peptide to confirm that any observed binding is specific to collagen. The force and energy underlying adhesion between collagen and MIN6 cells was determined using atomic force microscopy force spectroscopy (AFM-FS). Analysis of gene expression in MIN6 cells following culture on uncoated, collagen coated and methylglyoxal-modified collagen coated plates was used to assess MIN6 cell function and any impairment therein. Genes analysed were Ins1, Ins2, Glo1, E-cadherin, Cx36 and integrin beta 1 (Itgb1). This enabled the effect of methylglyoxal modification of collagen IV on binding to MIN6 cells, and related effects on insulin expression and cell-cell adhesion and cell-ECM adhesion to be determined.

Objective 3: To characterise and evaluate the effect of diet induced insulin resistance on dicarbonyls and the associated metabolism in an *in vivo* model of T2DM

Feeding C57BL6 mice a HFD for 6 - 12 weeks induces insulin resistance and diabetes (Surwit, *et al.*, 1988). The effects of this have been well studied, particularly in organs susceptible to insulin resistance such as skeletal muscle and the liver, and with regards to potential treatments (Hancock, *et al.*, 2008; Souza-Mello, *et al.*, 2010; Winzell and Ahrén, 2004). However, relatively little is known about the pancreas in this model, especially with regard to the glyoxalase system and dicarbonyl metabolism. To achieve this objective, diabetes was induced by feeding a HFD to C57BL6 mice. An additional treatment group in which mice were fed a HFD supplemented with EPA and DHA was maintained. Previous work has suggested that this supplementation prevents the detrimental effects of HFD in the development of obesity and insulin resistance (Jilkova, *et al.*, 2013; Rossmeisl, *et al.*, 2009; Rossmeisl, *et al.*, 2012). The activity of the glyoxalase system enzymes and the amount of related metabolites was measured in the pancreas from control diet fed, HFD fed and omega-3 fatty acid supplemented HFD fed mice. Glycation, oxidation and nitration adduct residues were quantified on the cytosolic and ECM pancreatic protein and the plasma protein. The concentration of glycation, oxidation and nitration free adducts in the pancreas and plasma was determined. This data enabled an understanding and comparison of dicarbonyl metabolism and associated protein glycation in control and insulin resistant diabetic mice. Immunostaining was also used to observe changes in localisation of collagen IV, insulin and the glycation adduct MG-H1 in the pancreas of mice fed these different diets.

4. Materials and Methods

4.1. Materials

4.1.1. Cell line and cell culture reagents

MIN6 cells were originally obtained from Professor Jun-ichi Miyazaki (Osaka Medical School, Japan). Dulbecco's Modified Eagles Medium (DMEM), CO_2-independent medium and 0.25% Trypsin-EDTA solution were purchased from Invitrogen Life Technologies (Paisley, UK) and Fetal Bovine Serum (FBS) from Biosera (Boussens, France). Penicillin-Streptomycin solution (10,000 units penicillin and 10 mg streptomycin per mL in 0.9% sodium chloride), trypan blue and thiazolyl blue tetrazolium bromide (MTT) were all purchased from Sigma Aldrich (Gillingham, Dorset, UK). Trypsin neutralising solution (0.05% trypsin inhibitor, 0.1% BSA) was from Promocell (Heidelberg, Germany). Neubauer haemocytometers for cell counting were purchased from Paul Marienfeld GmbH & Co. KG (Lauda-Königshofen, Germany).

4.1.2. Enzymes, peptides and proteins

L-Arginyl-glycyl-L-aspartic acid (RGD), human fibronectin purified from plasma and human placental collagen IV were obtained from Sigma Aldrich and mouse Engelbreth-Holm-Swarm (EHS) lathrytic tumour derived collagen IV was obtained from BD Bioscience (San Jose, USA). Collagenase from *Clostridium histolyticum* (type VII), pronase E from *Streptomyces griseus* (type XIV), pepsin from porcine gastric mucosa, prolidase from porcine kidney, leucine aminopeptidase from kidney microsomes (type VI-S), L-lactic dehydrogenase from rabbit muscle and D-lactic dehydrogenase from *Staphylococcus epidermidis* were all purchased from Sigma Aldrich.

4.1.3. Antibodies

Armenian hamster anti-mouse Itgb1 (functional grade purified) monoclonal antibody was from eBioscience (Hatfield, UK). Chicken polyclonal anti-insulin antibody and rabbit polyclonal anti-collagen IV antibodies were obtained from Abcam (Cambridge, UK). Mouse anti-MG-H1 monoclonal antibody clone 1H7G5 was a gift from Professor Michael Brownlee (Albert Einstein College of Medicine,

Bronx, NY). Alexa Fluor 555 goat anti-chicken IgG, Alexa Fluor 488 goat anti-mouse IgG, Alexa Fluor 488 goat anti-rabbit IgG and Alexa Fluor 555 goat anti-rabbit IgG were all obtained from Molecular Probes (Invitrogen, Eugene, Oregon, USA).

4.1.4. Analytical and preparative kits

RNeasy Mini Kit was from Qiagen (Manchester, UK). CBQCA protein quantitation kit was purchased from Invitrogen Life Technologies (Paisley, UK) and the protein assay dye concentrate from BioRad (Hemel Hempstead, Hertfordshire, UK). Glucose assay kits were obtained from Sigma Aldrich. Strong anion exchange solid phase extraction cartridges were from Alltech Associates Ltd. (Carnworth, Lancashire, UK) and 3,000 and 10,000 molecular weight cut-off centrifugal filters were from Millipore (Watford, UK).

4.1.5. Immunohistochemistry reagents

Microscope slides were from Fisher Scientific (Loughborough, UK) and cover glass from VWR International (Lutterworth, Leicestershire, UK). Embedding matrix was from Shandon Cryomatrix (ThermoFisher, Epsom, Surrey, UK). Mounting medium containing 4',6-diamidino-2-phenylindole (DAPI) and an ImmEdge hydrophobic barrier pen were purchased from Vector Laboratories (Peterborough, UK).

4.1.6. Chromatographic reagents

Hypercarb columns (50 x 2.1 mm, 150 x 2.1 mm and 250 x 2.1 mm) and octadecyl silane (ODS) columns (100 x 2.1 mm) for HPLC were purchased from Thermofisher (Epsom, Surrey, UK) and Waters (Elstree, Hertfordshire, UK) respectively. HPLC grade and Optima grade solvents were obtained from Fisher Scientific (Loughborough, UK).

4.1.7. Other analytical reagents

Nuclease-free water and 18S reference primers were from Qiagen (Manchester, UK). All other primers were ordered from Invitrogen custom primer service (Paisley, UK). dNTP mix was from Fermentas (Thermo Scientific, Epsom, Surrey, UK). Bioscript, RiboSafe RNase Inhibitor, Oligo (dT)18 Primer Mix and

SensiMix Sybr Low-ROX were all purchased from Bioline (London, UK). [*glycine*-$^{13}C_2{}^{15}N$]GSH, 98% ^{15}N and 99% ^{13}C was purchased from Sigma Aldrich. [$^{13}C_4{}^{15}N_2$]GSSG was synthesised from [*glycine*-$^{13}C_2{}^{15}N$]GSH. Standards and isotopic standards for dicarbonyl assay were available in house. 3-DG and [$^{13}C_6$]3-DG were synthesised from glucose and [$^{13}C_6$]glucose respectively. Glyoxal and [$^{13}C_2$]glyoxal were synthesised by oxidation of ethylene glycol and [$^{13}C_2$]ethylene glycol respectively using alcohol oxidase and catalase. High purity methylglyoxal and [$^{13}C_2$]methylglyoxal were available in house, prepared and purified as described (McLellan and Thornalley, 1992). Isotopically labelled citrulline and amino acids were purchased from Cambridge Isotope Laboratories (Andover, MA, USA) and glycation, oxidation and nitration adducts were available in house, prepared and purified as described (Ahmed, *et al.*, 2002; Thornalley, *et al.*, 2003). 2,5,5[$^{2}H_3$]DL-α-Aminoadipic acid ([$^{2}H_3$]-AAA) was purchased from CDN Isotopes (Quebec, Canada). ε-(γ-L-Glutamyl)–L-lysine was purchased from Bachem AG (Bubendorf, Switzerland) and [$^{13}C_5$]ε-(γ-L-glutamyl)–L-lysine was available in house, prepared and purified as described (Bertholet, *et al.*, 1977). S-p-Bromobenzyl-glutathione cyclopentyl diester (BrBzGSHCp$_2$) was available in house, prepared and purified as described (Thornalley, *et al.*, 1996). All other analytical reagents and buffers were purchased from either Sigma Aldrich or Fisher Scientific.

4.1.8. Instrumentation

Water used for all experiments was filtered through a Milli-Q Advantage A-10 System from Millipore (Watford, UK). Microplate assays were quantified using a FLUOstar Optima plate reader (BMG Labtech, Aylesbury, Buckinghamshire, UK) and enzymatic activity assays and stock calibrations performed using UVIKON XS spectrophotometer (NorthStar Scientific Ltd. Potton, Bedfordshire, UK). Liquid chromatography-tandem mass spectrometry (LC-MS/MS) analysis was performed using Waters Acquity ultra HPLC systems with a Quattro Premier XE Tandem mass spectrometer and Xevo triple quadrupole mass spectrometer (Waters, Elstree, Hertfordshire, UK). Enzymatic hydrolysis was performed using a CTC-PAL Automation System (CTC-Analytics, Zwingen, Switzerland). The centrifugal evaporator was a Savant Instruments SpeedVac (Thermo Scientific, Waltham MA). Quantification of RNA stocks was performed using a ND-1000 Nanodrop spectrophotometer (Nanodrop, Wilmington, USA). RNA expression analysis was

performed using a 7500 Fast Real-Time PCR machine from Applied Biosystems (Carlsbad, California, USA). A Sonics Vibra-Cell sonicator from Jencons Scientific (Leighton Buzzard, Bedfordshire, UK) was used for lysis of cell culture samples and a Lab Gen 7 homogeniser from Cole Parmer (Vernon Hills, USA) was used for isolation of protein and soluble extracts from pancreatic tissue samples. Pancreas samples were sectioned for immunohistochemistry using a CM1850 Cryostat from Leica Microsystems (Milton Keynes, UK). Confocal microscopy was performed using an AxioVert 200M laser scanning confocal microscope from Carl Zeiss Microscopy (Thornwood, NY, USA). AFM-FS was performed using a CellHesion module (JPK Instruments, Berlin, Germany).

4.1.9. Software

Mass spectrometry data was processed using MassLynx software Version 4.1 (Waters, Elstree, Hertfordshire, UK). Atomic force spectroscopy data was processed using CellHesion 200 software (JPK Instruments, Berlin, Germany). Confocal microscopy images were viewed using LSM Image Browser (Carl Zeiss Microscopy, Thornwood, NY, USA). Microplate assays were analysed using Optima software version 2.10 R2 (BMG Labtech, Aylesbury, Buckinghamshire, UK). Real-time PCR analysis was performed using 7500 Fast System Software version 1.4.0. RNA primers were designed using the Oligo perfect design tool (Invitrogen Life Technologies, Paisley, UK) with mRNA and genomic sequences obtained using the University of California, Santa Cruz genome browser tool (Genome Bioinformatics Group, University of California, Santa Cruz). ChemDraw Pro version 13.0 was used for chemical structures and associated analysis. Statistical analysis was performed using SPSS Statistics version 21.

4.2. Cell culture methods

4.2.1. MIN6 cell culture

MIN6 cells were maintained in DMEM supplemented with 15% FBS and 200 U/mL penicillin and 200 µg/mL streptomycin at 37 °C under aseptic conditions and an atmosphere of air/5% carbon dioxide. Cells were passaged approximately every 7 days with a seeding density of *ca.* 30,000 cells/cm^2. Cells were harvested

using 0.25% trypsin-EDTA, subsequently neutralised by media addition. For experiments performed in high glucose conditions, culture media was supplemented with β-D-glucose to a final concentration of 20 mM using a sterile aqueous solution. Unless stated otherwise, all experimental cultures were performed for 5 days on cells between passages 40 and 45, following which cell pellet samples (collected by trypsinisation) and media samples were stored for subsequent analysis. Cell viability was ≥ 98% at the start of all experiments determined using trypan blue dye exclusion.

4.2.2. Assessment of cell viability

Cell viability was assessed by the trypan blue dye exclusion technique (Strober, 2001) and also by the redox staining MTT method (Mosmann, 1983). For the MTT method, medium was removed from cells plated in 96 well cell culture plates. Wells were washed with 2 x 100 µL fresh medium and 2 x 100 µL PBS. MTT (100 µL; 0.5 mg/mL) in medium was added and the plate incubated for 2 h at 37 °C in a cell culture incubator. The MTT solution was removed, wells washed (2 x 100 µL medium) and cells lysed with 100 µL DMSO. Plates were mixed for 5 min until lysis solutions were of homogenous appearance and absorbance at 595 nm was measured using a reference wavelength of 650 nm.

4.2.3. Coating of plates with collagen

Type IV collagen was diluted in PBS and added to 24 well cell culture plates (Costar, Corning) to give a coating concentration of 10 µg/cm^2. Plates were incubated at room temperature overnight, the solution carefully aspirated off and wells washed with 500 µL PBS.

4.2.4. Modification of plated collagen

Methylglyoxal was diluted in PBS to a final concentration of 10 µM, sterile filtered through a 0.2 µm cellulose acetate filter and 500 µL added per well of the 24 well plate. Plates were incubated at 37 °C for 24 hours. Methylglyoxal solutions were removed and wells washed with 500 µL PBS.

4.2.5. Quantification of collagen adhered to wells

Plates were coated overnight with collagen as described in section 4.2.3. Collagen was removed from wells and wells washed twice with 500 µL PBS; PBS wash. Wells were then washed with 6 x 500 µL 0.1% Triton X-100 in PBS to remove the collagen from the well; the first three washes Triton wash 1 and the second three washes Triton wash 2. Samples were quantified by 3-(4-carboxybenzoyl)quinoline-2- carboxaldehyde (CBQCA) assay.

4.2.6. Cell adhesion assay

MIN6 cells at a density of 570,000 cells/mL in HEPES buffer (9.7 mM, pH 7.4, containing 5.4 mM KCl, 1 mM $CaCl_2$, 136.9 mM NaCl, 0.34 mM Na_2HPO_4 and 5.6 mM D-glucose) were seeded into wells of collagen coated plates to give coverage of 150,000 cells/cm^2. Plates were incubated at 37 °C for 2 h after which time non-adherent cells were removed and the adhered cells were trypsinised and counted. Cells were incubated with 5 µg/mL anti-Itgb1 antibody and 2 µg/mL RGD for 15 minutes at 37 °C prior to plating for the cell adhesion assay.

4.2.7. Atomic force microscopy force spectroscopy

AFM-FS was used to measure the detachment energy and initial force necessary to uncouple cells from collagen IV. The experimental set up is illustrated in Figure 8.

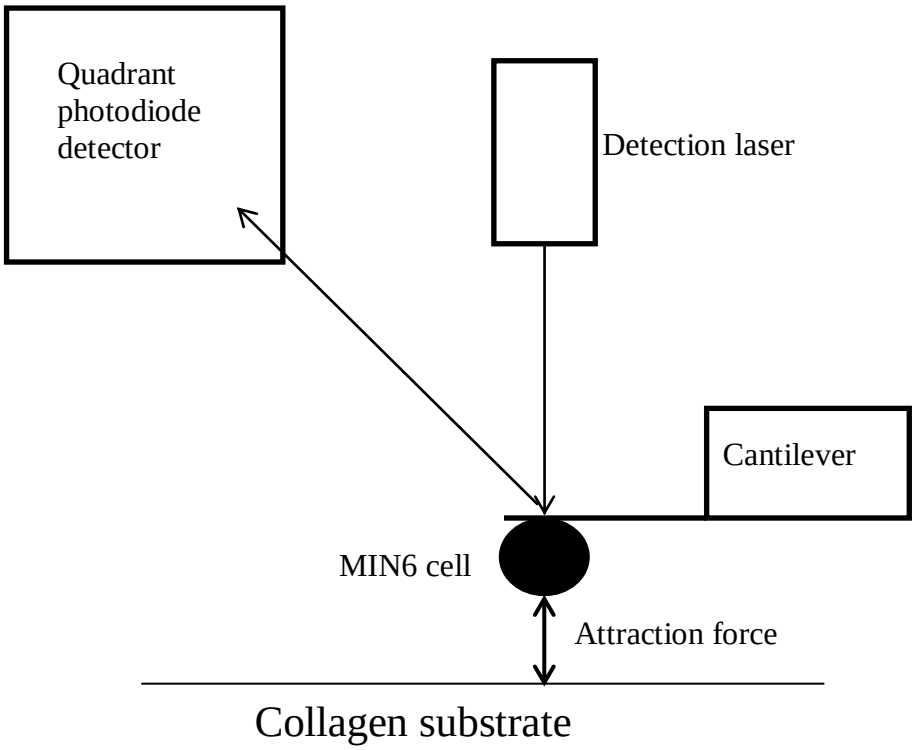

Figure 8: AFM experimental set-up.

Cantilevers were functionalised by sequential incubations in solutions of 2 µg/mL poly-L-lysine in PBS (30 min at room temperature), 20 µg/mL fibronectin in PBS (2 h at 37 °C) and PBS (overnight at 4 °C). Each cantilever was calibrated before use. MIN6 cells were removed from culture flasks into fresh CO_2-independent media using a cell scraper. Cell suspensions were incubated with 2 µg/mL RGD for 15 min at 37 °C prior to use as RGD treated cells. A single MIN6 cell was bound to a cantilever and brought into contact with collagen IV with a force of 3 nN. The cell remained in contact with the collagen substrate for 15 s while adhesion occurred. The cantilever was then retracted at a constant speed of 5 µm/s and the force (nN) and displacement - deflection of the cantilever - were measured using a laser until the cell was completely separated from the collagen (a maximum pulling length of 90 µm). Measurements, approximately 50, were performed with multiple cells and plates of collagen in separate experiments (n=3). Detachment energy (fJ) was calculated as force (nN) x displacement (µm).

4.3. Analytical methods

4.3.1. Bradford assay (samples)

Protein concentrations in cell lysates and tissue homogenates were determined by the Bradford method (Bradford, 1976) using BSA for calibration standards. Stock solutions of BSA were calibrated on a spectrophotometer using absorbance at 279 nm and the stock concentration deduced.

4.3.2. CBQCA protein assay

The CBQCA assay for proteins was performed according to the manufacturer's instructions to quantify collagen adhered to wells of a 24 well plate. This assay has higher sensitivity than the Bradford assay and quantifies protein concentrations in the ng range in the presence of detergents such as Triton X-100. Collagen was quantified against a collagen standard curve. All standards and samples were prepared using low binding pipette tips and glass tubes to minimise loss of protein during sample processing and to improve assay performance.

4.3.3. Calibration of stock solutions

4.3.3.1. MG

Stock solutions of MG were calibrated by derivatisation of MG with aminoguanidine at 37 °C and pH 7.4 which forms isomeric triazines, 3-amino-5-methyl-1,2,4-triazine and 3-amino-6-methyl-1,2,4-triazine with characteristic absorbance at 320 nm for which ε_{320} = 2.41 $mM^{-1}cm^{-1}$. MG was diluted to approximately 50 µM and 1 mM aminoguanidine added and incubated in 50 mM sodium phosphate buffer, pH 7.4 and 37 °C for 4 h. Control samples, containing 1 mM aminoguanidine in 50 mM sodium phosphate buffer, were incubated alongside. The absorbance of the product mixtures was measured and the concentration of the MG was deduced assuming a 1:1 reaction of MG with aminoguanidine to form triazine products. (Thornalley, *et al.*, 2000).

4.3.3.2. S-D-Lactoylglutathione

Stock solutions of S-D-lactoylglutathione were calibrated by absorbance at 240 nm using the extinction coefficient $\Delta\varepsilon_{240}$ = 3.30 $mM^{-1}cm^{-1}$ (Clelland and Thornalley, 1991).

4.3.4. Enzymatic activity assays

4.3.4.1. Sample preparation

MIN6 cells were collected after trypsinisation, washed in PBS and resuspended in 10 mM sodium phosphate buffer, pH 7.0, sonicated on ice at 110 Watts for 30 sec, and centrifuged at 20,000 g for 30 min at 4°C. The supernatant was removed and retained for enzymatic activity assays. Pancreas samples (5 - 10 mg) were homogenised on ice in 250 µL 10 mM sodium phosphate buffer, pH 7.0. Homogenates were centrifuged at 20,000 g for 30 min at 4°C and the supernatant used for enzymatic activity assays.

4.3.4.2. Glyoxalase 1

The activity of Glo1 was determined by measuring the initial rate of formation of S-D-lactoylglutathione from the GSH-MG hemithioacetal formed non-enzymatically from MG and GSH and followed spectrophotometrically at 240nm; $\Delta\varepsilon_{240}$ = 2.86 $mM^{-1}cm^{-1}$ (Allen, *et al.*, 1993b).

$$CH_3COCHO + GSH \rightleftharpoons CH_3COCH(OH)\text{-}SG \xrightarrow{Glo1} CH_3CH(OH)CO\text{-}SG$$

2 mM MG and 2 mM GSH were incubated in 50 mM sodium phosphate buffer, pH 6.6 for 10 min at 37°C to form the GSH-MG hemithioacetal. Cell lysate, or lysate buffer for the blank, was added at a 50-fold dilution to a final volume of 1 mL, the solution mixed well by inversion and absorbance at 240 nm monitored for five min at 37°C. The initial rate of change in absorbance was determined and the activity of Glo1 deduced. Glo1 activity was expressed as units per mg of protein where one unit is the amount of enzyme which catalyses the formation of 1 µmol of S-D-lactoylglutathione from the hemithioacetal substrate per minute under assay conditions.

4.3.4.3. Glyoxalase 2

The activity of Glo2 was determined by measuring the initial rate of hydrolysis of S-D-lactoylglutathione to D-lactate and GSH, followed spectrophotometrically at 240 nm; $\Delta\varepsilon_{240}$ = 3.10 $mM^{-1}cm^{-1}$. This extinction coefficient equates to the difference between the extinction coefficients of the substrate, S-D-lactoylglutathione, 3.3 $mM^{-1}cm^{-1}$, and the hydrolysed product GSH, 0.2 $mM^{-1}cm^{-1}$ (Ball and Vander Jagt, 1979).

$$CH_3CH(OH)CO\text{-}SG + H_2O \xrightarrow{Glo2} CH_3CH(OH)CO_2^- + H^+$$

S-D-Lactoylglutathione (0.3 mM) was incubated in 50 mM Tris/HCl, pH 7.4 and 37°C, and the cell lysate or lysate buffer for the blank was added at a 20-fold dilution to a final volume of 1 mL. The solution was mixed by inversion and absorbance at 240 nm monitored for 5 min at 37°C. The initial rate of change in absorbance was deduced (Allen, *et al.*, 1993a). One unit of Glo2 activity is the amount of enzyme which catalyses the hydrolysis of 1 µmol of S-D-lactoylglutathione per minute under assay conditions.

4.3.5. Assay of D-lactate

4.3.5.1. Assay of D-lactate in cell culture media

Since D-lactate is freely membrane permeable the cellular levels of D-lactate were established by measuring the amount in culture media. The end-point enzymatic assay was based on the fluorimetric assay developed by McLellan *et al.* (1992). D-Lactate is converted to pyruvate by the enzyme D-lactic dehydrogenase during incubation at 37 °C. This is associated with the reduction of NAD^+; the accumulation of NADH is measured by fluorescence, with 340 nm and 460 nm the excitation and emission wavelengths respectively.

$$\text{D-Lactate} + NAD^+ \rightleftharpoons \text{pyruvate} + NADH$$

The reaction is driven to endpoint in the forward reaction by the presence of hydrazine, removing pyruvate from the equilibrium as pyruvate hydrazine. Media samples (0.5 mL) were de-proteinised by the addition of 1 mL ice-cold 0.6 M

perchloric acid (PCA). The suspension was vortex mixed, incubated on ice for 10 min to enable the protein to precipitate and centrifuged (7,000 g, 4 °C, 5 min) to sediment the protein precipitate. An aliquot of supernatant (700 µL) was taken and neutralised to pH 7 by the addition of 2 M potassium bicarbonate (200 µL). Samples were again vortex mixed and centrifuged (7,000 g, 4 °C, 5 min) to sediment the potassium perchlorate precipitate. The supernatant was removed and placed in a centrifugal evaporator under vacuum (20 mm Hg) at room temperature for 5 min to remove dissolved carbon dioxide.

An aliquot of the resulting neutralised sample (100 µL) or D-lactate standard solution was added to each well of a black microplate together with 100 µL of glycine hydrazine buffer (1.2 M glycine, 0.5 M hydrazine hydrate, 2.5 mM diethylenetriaminepentaacetic acid (DETAPAC), pH 9.2) and 25 µL 4 mM NAD^+. The reaction was initialised by the addition of 25 µL D-lactic dehydrogenase (250 U/mL), the plate sealed and incubated in the dark at 37 °C for 2 h. A control without addition of enzyme was run for each sample. A standard curve over the range 0.5 – 3.0 nmol D-lactate was prepared as detailed in Table 7. A representative calibration curve is displayed in Figure 9.

Table 7: Solutions for preparing the calibration curve in the assay of D-lactate

Calibration solution	D-Lactate (nmol)	Volume of 100 µM D-lactate stock (µL)	Water (µL)
0	0	0	100
1	0.5	5	95
2	1.0	10	90
3	1.5	15	85
4	2.0	20	80
5	2.5	25	75
6	3.0	30	70

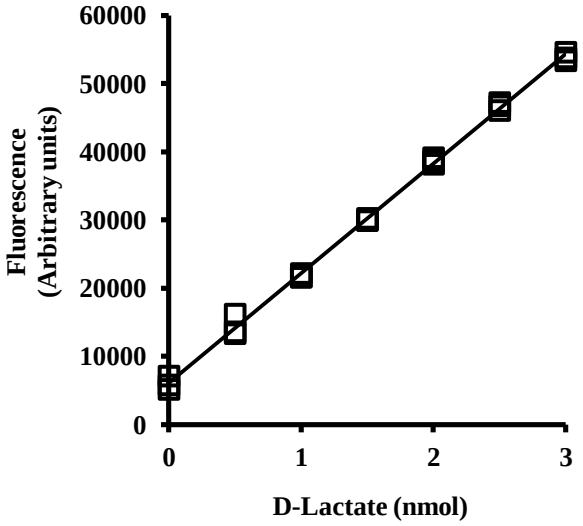

Figure 9: Standard curve for assay of D-lactate (fluorescence method). Regression of fluorescence on D-lactate (nmol) gave Fluorescence = ((16075 ± 169) x D-lactate (nmol)) + 6088 ± 304; $r^2 = 0.998$; n = 21.

4.3.5.2. Assay of D-lactate in mouse pancreas

Snap frozen mouse pancreas tissue (approximately 10 mg) was homogenised in 250 µL ice-cold 0.6 M PCA. Suspensions were incubated on ice for 10 min to enable the protein to precipitate and centrifuged (7,000 g, 4 °C, 5 min) to sediment the protein precipitate. The supernatant (200 µL) was removed and neutralised to pH 7 by the addition of 2 M potassium bicarbonate (60 µL). Samples were vortex mixed and centrifuged (7,000 g, 4 °C, 5 min) to sediment the potassium perchlorate precipitate. The supernatant was removed and placed in a centrifugal evaporator under vacuum (20 mm Hg) at room temperature for 5 min to remove dissolved carbon dioxide.

Samples were assayed in a clear microplate as described for cell culture media samples (section 4.3.5.1) against a calibration curve from 0.5 – 14 nmol D-lactate prepared as described in Table 8. A specimen calibration curve is shown in Figure 10. The resulting increase in NADH was monitored by absorbance at 340 nm.

Table 8: Solutions for preparing the calibration curve in the assay of D-lactate (absorbance detection)

Calibration solution	D-Lactate (nmol)	Volume of 100 µM D-lactate stock (µL)	Water (µL)
0	0	0	100
1	0.5	2.5	97.5
2	1.0	5	95.0
3	2.0	10	90.0
4	4.0	20	80.0
5	6.0	30	70.0
6	8.0	40	60.0
7	10.0	50	50.0
8	14.0	70	30.0

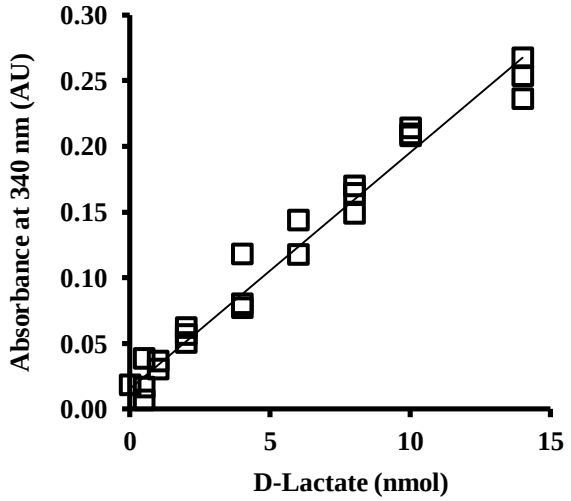

Figure 10: Standard curve for D-lactate (absorbance). Regression of absorbance on amount of D-lactate (nmol) gave Absorbance = ((0.018 ± 0.0007) x D-lactate (nmol)) + 0.0157 ± 0.0050; $r^2 = 0.968$; n = 24.

4.3.6. Assay of L-lactate

L-Lactate was assayed as described for D-lactate except using L-lactic dehydrogenase. Sample content of L-lactate is 50 - 100 fold higher than D-lactate and so media samples were diluted with water prior to assay. L-Lactate calibration

standards were prepared over the range 1-10 nmol - Figure 11. Samples were prepared and assayed according to the protocol for D-lactate (section 4.3.5).

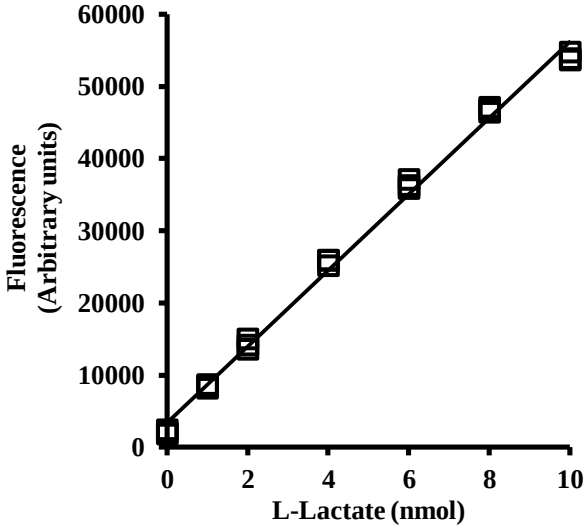

Figure 11: Standard curve for assay of L-lactate (fluorescence method). Regression of fluorescence on amount of L-lactate (nmol) gave: Fluorescence = ((5275 ± 86) x L-lactate (nmol)) + 3431 ± 484; $r^2 = 0.995$; n = 21.

4.3.7. D-Glucose assay

The concentration of glucose in culture media was determined using an end-point enzymatic assay using a commercial assay reagent containing 1.5 mM NAD^+, 1 mM ATP, 1 unit/mL hexokinase and 1 unit/mL G6P dehydrogenase. It was calibrated by assay of 0 – 37.5 nmol D-glucose standard. The D-glucose assay was performed according to the manufacturer's instructions; the enzymatic principle of the coupled assay is illustrated by the following equations:

$$\text{Glucose + ATP} \xrightarrow{\text{Hexokinase}} \text{G6P + ADP}$$

$$\text{G6P + } NAD^+ \xrightarrow{\text{G6PDH}} \text{6-Phosphogluconate + NADH}$$

The formation of NADH is measured by endpoint measurement spectrophotometrically at 340 nm. Since one nmol glucose leads to the formation of one nmol NADH in this reaction, the increase in absorbance at 340 nm is directly proportional to the concentration of glucose. A standard curve was constructed over

the range 0 – 37.5 nmol glucose, incubated for 15 min at room temperature alongside diluted test samples and the absorbance at 340 nm measured spectrophotometrically.

4.3.8. Assay of cellular thiols

The amount of total thiols in cell cytosolic extracts (mainly protein cysteine thiols, GSH, γ-glutamyl-cysteine and free cysteine) was determined by measuring the absorbance produced by the reaction of cytosolic extracts with 5,5'-dithiobis-(2-nitrobenzoic acid) (DTNB). The reaction between DTNB and protein thiols results in the formation of the chromophore 2-nitro-5-thiobenzoate anion (TNB) and a consequent increase in absorbance at 410 nm.

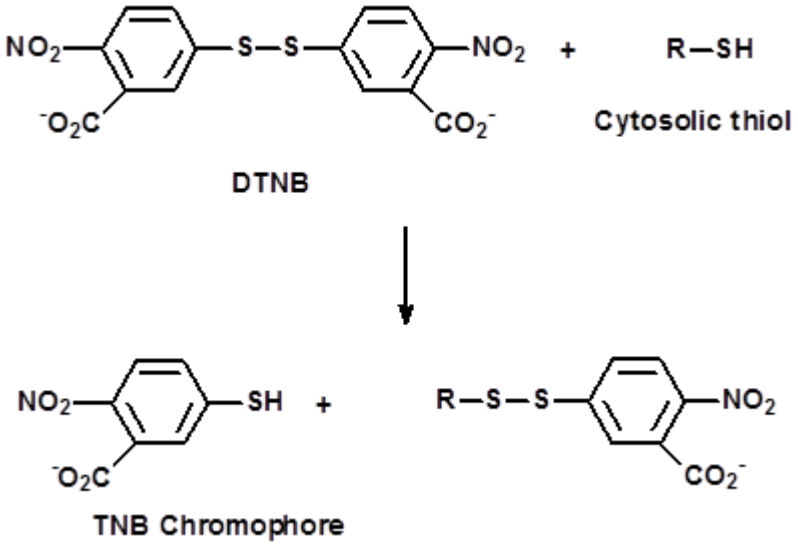

DTNB solution (125 µL, 1 mM DTNB in 100 mM sodium phosphate buffer, containing 0.2 mM DETAPAC, pH 7.4) and 100 µL of water were added to wells of a 96 well plate. Sample or standard (25 µL) was added and the absorbance at 410 nm was recorded after incubation for 20 min at room temperature. The assay was calibrated using GSH over the range 2 - 30 nmol and the measured absorbance used to deduce the amount of cellular thiols. A specimen calibration curve is displayed in Figure 12.

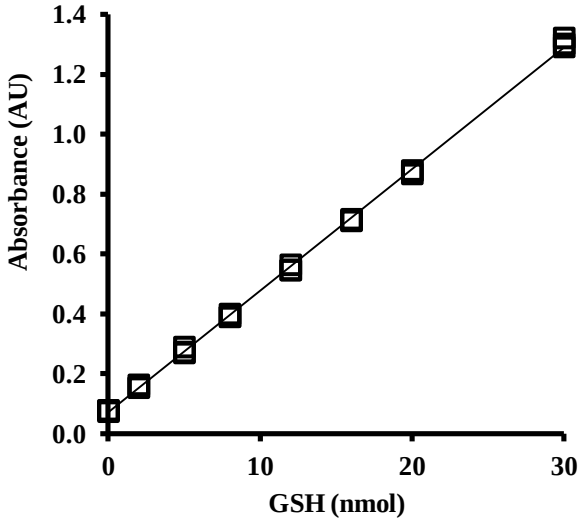

Figure 12: Standard curve for assay of thiols in cytosolic extracts of cells. Regression of absorbance on amount of Thiols (nmol) gave: Absorbance = ((0.0407 ± 0.0002) x GSH (nmol)) + 0.0708 ± 0.0035; $r^2 = 0.999$; n = 24.

4.3.9. Real-time quantitative PCR

4.3.9.1. Principle of assay

Real-time quantitative PCR (qPCR) was used to compare mRNA transcript copy number of specific genes in cell and tissue samples. Briefly, the cellular RNA was extracted and reverse transcribed into cDNA. cDNA was used as a template for the primers during real-time PCR analysis. SYBR green I dye was used for detection; it fluoresces when bound to double stranded DNA. This fluorescence was measured on each PCR cycle.

4.3.9.2. Primer design and testing

Primers were designed using the Invitrogen oligo perfect designer tool using mRNA and genomic DNA sequences obtained from the University of California, Santa Cruz genome browser. Multiple primer pairs were selected for each gene. Amplicon length (optimal 100 - 150 base pairs) was considered and primers spanning exon-exon junctions were chosen when possible; this acted as an additional quality control since any contaminant genomic DNA would not act as a template for amplification. All primer sequences used are given in Appendix A.

Dissociation plots were performed for all primers to test performance and $MgCl_2$ concentration was optimised further when necessary. Example dissociation

plots are shown in Figure 13. Dissociation plots were routinely performed for each assay plate; this ensured that the primers performed consistently.

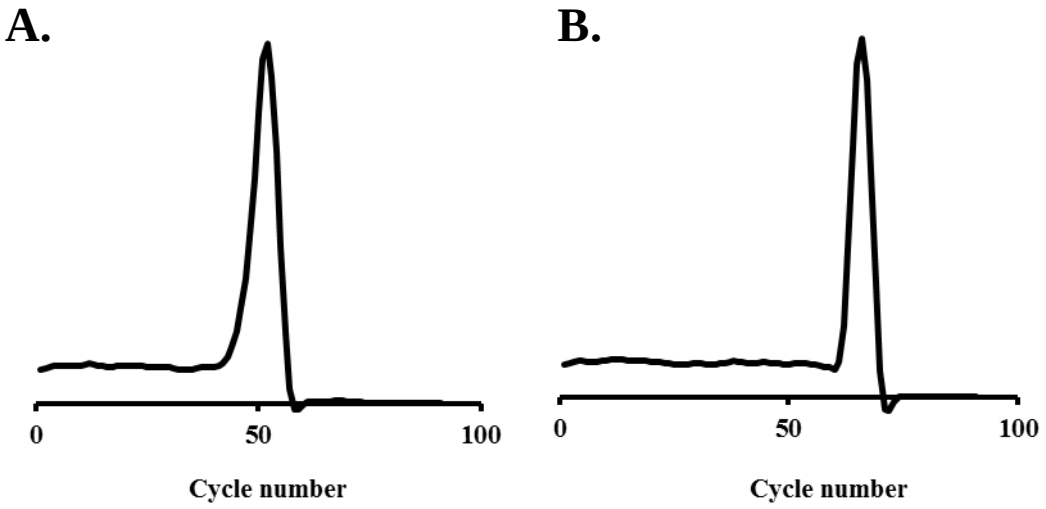

Figure 13: Representative dissociation plots for primers. A: Itgb1 in MIN6 cell sample. B: ICAM-1 in pancreas sample.

4.3.9.3. RNA extraction

RNA was extracted from both cell and pancreas samples using the Qiagen RNeasy Mini Kit. Extraction was performed according to the manufacturer's protocol. For pancreas samples 3 - 6 mg tissue was homogenised in 350 µL RLT lysis buffer using a micropestle before continuing according to the provided protocol. Quantity and quality of RNA was determined using a Nanodrop spectrophotometer; a pure solution of RNA should give a value of between 1.9 and 2.1 for the ratio of the absorbance at 260 nm and 280 nm.

4.3.9.4. Reverse transcription

Oligo-$(dT)_{18}$ primer (270 ng) was added to RNA (200 ng) and the volume made up to 12 µL with nuclease free water. Samples were incubated at 70 °C for 5 min to enable the primer to hybridise to the poly-adenylated tail at the 3' end of mRNA. Solutions were then cooled on ice before 8 µL of a master mix containing 200 U Bioscript Reverse Transcriptase, 10 U RNase inhibitor, 4 µL of 5x buffer and 1 µL of 10mM dNTP mix in nuclease free water was added. Samples were incubated for 60 min at 42 °C, heated at 72 °C for 10 min to terminate the reaction and then cooled at 4 °C. Samples were stored at -20 °C until analysis. Amounts of

RNA used for cDNA preparation was scaled up to 500 ng and 1 µg, as necessary, for tissue samples.

4.3.9.5. Sample analysis

PCR plates were loaded with 2 µL sample, 10 µL SensiMix SYBR Low-ROX, 2.5 pmol of forward and reverse primers and $MgCl_2$ to the optimised concentration in a final volume of 20 µL/well. Plates were sealed and analysed using a real-time PCR machine. Plates were heated to 95 °C for 10 min to activate the hot-start DNA polymerase, 40 cycles of 95 °C x 15 s and 60 °C x 60 s then followed. A standard curve of serially diluted pooled cDNA over the range 0.1 pg – 1000 ng was run alongside assay samples and used for quantification using 18S as a reference gene. RNA was quantified as a ratio to 18S RNA in the sample.

4.4. LC-MS/MS methodologies

4.4.1. Dicarbonyl assay

4.4.1.1. Principle of assay

The amount of MG, glyoxal and 3-DG in cultured cells and media, pancreas and plasma samples was determined by derivatisation with 1,2-diaminobenzene and quantification of the resulting quinoxaline adducts by stable isotopic dilution analysis LC-MS/MS (Figure 14).

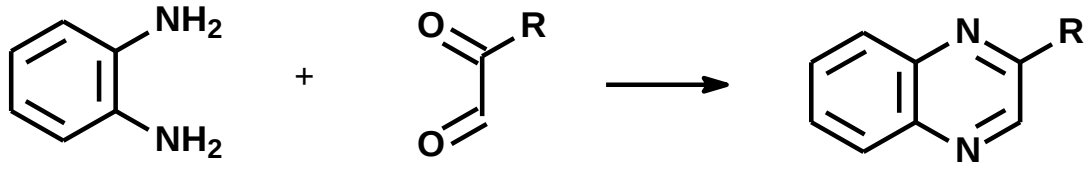

Figure 14: Derivatisation reaction in the dicarbonyl assay. For glyoxal, MG and 3-DG, R = H, CH_3, and $CH_2(CHOH)_2CH_2OH$, respectively.

4.4.1.2. Sample preparation

For collection of MIN6 cell culture samples, cells were trypsinised and then neutralised with trypsin neutralising solution (0.05% trypsin inhibitor, 0.1% BSA).

Cell suspensions were immediately centrifuged to pellet the cells, the supernatant removed and cell pellet samples frozen.

For analysis of cell pellets, 10 µL of cold 20% trichloroacetic acid (TCA) containing 0.9% sodium chloride solution (TCA-saline) was added to cell pellets to de-proteinise the samples and samples were vortex mixed well. An aliquot of water (40 µL) was added. For media samples, an aliquot of culture medium (20 µL) was taken, and 10 µL of TCA-saline and 20 µL of water were added. For plasma samples, an aliquot of plasma (5 µL) was taken, and 10 µL of TCA-saline and 35 µL of water were added. Subsequent preparation was identical for all three types of sample. An aliquot of 3% sodium azide in water (5 µL) was added to inhibit peroxidise activity and isotopic standard cocktail (5 µL containing 2 pmol of each [^{13}C]dicarbonyl) was added to each sample. The samples were vortex mixed and centrifuged (6,000 g, 10 min, 4°C). Supernatant (45 µL) was removed and added to 10 µL derivatisation agent solution (0.5 mM 1,2-diaminobenzene in 200 mM HCl containing 0.5 mM DETAPAC). Pancreas samples (5 - 10 mg) were homogenised using a micropestle in 100 µL TCA-saline and 5 µL of [^{13}C]dicarbonyl standard cocktail was added. Samples were vortex mixed and centrifuged (6,000 g, 10 min, 4°C). An aliquot of supernatant (40 µL) was transferred and 5 µL of 3% sodium azide was added to it. The derivatisation agent solution was added (10 µL 0.5 mM 1,2-diaminobenzene in 200 mM HCl containing 0.5 mM DETAPAC). Samples and standards were left at room temperature in the dark for 4 h for derivatisation to quinoxaline adducts and then analysed by LC-MS/MS. Standards (2 - 20 pmol for MG and 3-DG and 0.2 – 2.0 pmol for glyoxal) were derivatised concurrently with the samples for calibration of the analyte/isotopic standard response ratio.

4.4.1.3. Preparation of calibration standards

Cocktails of dicarbonyl normal standards containing 800 nM MG and 3-DG and 80 nM glyoxal and stable isotopic substituted dicarbonyls containing 400 nM [$^{13}C_3$]MG, [$^{13}C_2$]glyoxal and [$^{13}C_6$]3-DG were prepared and used to prepare standards over the range 0.2 - 2.0 for glyoxal and 2 - 20 pmol for MG and 3-DG - Table 9.

Table 9: Preparation of calibration standards in the assay of dicarbonyls

Calibration solution	MG, 3-DG (pmol)	Glyoxal (pmol)	20% TCA-0.9% NaCl (µL)	Water (µL)	3% sodium azide (µL)	800 nM MG and 3-DG, 80 nM glyoxal (µL)	400 nM [^{13}C]Dicarbonyl (µL)	0.5 mM 1,2-diaminobenzene in HCl-DETAPAC (µL)
0	0	0	10	25	5	-	5	10
1	2	0.2	10	22.5	5	2.5	5	10
2	4	0.4	10	20	5	5	5	10
3	8	0.8	10	15	5	10	5	10
4	12	1.2	10	10	5	15	5	10
5	16	1.6	10	5	5	20	5	10
6	20	2.0	10	-	5	25	5	10

4.4.1.4. LC-MS/MS conditions

LC was performed using a reversed phase ODS BEH C18, 1.7 µm particle size column (100 x 2.1 mm) fitted with a 5 x 2.1 mm pre-column. The column temperature was 30 ℃. Solvents used were 0.1% trifluoroacetic acid (TFA) in water (solvent A) and 0.1% TFA in 50:50 acetonitrile (MeCN): water (solvent B). The elution profile is shown in Table 10.

Table 10: Elution profile for dicarbonyl analysis

Injection Run

Time (min)	Flow rate (mL/min)	Solvent A (%)	Solvent B (%)	Gradient
Initial	0.2	100	0	
10	0.2	0	100	Linear
15	0.4	0	100	Immediate
30	0.4	100	0	Immediate

LC eluate was eluted into the electrospray source of the Waters Quattro Premier XE tandem mass spectrometer. For mass spectrometric detection, the capillary voltage was 0.6 kV, the ion source temperature 120 ℃, the desolvation gas temperature 350 ℃ and cone and desolvation gas flows 146 and 900 L/h respectively. Table 11 lists the optimised multiple reaction monitoring (MRM) conditions used for detection, along with their retention times, cone voltage and collision energy.

Table 11: Optimised MRMs for dicarbonyl analysis

Analyte	Parent ion (Da)	Fragment ion (Da)	Retention time (min)	Cone Voltage (V)	Collision Energy (eV)
MG	145.1	77.1	7.8	24	24
[$^{13}C_3$]MG	148.0	77.1	7.8	24	24
Glyoxal	131.0	77.1	7.1	24	23
[$^{13}C_2$]Glyoxal	133.0	77.1	7.1	24	23
3-DG	235.2	199.0	5.8	21	15
[$^{13}C_6$]3-DG	241.2	205.0	5.8	21	15

4.4.1.5. Data analysis

LC-MS/MS data was integrated using MassLynx software. Representative chromatograms of standard solutions of dicarbonyls are shown in Figure 15. Peak area ratios of analyte/isotopic standard were plotted against analyte amount to construct calibration curves - Figure 16. The amount of dicarbonyls in aliquots assayed was deduced from the peak area ratio using the calibration curves and the amount in original samples was calculated using appropriate dilution factors.

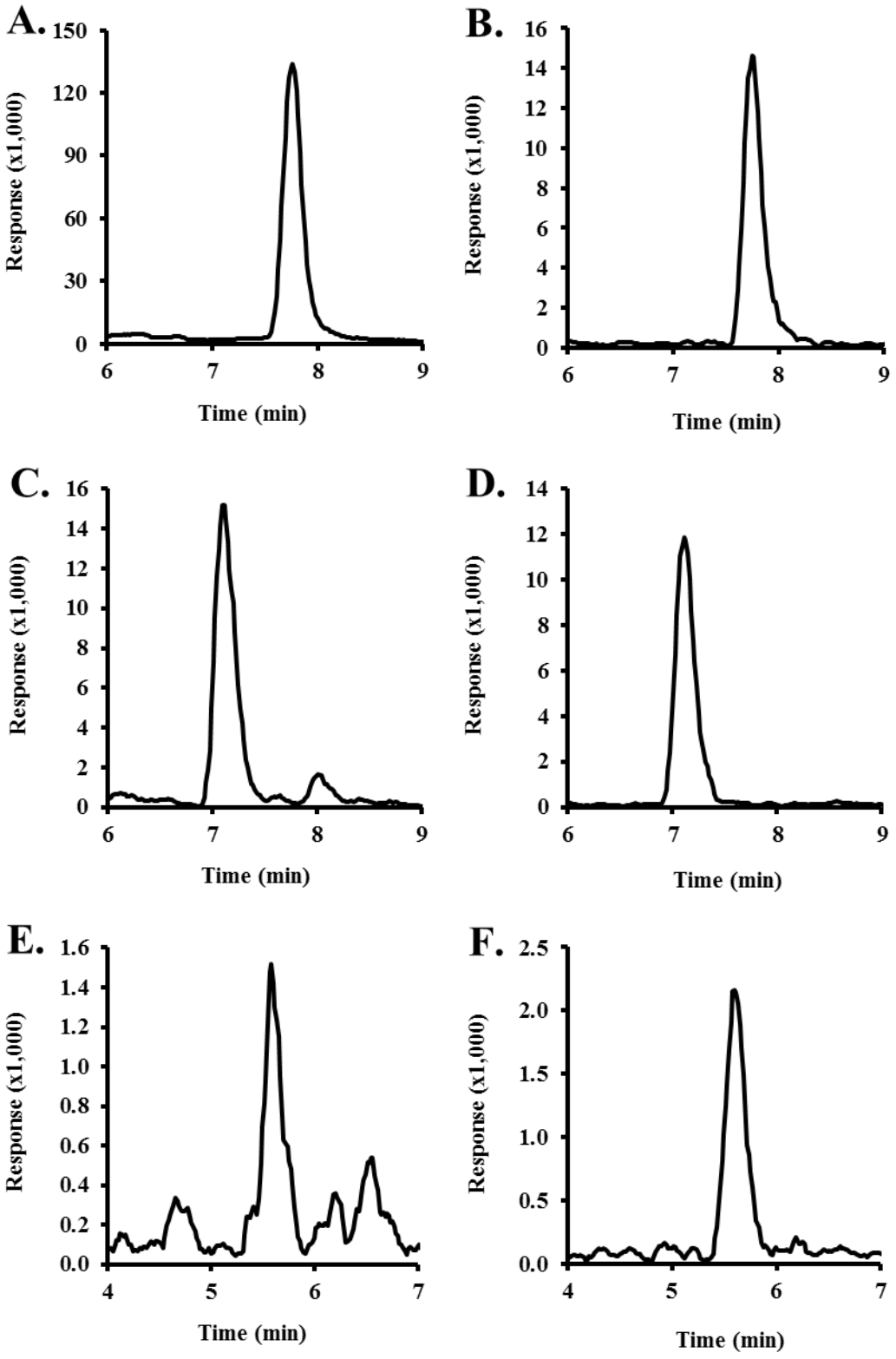

Figure 15: Chromatograms of dicarbonyl compounds in mouse pancreas. A: MG. B: [$^{13}C_3$]MG (2 pmol). C: Glyoxal. D: [$^{13}C_2$]Glyoxal (2 pmol). E: 3-DG. F: [$^{13}C_6$]3-DG (2 pmol).

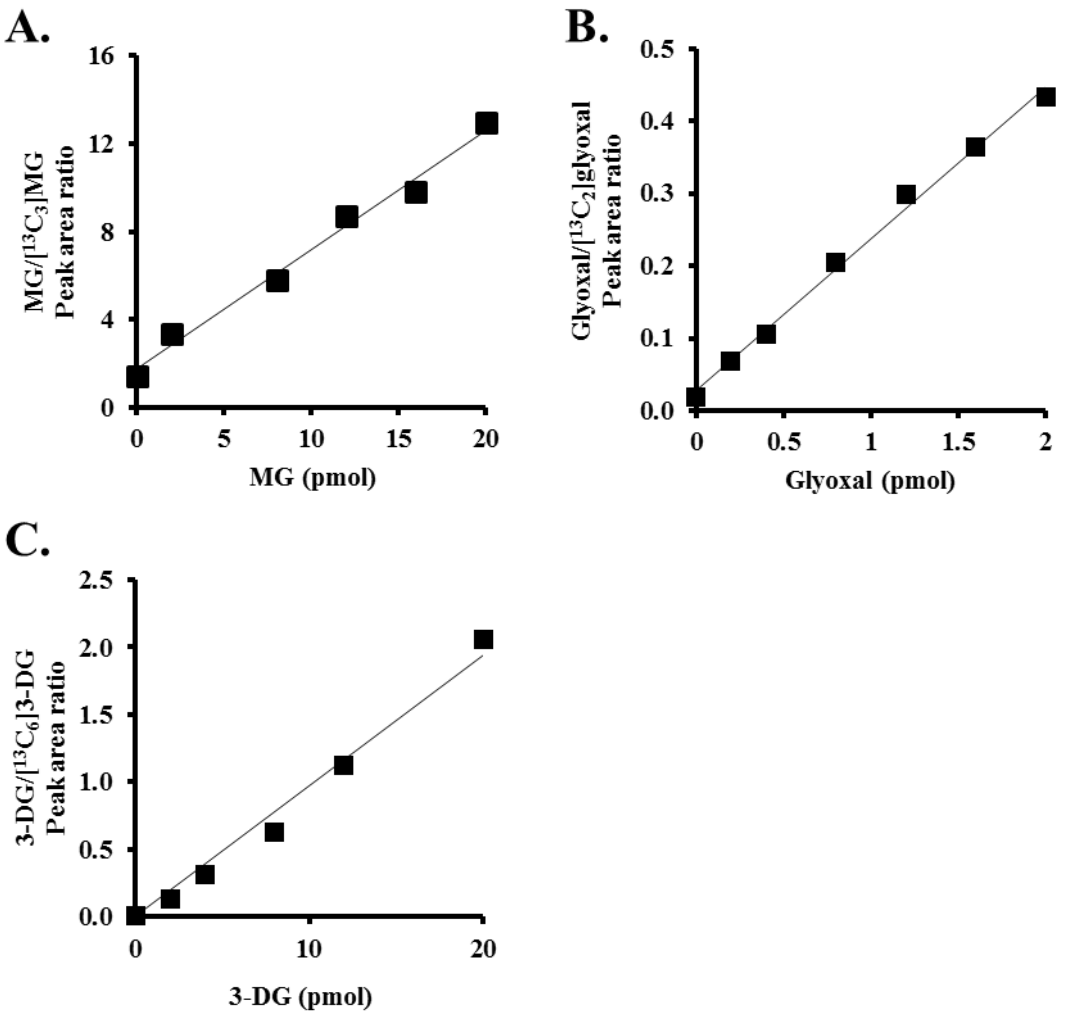

Figure 16: Typical calibration curves of dicarbonyls by LC-MS/MS. A. Standard curve for MG. Regression of Peak area ratio on amount of MG (pmol) gave: Peak area ratio = ((0.544 ± 0.030) x MG (pmol)) + 1.75 ± 0.007; r^2 = 0.988; n = 6. B. Standard curve for Glyoxal. Regression of Peak area ratio on amount of glyoxal (pmol) gave: Peak area ratio = ((0.211 ± 0.007) x glyoxal (pmol)) + 0.027 ± 0.0074; r^2 = 0.995; n = 7. C. Standard curve for 3-DG. Regression of Peak area ratio on amount of 3-DG (pmol) gave: Peak area ratio = ((0.0971 ± 0.0050) x 3-DG (pmol)) ± 0.0515; r^2 = 0.984; n = 6.

4.4.2. Glutathione assay

4.4.2.1. Principle of assay

A stable isotopic dilution analysis LC-MS/MS method for the detection and quantification of GSH, GSSG and S-D-lactoylglutathione in cell culture samples was developed.

4.4.2.2. Synthesis of [$^{13}C_4{}^{15}N_2$]GSSG

Stable labelled [*glycine*-$^{13}C_2{}^{15}N_1$]GSH was oxidised using diamide (Kosower, *et al.*, 1969) to obtain stable labelled [$^{13}C_4{}^{15}N_2$]GSSG for use in the LC-MS/MS method to quantify cellular GSSG.

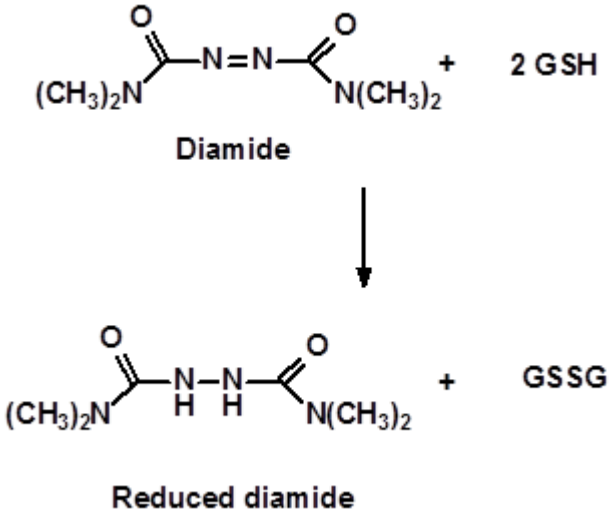

An aliquot of [$^{13}C_2{}^{15}N_1$]GSH solution (3.2 mM, 100 µL) and 10 mM diamide in methanol (30 µL) were added to 100 µL of 10 mM sodium phosphate buffer, pH 7.4 and incubated at 37°C for 30 min. The reaction mixture was purified by elution onto a 500 mg strong anion-exchange solid-phase extraction (SAX SPE) cartridge in the formate form. [$^{13}C_4{}^{15}N_2$]GSSG was retained on the SAX-SPE cartridge but diamide and reduced diamide were not. The SAX-SPE cartridge was washed with 10 mL water to remove the diamide and reduced diamide. [$^{13}C_4{}^{15}N_2$]GSSG was collected by eluting off the SAX-SPE cartridge with 5 mL 100 mM formic acid. The solution was lyophilised to dryness, reconstituted in water (1 mL) and filtered through a 0.2 µm nylon filter. The concentration of [$^{13}C_4{}^{15}N_2$]GSSG was deduced by isotopic dilution analysis with known amounts of GSSG. The synthesis yield was 28%.

4.4.2.3. Preparation of calibration standards

Stock solutions of GSH, GSSG, S-D-lactoylglutathione and [*glycine*-$^{13}C_2{}^{15}N_1$]GSH were prepared in filtered water to 1 mg/mL. Further dilutions of these stocks were prepared in 0.1% TFA in water. Calibration standards were prepared for sample analysis over the range 100 - 2000 pmol and 5 - 100 pmol for GSH and GSSG respectively (Table 12) by the protocol detailed in Table 13.

Table 12: Calibration range for glutathione analysis

Calibration solution	GSH (pmol)	GSSG (pmol)	[$^{13}C_2{}^{15}N_1$]GSH (pmol)	[$^{13}C_4{}^{15}N_2$]GSSG (pmol)
0	0	0	100	20
1	100	5	100	20
2	200	10	100	20
3	400	20	100	20
4	1000	50	100	20
5	1600	80	100	20
6	2000	100	100	20

Table 13: Preparation of glutathione standards

Calibration solution	GSH (µL)		GSSG (µL)		0.1% TFA in water (µL)	12.5% TCA (µL)	Isotopic cocktail (µL)
	40 µM	200 µM	2 µM	10 µM			
0	-	-	-	-	20	20	10
1	2.5	-	2.5	-	15	20	10
2	5	-	5	-	10	20	10
3	10	-	10	-	-	20	10
4	-	5	-	5	10	20	10
5	-	8	-	8	4	20	10
6	-	10	-	10	-	20	10

4.4.2.4. Preparation of samples

Pelleted cells were resuspended in 40 µL of a solution containing 10% TCA, 0.15% NaCl and 0.25% sodium azide in water. This solution precipitates proteins and acts as a preservative by inhibiting peroxidase activity in the sample; residual peroxidase activity otherwise remains in TCA extracts. Samples were centrifuged at 20,000 g for 30 min at 4 °C and aliquots of supernatant (10 µL) transferred to vials for LC-MS/MS analysis with the addition of 10 µL isotopic standard cocktail.

4.4.2.5. LC-MS/MS conditions

Two graphite Hypercarb HPLC columns were used in series (50 x 2.1 mm and 250 x 2.1 mm, particle size 5 µm) with column temperature of 30 °C. Solvents used were 0.1% TFA in water (Solvent A) and 0.1% TFA in 50:50 MeCN: water (Solvent B1) and 0.1% TFA in 50:50 Tetrahydrafuran (THF): water (Solvent B2). The gradients used during the analytical run and post run are displayed in Table 14.

Table 14: Elution profile for glutathione analysis

Time (min)	Flow rate (mL/min)	Solvent A1 (%)	Solvent B1 (%)	Solvent B2 (%)	Gradient
Injection Run					
Initial	0.2	100	0	-	
1	0.2	100	0	-	Isocratic
15	0.2	40	60	-	Linear
16	0.2	40	60	-	Isocratic
Postrun					
Initial	0.4	0	-	100	
10	0.4	0	-	100	Isocratic
25	0.4	100	-	0	Immediate

Flow from the column was eluted into the electrospray source of the MS/MS detector between 4 and 16 min for data collection. Mass spectrometric analysis was performed using electrospray positive ionisation mode. For mass spectrometric detection, the capillary voltage was 3.4 kV, the ion source temperature 120 °C, the desolvation gas temperature 350 °C and cone and desolvation gas flows 146 and 550 L/h respectively. Table 15 shows the optimised MRM conditions used for detection,

along with their retention times, cone voltage and collision energy. Fragmentation analysis of the MRM transitions is detailed in Figure 17.

Table 15: Optimised MRMs for glutathione analysis

Analyte	Parent ion (Da)	Fragment ion (Da)	Retention time (min)	Cone Voltage (V)	Collision Energy (eV)
GSH	308.2	179.1	11.7	30	13
[$^{13}C_2{}^{15}N_1$]GSH	311.2	182.1	11.7	30	13
GSSG	613.2	483.7	14.4	52	18
[$^{13}C_4{}^{15}N_2$]GSSG	619.2	489.7	14.4	52	18
S-D-lactoylglutathione	380.2	76.2	13.1	32	35

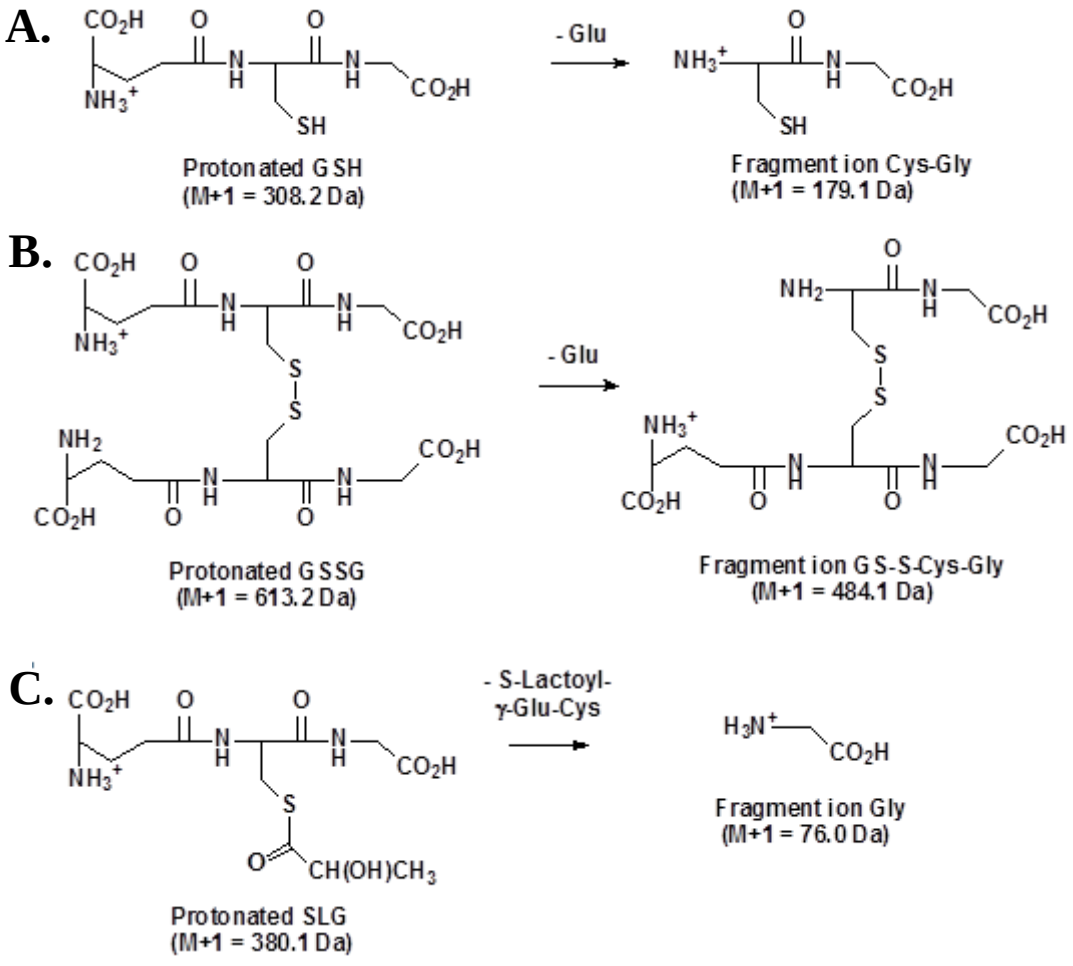

Figure 17: Fragmentation of glutathione. MRM mass transition fragmentations: A. GSH, B. GSSG and C. S-D-lactoylglutathione.

4.4.2.6. Data analysis

Data analysis was performed using MassLynx software. Specimen chromatograms of GSH and GSSG are shown in Figure 18. Calibration curves were constructed plotting peak area ratio of analyte/isotopic standard against analyte concentration as shown in Figure 19. The amount of glutathione in assayed aliquots was deduced using the peak area ratio and the appropriate calibration curve and the amount in the original sample calculated taking account of any dilution factors.

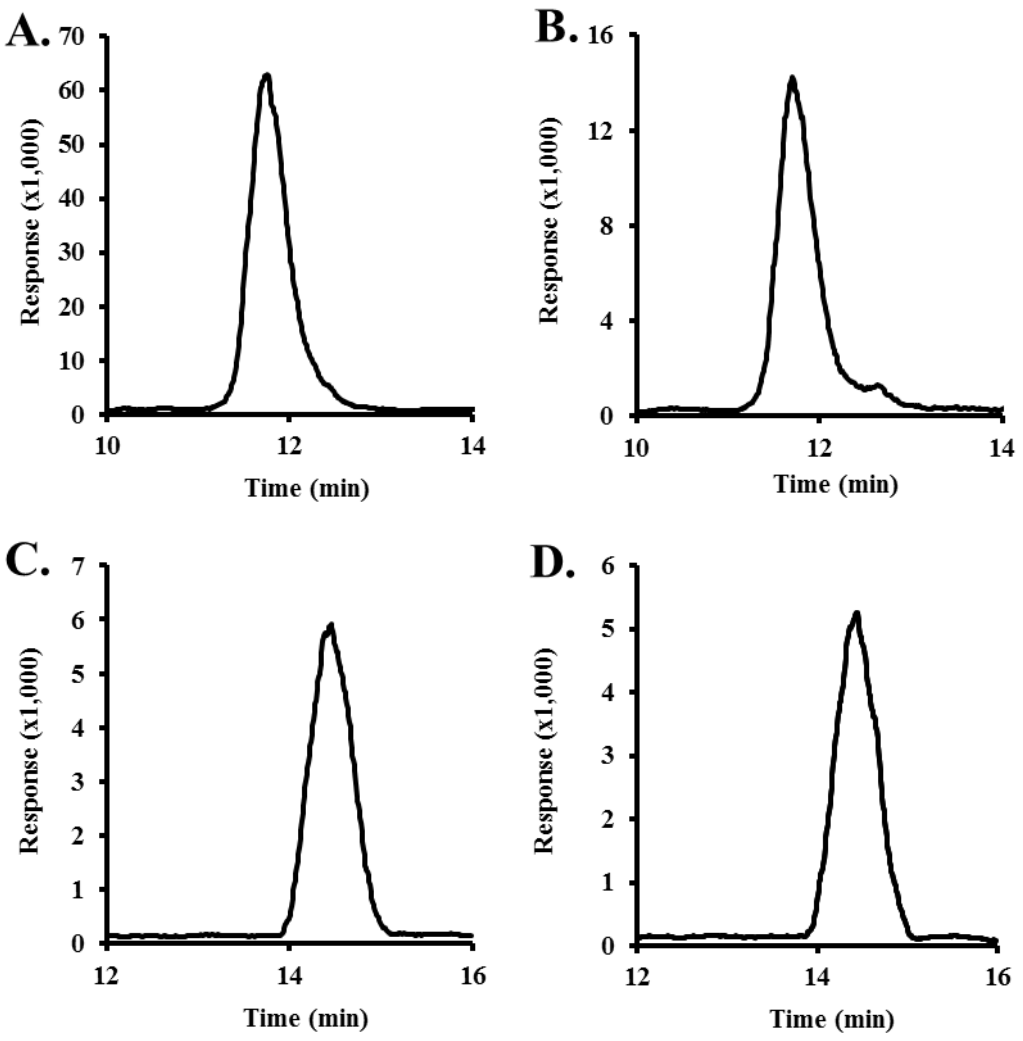

Figure 18: Representative chromatograms in of glutathione in MIN6 cells. A: GSH. B: [$^{13}C_2{}^{15}N_1$]GSH (100 pmol). C: GSSG. D: [$^{13}C_4{}^{15}N_2$]GSSG (20 pmol).

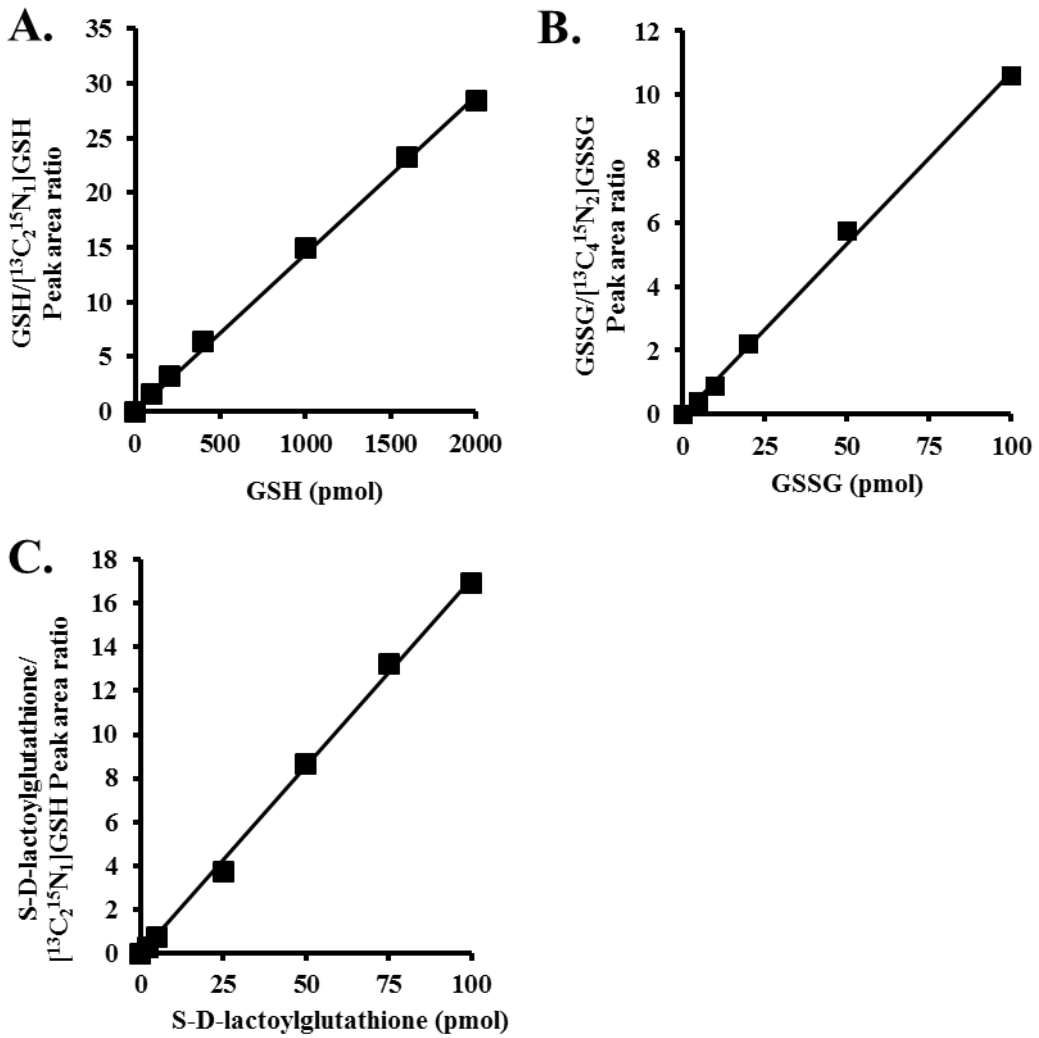

Figure 19: Typical calibration curves of glutathione by LC-MS/MS. A: Standard curve for GSH. Regression of Peak area ratio on amount of GSH (pmol) gave: Peak area ratio = ((0.0145 ± 0.002) x GSH (pmol)) ± 0.180; r^2 = 0.999; n = 7. B: Standard curve for GSSG. Regression of Peak area ratio on amount of GSSG (pmol) gave: Peak area ratio = ((0.1072 ± 0.0027) x GSSG (pmol)) ± 0.124; r^2 = 0.998; n = 6. C: Standard curve for S-D-lactoylglutathione. Regression of Peak area ratio on amount of S-D-lactoylglutathione (pmol) gave: Peak area ratio = ((0.1711 ± 0.0032) x S-D-lactoylglutathione (pmol)) ± 0.167; r^2 = 0.998; n = 7.

4.4.2.7. Limit of detection, recovery and intra-batch coefficient of variation

The calibration curves for GSH, GSSG and S-D-lactoylglutathione were linear (see Figure 19) and reproducible when prepared and assayed on different days. The limit of detection (LoD) was 0.92 pmol, 1.46 pmol and 0.54 pmol for GSH, GSSG and S-D-lactoylglutathione respectively. Example chromatograms of GSH and GSSG in MIN6 cells are shown in Figure 18. Analytical recovery was assessed by addition of 500 pmol GSH and 50 pmol GSSG and S-D-lactoylglutathione to cell

samples. Analytical recoveries were: GSH, 97.1 ± 1.6%; GSSG, 92.7 ± 5.7%; and S-D-lactoylglutathione, 99.3 ± 14.1%. Intra-batch coefficient of variation was determined by analysis of replicate samples. Intra-batch coefficient of variation was: GSH, 8.8% (n = 6); and GSSG, 10.9% (n = 6).

4.4.3. Assay of protein glycation, oxidation and nitration adducts

4.4.3.1. Principle of assay

The glycation, oxidation and nitration adduct and the corresponding amino acid residue content of cytosolic protein extracts of cultured cells and mouse pancreas and plasma protein were measured, after exhaustive enzymatic hydrolysis, by stable isotopic dilution analysis LC-MS/MS as described (Thornalley, *et al.*, 2003). Glycation, oxidation and nitration free adduct concentration of culture medium, mouse pancreas and plasma were measured similarly without exhaustive enzymatic hydrolysis.

4.4.3.2. Sample preparation

Extraction of soluble protein

Trypsinised MIN6 cells were washed 3 times in PBS and then resuspended in 250 µL 10 mM sodium phosphate buffer, pH 7.4, sonicated on ice (110 W, 30 sec) and centrifuged (20,000 g, 30 min, 4°C). The supernatant was transferred to a 10 kDa ultrafilter and washed by diafiltration - 4 cycles of dilution to 500 µL with argon-purged water and concentration to 50 µL by centrifugation (14,000 g, 20 min, 4 °C). The resultant washed protein concentrate was quantified by Bradford assay and subjected to exhaustive enzymatic hydrolysis. Culture media samples were filtered through 3 kDa ultrafilters (14,000 g, 20 min, 4 °C) and the resulting ultrafiltrate analysed for protein glycation, oxidation and nitration free adducts.

Pancreas samples (approximately 10 mg wet weight) were homogenised in 250 µL 10 mM sodium phosphate buffer, pH 7.4 and 4 °C and centrifuged (20,000 g, 30 min, 4 °C) to sediment the membranes. The resulting supernatants were transferred to 10 kDa ultrafilters. Plasma samples (5 µL) were diluted with 45 µL water and transferred to 10 kDa ultrafilters. Samples were washed by diafiltration. The resultant protein was quantified by Bradford assay and hydrolysed by exhaustive

enzymatic hydrolysis. The first filtrates were retained for analysis as pancreatic and plasma filtrate.

Enzymatic hydrolysis of soluble protein

Protein (100 µg) was transferred to vials for hydrolysis and all samples/controls in a sample set were made up to the same volume (20 - 40 µL) using argon-purged filtered water. Samples were argon-purged using a centrifugal evaporator and the remaining procedure carried out on the CTC-PAL sample preparation automation system. Aliquots of HCl (100 mM, 10 µL), pepsin (2 mg/mL in 20 mM HCl, 5 µL) and the antioxidant thymol (1 mg/mL in 20 mM HCl, 5 µL) were added and the samples incubated for 24 h at 37 °C. Samples were buffered and neutralised by the additions of potassium phosphate buffer (100 mM, pH 7.4, 12.5 µL) and potassium hydroxide (260 mM, 5 µL) respectively. Pronase E (2 mg/mL in 10 mM potassium phosphate buffer, pH 7.4, 5 µL) and prolidase (2 mg/mL in 10 mM potassium phosphate buffer, pH 7.4, 5 µL) were added and the samples incubated for a further 24 h at 37 °C. Aliquots of aminopeptidase (2 mg/mL in 10 mM potassium phosphate buffer, pH 7.4, 5 µL) and prolidase (2 mg/mL in 10 mM potassium phosphate buffer, pH 7.4, 5 µL) were added, the samples incubated for a further 48 h at 37 °C and frozen at -20 °C until subsequent LC-MS/MS analysis. Triplicate samples of water and human serum albumin (HSA) (100 µg) were hydrolysed alongside analytical samples as hydrolysis controls. These were made up to the same volume as protein samples.

Extraction of ECM protein

Pancreas samples (approximately 2 mg) were homogenised in 100 µL of ice-cold PBS and centrifuged at 10,000 g for 30 min at 4 °C. The supernatant was removed and pellets were washed with two cycles of 500 µL PBS addition and centrifugation (6,000 g, 15 min, 4 °C). Lipid components were then extracted with 500 µL chloroform: methanol (2:1 v/v) for 24 h at 4 °C whilst shaking continuously (Dobler, *et al.*, 2006; Folch, *et al.*, 1957). Samples were centrifuged (6,000 g, 15 min, 4 °C) and the chloroform-methanol mixture removed. Pellets were washed with two cycles of 500 µL water addition and centrifugation (6,000 g, 15 min, 4 °C) and the pellets stored at -20 °C until subsequent enzymatic hydrolysis.

Enzymatic hydrolysis of ECM protein

The enzymatic hydrolysis protocol used for soluble cellular proteins was adapted for hydrolysis of insoluble matrix proteins. Argon-purged filtered water (40 µL) was added to the pelleted protein. Aliquots of thymol (1 mg/mL in 10 mM TES buffer, pH 7.4, 5 µL) and bacterial collagenase (1 mg/mL in 50 mM TES buffer, pH 7.4 with 5 mM $CaCl_2$, 10 µL) were added, the sample purged with argon in a centrifugal evaporator and incubated for 24 h at 37 °C with shaking. Pronase E solution (2 mg/mL in 10 mM TES buffer, pH 7.4, 5 µL) and penicillin/streptomycin (1000 U/mL and 1 mg/mL in 10 mM TES buffer, pH 7.4, 5 µL) were added, the samples again argon purged in a centrifugal evaporator and incubated for 24 h at 37 °C with shaking. Further aliquots of aminopeptidase (2 mg/mL in 10 mM TES buffer, pH 7.4, 5 µL) and prolidase (2 mg/mL in 10 mM TES buffer, pH 7.4, 5 µL) were added to give a final hydrolysate volume of 75 µL. Samples were purged with argon in a centrifugal evaporator and incubated, shaking, at 37 °C for 48 h. Hydrolysates were frozen at -20 °C until subsequent LC-MS/MS analysis. Additional control samples were run: water alone (no protein), 100 µg and 200 µg HSA in 40 µL of argon purged water – to investigate the effect of protein concentration on autohydrolysis of hydrolytic enzymes.

Preparation of samples for analysis

Samples were prepared for LC-MS/MS analysis as detailed in Table 16. MIN6 culture samples and pancreatic hydrolysed protein were analysed on the Quattro Premier mass spectrometer. Pancreatic filtrates, plasma filtrates and plasma samples were all analysed on the Xevo TQ-S system.

Table 16: Sample preparation for analysis of protein glycation, oxidation and nitration adducts

Sample type	Sample (µL)	Isotopic standard cocktail (µL)	0.1% TFA in water (µL)
MIN6 protein hydrolysate	25	25	-
MIN6 Culture media filtrate	25	25	-
Pancreatic protein hydrolysate	25	25	-
Pancreatic ECM protein	12.5	25	12.5
Pancreatic filtrate	10	25	15
Plasma hydrolysate	5	25	20
Plasma filtrate	10	25	15

4.4.3.3. Preparation of calibration standards

Calibration cocktail stocks of both analytes and isotopically labelled analytes were prepared. These were diluted as shown in Table 17. Different stocks were prepared for calibrations and samples to be run on the Quattro Premier and the more sensitive Xevo TQ-S system, enabling the same dilutions to be used for both. Details of the calibration range for all analytes for the two instruments are listed in Table 18 and Table 19 for the Quattro Premier and Xevo TQ-S respectively.

Table 17: Preparation of calibration standards for analysis of protein glycation, oxidation and nitration adducts

Calibration solution	Standard cocktail (µL)	0.1 % TFA in water (µL)	Isotopic cocktail (µL)	Total volume (µL)
0	0	25.0	25.0	50.0
1	1.25	23.75	25.0	50.0
2	2.5	22.5	25.0	50.0
3	6.3	18.7	25.0	50.0
4	12.5	12.5	25.0	50.0
5	18.8	6.2	25.0	50.0
6	25.0	0	25.0	50.0

Table 18: Calibration range for analysis of protein glycation, oxidation and nitration adducts (Quattro Premier)

Calibration solution	0	1	2	3	4	5	6	Isotopic standard
Analyte	pmol	pmol	pmol	pmol	pmol	pmol	pmol	pmol
MG-H1	0	2.50	5.00	12.5	25.0	37.5	50.0	25.0
CEL	0	0.50	1.00	2.5	5.0	7.5	10.0	5.0
MOLD	0	0.50	1.00	2.5	5.0	7.5	10.0	5.0
G-H1	0	0.50	1.00	2.5	5.0	7.5	10.0	5.0
CML	0	1.25	2.50	6.25	12.5	18.75	25.0	5.0
CMA	0	0.50	1.00	2.5	5.0	7.5	10.0	2.5
3DG-H	0	2.50	5.00	12.5	25.0	37.5	50.0	25.0
FL	0	5.00	10.0	25.0	50.0	75.0	100.0	6.0
Glucosepane	0	0.50	1.00	2.5	5.0	7.5	10.0	5.0
Pentosidine	0	0.05	0.10	0.25	0.50	0.75	1.00	n/a
MetSO	0	2.50	5.00	12.5	25.0	37.5	50.0	25.0
Dityrosine	0	0.50	1.00	2.5	5.0	7.5	10.0	5.0
NFK	0	0.50	1.00	2.5	5.0	7.5	10.0	5.0
Ornithine	0	2.50	5.00	12.5	25.0	37.5	50.0	50.0
3-NT	0	0.50	1.00	2.5	5.0	7.5	10.0	5.0

AASA	0	0.50	1.00	2.5	5.0	7.5	10.0	5.0
GSA	0	0.50	1.00	2.5	5.0	7.5	10.0	5.0
	nmol	nmol	nmol	nmol	nmol	nmol	nmol	nmol
Arginine	0	1.0	2.0	5.0	10.0	15.0	20.0	5.0
Lysine	0	1.0	2.0	5.0	10.0	15.0	20.0	5.0
Methionine	0	1.0	2.0	5.0	10.0	15.0	20.0	5.0
Tyrosine	0	0.2	0.4	1.0	2.0	3.0	4.0	2.0
Tryptophan	0	0.2	0.4	1.0	2.0	3.0	4.0	1.0
Valine	0	1.0	2.0	5.0	10.0	15.0	20.0	5.0

Table 19: Calibration range for analysis of protein glycation, oxidation and nitration adducts (Xevo TQ-S)

Calibration solution	0	1	2	3	4	5	6	Isotopic standard
Analyte	pmol	pmol	pmol	pmol	pmol	pmol	pmol	pmol
MG-H1	0	0.125	0.250	0.625	1.250	1.875	2.500	1.25
CEL	0	0.025	0.050	0.125	0.250	0.375	0.500	0.25
MOLD	0	0.025	0.050	0.125	0.250	0.375	0.500	0.25
G-H1	0	0.025	0.050	0.125	0.250	0.375	0.500	0.25
CML	0	0.125	0.250	0.625	1.250	1.875	2.500	0.25

CMA	0	0.025	0.050	0.125	0.250	0.375	0.500	0.25
3DG-H	0	0.125	0.250	0.625	1.250	1.875	2.500	1.25
FL	0	0.250	0.500	1.250	2.500	3.750	5.000	0.30
Glucosepane	0	0.025	0.050	0.125	0.250	0.375	0.500	0.25
Pentosidine	0	0.0025	0.005	0.0125	0.025	0.0375	0.050	n/a
MetSO	0	0.125	0.250	0.625	1.250	1.875	2.500	1.25
Dityrosine	0	0.025	0.050	0.125	0.250	0.375	0.500	0.25
NFK	0	0.025	0.050	0.125	0.250	0.375	0.500	0.25
Ornithine	0	0.125	0.250	0.625	1.250	1.875	2.500	2.50
3-NT	0	0.025	0.050	0.125	0.250	0.375	0.500	0.25
AASA	0	0.025	0.050	0.125	0.250	0.375	0.500	2.50
GSA	0	0.025	0.050	0.125	0.250	0.375	0.500	2.50
	nmol	nmol	nmol	nmol	nmol	nmol	nmol	nmol
Arginine	0	0.05	0.10	0.25	0.50	0.75	1.00	0.25
Lysine	0	0.05	0.10	0.25	0.50	0.75	1.00	0.25
Methionine	0	0.05	0.10	0.25	0.50	0.75	1.00	0.25
Tyrosine	0	0.01	0.02	0.05	0.10	0.15	0.20	0.10
Tryptophan	0	0.01	0.02	0.05	0.10	0.15	0.20	0.05
Valine	0	0.05	0.10	0.25	0.50	0.75	1.00	0.25

4.4.3.4. LC-MS/MS conditions (Quattro Premier)

Two graphite Hypercarb HPLC columns were used in series (50 x 2.1 mm and 250 x 2.1 mm, particle size 5 µm) with column temperature of 30 °C. Solvents used were 0.1% TFA in water (Solvent A) and 0.1% TFA in 50:50 MeCN: water (Solvent B1) and 0.1% TFA in 50:50 THF: water (Solvent B2). The gradients used during the analytical run and post run are detailed in Table 20. Flow went through both columns in series until 10.8 min. From 10.8 min until 26 min eluate from the 50 x 2.1 mm column was eluted into the mass spectrometer detector, and for the remainder of the analytical run eluate was from both columns in series.

Table 20: Elution profile for analysis of protein glycation, oxidation and nitration adducts (Quattro Premier)

Injection Run					
Time (min)	Flow rate (mL/min)	Solvent A1 (%)	Solvent B1 (%)	Solvent B2 (%)	Gradient
Initial	0.2	100	0	-	
5	0.2	100	0	-	
8	0.2	97	3	-	Linear
12	0.2	97	3	-	Isocratic
15	0.2	83	17	-	Linear
18	0.2	83	17	-	Isocratic
24	0.2	20	80	-	Linear
26	0.2	97	3	-	Linear
27	0.2	50	50	-	Linear
35	0.2	50	50	-	Isocratic
Postrun					
Initial	0.4	0	-	100	
10	0.4	0	-	100	Isocratic
20	0.2	0	-	100	Immediate
25	0.2	100		0	Immediate
40	0.4	100		0	Immediate

Flow from the column was eluted into the electrospray source of the MS/MS detector between 4 and 35 min for data collection. Mass spectrometric analysis was performed using electrospray positive ionisation mode. For mass spectrometric detection, the capillary voltage was 1.0 kV, the ion source temperature 120 ℃, the desolvation gas temperature 350 °C and cone and desolvation gas flows 96 and 900 L/h respectively. Table 21 lists the optimised MRM conditions used for detection, along with their retention times, cone voltage and collision energy.

Table 21: Optimised MRM mass transitions for analysis of protein glycation, oxidation and nitration adducts (Quattro Premier)

Analyte	Parent ion (Da)	Fragment ion (Da)	Retention time (min)	Cone Voltage (V)	Collision Energy (eV)
Arginine	175.1	70.1	31.2	30	24
[$^{15}N_2$]Arginine	177.1	70.1	31.2	30	24
Lysine	147.1	84.1	5.7	20	18
[$^{13}C_6$]Lysine	153.1	89.1	5.7	20	18
Methionine	150.1	104.0	31.4	21	13
[$^{2}H_3$]Methionine	153.1	107.0	31.4	21	13
Tyrosine	181.9	136.0	18.8	20	16
[$^{2}H_4$]Tyrosine	185.9	140.0	18.8	20	16
Tryptophan	205.2	158.8	23.8	20	20
[$^{15}N_2$]Tryptophan	207.2	160.8	23.8	20	20
Valine	117.8	72.0	8.5	19	8
[$^{2}H_8$]Valine	125.8	80.0	8.5	19	8
MG-H1	229.0	114.0	11.3	30	18
[$^{15}N_2$]MG-H1	231.0	116.0	11.3	30	18
CEL	219.0	130.0	30.7	25	16
[$^{13}C_6$]CEL	225.0	136.0	30.7	25	16
MOLD	341.0	84.1	14.8	48	33
[$^{2}H_8$]MOLD	349.0	88.1	14.8	48	33
G-H1	214.9	100.2	12.9	25	18
[$^{15}N_2$]G-H1	216.9	102.2	12.9	25	18
CML	204.9	84.1	30.5	24	19

[$^{13}C_6$]CML	210.9	89.1	30.5	24	19
CMA	233.0	70.1	12.4	30	27
[$^{13}C_2$]CMA	235.0	70.1	12.4	30	27
3DG-H	319.0	70.1	11.3	45	34
[$^{15}N_2$]3DG-H	321.0	70.1	11.3	45	34
FL	291.0	84.1	30.5	35	32
[$^{2}H_4$]FL	295.0	88.1	30.5	35	32
Glucosepane	429.2	269.2	16.4	49	30
[$^{13}C_6$]Glucosepane	435.2	275.1	16.4	49	30
MetSO	166.1	56.2	8.6	21	20
[$^{2}H_3$]MetSO	169.1	56.2	8.6	21	20
Dityrosine	361.0	315.1	20.5	35	22
[$^{2}H_6$]Dityrosine	367.0	321.1	20.5	35	22
NFK	237.0	191.1	21.7	20	11
[$^{15}N_2$]NFK	239.0	193.1	21.7	20	11
Ornithine	133.1	70.1	5.2	20	13
[$^{2}H_6$]Ornithine	139.1	76.1	5.2	20	13
3-NT	226.9	180.9	23.5	25	18
[$^{2}H_3$]3-NT	229.9	183.9	23.5	25	18
AASA	127.9	82.0	31.3	26	12
[$^{2}H_3$]-AAA	164.9	146.8	31.7	17	10
GSA	113.8	67.9	31.0	26	12

Pentosidine	Ex 320 nm	Em 365 nm	20.7
NFK	Ex 320 nm	Em 424 nm	21.2
Dityrosine	Ex 284 nm	Em 407 nm	20.3

4.4.3.5. LC-MS/MS conditions (Xevo TQ-S)

A similar HPLC elution gradient and postrun wash was optimised as used with the Quattro Premier system – section 4.4.3.4 above. Mass spectrometric analysis was performed using electrospray positive ionisation mode. For mass spectrometric detection, the capillary voltage was 0.5 kV, the ion source temperature 150 °C, the desolvation gas temperature 500 °C and cone and desolvation gas flows

150 and 1000 L/h respectively. Similar MRM mass transitions were optimised and established for quantification on the Xevo TQ-S system as optimised on the Quattro Premier (Table 21).

4.4.3.6. Data analysis

Data analysis was performed using MassLynx software. Calibration curves were constructed by plotting peak area ratio of analyte/isotopic standard against analyte concentration as shown in Figure 20. Example chromatograms are displayed in Figure 21. The amounts in assayed aliquots were deduced using the peak area ratio and the appropriate calibration curve. Concentrations of glycation, oxidation and nitration free adducts in filtrates (from culture media, plasma and pancreas) were calculated using appropriate dilution factors. Glycation, oxidation and nitration adduct residues in hydrolysed protein samples were normalised to the appropriate amino acid, taking into account any necessary correction factors for hydrolysis.

In the analysis of protein glycation, oxidation and nitration adduct residues of proteins, a robust basis for correction of the contribution to protein glycation, oxidation and nitration adducts by autohydrolysis of proteases is required. Hydrolysis in protein free blanks overestimates this contribution since autohydrolysis of proteases is faster when no protein substrate is present. An initial strategy employed was correction from digestion of a polypeptide that could not contain protein glycation, oxidation and nitration adduct residues – such as polythreonine. This however, only presents the proteases with one type of peptide bond – different from all other samples. The current method uses triplicate digests of zero protein blanks and a known amount of HSA to quantify an amino acid that is not modified – valine. In the HSA digests the amount of valine detected is that from HSA + autohydrolysis of proteases (V_{HSA} + $V_{Proteases\ (Protein)}$). In the zero protein blanks the valine detected is only from autohydrolysis ($V_{Proteases\ (Blank)}$). The valine liberated from proteases in the presence of HSA is decreased by the suppression of autohydrolysis by presence of HSA. The factor $V_{Proteases\ (Protein)}$/ $V_{Proteases\ (Blank)}$, typically *ca.* 0.7, is applied to the amount of protein glycation, oxidation and nitration adducts quantified in the blank to produce correction factors to apply to sample protein digests. That is, the presence of protein substrate slows autohydrolysis of proteases by *ca*. 30%. This correction factor is determined for each batch of samples for enzymatic hydrolysis.

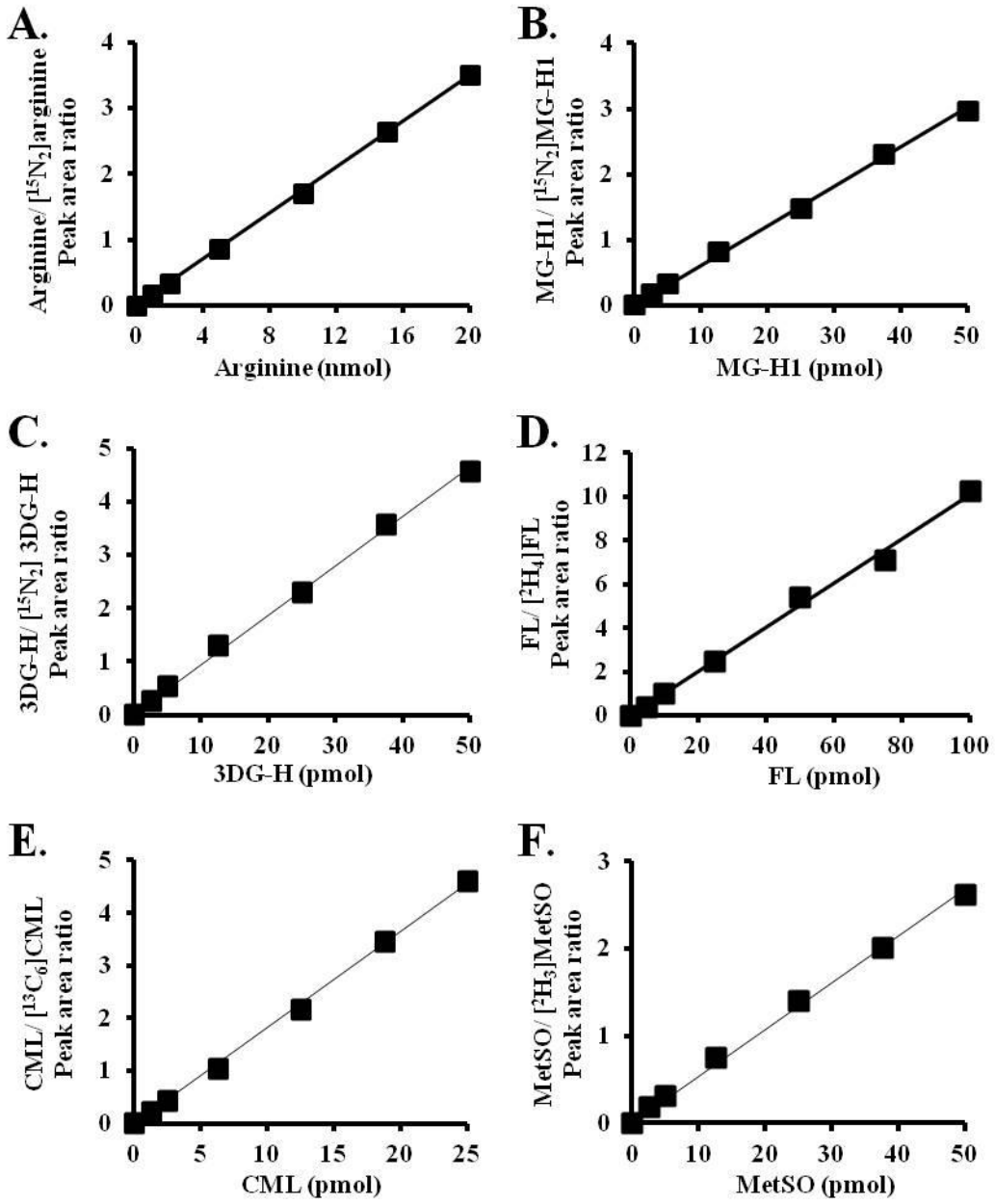

Figure 20: Typical calibration curves for glycation and oxidation adduct residues and amino acids by LC-MS/MS. A: Standard curve for arginine. Regression of Peak area ratio on amount of arginine (nmol) gave: Peak area ratio = (0.175 ± 0.001 x arginine (nmol)) ± 0.0105; r^2 = 1.00 (n = 7). B: Standard curve for MG-H1. Regression of Peak area ratio on amount of MG-H1 (pmol) gave: Peak area ratio = (0.0605 ± 0.0008 x MG-H1 (pmol)) ± 0.0220; r^2 = 0.998 (n = 7). C: Standard curve for 3DG-H. Regression of Peak area ratio on amount of 3DG-H (pmol) gave: Peak area ratio = (0.093 ± 0.001 x 3DG-H (pmol)) ± 0.0378; r^2 = 0.998 (n = 7). D: Standard curve for FL. Regression of Peak area ratio on amount of FL (pmol) gave: Peak area ratio = (0.101 ± 0.003 x FL (pmol)) ± 0.150; r^2 = 0.996 (n = 7). E: Standard curve for CML. Regression of Peak area ratio on amount of CML (pmol) gave: Peak area ratio = (0.183 ± 0.003 x CML (pmol)) ±0.0340; r^2 = 0.999 (n = 7). F: Standard curve for MetSO. Regression of Peak area ratio on amount of MetSO (pmol) gave: Peak area ratio = (0.0536 ± 0.0008 x MetSO (pmol)) ± 0.0219; r^2 = 0.997 (n = 7).

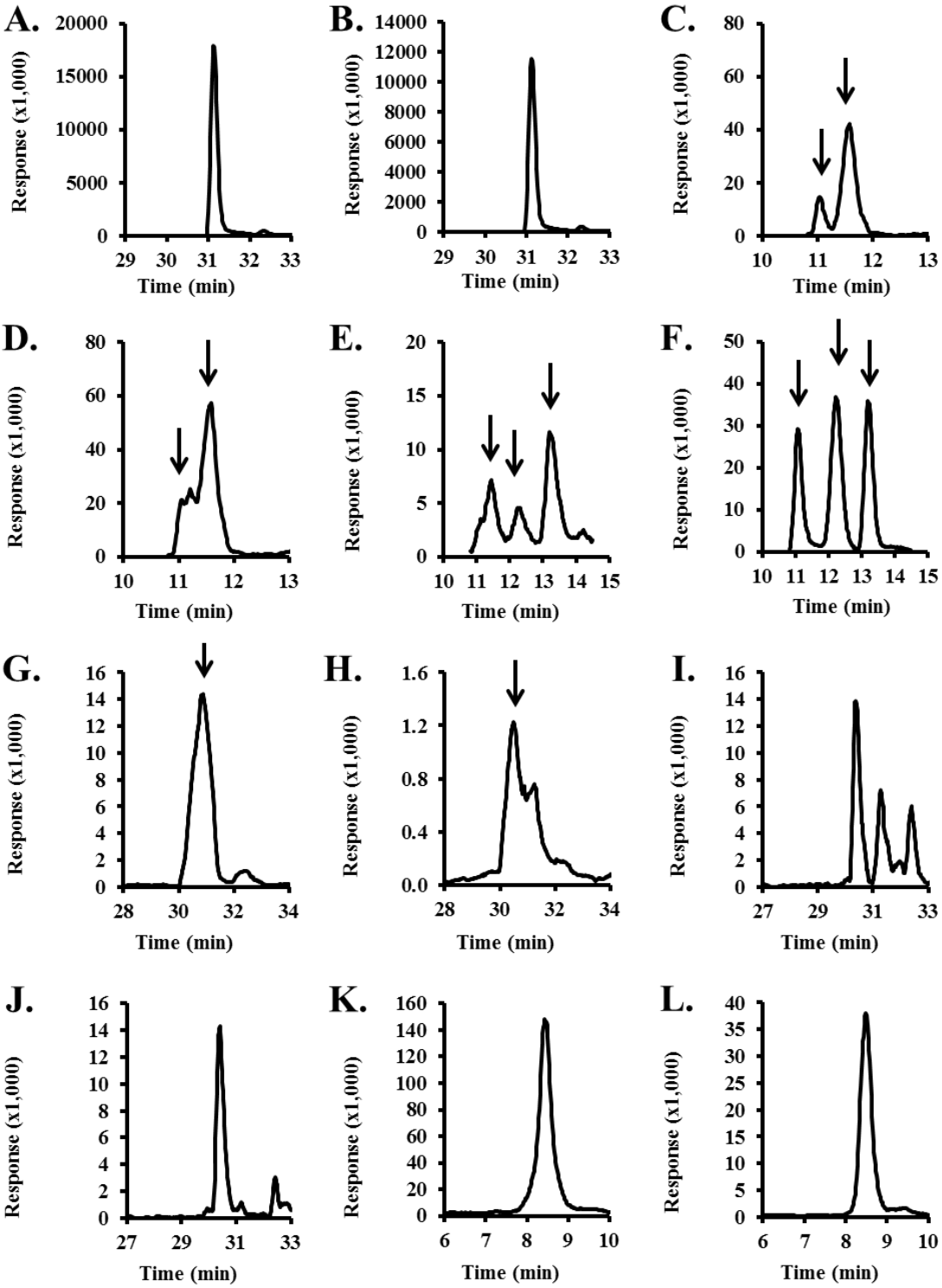

Figure 21: Representative chromatograms of glycation and oxidation adduct residues and amino acids in mouse pancreas. Chromatograms are: A. arginine; B. [$^{15}N_2$]arginine; C. MG-H1 (2 epimers); D. [$^{15}N_2$]MG-H1 (2 epimers); E. 3DG-H (3 isomers); F. [$^{15}N_2$]3DG-H (3 isomers); G. FL; H. [$^{2}H_4$]FL; I. CML; J. [$^{13}C_6$]CML; K. MetSO; L. [$^{2}H_3$]MetSO.

4.4.4. Assay of ε-(γ-Glutamyl)lysine

4.4.4.1. Principle of assay

The amount of ε-(γ-glutamyl)lysine (GEEK) in pancreas homogenates was measured by LC-MS/MS assay.

4.4.4.2. Sample preparation

Hydrolysates of soluble and ECM pancreatic protein prepared as in section 4.4.3.2 were used. Soluble pancreatic protein digest (25 µL) was added to a solution of [$^{13}C_5$]GEEK (10 pmol, 25 µL) for analysis. ECM pancreatic protein digest (12.5 µL) was diluted with 0.1% TFA in 3.75% MeCN (12.5 µL) and added to [$^{13}C_5$]GEEK (10 pmol, 25 µL) for analysis.

4.4.4.3. Preparation of calibration standards

Stocks of GEEK (0.5 µM and 10 µM) and γ-[$^{13}C_5$]GEEK (0.4 µM) were prepared. Aliquots of [$^{13}C_5$]GEEK (25 µL) were mixed with GEEK diluted to 25 µL with 0.1% TFA in 3.75% MeCN. Standards were prepared over the range 1 - 200 pmol as detailed in Table 22.

4.4.4.4. LC-MS/MS conditions

Special LC elution conditions were required to resolve GEEK chromatographically from isobaric interferences of α-Glu-Lys, α-Lys-Glu and γ-Glu-α-Lys. A graphite Hypercarb HPLC column was used (150 x 2.1 mm, particle size 3 µm) with column temperature of 30 °C. Solvents used were 0.1% TFA in 3.75% MeCN (Solvent A) and 0.1% TFA in 50:50 THF: water (Solvent B). The elution profile is detailed in Table 23.

Table 22: Preparation of GEEK calibration standards

Calibration solution	GEEK (pmol)	GEEK (µL)		0.1% TFA in 3.75% MeCN (µL)	[$^{13}C_5$]GEEK (0.4 µM) (µL)	Total volume (µL)
		0.5 µM	10 µM			
0	0	-	-	25.0	25.0	50.0
1	1	2	-	23.0	25.0	50.0
2	5	10	-	15.0	25.0	50.0
3	10	20	-	5.0	25.0	50.0
4	25	-	2.5	22.5	25.0	50.0
5	50	-	5.0	20.0	25.0	50.0
6	100	-	10.0	15.0	25.0	50.0
7	150	-	15.0	10.0	25.0	50.0
8	200	-	20.0	5.0	25.0	50.0

Table 23: Elution profile for GEEK analysis

Injection Run

Time (min)	Flow rate (mL/min)	Solvent A (%)	Solvent B (%)	Gradient
Initial	0.2	100	0	
5	0.2	100	0	Isocratic
15	0.2	100	0	Isocratic
35	0.2	0	100	Immediate
40	0.2	100	0	Immediate
55	0.4	100	0	Immediate

Flow from the column was eluted into the electrospray source of the MS/MS detector between 2 and 15 min for data collection. Mass spectrometric analysis was performed using electrospray positive ionisation mode. For mass spectrometric detection, the capillary voltage was 1.0 kV, the ion source temperature 120 °C, the desolvation gas temperature 350 °C and cone and desolvation gas flows 96 and 900 L/h respectively. The optimised MRM conditions used for detection, along with their retention times, cone voltage and collision energy are listed in Table 24.

Table 24: Optimised MRM mass transitions for GEEK analysis

Analyte	Parent ion (Da)	Fragment ion (Da)	Retention time (min)	Cone Voltage (V)	Collision Energy (eV)
GEEK	276.1	147.1	10.0	32	12
[$^{13}C_5$]GEEK	281.1	147.1	10.0	32	12

4.4.4.5. Data analysis

Specimen chromatograms are shown in Figure 22. Calibration curves were constructed by plotting peak area ratio of GEEK / [$^{13}C_5$]GEEK against GEEK concentration (Figure 23). The amounts in assayed aliquots were deduced using the peak area ratio and the appropriate calibration curve. The amount of GEEK in hydrolysed samples was normalised to the lysine measured in the corresponding assay of glycation, oxidation and nitration adduct residues.

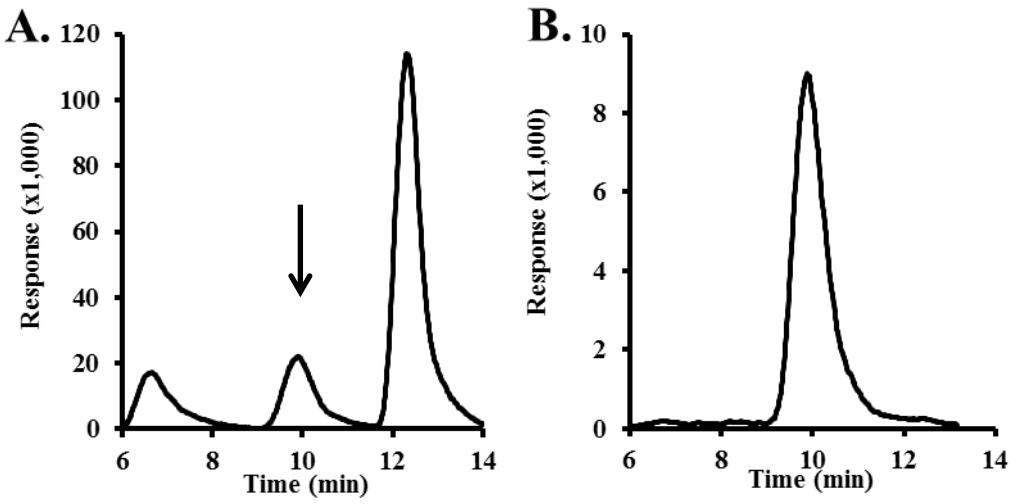

Figure 22: Representative chromatograms of GEEK in pancreatic protein digest. A: GEEK. B: [$^{13}C_5$]GEEK (10 pmol).

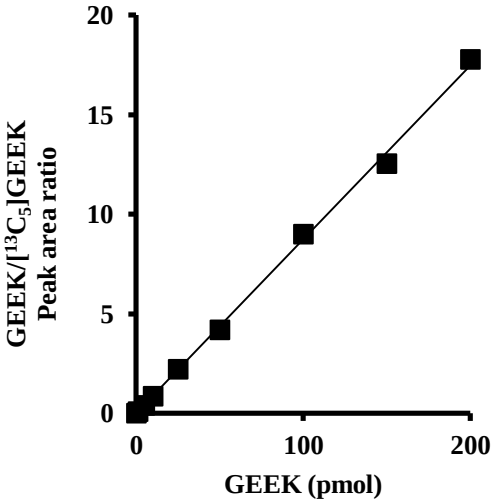

Figure 23: Typical calibration curve for GEEK by LC-MS/MS. Regression of Peak area ratio on amount of GEEK (pmol) gave: Peak area ratio = ((0.0873 ± 0.0013) x GEEK (pmol)) ± 0.119; $r^2 = 0.998$; n = 9.

4.4.5. Citrulline assay

4.4.5.1. Principle of assay

The amount of free citrulline in pancreatic and plasma filtrates was measured by an established stable isotopic dilution analysis LC-MS/MS assay.

4.4.5.2. Sample preparation

Pancreatic and plasma ultra-filtrates prepared for analysis of glycation, oxidation and nitration free adducts were diluted for analysis to measure citrulline free adducts. Pancreatic filtrates (10 µL) and plasma filtrates (2.5 µL) were diluted with 0.1% TFA in water to a final volume of 25 µL and added to [$^{13}C_6$]citrulline (2.5 pmol, 25 µL) for analysis.

4.4.5.3. Preparation of calibration standards

Stocks of citrulline (0.2 µM and 2 µM) and [$^{13}C_6$]citrulline (0.1 µM) were prepared. Aliquots of [$^{13}C_6$]citrulline (25 µL) were mixed with known amounts of citrulline diluted to 25 µL with 0.1% TFA in water. Standards were prepared over the range 0.25 – 50.0 pmol as detailed in Table 25.

Table 25: Preparation of citrulline calibration standards

Calibration solution	Citrulline (pmol)	Citrulline (µL)		0.1% TFA in water (µL)	[$^{13}C_6$]Citrulline (0.1 µM) (µL)	Total volume (µL)
		0.2 µM	2 µM			
0	0	-	-	25.00	25	50
1	0.25	1.25	-	23.75	25	50
2	0.50	2.50	-	22.50	25	50
3	1.25	6.25	-	18.75	25	50
4	2.50	12.5	-	12.50	25	50
5	3.75	18.75	-	6.25	25	50
6	5.00	25.0	-	-	25	50
7	10.0	-	5.00	20.00	25	50
8	25.0	-	12.5	12.50	25	50
9	50.0	-	25.0	-	25	50

4.4.5.4. LC-MS/MS conditions

Special LC elution conditions were required to clearly resolve citrulline from arginine chromatographically as a minor fraction of arginine degrades to citrulline in the electrospray source of the mass spectrometer. Although minor for arginine detection this would overestimate citrulline significantly if arginine and citrulline were not resolved chromatographically. A graphite Hypercarb HPLC column was used (150 x 2.1 mm, particle size 3 µm) with column temperature of 30 °C. Solvents used were 0.1% TFA in water (Solvent A), 0.1% TFA in 50% MeCN (Solvent B1) and 0.1% TFA in 50% THF (Solvent B2). The elution profile for the analytical run and postrun is detailed in Table 26. Eluate from the column was eluted into the electrospray source of the Quattro Premier MS/MS detector between 4 and 20 min for data collection. Mass spectrometric analysis was performed using electrospray positive ionisation mode. For mass spectrometric detection the capillary voltage was 1.0 kV, the ion source temperature 120 °C, the desolvation gas temperature 350 °C and cone and desolvation gas flows 96 and 900 L/h respectively. The optimised MRMs used for detection and quantification of citrulline, along with their retention time, cone voltage and collision energy are displayed in Table 27.

Table 26: Elution profile for citrulline analysis

Time (min)	Flow rate (mL/min)	Solvent A1 (%)	Solvent B1 (%)	Solvent B2 (%)	Gradient
Injection Run					
Initial	0.2	100	0	-	
5	0.2	100	0	-	
20	0.2	95	5	-	Linear
Postrun					
Initial	0.2	0	-	100	
20	0.2	0	-	100	Isocratic
25	0.2	100	-	0	Immediate
40	0.4	100	-	0	Immediate

Table 27: Optimised MRM mass transitions for citrulline analysis

Analyte	Parent ion (Da)	Fragment ion (Da)	Retention time (min)	Cone Voltage (V)	Collision Energy (eV)
Citrulline	176.1	158.9	11.8	20	8
[$^{13}C_6$]Citrulline	181.1	163.9	11.8	20	8

4.4.5.5. Data analysis

Specimen chromatograms are shown in Figure 24. Calibration curves were constructed by plotting the peak area ratio of citrulline/ [$^{13}C_6$]citrulline against citrulline concentration (Figure 25). The amount in assayed samples was deduced using the calibration curve and the concentration in the original filtrate calculated with use of appropriate dilution factors. The amount of citrulline in pancreatic filtrates was normalised to the wet weight of the pancreas sample.

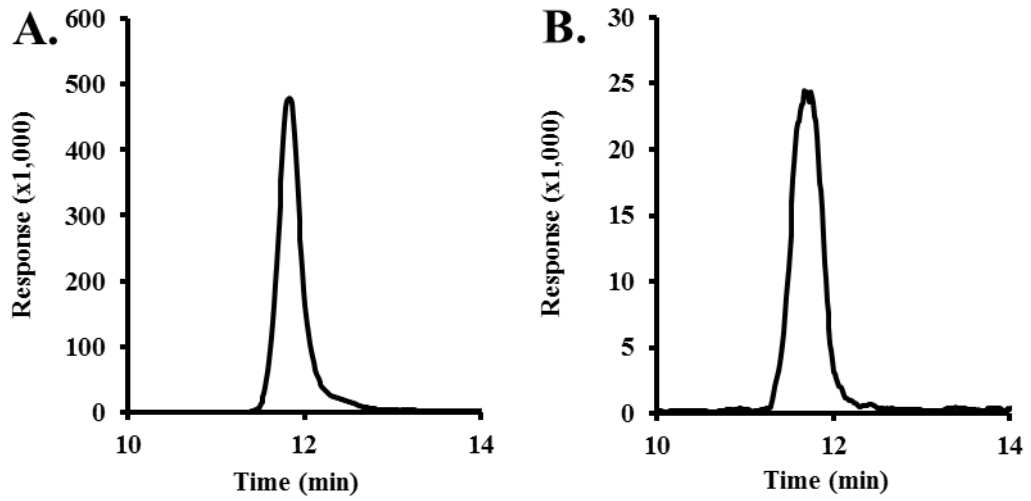

Figure 24: Representative chromatograms of citrulline in mouse pancreas. A: Citrulline. B: [$^{13}C_6$]Citrulline (2.5 pmol).

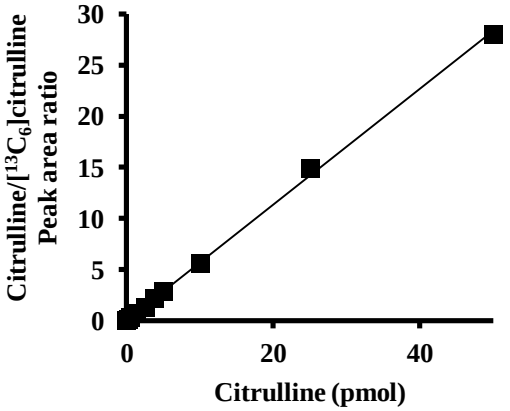

Figure 25: Typical calibration curve for citrulline by LC-MS/MS. Regression of Peak area ratio on amount of citrulline (pmol) gave: Peak area ratio = ((0.5673 ± 0.0059) x citrulline (pmol)) ± 0.107; $r^2 = 0.999$; n = 10.

4.5. Immunohistochemistry

Frozen mouse pancreas samples were covered in cryomatrix embedding resin and placed on dry ice to solidify. Samples were sectioned into 0.8 µm slices and mounted onto glass slides. Sections were air dried and fixed using 4% paraformaldehyde (PFA) in PBS for 10 min. PFA was removed, sections washed with PBS and permeabilised with 0.1% Triton X-100 in PBS for 10 min. Triton X-

100 was removed and sections were washed with TBS for 10 min and blocked with 1% poly-L-asparagine for 1 h at room temperature. Sections were washed again with PBS and incubated with primary antibodies overnight at 4 °C. Antibodies were 10 ng/mL mouse anti-MG-H1 monoclonal antibody, 11 µg/mL chicken anti-insulin polyclonal antibody and 2.5 µg/mL rabbit anti-collagen IV polyclonal antibody. Sections were then washed with PBS (2 x 5 min) and incubated with the Alexa labelled secondary antibodies for 1 h at room temperature. Secondary antibodies were goat anti-mouse IgG-Alexa488 conjugate, goat anti-chicken IgG-Alexa555 conjugate, goat anti-rabbit IgG-Alexa555 conjugate and goat anti-rabbit IgG-Alexa488 conjugate; all diluted to 5 µg/mL. Samples were then mounted using mounting medium containing 4',6-diamidino-2-phenylindole (DAPI). Images were acquired under a 63x NA oil immersion objective using a laser scanning Zeiss confocal microscope at 1x zoom. Additional pancreas sections were incubated with PBS without antibody addition and with secondary antibodies only as controls for tissue auto-fluorescence and non-specific antibody binding respectively.

4.6. Animal Study

The in-life study was performed by Professor Jan Kopecky and co-workers, Institute of Physiology, Academy of Sciences of the Czech Republic. Experiments were conducted under the guidelines for the use and care of laboratory animals of the Institute of Physiology and followed the 'Principles of laboratory animal care'. C57BL6/N male mice were randomised into control chow fed (3.4% fat) and HFD (approximately 35% fat) fed groups at the age of 3 months. Control animals remained on a standard chow diet whilst HFD animals were fed high fat chow for one week. Following this one week of adaptation, HFD fed animals were again randomised, into HFD and omega-3 fatty acid supplemented HFD groups. HFD and control groups continued on the same chow diet, whilst supplemented animals were fed HFD with 15% dietary lipids replaced by fish oils for a further 9 weeks. Details of the macronutrient composition of these diets are given by Kuda *et al*. (2009). The mice were sacrificed by cervical dislocation under anaesthesia following overnight access to food. All mice were caged separately throughout. Fasting glucose and insulin levels and the glucose tolerance test were performed after 8 weeks of the

dietary regimes – one week prior to sacrifice. Blood glucose and insulin were measured using calibrated glucometers and radioimmunoassay respectively. Plasma triglycerides and cholesterol were measured using a clinical analyser. NEFA were measured using a commercial kit (Waco Chemicals, Neuss, Germany). Glucose tolerance was assessed by measuring blood glucose after an overnight fast and following injection of D-glucose and expressed as "area under the curve". Food consumption over a 24 h period was measured weekly and used to calculate the cumulative food intake over the study period. Pancreas and plasma samples were sent on dry ice for subsequent analysis.

4.7. Statistical Analysis

Experiments were performed using analysis in replicates of triplicates or greater. Difference between normally distributed experimental groups was tested using Student's t-test assuming equal or unequal variance as appropriate based on the result of the F-test two sample for variance. Significance was defined as $P \leq 0.05$. Regression analysis was performed and used to determine the statistical LoD; using 3 x standard error at the intercept to calculate the LoD. Normality of data was tested using Kolmogorov-Smirnov test and difference between non-parametric data groups determined using Mann Whitney U test. Where smoothing has been applied to chromatograms it is based on the number of scans for peak width at half-height.

5. Results: The glyoxalase system and dicarbonyl metabolism in MIN6 cells *in vitro*

5.1. Growth of MIN6 cells *in vitro*

A growth curve was constructed to assess the growth and viability of MIN6 cells *in vitro*. The growth of MIN6 cells was studied in low and high glucose concentrations, 5.5 mM and 20 mM, respectively - Figure 26. When MIN6 cells were seeded at a density of 32,200 cells/cm^2 or 322,000 cells per well in medium containing 5.5 mM glucose, the viable cell density and number increased progressively for 5 days, reaching a maximum density of 197,000 cells/cm^2 or 1.97 million cells per well. Thereafter the viable cell density and number decreased progressively at days 6 and 7. The decrease in cell number at days 6 and 7 was associated with an increased number of detached cells rather than a decrease in viability of cells recovered by trypsinisation. When MIN6 cells were incubated with 20 mM glucose there was similar growth kinetics as in cultures with 5.5 mM glucose - Figure 26. In subsequent experiments MIN6 cells were incubated for a maximum of 5 days.

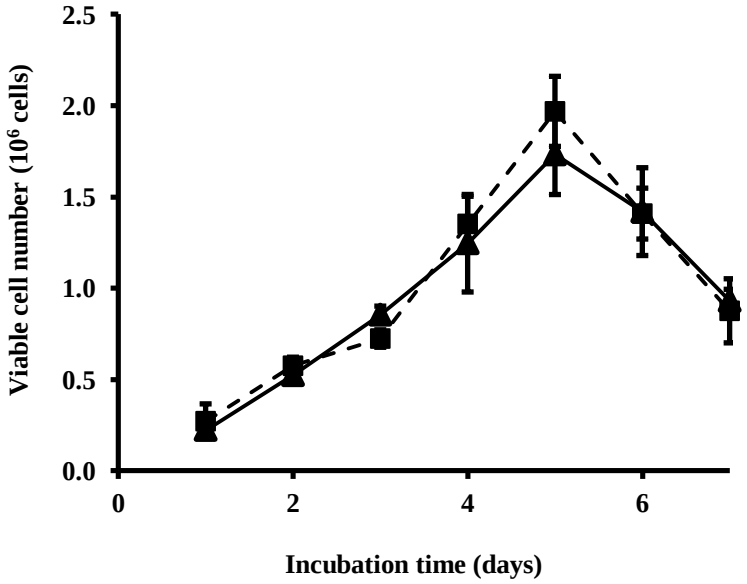

Figure 26: Growth curve of MIN6 cells cultured *in vitro* with media containing 5.5 mM and 20 mM glucose. Data are mean ± SD; n = 3. Key: ■- - ■, medium containing 5.5 mM glucose; ▲—▲, medium containing 20 mM glucose.

5.2. Characterisation of the glyoxalase system of MIN6 cells *in vitro*

5.2.1. Activity of glyoxalase 1 and glyoxalase 2 of MIN6 cells *in vitro*

The mean activity of Glo1 in MIN6 cells *in vitro* incubated in medium with 5.5 mM glucose was 600 ± 87 mU per million cells. The mean activity of Glo2 in MIN6 cells *in vitro* incubated in medium with 5.5 mM glucose was 549 ± 82 mU per million cells. The activity of Glo1 and Glo2 was not changed significantly by incubation with 20 mM glucose – Figure 27. The activity of MG reductase and dehydrogenase was measured in MIN6 cell lysates but was below the limit of detection (<0.5 mU per million cells). Glo1 and the glyoxalase system is therefore the main enzymatic route for metabolism of MG in MIN6 cells *in vitro*.

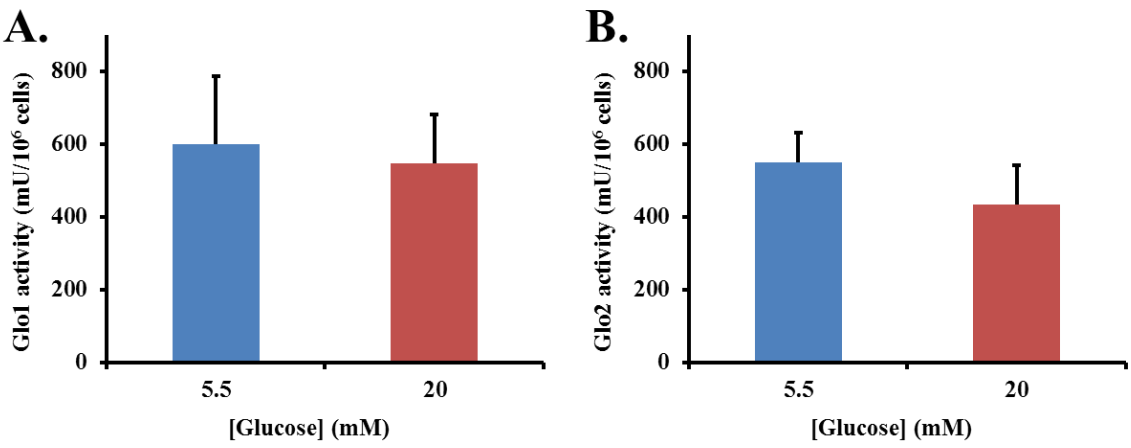

Figure 27: Enzymatic activities of the glyoxalase system in MIN6 cells.
A. Activity of Glo1. B. Activity of Glo2. MIN6 cells were cultured in medium for 5 days. Data are mean ± SD; n = 5 - 6.

5.2.2. Glyoxalase 1 gene expression of MIN6 cells *in vitro*

The expression of Glo1 in MIN6 cells incubated *in vitro* in medium with 5.5 mM glucose was studied by quantifying Glo1 mRNA by RT-PCR and normalising to 18S rRNA. Normalised Glo1/ 18S RNA was 0.404 ± 0.014 and 0.407 ± 0.008 at passage 40 and 46 respectively (n = 3). The mean expression of Glo1 in MIN6 cells incubated *in vitro* in medium with 20 mM glucose was 0.412 ± 0.006 and 0.403 ±

0.009 at passage 40 and 46 respectively (n = 3). Hence, the expression was not significantly altered by either passage or incubation with 20 mM glucose.

5.2.3. Dicarbonyls in MIN6 cells *in vitro*

The MG content of MIN6 cells incubated in medium with 5.5 mM glucose was 5.95 ± 2.88 pmol per million cells. The glyoxal content of MIN6 cells incubated in medium with 5.5 mM glucose was 0.31 ± 0.03 pmol per million cells. The 3-DG content of MIN6 cells incubated in medium with 5.5 mM glucose was 2.09 ± 1.01 pmol per million cells. The cellular contents of MG, glyoxal and 3-DG were not changed significantly when MIN6 cells were incubated with 20 mM glucose - Figure 28. The concentration of MG, glyoxal and 3-DG in media of MIN6 cells incubated in 5.5 mM glucose was 76.1 ± 13.8 nM, 30.7 ± 1.8 nM and 1120 ± 145 nM respectively. There was a 2.4-fold increase in the concentration of 3-DG measured in MIN6 culture media when MIN6 cells were cultured in 20 mM glucose - Figure 28. The concentration of MG and glyoxal in the medium was not significantly changed by incubation of MIN6 cells with 20 mM glucose.

5.2.4. Glutathione and thiols in MIN6 cells *in vitro*

The cellular amounts of reduced and oxidised glutathione and total thiols were measured in MIN6 cells following 5 day culture - Table 28. There was no change in the amount of GSH, GSSG or total thiols in MIN6 cells following culture in media containing 20 mM glucose compared to in 5.5 mM glucose control. The amount of S-D-lactoylglutathione in MIN6 cells was below the limit of detection (<1.1 pmol/10^6 cells).

Table 28: Cellular glutathione and thiols in MIN6 cultured for 5 days *in vitro*

Analyte	5.5 mM glucose	20 mM glucose
GSH (pmol/10^6 cells)	858 ± 114	879 ± 60
GSSG (pmol/10^6 cells)	11.1 ± 3.5	13.7 ± 4.9
Total thiols (nmol/10^6 cells)	34.5 ± 1.8	35.0 ± 1.2
Protein thiols (nmol/10^6 cells)	33.7 ± 1.9	34.1 ± 1.2

GSH, GSSG and total thiols data are mean ± SD; n = 4 - 6. Protein thiols were deduced from the total thiols and GSH.

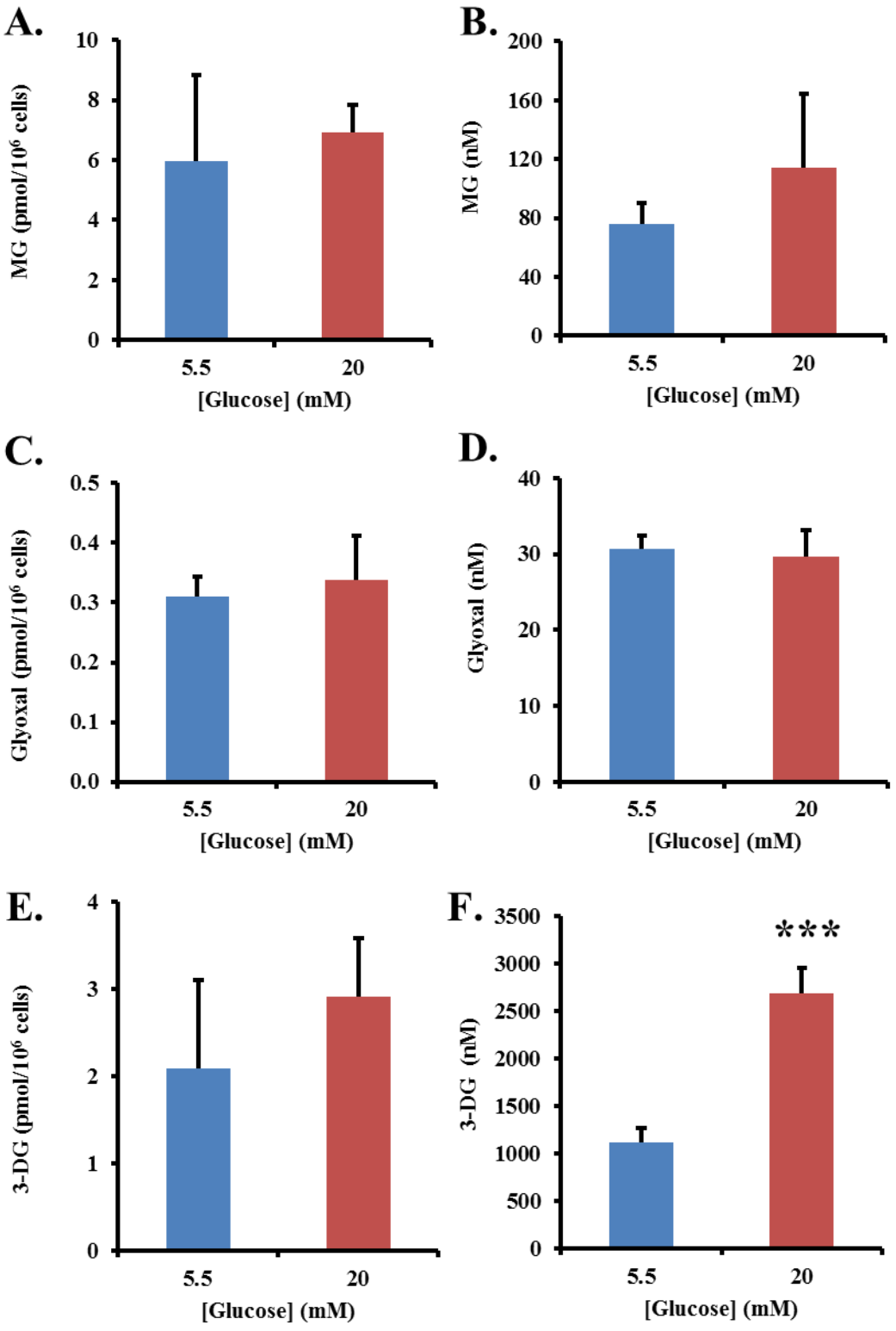

Figure 28: Dicarbonyls in MIN6 cells *in vitro*. Panels A, C and E, cellular content of MG, glyoxal and 3-DG in MIN6 cells; panels B, D and F, concentration of MG, glyoxal and 3-DG in culture medium. Data are mean ± SD; n = 5 - 6. Significance: ***, P<0.001.

5.2.5. Flux of formation of D-lactate and concentration of L-lactate in MIN6 cells *in vitro*

The flux of formation of D-lactate is an approximate measure of the flux of production of MG where the metabolism of D-lactate is low or negligible. The rate of formation of D-lactate in MIN6 cells over 5 days was 1.02 ± 0.34 nmol per 10^6 cells per day. The concentration of D-lactate in the culture medium at baseline was 6.25 ± 0.67 µM and increased to 12.0 ± 1.2 µM after 5 days. When cell cultures were spiked with 10 µM exogenous D-lactate, the increment in flux of formation of D-lactate was not significantly different to in unspiked controls indicating that D-lactate was not metabolised significantly in MIN6 cells. Analysis of D-lactate in baseline medium and medium following incubation of MIN6 cells for 5 days in 5.5 mM and 20 mM glucose showed a 41% increase in flux of formation of D-lactate when the cells were cultured in 20 mM glucose (P<0.01) – Figure 29.

The concentration of L-lactate in the medium of MIN6 cell cultures was 0.529 ± 0.011 mM (n = 5). Following incubation of MIN6 cells with 5.5 mM and 20 mM glucose for 5 days the concentration of L-lactate was 1.15 ± 0.07 mM and 1.19 ± 0.03 mM respectively (P<0.001 with respect to baseline; n = 5). L-Lactate concentration in medium was not significantly altered by incubation with 20 mM glucose.

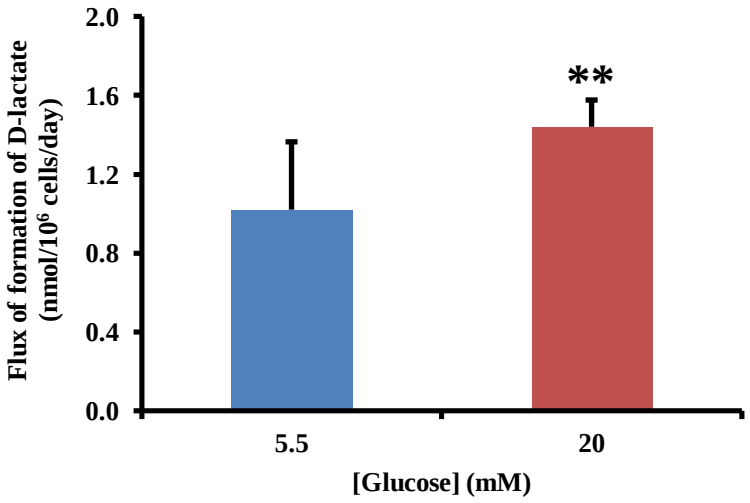

Figure 29: Flux of formation of D-lactate by MIN6 cells *in vitro*. MIN6 cells were cultured for 5 days. Data are mean ± SD; n = 9. Significance: **, P<0.01.

5.2.6. Consumption of D-glucose by MIN6 cells *in vitro*

The glucose consumption in MIN6 cells *in vitro* incubated in 5.5 mM glucose was 0.716 ± 0.068 µmol/10^6 cells/day - Figure 30. The consumption of glucose increased by 28% to 0.914 ± 0.098 µmol/10^6 cells/day when culture medium contained 20 mM glucose - Figure 30.

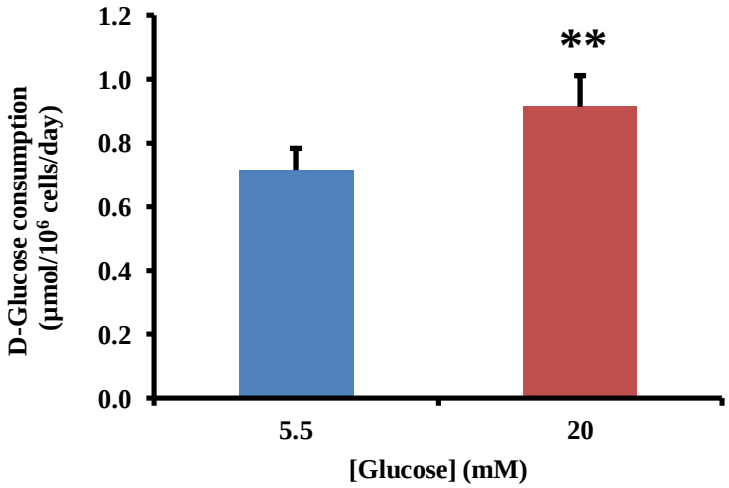

Figure 30: D-Glucose consumption in MIN6 cells *in vitro*. MIN6 cells were cultured for 5 days. Data are mean ± SD; n = 6. Significance: **, P<0.01.

The flux of formation of D-lactate from glucotriose was 0.0771 ± 0.0161 % when MIN6 cells were incubated in medium containing 5.5 mM glucose and was not changed significantly when MIN6 cells were cultured in 20 mM glucose.

5.2.7. Glycation, oxidation and nitration adduct residue content of cytosolic protein of MIN6 cells

Analysis of glycation, oxidation and nitration adduct residues in hydrolysed protein from MIN6 cells cultured for 5 days in media containing 5.5 mM and 20 mM glucose showed no significant change in the adduct residues measured – Table 29.

Table 29: Protein glycation, oxidation and nitration adduct residues in MIN6 cells *in vitro*

Protein adduct residue	5.5 mM glucose	20 mM glucose
FL (mmol/mol lys)	0.850 ± 0.143	0.898 ± 0.381
CML (mmol/mol lys)	0.213 ± 0.026	0.175 ± 0.043
CML/FL ratio	0.235 ± 0.045	0.224 ± 0.058
CEL (mmol/mol lys)	0.0461 ± 0.0057	0.0415 ± 0.0126
MG-H1 (mmol/mol arg)	0.351 ± 0.068	0.376 ± 0.117
CMA (mmol/mol arg)	0.0182 ± 0.0029	0.0166 ± 0.0060
3DG-H (mmol/mol arg)	0.153 ± 0.019	0.147 ± 0.015
MetSO (mmol/mol met)	2.87 ± 0.80	3.63 ± 1.19
NFK (mmol/mol trp)	1.09 ± 0.14	0.918 ± 0.14
3-NT (mmol/mol tyr)	0.00227 ± 0.00024	0.00234 ± 0.00149

Data are mean ± SD; n = 4 - 6.

5.2.8. Protein glycation, oxidation and nitration free adducts in culture media

Protein glycation, oxidation and nitration free adducts were quantified in MIN6 cell culture medium – Table 30. Quantitatively, FL was the major glycation free adduct formed. There were increases in the rate of formation of FL free adduct (4.1-fold) and 3DG-H free adduct (2-fold) when MIN6 cells were cultured *in vitro* in 20 mM glucose. There were no quantifiable increases in MOLD, NFK, MetSO, dityrosine or 3-NT in the medium during the culture.

DMEM medium contains 798 µM lysine and 398 µM arginine and therefore part of the flux of glycation free adducts occurs by glycation of lysine and arginine in the extracellular medium. To deduce the contribution of extracellular glycation to the flux of glycation free adducts, culture medium was incubated without cells to find the rate of glycation of lysine and arginine from glucose and dicarbonyls present – from serum and degradation of serum protein glycated by glucose and spontaneous fragmentation of glucose. The rates were then corrected for a factor reflecting the effect of the presence of cells on the glycating agent. The correction factor = (mean concentration of glycating agent in cell incubations/mean concentration of glycating agent in cell-free incubations). For 5.5 mM and 20 mM glucose incubations

respectively: 0.68 and 0.89 for glucose; 0.20 and 0.32 for methylglyoxal; and 0.07 and 0.06 for glyoxal. The presence of cells did not change the extracellular concentration of 3-DG significantly. Accordingly, rates of glycation free adduct production in cell cultures, the contribution of glycation in the extracellular medium to this and the proportion of glycation free adduct production due to cells was deduced- Table 30. This showed that most (>905) of FL free adduct was formed in the medium whereas for dicarbonyl derived AGEs, most AGE free adduct was formed in cells.

5.3. Insulin expression in MIN6 cells *in vitro*

The expression of the mouse insulin genes were measured in MIN6 cells cultured in medium containing 5.5 mM and 20 mM glucose at both passage 40 and 46 - Table 31. Expression of Ins1 and Ins2 was equivalent and unaltered by culture in medium containing 20 mM glucose. The expression of both Ins1 and Ins2 decreased with passage; Ins1 declined by 11% and 9% and Ins2 by 3% and 5% in 5.5 mM and 20 mM glucose respectively. The ratio of Ins1:Ins2 expression also decreased with passage by 7% and 4% in 5.5 mM and 20 mM glucose respectively. A similar ratio change was observed in passage 40 MIN6 cells cultured in 20 mM glucose – the Ins1:Ins2 ratio decreased by 4% compared to cells cultured in 5.5 mM glucose.

Table 30: Protein glycation, oxidation and nitration free adduct flux of formation by MIN6 cells *in vitro*

	Incubation with MIN6 cells		Extracellular formation†		% Adduct formed from cell proteolysis	
Free adduct	5.5 mM glucose	20 mM glucose	5.5 mM glucose	20 mM glucose	5.5 mM glucose	20 mM glucose
FL	248 ± 18	1025 ± 32***	214 ± 18°	881 ± 109$^{***,\circ}$	14	14
CML	6.3 ± 2.4	6.9 ± 3.1	ND	ND	ND	ND
CEL	2.9 ± 1.1	2.5 ± 0.7	<LOD	<LOD	---	---
MG-H1	16.7 ± 3.1	14.6 ± 1.8	3.3 ± 0.2°°°	6.1 ± 0.9$^{***,\circ\circ\circ}$	80	58
CMA	22.0 ± 1.8	19.7 ± 2.3	1.9 ± 0.2°°°	1.6 ± 0.1°°°	91	92
3DG-H	5.7 ± 1.4	11.5 ± 1.3***	3.6 ± 0.7°	7.2 ± 0.5 $^{***,\circ}$	37	37

Protein glycation, oxidation and nitration free adduct flux of formation (pmol/10^6 cells/day). Data are mean ± SD; n = 4 - 6. Significance: ***, P<0.001 with respect to low glucose control; ° and °°°, P<0.05 and P<0.001 with respect to cell incubation production rate.

† Extracellular formation rate was deduced in pmol/10^6 cells/day equivalents from incubation without cells. A correction factor to the rate in cell-free incubation is applied to allow for the decrease in glucose, methylglyoxal and glyoxal in the presence of cells. This factor, mean concentration of glycating agent in cell incubations/ mean concentration of glycating agent in cell-free incubations, for 5.5 mM and 20 mM glucose incubations was respectively: 0.68 and 0.89 for glucose, 0.20 and 0.32 for methylglyoxal; and 0.07 and 0.06 for glyoxal. The presence of cells did not change the extracellular concentration of 3-DG significantly. Abbreviation: ND, not determined.

Table 31: Insulin gene expression in MIN6 cells

	5.5 mM glucose		20 mM glucose	
	Passage 40	Passage 46	Passage 40	Passage 46
Ins1	0.644 ± 0.008	0.576 ± 0.013**	0.631 ± 0.005	0.577 ± 0.021*
Ins2	0.603 ± 0.011	0.582 ± 0.006*	0.618 ± 0.005	0.585 ± 0.015*
Ins1:Ins2 ratio	1.07 ± 0.01	0.990 ± 0.033*	1.02 ± 0.02°°	0.985 ± 0.012*

MIN6 cells (30,000 cells per cm^2) were incubated for 5 days. Data are mean ± SD; n = 3 normalised to 18S RNA. Significance: * and **, P< 0.05 and P<0.01 respectively, compared to passage 40 cells in the same glucose concentration; °°, P<0.01 compared to 5.5 mM glucose condition of the same passage.

5.4. The glyoxalase system and MIN6 cells under dicarbonyl stress

5.4.1. Treatment of MIN6 with exogenous MG *in vitro*

Treatment of MIN6 cells with 500 µM MG for 30 min produced a 2-fold increase in the cellular content of MG (5.69 ± 0.18 pmol per million cells in control samples to 12.6 ± 3.9 pmol per million cells in treated cells (P<0.05)). The concentration of MG in the medium decreased from 500 µM at baseline to 356 ± 57 µM at 30 min and was 0.546 ± 0.133 µM in control media (P<0.001).

5.4.2. Effect of the cell permeable Glo1 inhibitor, $BrBzGSHCp_2$ on MIN6 cell growth *in vitro*

Endogenous dicarbonyls were increased by using a cell permeable inhibitor of Glo1 – $BrBzGSHCp_2$. A concentration-response of $BrBzGSHCp_2$ for the effect on MIN6 cell growth was constructed - Figure 31. There was no significant impairment in cell viability until MIN6 cells were treated with doses of $BrBzGSHCp_2$ greater than 12 µM. The median growth inhibitory concentration GC_{50} value of $BrBzGSHCp_2$ was 27.3 ± 0.9 µM with a logistic regression coefficient n = 2.47 ± 0.22.

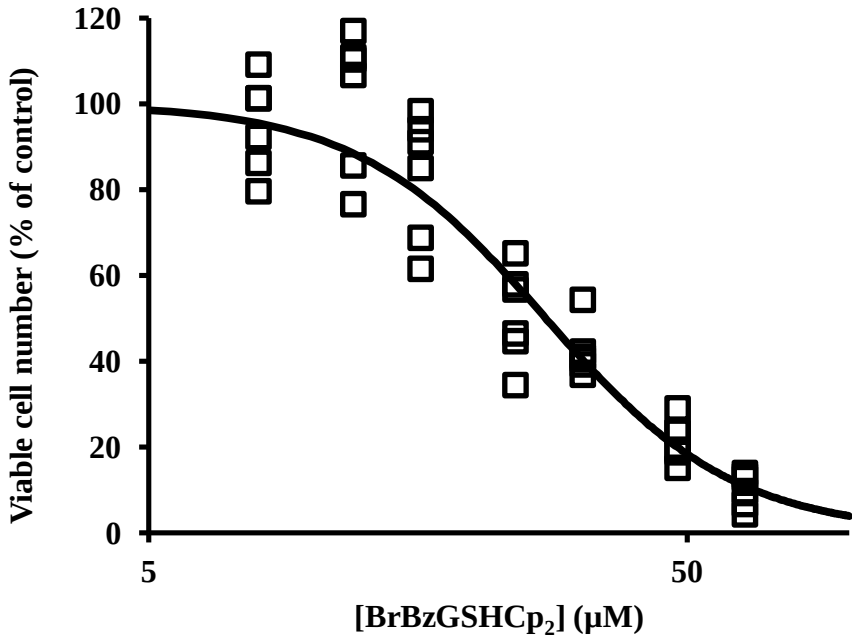

Figure 31: Dose response of MIN6 cells treated with $BrBzGSHCp_2$ for 48 h. Data are mean ± SD; n = 6 for 7 concentrations. Data were fitted to the equation: Viable cell number (% of control) = 100 x $GC_{50}^n/(GC_{50}^n = [BrBzGSHCp_2]^n)$, solving for GC_{50} and n.

5.4.3. Effect of $BrBzGSHCp_2$ on dicarbonyls

MIN6 cells were treated with 10 µM $BrBzGSHCp_2$ with 5.5 mM and 20 mM glucose for 48 h - Figure 32. The cellular content of MG was not increased significantly by incubation with 10 µM $BrBzGSHCp_2$, 20 mM glucose or both. Incubation with 10 µM $BrBzGSHCp_2$ did however increase the cellular MG content when MIN6 cells were incubated with either 5.5 mM or 20 mM glucose (6.55 ± 1.84 versus 13.4 ± 4.57 pmol per 10^6 cells, $P<0.05$).

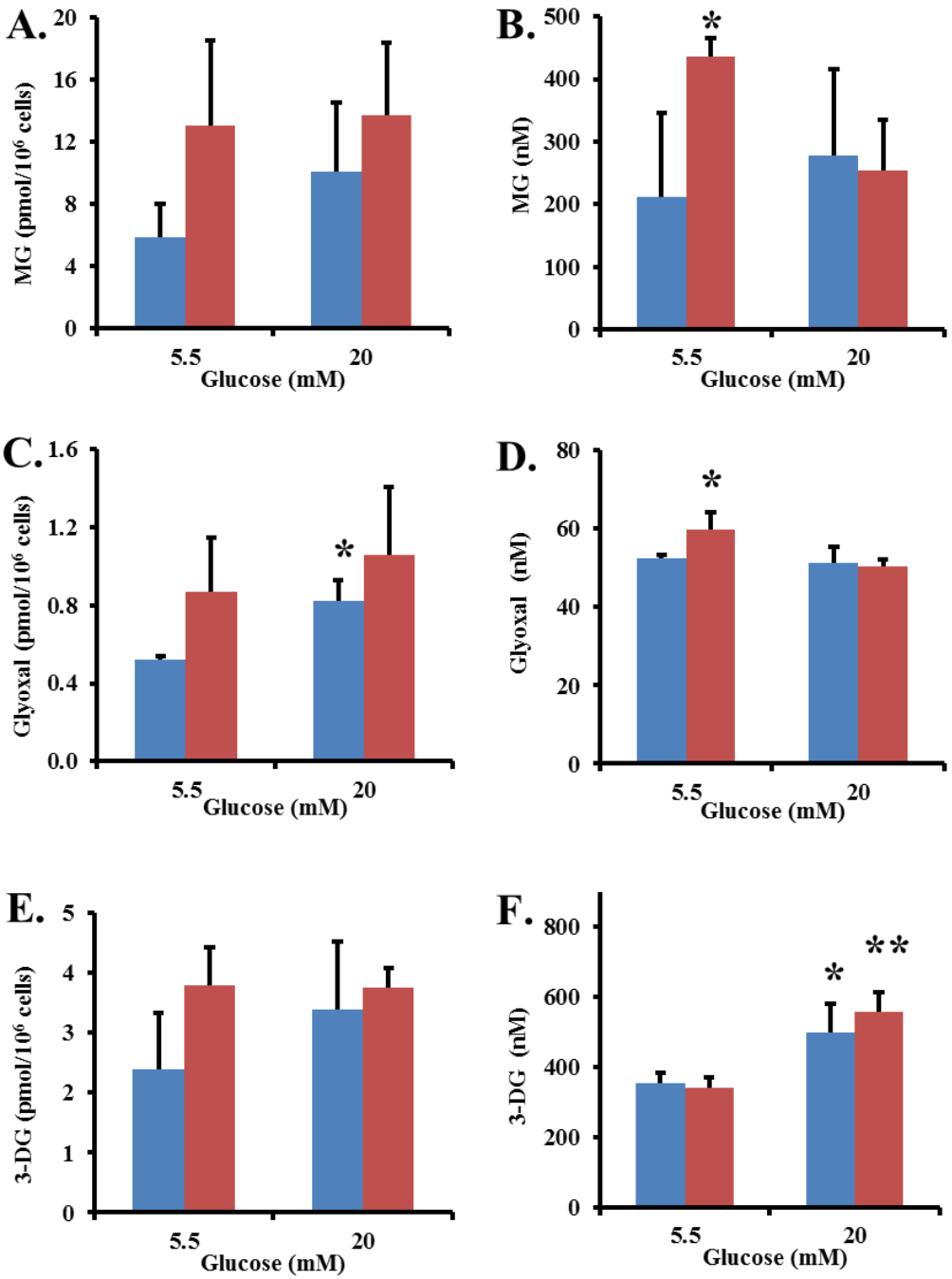

Figure 32: Effect of 10 µM BrBzGSHCp$_2$ and 20 mM glucose on the dicarbonyl content of MIN6 cells and culture medium. Panels A, C and E, cellular content of MG, glyoxal and 3-DG; panels B, D and F concentrations of MG, glyoxal and 3-DG in culture medium. Data are mean ± SD; n = 3. Significance: * and **, P<0.05 and P<0.01 respectively. Key: ■, Control MIN6 cells; ■ MIN6 cells treated with 10 µM BrBzGSHCp$_2$.

The concentration of MG in the medium was increased *ca.* 2-fold by incubation with 10 µM BrBzGSHCp$_2$. The cellular content of glyoxal was increased 58% by incubation with 20 mM glucose and the glyoxal concentration of culture medium was increased 14% by incubation with 10 µM BrBzGSHCp$_2$. The 3-DG

concentration of culture medium was increased 41% by incubation with 20 mM glucose.

5.4.4. Effect of $BrBzGSHCp_2$ on glutathione content of MIN6 cells *in vitro*

Incubation of MIN6 cells *in vitro* with 10 µM $BrBzGSHCp_2$ for 48 h produced *ca.* 2-fold increase in the cellular content of GSH and *ca.* 3-fold increase in the cellular content of GSSG in both low and high glucose conditions - Figure 33.

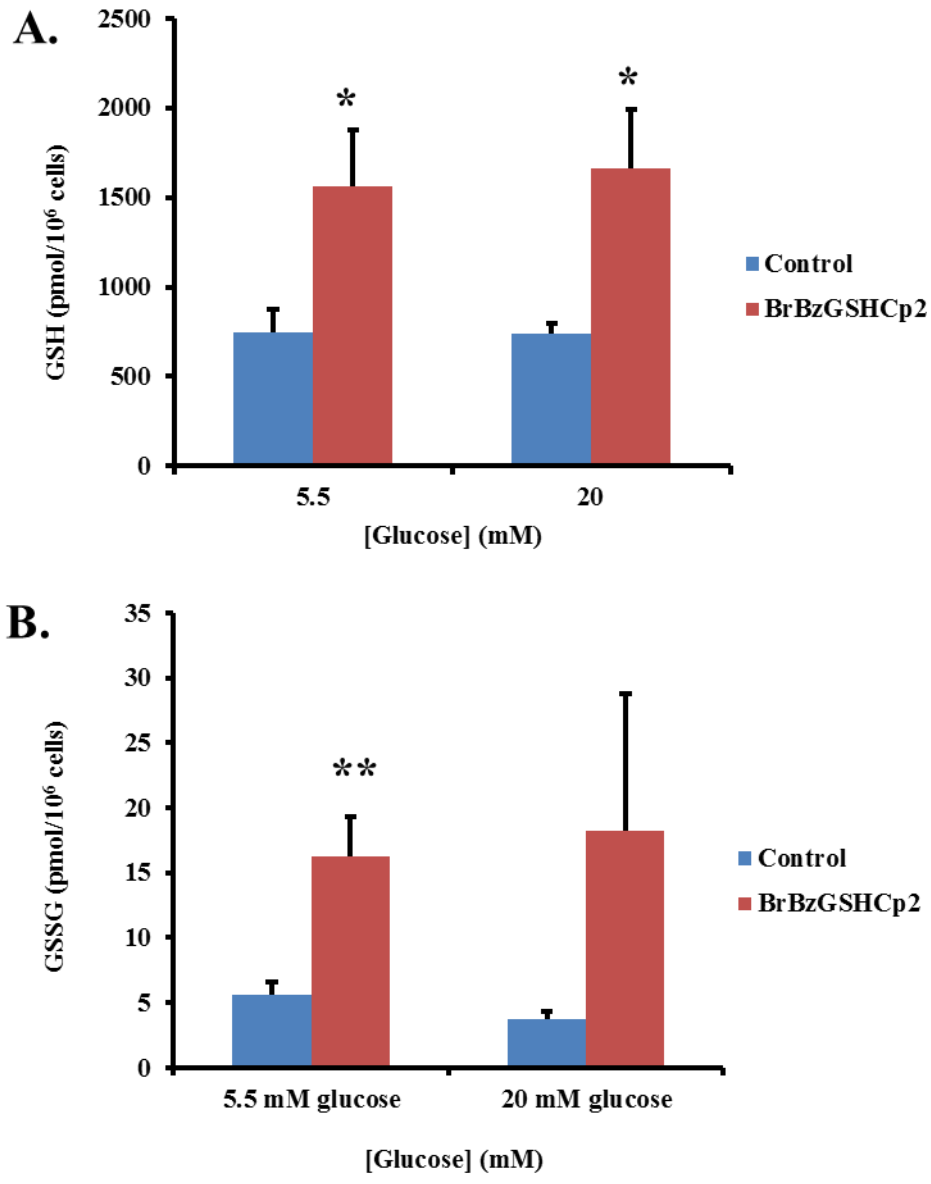

Figure 33: The effect of $BrBzGSHCp_2$ on glutathione content in MIN6 cells. A. GSH and B. GSSG in MIN6 cells. Data are mean ± SD; n = 3. Significance: * and **, P<0.05 and P<0.01, respectively.

5.4.5. Effect of $BrBzGSHCp_2$ on glyoxalase 1 and insulin expression of MIN6 cells *in vitro*

The effect of $BrBzGSHCp_2$ on Glo1 and insulin expression in MIN6 cells *in vitro* was analysed by measurement of Glo1 and insulin mRNA. There was no significant change in Glo1 mRNA level when MIN6 cells were treated with 10 µM $BrBzGSHCp_2$ for 48 h - Figure 34. However, the combination of 20 mM glucose and $BrBzGSHCp_2$ led to a 17% decrease in Glo1 mRNA, compared to control cultures in 5.5 mM glucose.

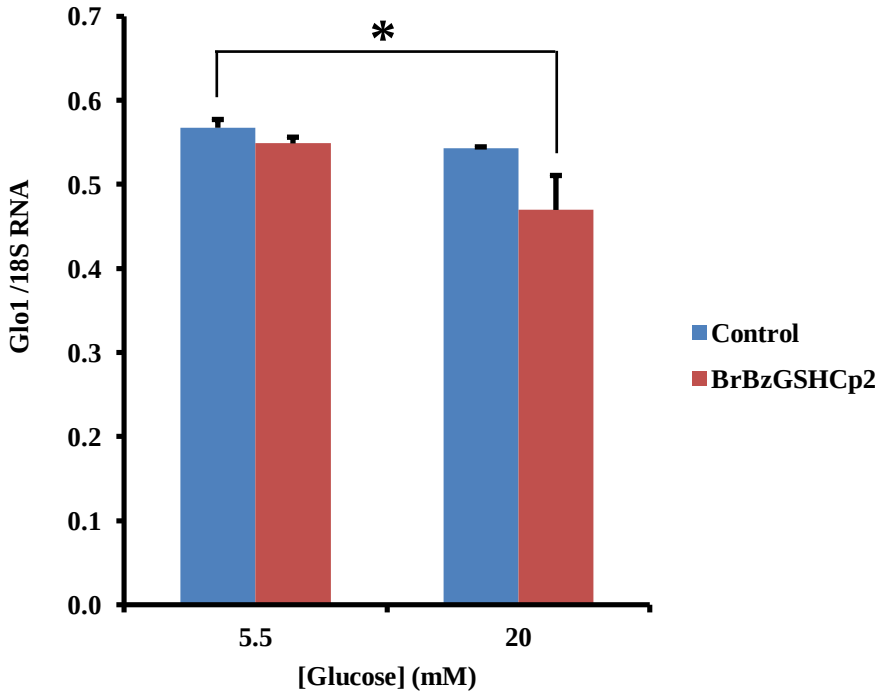

Figure 34: Expression of Glyoxalase 1 in MIN6 cells treated with $BrBzGSHCp_2$ *in vitro*. Glo1 expression in MIN6 cells treated with 10 µM $BrBzGSHCp_2$ for 48 h, normalised to expression of 18S RNA. Data are mean ± SD; n = 3. Significance: *, $P<0.05$.

There was a significant increase in Ins1 expression in MIN6 cells treated with 10 µM $BrBzGSHCp_2$ for 48 h - 7% and 3% in 5.5 mM and 20 mM glucose conditions respectively, compared to control - Figure 35. Ins1 and Ins2 mRNA decreased by 3% and 4% respectively when MIN6 cells were cultured in 20 mM glucose compared to in 5.5 mM glucose. The level of Ins2 mRNA did not significantly change when MIN6 cells were treated with $BrBzGSHCp_2$ - Figure 35. There was consequently a shift in the ratio of Ins1:Ins2 mRNA, with an 8% ($P<0.01$)

and 11% (P<0.05) higher proportion of Ins1 in 5.5 mM and 20 mM glucose respectively when MIN6 cells were treated with 10 µM $BrBzGSHCp_2$.

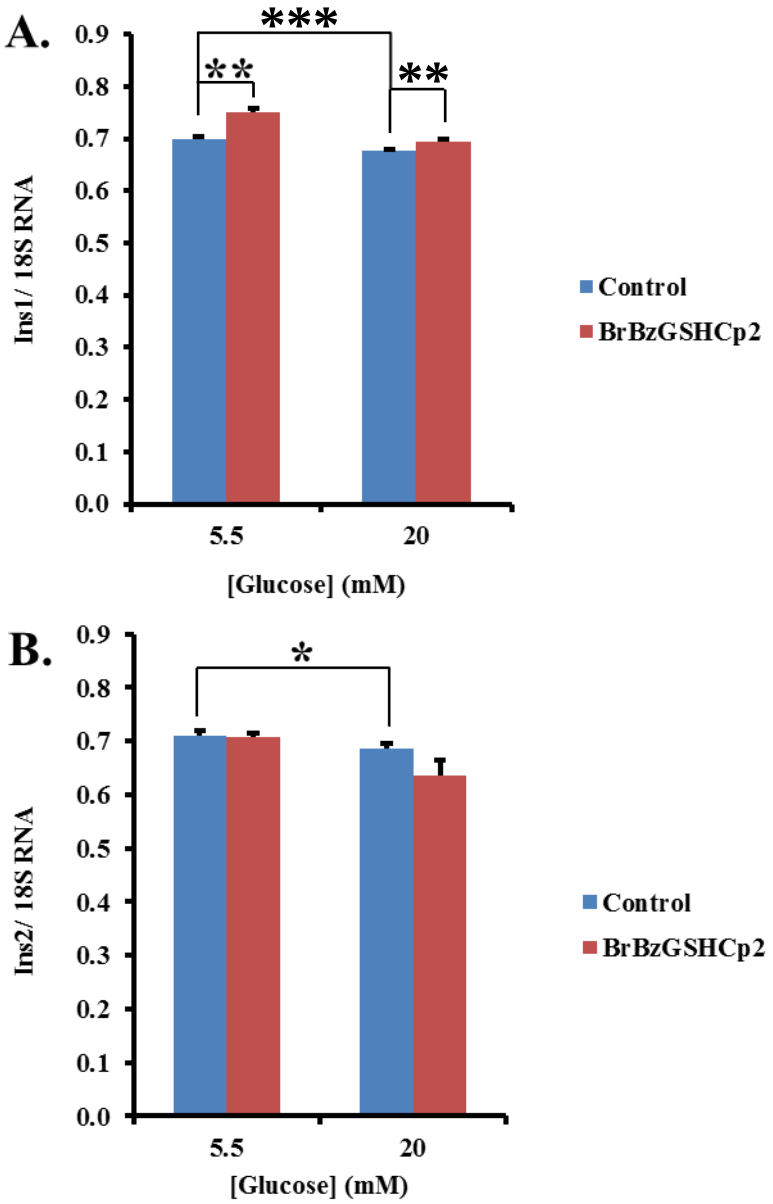

Figure 35: Expression of Ins1 and Ins2 in MIN6 cells treated with $BrBzGSHCp_2$
A. Ins1 expression and B. Ins2 expression. Data are mean ± SD; n = 3 of expression normalised to expression of 18S RNA. Significance: *, ** and ***, P<0.05, P<0.01 and P<0.001, respectively.

6. Results: Effect of modification of collagen IV on MIN6 cell adhesion and function

6.1. Characterisation of collagen IV coated plates

Twenty-four well plates were coated with collagen IV overnight. Coating of plates resulted in 6.29 ± 2.93 µg collagen/well adherence; 33.1% of the collagen added. Total collagen was measured by CBQCA assay following extraction by washing wells twice with PBS and six times with 0.1% Triton X-100 in PBS. In total, 96.6% of the collagen added to each well (19 µg) was recovered - Figure 36.

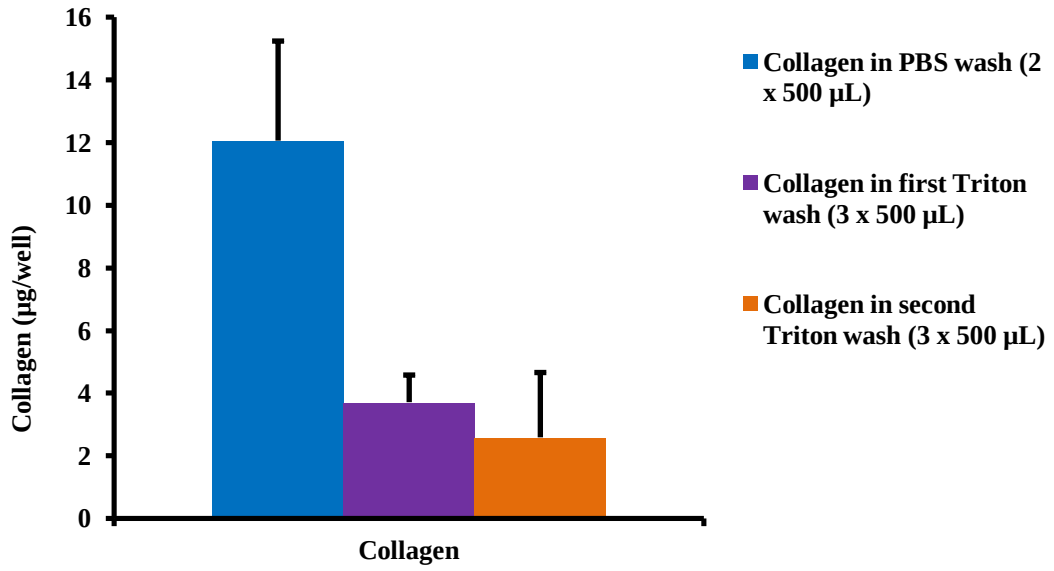

Figure 36: Recovery of collagen from 24 well plate. Data are mean ± SD; n = 3-4.

6.2. Effect of collagen IV on MIN6 cell adhesion

Coating plates with human collagen IV increased the adhesion of MIN6 cells 2-fold with respect to uncoated culture plates. This increase was prevented by pre-incubation of MIN6 cells with either anti-Itgb1 antibody or RGD peptide before plating onto coated plates; a 50% and 47% decrease relative to control cells was demonstrated for anti-Itgb1 antibody and RGD peptide respectively - Figure 37. The initial adhesion showed more clustering of cells when plated onto collagen, compared to the equally dispersed cells plated onto control uncoated plates.

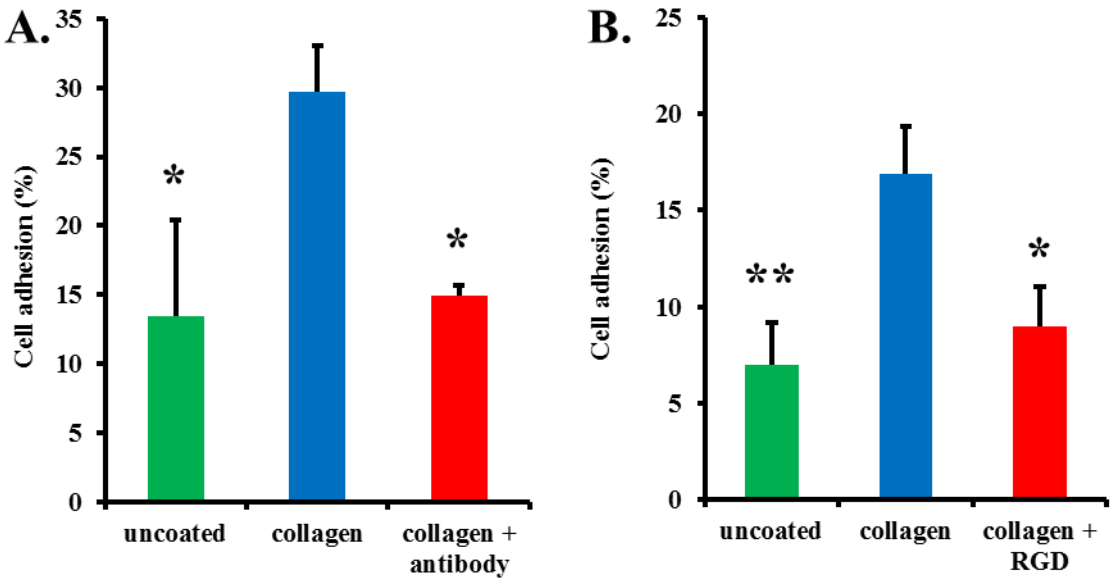

Figure 37: Collagen dependent adhesion of MIN6 cells *in vitro*. Collagen dependent adhesion of MIN6 to human collagen was blocked by A. 5 µg/mL anti-Itgb1 antibody and B. 2 µg/mL RGD. Data are mean ± SD; n = 3. Significance: * and **, $P<0.05$ and $P<0.01$, respectively.

6.3. Effect of glycation of collagen IV with methylglyoxal on MIN6 cell adhesion

6.3.1. Determination of adhesion by cell adhesion assay

The use of 100 µM MG to modify the collagen resulted in a visual increase in the number of rounded and floating cells after 24 hours as well as a change in morphology. There were less adherent, healthy cells and less cell-cell interactions with this MG-modified collagen coating of the wells. In all other experiments with MG-glycated collagen, cells had a healthy morphology at the time points monitored. At both 24 and 72 h incubation on collagen, there was no clear difference in MIN6 cell morphology when compared to collagen glycated with 4 µM or 10 µM MG. The effect of the modification of human collagen IV with MG on the adhesion of MIN6 cells is shown in Figure 38. Adhesion compared to control collagen was increased by 66% and 98% when collagen was incubated for 24 h with 4 µM and 10 µM MG respectively. The same trends could be observed when experiments were repeated using mouse collagen IV - Figure 39. Adhesion to mouse collagen coated plates was increased by 76% compared to uncoated plates, and adhesion increased a further 67% over control collagen when collagen had been glycated with 10 µM

MG. Although cells on glycated collagen appeared loose when viewed under the microscope, there were large clusters of cells visible; this clustering may account for the increased number of cells adhered.

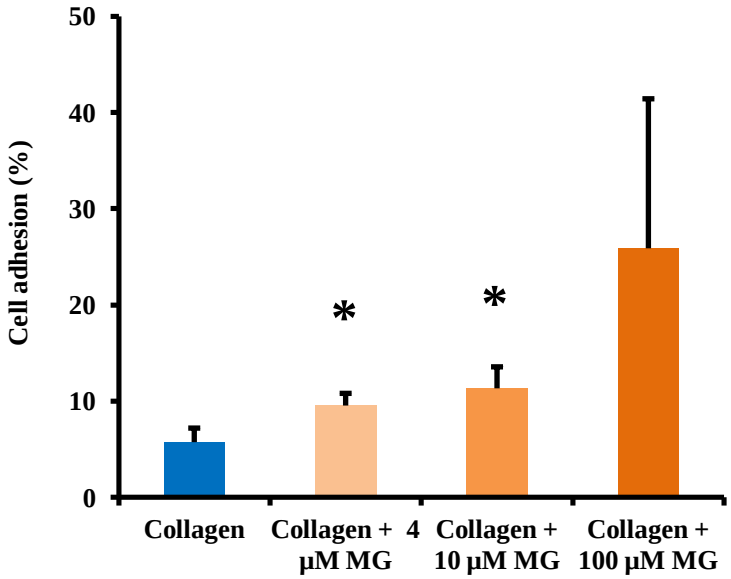

Figure 38: MIN6 cell adhesion to human collagen IV modified with MG. Percentage cell adhesion after 2 h incubation. Data are mean ± SD; n = 3. Significance: *, P<0.05.

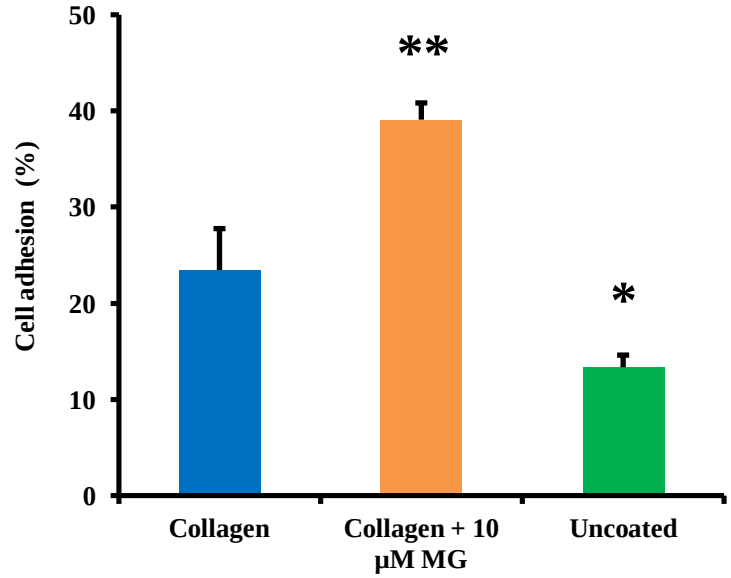

Figure 39: MIN6 cell adhesion to mouse collagen and MG-glycated collagen. Percentage cell adhesion after 2 h incubation on uncoated wells, mouse collagen IV and mouse collagen IV glycated with 10 µM MG for 24 hr. Data are mean ± SD; n = 3 - 4. Significance: * and **, P<0.05 and P<0.01, respectively.

6.3.2. Determination of force and energy of adhesion between MIN6 cells and collagen IV

The maximum unbinding force and energy needed to detach MIN6 cells from collagen and MG-glycated collagen were measured using AFM-FS - Figure 40. The median maximum unbinding force was 45% lower for collagen glycated with 10 μM compared to control collagen. The total energy required to detach MIN6 cells from the collagen matrix also decreased – the median was 92% lower when collagen was glycated with MG. The same effect was observed when MIN6 cells were pre-incubated with RGD before plating onto control collagen – the median detachment energy had decreased by 91%. Figure 41 shows the unbinding force and detachment energy for the three treatment groups.

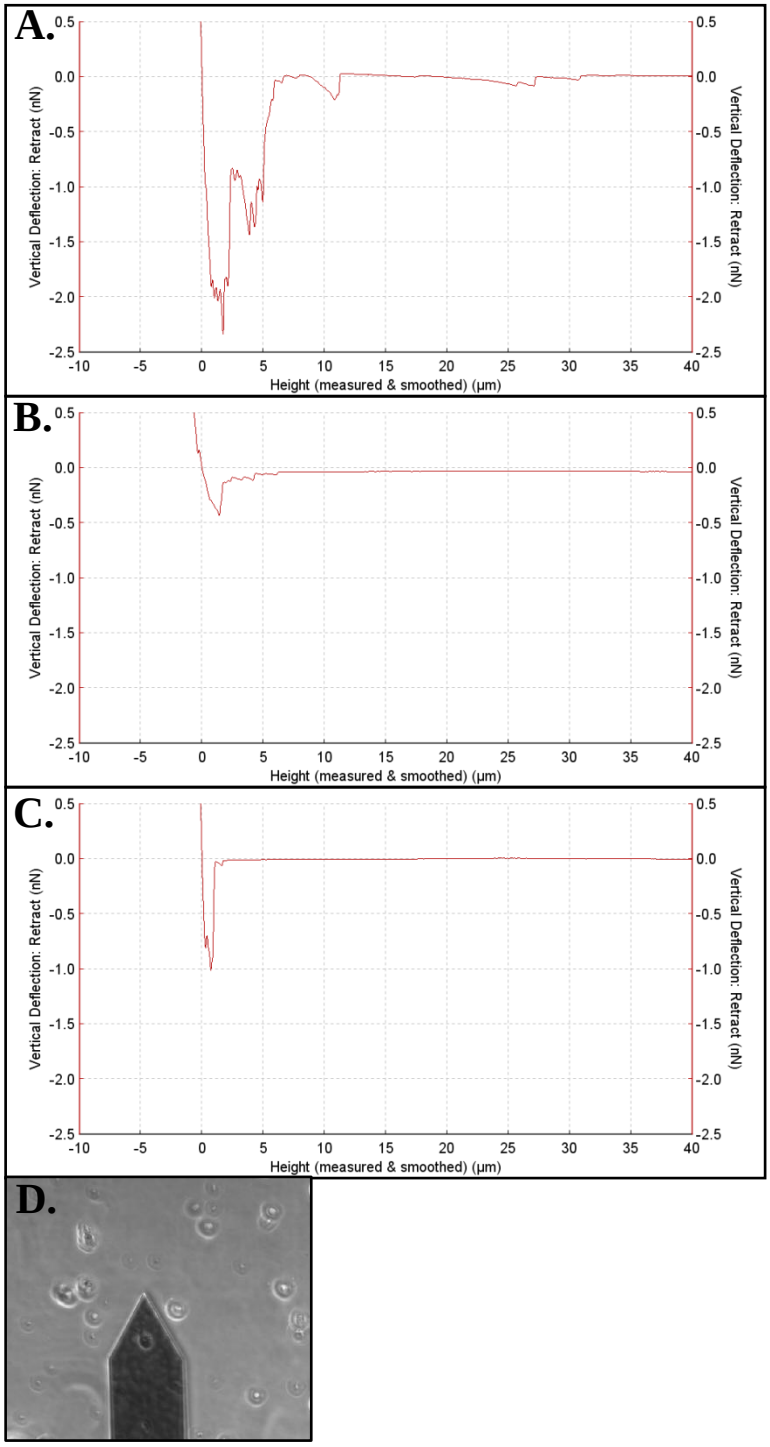

Figure 40: Atomic Force Spectroscopy traces. A. Force Spectroscopy trace for MIN6 cell on control collagen. The cantilever was retracted (5 µm/s) and the force versus deflection measured until the cell and matrix were completely separated. The same experiment was repeated using B. collagen glycated with 10 µM MG for 24 h and C. MIN6 cells pre-incubated with 2 µg/mL RGD. D. A representative phase contrast image of a single MIN6 cell bound to the cantilever (cantilever width 50 µm).

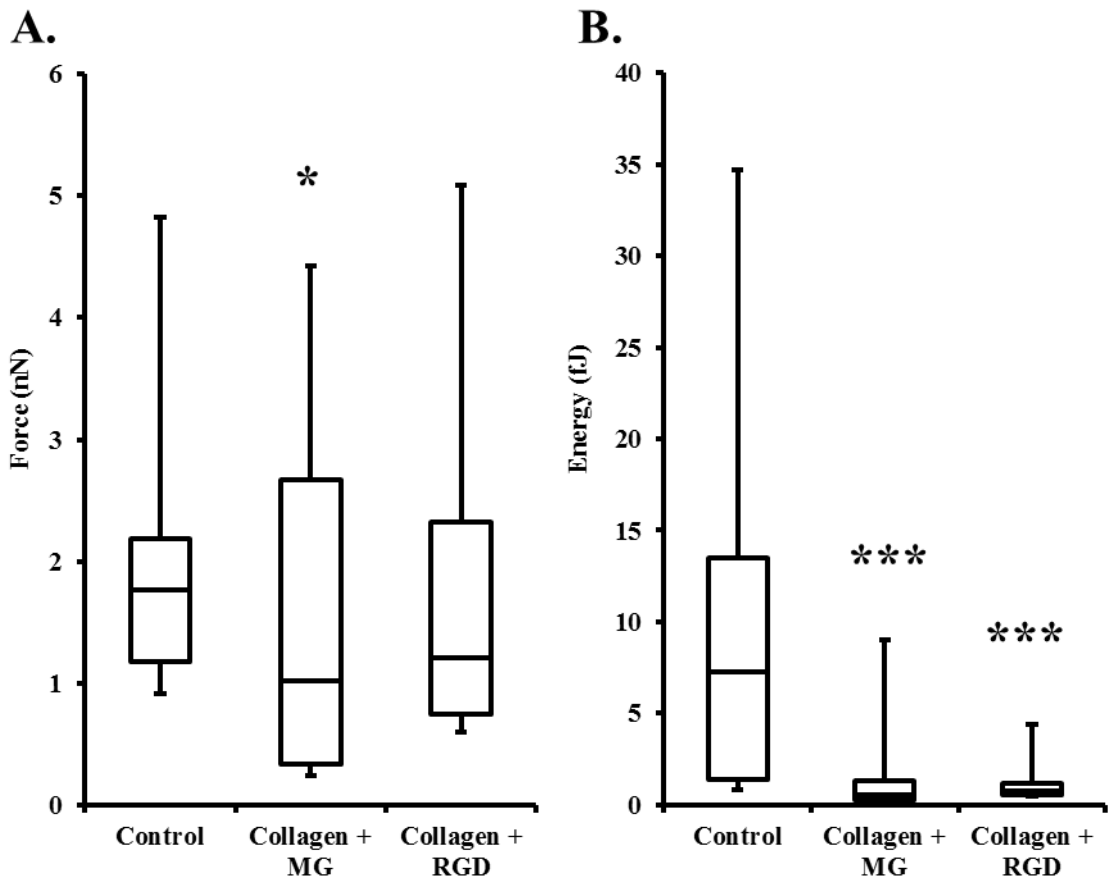

Figure 41: MG-glycation of collagen decreases MIN6-collagen adhesion. Quantification of (A) maximum unbinding force and (B) detachment energy. Data of multiple cells from three separate experiments (42 - 59 data points) are expressed as box plots displaying minimum and maximum data points, median and interquartile range. Significance: * and ***: $P<0.05$ and $P<0.001$, respectively.

6.4. Effect of culture on collagen IV and MG-glycated collagen IV on gene expression in MIN6 cells

MIN6 cells were plated onto 24 well plates coated with collagen, collagen glycated with 10 µM MG and onto uncoated wells. Cells were cultured for 3 days, the RNA extracted and the expression of genes of interest analysed - Table 32. The expression of Glo1 in MIN6 cells was not altered by either culture on collagen IV or MG-glycation of the collagen matrix. Expression of Ins2 was also unaltered by coating of plates with either collagen or MG-glycated collagen. Ins1 expression tended to increase in MIN6 cells cultured on collagen, although this was regardless of whether or not the collagen was glycated. Culture on MG-glycated mouse collagen resulted in a slight increase in the expression of Ins1 of 0.82% over culture

on uncoated plastic, whilst the same trend showed a 1.6% increase in expression in cells cultured on control human collagen compared to the uncoated control. There was a 5% decrease in the expression of Itgb1 when MIN6 cells were cultured on MG-glycated collagen compared to culture on control collagen substrate. E-cadherin expression decreased by 6% when MIN6 cells were cultured on MG-glycated collagen, compared to culture in uncoated wells. Whilst there was no quantifiable change in Cx36 expression in MIN6 cells cultured on mouse collagen, this was potentially due to the variability in measurements, particularly of the expression in MIN6 cells cultured on MG-glycated mouse collagen. In experiments performed using human collagen, there was a decrease (5%) in the expression of Cx36 in MIN6 cells cultured on glycated collagen, compared to MIN6 cells cultured on control collagen – as shown in Figure 42.

Table 32: Gene expression analysis of MIN6 cells cultured on mouse collagen

Gene	Uncoated	Collagen coated	Collagen coated + 10 μM MG
Ins1	0.725 ± 0.003	0.729 ± 0.004	0.731 ± 0.002°
Ins2	0.654 ± 0.008	0.657 ± 0.009	0.653 ± 0.008
Glo1	0.533 ± 0.010	0.541 ± 0.008	0.534 ± 0.012
Itgb1	0.628 ± 0.002	0.633 ± 0.014	0.602 ± 0.011*
E-cadherin	0.619 ± 0.005	0.610 ± 0.032	0.584 ± 0.016°
Connexin36	0.436 ± 0.034	0.406 ± 0.009	0.402 ± 0.020

Data are mean ± SD; n = 3 - 4. Significance: * and $^{\circ}$, $P<0.05$ compared to control collagen and uncoated wells respectively. Gene expression normalised to 18S RNA.

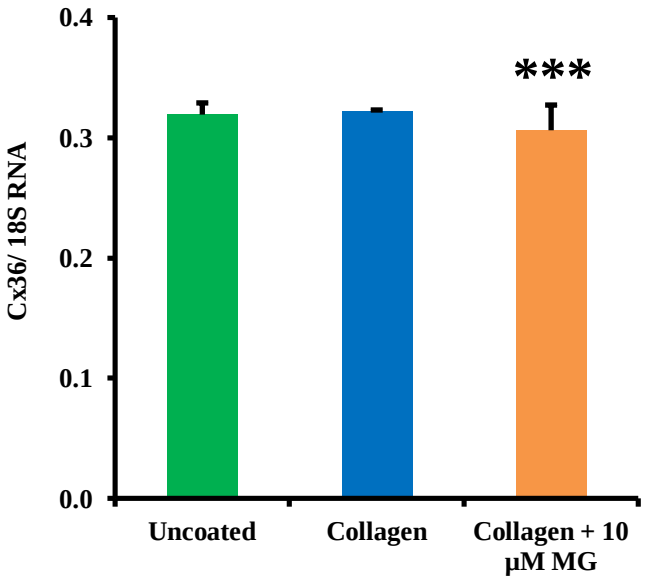

Figure 42: Expression of Cx36 in MIN6 cells cultured on human collagen IV. Cx36 mRNA normalised to 18S RNA in MIN6 cells following culture for 3 days in uncoated wells, on human collagen IV and human collagen IV glycated with 10 µM MG for 24 h. Data are mean ± SD; n = 4. Significance: ***, P<0.001.

7. Results: The glyoxalase system and dicarbonyl metabolism in an *in vivo* model of insulin resistance

7.1. Impairments in glucose tolerance in high fat diet fed mice

The effects of the three different dietary regimes on body and organ weight, food intake and parameters relating to glucose tolerance and lipid content in C57BL6 mice are detailed in Table 33. The cumulative food consumption (kJ) was increased by 16% in the HFD group compared to the mice fed control chow. When the HFD was supplemented with omega-3 fatty acids the food intake was not significantly different to that of the control mice. Both the HFD and omega-3 fatty acid supplemented HFD led to increased weight gain compared to the control mice (3-fold and 2.3-fold respectively). Consequently, the total body weight at the end of the study was 40% and 29% higher in the HFD and supplemented groups respectively, when compared to those mice fed a diet of control chow. The liver and brown adipose tissues were both significantly larger following HFD feeding – 17% and 2.5-fold respectively. When animals were fed a HFD supplemented with omega-3 fatty acids only the brown adipose tissue was significantly larger than the mass measured in control animals, however, the increase – 1.9-fold – was smaller than observed without the supplementation of the HFD. The pancreas mass was not significantly different between the treatment groups. Mice fed a HFD had increased plasma fasting glucose concentration (+73%), insulin (+5.2-fold), cholesterol (+2.1-fold), NEFA (+37%) and triglycerides (48%), compared to mice fed a normal chow diet. In addition, the hepatic steatosis – judged by measuring the lipid content of the liver - had increased 3.3-fold in HFD fed mice. Mice fed a HFD also had impaired glucose tolerance – as judged by the 2.2-fold increase in the area under curve measurement in a glucose tolerance test. Fasting plasma insulin was 2.2-fold higher in mice fed HFD supplemented with omega-3 fatty acids than in control mice and the increase in fasting plasma glucose was 48% over control animals - substantially less than the increases observed in mice fed a HFD without omega-3 fatty acid supplementation.

Table 33: Parameters relating to body weight, glucose tolerance and adiposity in mice fed three different feeding regimes

Parameter	Control	HFD	HFD + omega-3 fatty acids
Whole body parameters:			
Body weight (g)	32.2 ± 1.9	45.0 ± 2.8***	41.4 ± 5.2***
Body weight gain (g)	6.0 ± 1.6	18.1 ± 2.8***	14.2 ± 3.3$^{***,\circ}$
Cumulative food intake (kJ)	2920 ± 258	3400 ± 170***	3040 ± 286
Tissue weight (mg):			
Pancreas	137 ± 27	159 ± 24	145 ± 22
Liver	1680 ± 175	1960 ± 300*	1650 ± 310
Brown adipose tissue	117 ± 35	292 ± 92***	227 ± 85**
Plasma parameters:			
Fasting glucose (mmol/L)	5.0 ± 0.9	8.6 ± 1.6***	7.3 ± 1.4***
Fasting insulin (ng/mL)	0.281 ± 0.097	1.45 ± 0.46***	0.609 ± 0.265$^{**,\circ\circ\circ}$
Cholesterol (mmol/L)	2.01 ± 0.25	4.30 ± 0.47***	3.52 ± 0.48$^{***,\circ\circ}$
NEFA (mmol/L)	0.582 ± 0.195	0.797 ± 0.176*	0.495 ± 0.080$^{\circ\circ\circ}$
Triglycerides (mmol/L)	1.27 ± 0.35	1.88 ± 0.62*	1.28 ± 0.36°
Other:			
Glucose tolerance (AUC, mmol/L x 180 min)	1520 ± 184	3300 ± 790***	2530 ± 331$^{***,\circ}$
Hepatic steatosis (mg/g tissue)	33.5 ± 4.9	111 ± 42***	62.6 ± 25.6$^{*,\circ}$

Data are mean ± SD; n = 8 - 9. AUC: area under curve. Significance: *, ** and ***, P<0.05, P<0.01 and P<0.001 compared to control group; and °, °° and °°°, P<0.05, P<0.01 and P<0.001 compared to HFD group.

7.2. Analysis of gene expression in HFD fed mice

RNA was extracted from the pancreas of control fed, HFD fed and omega-3 fatty acid supplemented HFD fed mice and the expression of Ins1, Ins2, Glo1 and ICAM-1 was analysed, using 18S RNA as a reference gene for normalisation. The expression of Ins1 and ICAM-1 showed no significant difference between the three treatment groups - Figure 43. Ins2 and Glo1 mRNA were below the limit of quantification.

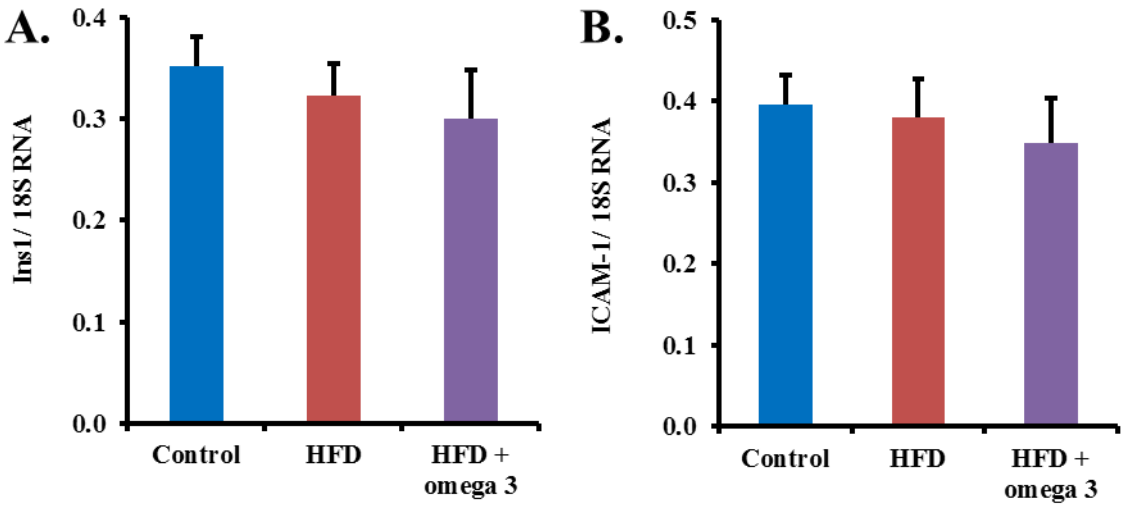

Figure 43: Gene expression in the pancreas of HFD fed mice. Expression of A. Ins1 and B. ICAM-1 in the pancreas. Data are mean ± SD; n = 7.

7.3. Activities of the glyoxalase system enzymes and pathway flux

The activity of Glo1 in the pancreas of control mice was 663 ± 120 mU per mg protein. The activity of Glo2 in the pancreas of control mice was 130 ± 39 mU per mg protein. The activity of Glo1 and Glo2 in the pancreas was not changed significantly by the three different dietary regimes - Figure 44. D-Lactate was also measured in the pancreas – indicative of *in situ* flux through the glyoxalase system. The pancreas content of D-lactate of control mice was 0.583 ± 0.171 nmol per mg wet weight. There was no significant change in the pancreas content of D-lactate with HFD and HFD with omega-3 fatty acid supplementation - Figure 45. Total thiol content of the pancreas was also unchanged by the different diets. Pancreas thiol contents were: 330 ± 62, 333 ± 116 and 327 ± 61 nmol per mg protein in control, HFD and HFD supplemented with omega-3 supplementation, respectively (n = 7 for each group).

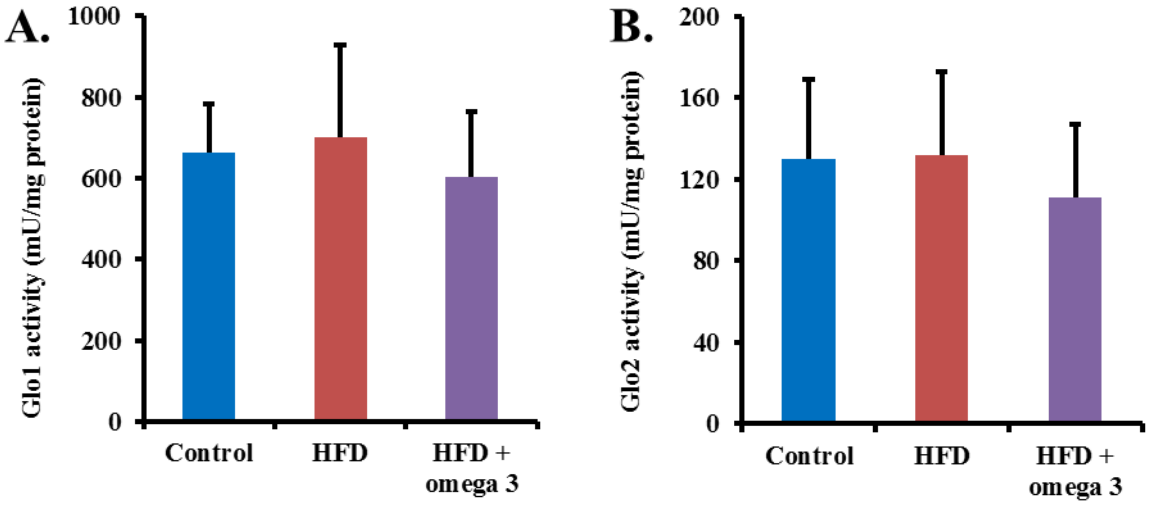

Figure 44: Enzymatic activities of the glyoxalase system in the mouse pancreas. A. Activity of Glo1. B. Activity of Glo2. Mice were fed a control chow diet, HFD and HFD supplemented with omega-3 fatty acids. Data are mean ± SD; n = 6 - 7.

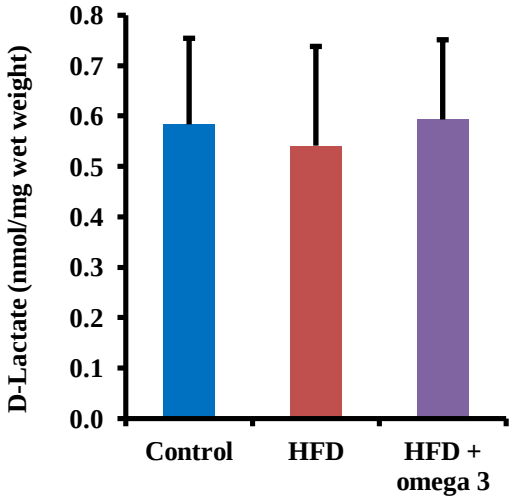

Figure 45: D-Lactate content of the mouse pancreas. Mice were fed a control chow diet, HFD and HFD supplemented with omega-3 fatty acids. Data are mean ± SD; n = 6 - 7.

7.4. Effect of HFD feeding on dicarbonyls in pancreas and plasma

The concentration of dicarbonyls in the plasma of mice fed a control diet, HFD and HFD supplemented with omega 3 were measured - Figure 46. There was no difference in the plasma concentration of MG, glyoxal or 3-DG in the three diet

groups. The dicarbonyls were also measured in the pancreas – Figure 47. There was a 24% and 35% increase in the MG in the pancreas in the HFD fed and the HFD supplemented with omega-3 fatty acid fed mice, respectively, compared to the amount in the pancreas of control chow fed mice. The amount of glyoxal also increased in HFD fed mice supplemented with omega-3 fatty acids with respect to control (+55%) and with respect to HFD fed mice (+70%). The glyoxal content of the pancreas of HFD fed mice was not significantly different to in the pancreas of control chow fed mice. The 3-DG content of the pancreas was decreased 47% in HFD fed mice compared to control chow fed mice but not in HFD fed mice supplemented with omega-3 fatty acids. The amount of MG in the pancreas was approximately 10-fold higher than both glyoxal and 3-DG.

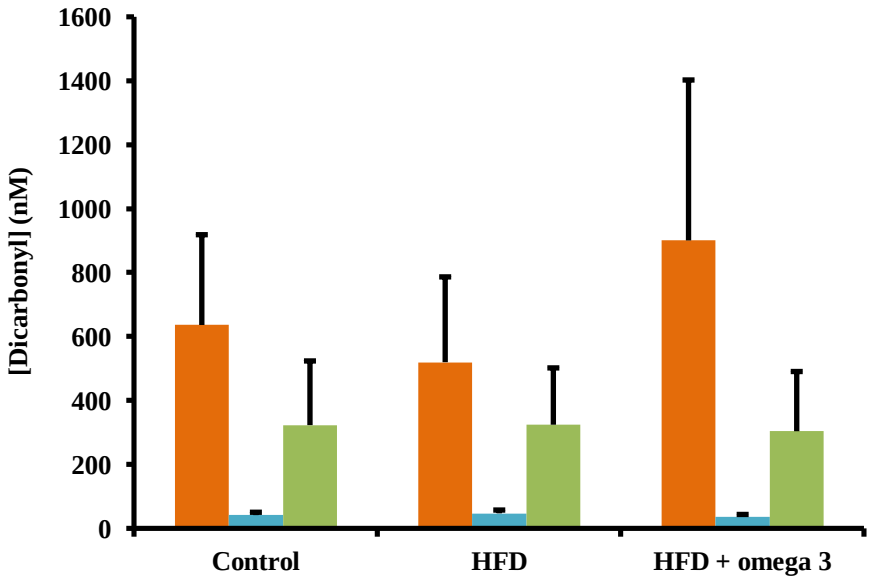

Figure 46: Concentration of dicarbonyls in mouse plasma. Data are mean ± SD; n = 6 - 9. Key: ■, MG; ■ glyoxal; ■ 3-DG.

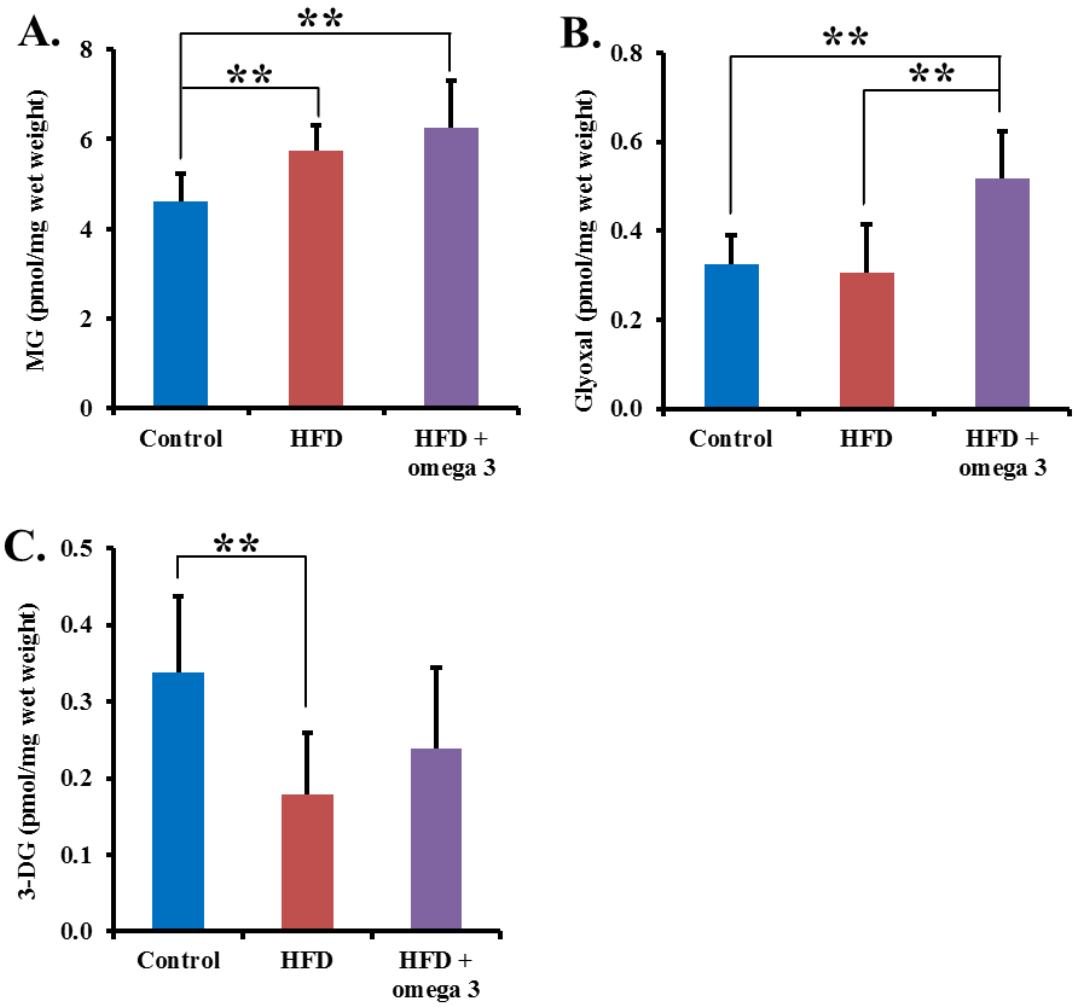

Figure 47: Dicarbonyls in mouse pancreas. A. Amount of MG. B. Amount of glyoxal. C. Amount of 3-DG. Pancreas of mice fed a control chow diet, HFD and HFD supplemented with omega-3 fatty acids. Data are mean ± SD; n = 6 - 7. Significance: **, P<0.01.

7.5. Formation of glycation, oxidation and nitration adduct residues on pancreatic and plasma protein

7.5.1. Pancreatic and plasma protein

Analysis of AGE residues of cytosolic protein of mouse pancreas indicated that MG-H1 was a major glycation adduct residue – 1.04 ± 0.21 mmol/mol arg of mice fed a control chow diet. HFD feeding with and without omega-3 fatty acid supplementation did not change MG-H1 residue content - Table 34. CMA adduct residue content of cytosolic protein of the mouse pancreas was decreased in both the HFD fed and HFD supplemented with omega-3 fatty acid fed mice by 30% and 37% respectively. Similar decreases were observed in 3DG-H (20% and 17%) and

MetSO (20% and 19%) residue contents. FL residue content of pancreatic protein was increased 24% in mice fed HFD supplemented with omega-3 fatty acids, compared to those fed HFD without omega-3 fatty acid supplementation.

Protein glycation, oxidation and nitration adduct residues were also analysed in ECM pancreatic protein. FL was decreased 54% in the pancreatic ECM protein of HFD and HFD supplemented with omega-3 fatty acid fed mice, compared to those fed control chow. CML was also 27% higher in mice fed a HFD supplemented with omega-3 fatty acid, compared to mice fed control chow. This resulted in a 3-fold increase in the CML/FL ratio. Other oxidative adduct residues - MetSO, dityrosine and NFK residues - did not change between the treatment groups. The glycation, oxidation and nitration adduct residue content on pancreatic ECM protein are given in Table 35.

In the plasma protein there were 2.4-fold and 1.8-fold increases in MOLD in HFD and omega-3 fatty acid supplemented HFD respectively, when compared to mice fed control chow - Table 36. FL also showed increased levels in HFD and omega-3 fatty acid supplemented HFD (33% and 24% respectively) when compared to control chow fed mice. However, CEL was 43% lower in the plasma of HFD fed mice than control chow fed mice. G-H1 residues on plasma proteins decreased by 39% when the HFD was supplemented with omega-3 fatty acid compared to HFD without supplementation. There were 37% and 28% increases in MetSO in the plasma of HFD fed and HFD supplemented with omega-3 fatty acid fed mice respectively, compared to the amount of this adduct in control chow fed mice, indicative of increased oxidative stress.

Table 34: Glycation, oxidation and nitration adduct residues in cytosolic protein of the mouse pancreas

Protein adduct residue	Control	HFD	HFD + omega-3 fatty acids
MG-H1 (mmol/mol arg)	1.04 ± 0.21	0.911 ± 0.124	1.02 ± 0.16
CEL (mmol/mol lys)	0.0210 ± 0.0090	0.0229 ± 0.0048	0.0194 ± 0.0048
MOLD (mmol/mol lys)	0.308 ± 0.045	0.337 ± 0.110	0.385 ± 0.075
G-H1 (mmol/mol arg)	0.0248 ± 0.0058	0.0236 ± 0.0071	0.0300 ± 0.0082
CML (mmol/mol lys)	0.289 ± 0.038	0.281 ± 0.031	0.287 ± 0.036
CMA (mmol/mol arg)	0.0371 ± 0.0059	0.0259 ± 0.0053**	0.0236 ± 0.0027***
3DG-H (mmol/mol arg)	0.257 ± 0.038	0.206 ± 0.017*	0.212 ± 0.029*
Pentosidine (mmol/mol arg)	0.00400 ± 0.00063	0.00361 ± 0.00045	0.00369 ± 0.00039
FL (mmol/mol lys)	12.4 ± 3.8	9.23 ± 0.95	11.4 ± 2.3°
Glucosepane (mmol/mol arg)	0.150 ± 0.047	0.107 ± 0.026	0.102 ± 0.023
MetSO (mmol/mol met)	9.84 ± 1.13	7.89 ± 0.59**	8.02 ± 0.44**
Dityrosine (mmol/mol tyr)	0.602 ± 0.192	0.697 ± 0.156	0.679 ± 0.147
NFK (mmol/mol trp)	0.615 ± 0.109	0.653 ± 0.077	0.712 ± 0.108
CML/FL ratio	0.0254 ± 0.0085	0.0306 ± 0.0036	0.0258 ± 0.0050
GEEK (mmol/mol lys)	2.42 ± 0.36	2.52 ± 0.61	2.69 ± 0.59

Data are mean ± SD; n = 6 - 7. Significance: *, ** and ***, P<0.05, P<0.01 and P<0.001, respectively, compared to control chow fed mice; °, P<0.05 compared to HFD fed mice.

Table 35: Glycation, oxidation and nitration adduct residues of extracellular matrix protein of mouse pancreas

Protein adduct residue	Control	HFD	HFD + omega-3 fatty acids
MG-H1 (mmol/mol arg)	0.373 ± 0.043	0.371 ± 0.049	0.417 ± 0.068
CEL (mmol/mol lys)	0.0697 ± 0.0102	0.0743 ± 0.0240	0.0768 ± 0.0244
G-H1 (mmol/mol arg)	0.0152 ± 0.0078	0.0179 ± 0.0074	0.0178 ± 0.0053
CML (mmol/mol lys)	0.161 ± 0.015	0.190 ± 0.043	0.203 ± 0.033*
CMA (mmol/mol arg)	0.0840 ± 0.0116	0.0768 ± 0.0119	0.0825 ± 0.0085
3DG-H (mmol/mol arg)	0.283 ± 0.060	0.265 ± 0.065	0.284 ± 0.049
Pentosidine (mmol/mol arg)	0.00266 ± 0.00071	0.00313 ± 0.00085	0.00297 ± 0.00073
FL (mmol/mol lys)	16.4 ± 5.8	7.61 ± 3.87**	5.95 ± 1.65**
Glucosepane (mmol/mol arg)	0.0181 ± 0.0042	0.0287 ± 0.0127	0.0202 ± 0.0036
MetSO (mmol/mol met)	34.1 ± 2.4	32.8 ± 2.9	31.2 ± 2.3
Dityrosine (mmol/mol tyr)	1.35 ± 0.25	1.54 ± 0.37	1.51 ± 0.10
NFK (mmol/mol trp)	0.735 ± 0.261	0.759 ± 0.254	0.580 ± 0.165
CML/FL ratio	0.0109 ± 0.0038	0.0317 ± 0.0164*	0.0326 ± 0.0031***
3-NT (mmol/mol tyr)	0.00710 ± 0.00278	0.00771 ± 0.00192	0.00838 ± 0.00247
GEEK (mmol/mol lys)	3.62 ± 1.60	3.30 ± 0.65	3.76 ± 1.84

Data are mean ± SD; n = 6 - 7. Significance: *, ** and ***, P<0.05, P<0.01 and P<0.001, respectively, compared to control chow fed mice.

Table 36: Glycation, oxidation and nitration adduct residues of mouse plasma protein

Protein adduct residue	Control	HFD	HFD + omega-3 fatty acids
MG-H1 (mmol/mol arg)	0.310 ± 0.039	0.325 ± 0.043	0.274 ± 0.029
CEL (mmol/mol lys)	0.287 ± 0.146	0.164 ± 0.031*	0.228 ± 0.071
MOLD (mmol/mol lys)	0.0515 ± 0.0380	0.125 ± 0.033**	0.0914 ± 0.0176*
G-H1 (mmol/mol arg)	0.0420 ± 0.0207	0.0584 ± 0.0143	0.0354 ± 0.0045°°
CML (mmol/mol lys)	0.814 ± 0.161	0.841 ± 0.129	0.770 ± 0.093
CMA (mmol/mol arg)	0.0306 ± 0.0085	0.0351 ± 0.0089	0.0289 ± 0.0041
3DG-H (mmol/mol arg)	0.254 ± 0.066	0.302 ± 0.065	0.203 ± 0.029
FL (mmol/mol lys)	1.89 ± 0.29	2.52 ± 0.44**	2.35 ± 0.38*
Glucosepane (mmol/mol arg)	0.134 ± 0.026	0.151 ± 0.026	0.126 ± 0.030
MetSO (mmol/mol met)	3.26 ± 0.48	4.49 ± 0.35***	4.17 ± 0.86*
Dityrosine (mmol/mol tyr)	4.32 ± 0.92	4.39 ± 0.61	4.56 ± 0.72
NFK (mmol/mol trp)	2.62 ± 0.35	2.46 ± 0.17	2.68 ± 0.19
CML/FL ratio	0.440 ± 0.083	0.338 ± 0.065*	0.334 ± 0.064*
Ornithine (mmol/mol arg)	0.133 ± 0.064	0.167 ± 0.048	0.179 ± 0.049

Data are mean ± SD; n = 7 - 9. Significance: *, ** and ***, P<0.05, P<0.01 and P<0.001, respectively, compared to control chow fed mice; °°, P<0.01 compared to HFD fed mice.

7.5.2. Glycation, oxidation and nitration free adducts and related amino acids in the pancreas

Glycation, oxidation and nitration free adducts and related amino acids in the pancreas cytosolic ultrafiltrates were analysed. There were decreases in the concentration of glycation free adducts in the pancreas in HFD fed mice when compared to control chow fed mice - Table 37. These decreases were also found in mice fed a HFD with omega-3 fatty acid supplementation. Decreases in free adduct concentration in HFD fed mice were: MG-H1, 78%; G-H1, 40%; CMA, 67%; 3DG-H, 58%; and FL, 57%. CML was decreased by 18% in mice fed a HFD

supplemented with omega-3 fatty acid compared to in mice fed a HFD without supplementation. Pentosidine increased by 11% in the pancreatic filtrate of HFD fed mice compared to control fed mice. There were no significant changes in free adduct concentrations of MetSO or NFK in the pancreatic filtrates. Dityrosine also decreased 28% in HFD when supplemented with omega-3 fatty acids, compared to control.

Related amino acid concentrations were also measured in the pancreatic cytosol extracts - Table 37. The concentration of tryptophan was lower in HFD and HFD supplemented with omega-3 fatty acid fed mice (43% and 65% respectively) compared to control chow fed mice, and the concentration of arginine was 22% lower in the pancreas of mice fed a HFD supplemented with omega-3 fatty acid than in control mice.

Table 37: Glycation, oxidation and nitration free adducts and related amino acids in pancreas cytosolic extracts

Free adduct	Control	HFD	HFD + omega-3 fatty acid
Glycation, oxidation and nitration free adducts (pmol/mg wet weight)			
MG-H1	1.61 ± 0.31	0.348 ± 0.036***	0.325 ± 0.035***
CEL	0.342 ± 0.063	0.349 ± 0.124	0.428 ± 0.104
MOLD	0.125 ± 0.040	0.155 ± 0.062	0.135 ± 0.052
G-H1	0.375 ± 0.043	0.226 ± 0.060***	0.163 ± 0.047***
CML	18.1 ± 2.8	20.1 ± 1.8	16.5 ± 2.0°°
CMA	0.154 ± 0.017	0.0502 ± 0.0046***	0.0468 ± 0.0099***
3DG-H	0.734 ± 0.113	0.312 ± 0.085***	0.255 ± 0.044***
Pentosidine	0.109 ± 0.009	0.122 ± 0.007*	0.111 ± 0.009
FL	11.8 ± 2.2	5.04 ± 0.68***	4.69 ± 0.91***
MetSO	0.616 ± 0.232	0.498 ± 0.049	0.619 ± 0.098
Dityrosine	0.835 ± 0.220	0.654 ± 0.141	0.604 ± 0.136*
NFK	0.134 ± 0.042	0.113 ± 0.037	0.108 ± 0.026
Amino acids (nmol/mg wet weight)			
Arg	0.357 ± 0.070	0.299 ± 0.067	0.277 ± 0.045*
Lys	1.05 ± 0.10	0.974 ± 0.074	0.970 ± 0.117
Met	0.408 ± 0.101	0.385 ± 0.051	0.387 ± 0.048
Tyr	0.402 ± 0.098	0.418 ± 0.092	0.447 ± 0.075
Trp	0.0379 ± 0.0106	0.0217 ± 0.0115*	0.0134 ± 0.0070***

Data are mean ± SD; n = 6 - 7. Significance: * and ***, P<0.05 and P<0.001, respectively, compared to control chow fed mice; °°, P<0.01 compared to HFD fed mice.

7.5.3. Glycation, oxidation and nitration free adducts and related amino acids in plasma

Glycation, oxidation and nitration free adducts and related amino acid concentrations of plasma were also determined. There were significant decreases in the adduct concentration of a number of glycation markers in both HFD fed and HFD supplemented with omega-3 fatty acid fed mice, compared to control chow fed mice - Table 38. These decreases were: MG-H1, 70%; CMA, 60%; 3DG-H, 89%;

and FL, 90%. CML free adduct was decreased 23% in plasma from HFD fed mice compared to control mice. The plasma filtrate concentration of the oxidative marker MetSO was unchanged in the different feeding regimes. Free adduct concentrations of NFK in the plasma were higher in the mice fed a HFD, compared with both control chow fed and omega-3 fatty acid supplemented HFD fed mice.

Analysis of amino acids in the plasma filtrates indicated a 24% decreased concentration of arginine in the HFD fed mice, compared with control chow fed mice. There were no significant changes in arginine in mice fed a HFD supplemented with omega-3 fatty acid. The concentration of tyrosine was increased 47% in plasma of mice fed a HFD supplemented with omega -3 fatty acids compared with control chow fed mice.

Table 38: Glycation, oxidation and nitration free adducts and related amino acids in plasma

Free adduct	Control	HFD	HFD + omega-3 fatty acid
Glycation, oxidation and nitration free adducts (nM)			
MG-H1	525 ± 139	160 ± 41***	146 ± 40***
CEL	6440 ± 410	5940 ± 3170	9130 ± 1620
CML	4600 ± 1100	3560 ± 657*	4120 ± 1220
CMA	14.0 ± 3.1	5.54 ± 1.13***	5.52 ± 2.75***
3DG-H	862 ± 260	91.4 ± 56.5***	183 ± 41***
FL	1870 ± 1298	188 ± 99**	-
MetSO	435 ± 112	384 ± 115	450 ± 49
NFK	67.4 ± 14.9	93.1 ± 21.9*	52.5 ± 20.1°°
Amino acids (µM)			
Arg	80.4 ± 12.0	60.9 ± 11.1**	70.7 ± 15.8
Lys	252 ± 52	276 ± 39	287 ± 54
Met	94.1 ± 21.4	86.2 ± 9.6	98.2 ± 8.7
Tyr	58.7 ± 12.3	69.4 ± 15.3	86.4 ± 19.6**

Data are mean ± SD; n = 7 - 9. Significance: *, ** and ***, P<0.05, P<0.01 and P<0.001, respectively, compared to control chow fed mice; °°, P<0.01 compared to HFD fed mice.

7.6. Localisation of insulin, collagen IV and MG-H1 residues in the mouse pancreas

Immunostaining was used to observe localisation of insulin, collagen IV and MG-H1 residues in sections of the mouse pancreas as well as any changes in localisation or co-localisation of these proteins and protein adducts following the different dietary regimes. Sections of pancreas from control, HFD and HFD supplemented with omega-3 fatty acid fed mice were analysed for these markers. Additional controls were analysed from each pancreas for auto-fluorescence and non-specific binding of secondary antibodies – an example is show in Figure 48. This showed no significant non-specific binding of secondary antibodies. Co-staining for collagen IV and insulin in pancreas sections is shown in Figure 49. Small amounts of collagen IV were present around the immunostaining of insulin, but this was different in appearance to the extensive collagen IV network observed in other regions of the pancreas. Co-staining of MG-H1 residues and insulin showed no clear co-localisation - Figure 50. Background fluorescence was also higher in these sections. Immunostaining for collagen and MG-H1 residues showed some co-localisation, particularly in the sections from the pancreas of a HFD fed mouse – Figure 51. There is a defined network of collagen IV within the pancreas sections; this is particularly evident in the pancreas sections from a control chow fed mouse.

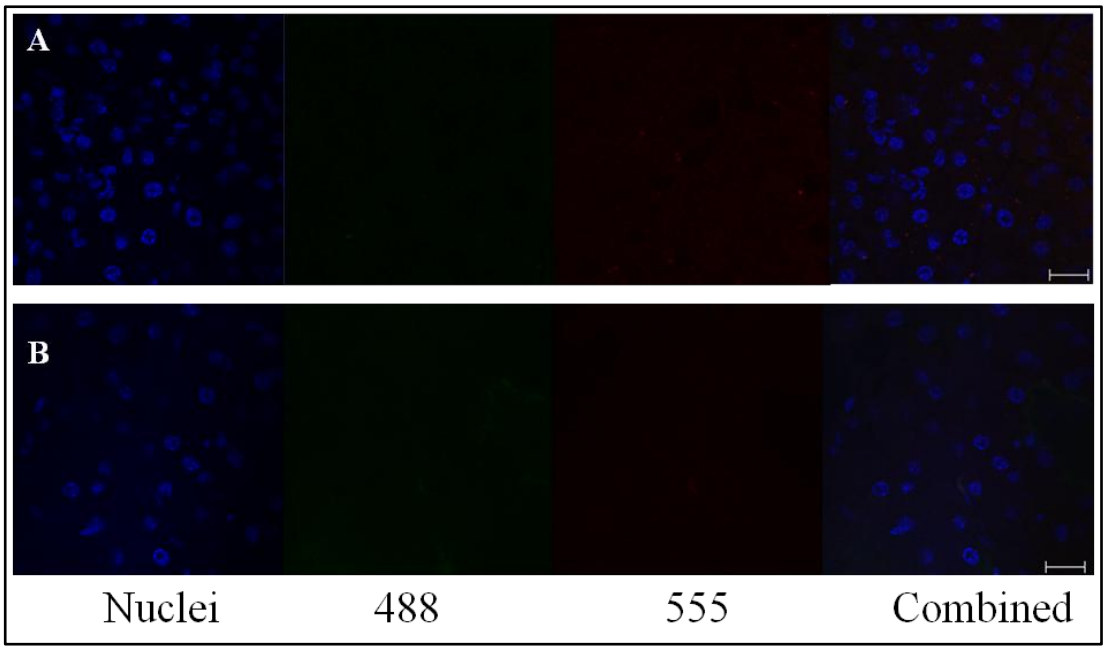

Figure 48: Examples of Immunostaining control sections. Representative sections showing (A) background fluorescence in HFD pancreas section and (B) staining using secondary antibodies alone in omega-3 fatty acid supplemented HFD pancreas section (goat anti-mouse 488 and goat anti-chicken 555). Scale bar: 20 µm.

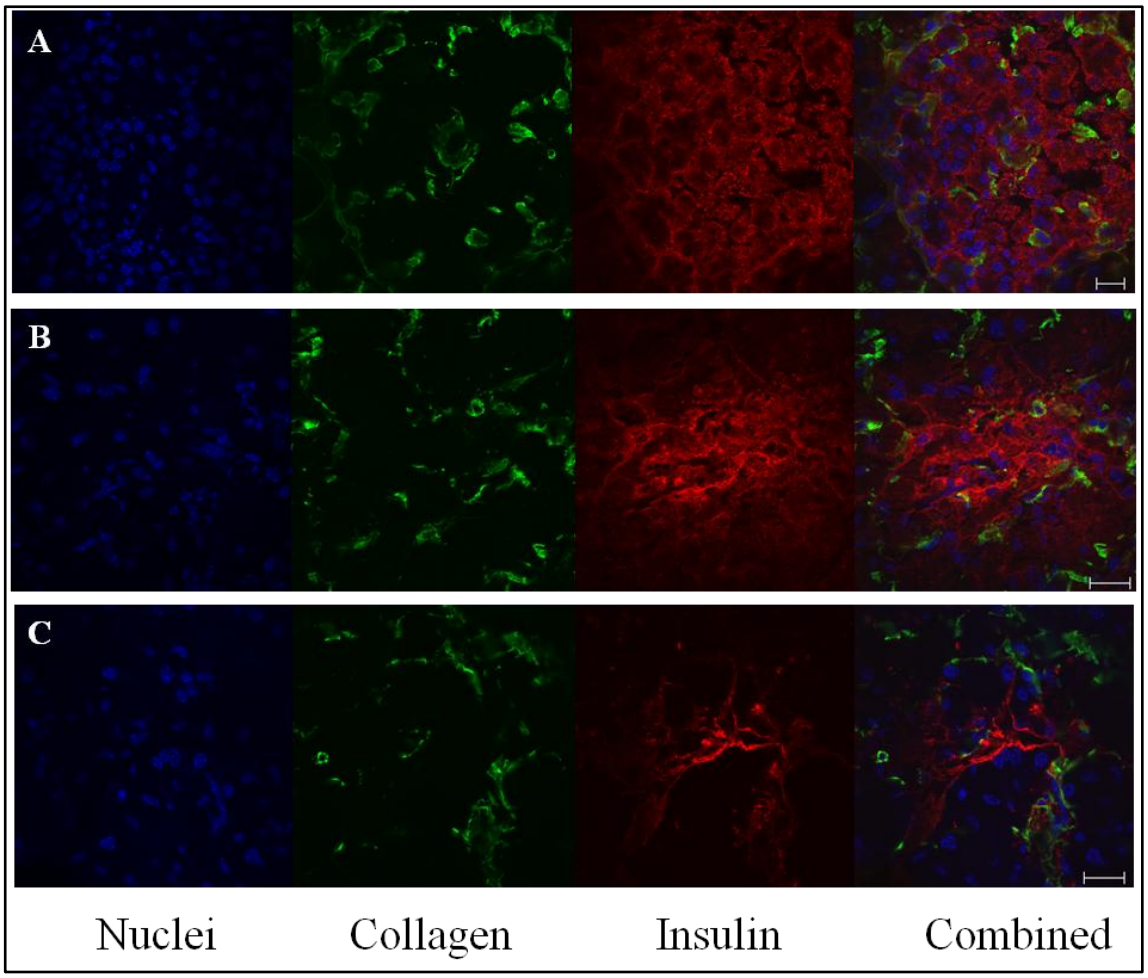

Figure 49: Immunostaining of collagen IV and insulin in the mouse pancreas. Co-staining of collagen IV and insulin in sections of the pancreas from (A) control chow fed mouse, (B) HFD fed mouse and (C) HFD supplemented with omega-3 fatty acid fed mouse. Scale bar: 20 µm.

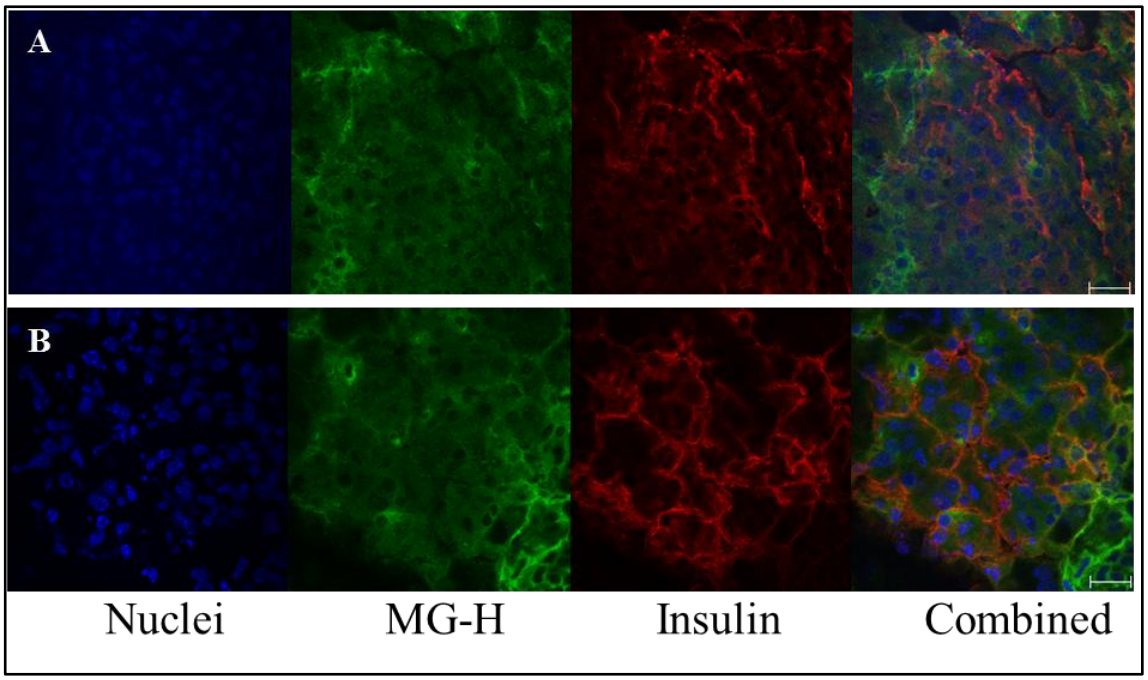

Figure 50: Immunostaining of MG-H1 residues and insulin in the mouse pancreas. Co-staining of MG-H1 residues and insulin in sections of the pancreas from (A) control chow fed mouse and (B) HFD fed mouse. Scale bar: 20 µm.

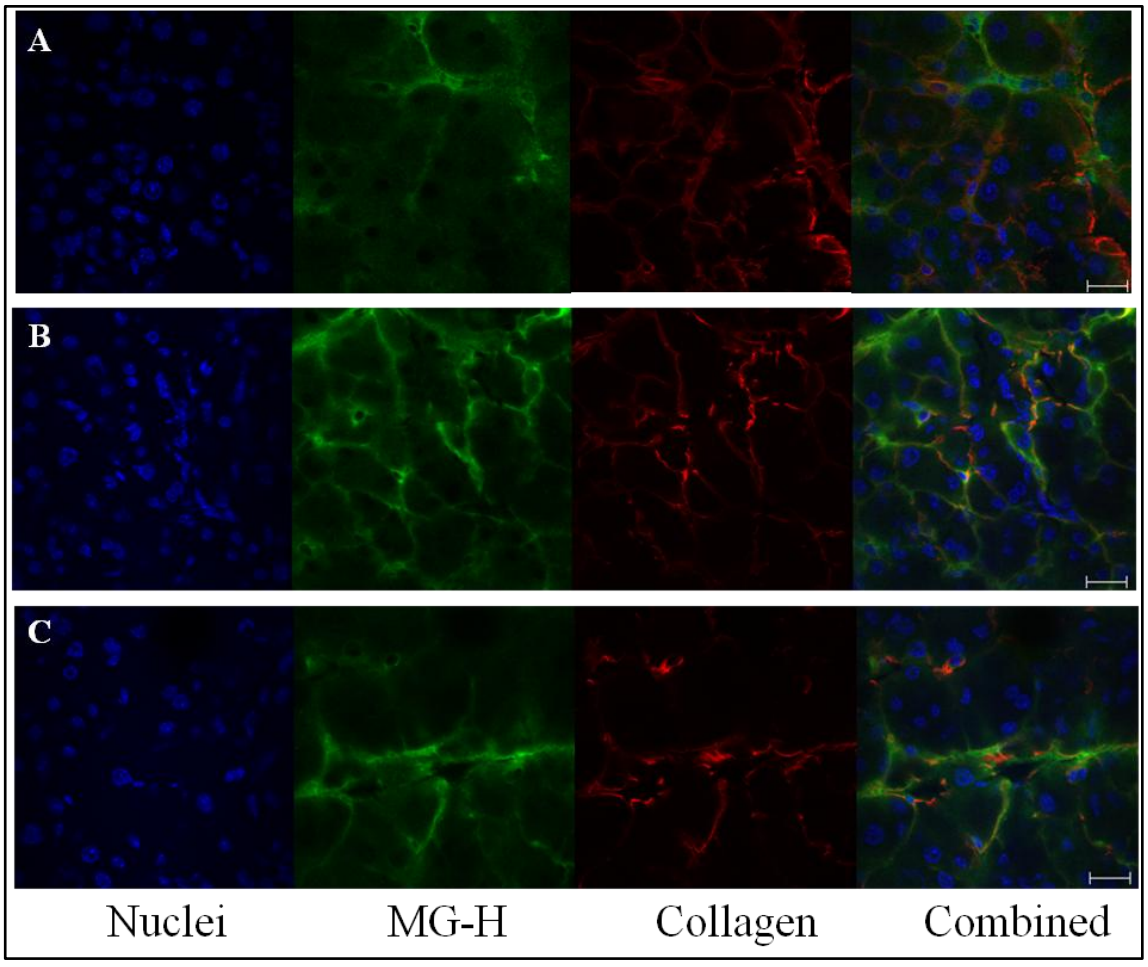

Figure 51: Immunostaining of collagen IV and MG-H1 residues in the mouse pancreas. Co-staining of collagen IV and MG-H1 residues in sections of the pancreas from (A) control chow fed mouse, (B) HFD fed mouse and (C) HFD supplemented with omega-3 fatty acid fed mouse. Scale bar: 20 µm.

8. Discussion

8.1. Effect of increased glucose concentration on pancreatic beta cell function – a possible role of dicarbonyl stress

In 1948 Dohan and Lukens showed that hyperglycaemia *per se* could play a pathogenic role in damage to the pancreas and development of diabetes (Dohan and Lukens, 1948). Others showed that infusion of glucose in Sprague-Dawley rats for 48 to 96 h caused a loss of GSIS (Leahy, *et al.*, 1987). However, modest increases in basal plasma glucose concentration from 4.7 to 6.0 mM for 53 h in adult humans increased beta cell function and insulin secretion (Flax, *et al.*, 1991). Loss of beta cell responsiveness to elevated glucose concentrations was termed "glucose toxicity" or "glucotoxicity" (Yki-Järvinen, 1992). Mechanisms involved are thought to include oxidative stress – where dicarbonyl stress by methylglyoxal is also implicated, dysregulation of beta cell glucose metabolism and other mechanisms that disrupt normal nutrient sensing (Liu, *et al.*, 1998; Nolan and Prentki, 2008; Robertson and Harmon, 2006).

Protein glycation may have a role in early stage beta cell dysfunction. If so, it is unlikely to be via glucose-mediated glycation as this is relatively slow and unresponsive to IGT. In addition, genetic knockout of fructosamine-3-kinase, responsible for FL repair, did not impair beta cell function (Pascal, *et al.*, 2010). Rather, increased methylglyoxal formation and dicarbonyl stress are more likely involved as increased methylglyoxal formation occurs even in short term increases in glucose concentration (Beisswenger, *et al.*, 2001). The methylglyoxal scavenger, aminoguanidine, partly prevented glucotoxicity both *in vitro* and *in vivo* (Piercy, *et al.*, 1998; Tanaka, *et al.*, 1999; Thornalley, *et al.*, 2000). If methylglyoxal and related dicarbonyls have an important role in glucotoxicity, it is likely that inducers of endogenous enzymatic protection of dicarbonyl stress – particularly Glo1 inducers – will be more effective and potentially less toxic than dicarbonyl scavengers (Kim, *et al.*, 2013; Xue, *et al.*, 2012).

The glyoxalase system and dicarbonyl metabolism have not been characterised in insulinoma cell lines *in vitro* or in the pancreas in an *in vivo* study relating to diabetes or beta cell dysfunction. Current research related to glycation

damage and diabetes is largely in the area of diabetic complications and how these can be limited and treated most effectively. In this study methylglyoxal metabolism by the glyoxalase system is investigated in the MIN6 insulinoma cell line and in an *in vivo* model of insulin resistance – HFD fed C57BL6 mice, to advance understanding of dicarbonyl metabolism in beta cell dysfunction and glucotoxicity.

8.2. The glyoxalase system and dicarbonyl metabolism in an *in vitro* beta cell line model – insulinoma MIN6 cells

MIN6 cells are widely used as a cell line model of pancreatic beta cells. Methylglyoxal, formed mainly from triosephosphate intermediates of glycolysis, reacts reversibly with GSH and protein thiols to form hemithioacetal adducts - Figure 52. There are also initial reversible adducts of methylglyoxal with arg and lys residues of protein. To characterise methylglyoxal metabolism by glyoxalase in MIN6 cells activities of Glo1 and Glo2, concentrations of methylglyoxal, GSH and protein thiols and flux of D-lactate formation were measured. When exogenous D-lactate was added to MIN6 cell cultures there was no significant metabolism of it, suggesting that formation of D-lactate by the glyoxalase system in this case represents flux of formation of methylglyoxal. D-lactate is metabolised in mammalian cells by mitochondrial 2-hydroxyacid dehydrogenase (Thornalley, 1993).

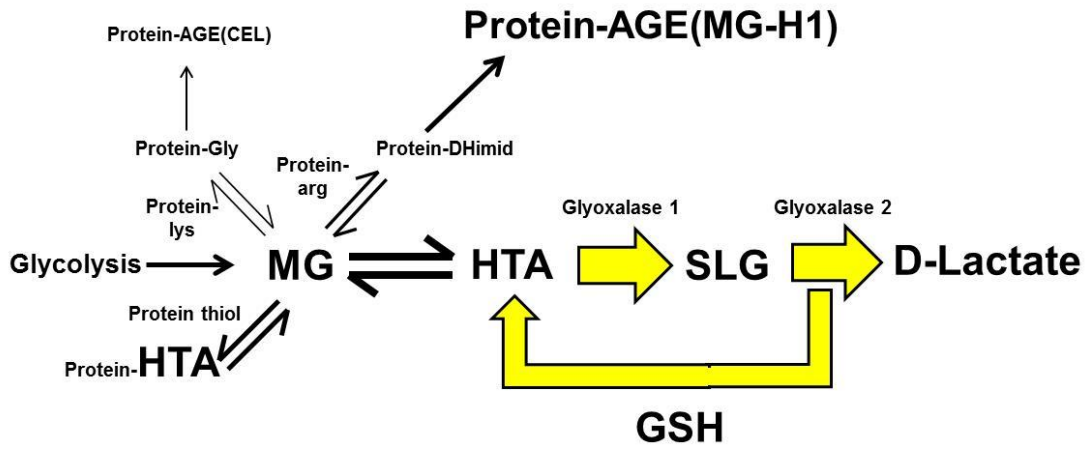

Figure 52: Methylglyoxal in MIN6 cells – formation, protein glycation and metabolism by glyoxalase. Key: DHimid, Dihydroxyimidazolidine; Gly, Glycosyl adduct; SLG, S-D-lactoylglutathione; HTA, hemithioacetal.

8.2.1. The effect of high glucose and dicarbonyl stress on dicarbonyl metabolism in MIN6 cells *in vitro*

Incubation of MIN6 cells in high glucose concentration (20 mM) showed no decrease in cell growth or viability. Glucose concentrations of up to 25 mM are routinely used in the culture medium for the growth of MIN6 cells by others (Cheng, *et al.*, 2012b; Kelly, *et al.*, 2010). MIN6 cells could be cultured for up to 5 days without cell detachment. Beyond this the viable cell number was decreased at six and seven days where cell detachment was evident.

Activities of the glyoxalase enzymes were present in MIN6 cells whereas activities of methylglyoxal dehydrogenase and methylglyoxal reductase were not detected. Measurement of enzymatic activities of Glo1 and Glo2 showed that the glyoxalase system was dominant – activities of methylglyoxal dehydrogenase and methylglyoxal reductase were below the limit of detection in MIN6 cells (<0.5 mU per million cells) and do not have a significant role in dicarbonyl metabolism in MIN6 cells. This suggests that the glyoxalase system is the major defence against dicarbonyl stress in MIN6 cells. Our research team has previously reported the metabolism of methylglyoxal to D-lactate in isolated rat pancreatic beta cells, indicating metabolism of methylglyoxal via the glyoxalase pathway in mature beta cells (Cook, *et al.*, 1998). Glo1 and aldoketo reductases metabolising methylglyoxal may be induced and the *in situ* activity of Glo1 is impaired by GSH depletion. Aldoketo reductases may therefore be important in supporting the detoxification of methylglyoxal in some circumstances (Rabbani and Thornalley, 2012c).

The expression of Glo1 in MIN6 cells was not altered by either culture from passage 40 to passage 46 or by the glucose concentration in the medium. The protective capacity of the glyoxalase system does not therefore deteriorate with passage over this range in this cell line, nor is its expression influenced by the glucose concentration within this physiological range. The activity of Glo1 and Glo2 were not significantly altered when MIN6 cells were cultured in 20 mM glucose. This demonstrates that in 20 mM glucose the protective capacity of the glyoxalase system in MIN6 cells is not increased, indicating that MIN6 cells are more at risk of glycation damage due to higher amounts of glucose and associated metabolites.

The dicarbonyl content of MIN6 cells and culture medium were measured to indicate the cellular exposure of MIN6 cells to dicarbonyls and whether this was

altered by a higher concentration of glucose in the culture medium. The content of MG, glyoxal and 3-DG in MIN6 cells *in vitro* was not altered by culture in media containing 20 mM glucose. The media concentrations of MG and glyoxal were not affected by the glucose concentration. The concentration of 3-DG in the medium increased 2.4-fold when cells were cultured in 20 mM glucose, compared to control cultures. Methylglyoxal is formed mainly in the cytosol of cells and a minor fraction leaks from cells by passive diffusion of the unhydrated form across membranes. There is also a slow formation from spontaneous degradation of glycated protein and glucose in the medium (Thornalley, *et al.*, 1999). The methylglyoxal measured is the sum of free methylglyoxal and methylglyoxal bound reversibly to protein. As Glo1 activity was not changed in high glucose cultures – nor was GSH (see later), the lack of increase in methylglyoxal concentration in cells and medium suggests that MIN6 cells are resistant to increases of triosephosphates when incubated in high glucose concentration. This is consistent with previous studies showing that decrease of glyceraldehyde-3-phosphate dehydrogenase by *ca.* 36% in high glucose cultures or in hydrogen peroxide treatment did not increase triosephosphates in MIN6 cells (Sakai, *et al.*, 2003). Lack of increase in glyoxal is consistent with no marked increase in lipid peroxidation. Increased 3-DG concentration in the culture medium may relate to increased degradation of glucose in culture medium to 3-DG non-enzymatically.

Cellular glutathione content was analysed to indicate whether this could affect the *in situ* activity of the glyoxalase system. Total glutathione in MIN6 cells, GSH + 2 x GSSG, was *ca.* 880 pmol per 10^6 cells. This is intermediate between *ca.* 200 and 3000 pmol per 10^6 cells of previous reports – determined by redox cycling assays (Kaneko, *et al.*, 2009; Kondo, *et al.*, 2000). The proportion of total glutathione present as GSSG (2.5%) is also much lower than the 36% previously reported (Kitiphongspattana, *et al.*, 2007). Kitiphongspattana *et al*. (2007) likely oxidised the cell extracts during sample processing. The assay for GSH and GSSG developed herein using stable isotopic dilution analysis LC-MS/MS has higher specificity, sensitivity and analytical recovery than previous techniques and is likely an improved estimate. There were no differences in the GSH or GSSG content of MIN6 cells cultured in 5.5 mM or 20 mM glucose, indicating that the *in situ* activity of Glo1 is not impaired or enhanced by change in the cellular content of GSH. In addition, this also showed that the absolute cell content of GSSG and GSSG/total

glutathione were not affected by the glucose concentration. An increase in absolute cell content of GSSG and GSSG/total glutathione would be indicative of an increase in oxidative stress. Lack of change suggests that there is no evidence of increased cytoplasmic oxidative stress in high glucose cultures. MIN6 cells incubated in high glucose concentration do not appear to suffer marked oxidative stress – as previous reports have suggested (Sakai, *et al.*, 2003). This was further supported by no differences in the total thiol or the protein thiol content in MIN6 cells cultured *in vitro* in the two different glucose conditions. Previous estimates of increased formation of ROS in MIN6 cells in high glucose appear to have been rates of ROS formation within the ability of the cells to metabolise them and prevent oxidative damage (Sakai, *et al.*, 2003).

The rate of formation of D-lactate by MIN6 cells in control cultures was 1.02 ± 0.34 nmol per 10^6 cells per day or 0.0771 ± 0.0161% of glucotriose flux. This was a slightly higher rate of formation, than found in the transformed endothelial cell line, HMEC-1, where the rate of formation of D-lactate in cultures with 5 mM glucose was *ca*. 0.4 nmol per 10^6 cells per day and *ca*. 0.04% of glucotriose flux (Z Irshad, unpublished observations). The rate of formation of D-lactate by MIN6 cells increased 41% cultured in high glucose *in vitro*, compared to 5.5 mM glucose. This indicates a higher flux of formation of D-lactate, and hence a higher flux of methylglyoxal through the glyoxalase system. With unchanged activity of Glo1, GSH or protein thiols this is expected to have produced a similar increase in cellular methylglyoxal concentration but this was not found. The concentration of L-lactate was not altered by culture in medium containing 5.5 or 20 mM glucose.

The rate of glucose consumption increased 28% when MIN6 cells were incubated in 20 mM glucose, and consequently the proportion of glucotriose leading to formation of D-lactate was unaltered. Therefore, the increased metabolism of glucose by MIN6 cells in 20 mM glucose only increased the flux of formation of methylglyoxal proportionate to the increase in glucose metabolism. There was no evidence for increased 'leak' of methylglyoxal from glycolysis in high glucose. This was different to the increased proportion of glucotriose flux converted to methylglyoxal in high glucose concentration, as found for red blood cells (Thornalley, 1988). The increased rate of glucotriose metabolism and D-lactate formation in hyperglycaemia, therefore, appears to be *ca*. 28 – 41%. With no change in Glo1 activity, GSH and protein thiols a similar increase in cellular concentration

of methylglyoxal was expected. Relatively high data dispersion in methylglyoxal measurement may have obscured detection of this.

Protein glycation, oxidation and nitration adduct residues were measured in cytosolic protein of MIN6 cells herein for the first time. Quantification of glycation, oxidation and nitration adduct residues on cellular protein of MIN6 cells indicated that glycation, oxidation and nitration adducts were present on the protein. The major AGE residue was MG-H1 at 0.351 mmol/mol arg. This is similar to the level previously reported in the mouse brain cortex (Kurz, *et al.*, 2011). CEL residue content was *ca*. 8-fold lower, as expected for the arginine-directed glycation of methylglyoxal (Thornalley, 2005). FL residue content was relatively low at 0.85 mmol/mol lys. There were no significant changes in the amount of protein glycated, oxidised or nitrated in MIN6 cells incubated in 5.5 mM and 20 mM glucose *in vitro*. There was also no change in the CML/FL residue ratio – a marker of oxidative stress (Knecht, *et al.*, 1991). This suggests there is no detectable increase in proteome damage by glycation, oxidation and nitration in the cytosol of MIN6 cells incubated in high glucose concentration.

Glycated, oxidised and nitrated cellular proteins undergo cellular proteolysis and related glycation, oxidation and nitration free adducts are released into the culture medium. The flux of formation of these was measured in MIN6 cell cultures. Some free adducts are further metabolised - NFK and MetSO – and fluxes could not therefore be deduced. The production of MG-H1, CEL, CML and CMA was not affected by the culture of MIN6 cells in 5.5 mM or 20 mM glucose, although these markers were produced indicating clearance of protein glycated by both MG and glyoxal from MIN6 cells. The flux of formation of FL and 3DG-H free adducts in MIN6 cells *in vitro* was increased *ca*. 4.1-fold and 2-fold, respectively, when MIN6 cells were cultured in 20 mM glucose. There are contributions to the formation of FL and 3DG-H free adducts by the direct reaction of glucose with lysine (798 μM) and 3-DG with arginine (398 μM) in the DMEM culture medium. Glucose (5.5 mM and 20 mM) is present in the culture medium and methylglyoxal, glyoxal and 3-DG are present from that in serum and that formed by degradation of glucose and serum protein glycated by glucose (Thornalley, *et al.*, 1999). The rate of formation of glycation free adducts in the culture medium and contributions from the medium were deduced. Greater than 90% of FL free adduct formation occurred in the medium. This is because the glucose concentration is low inside MIN6 cells and the

cell volume is low - *ca.* 0.1% of the volume of the culture. In addition, FL may be deglycated in cells by fructosamine-3-phosphokinase (Pascal, *et al.*, 2010). In contrast, the flux of formation of the dicarbonyl derived AGEs originate mainly from the cells. This is because the concentration of the dicarbonyls is 10 – 100 fold higher inside cells, and arg and lys residues inside cells are *ca*. 100 fold higher than the lys and arg concentration in the medium. Therefore, although the volume of the medium is *ca*. 1000-fold greater than the volume of the MIN6 cells in the medium, the markedly higher rate of dicarbonyl glycation inside cells contributes mostly to the flux of dicarbonyl-derived AGE formation.

Analysis of the basal expression of Ins1 and Ins2 in MIN6 cells confirmed that these genes are expressed. Whilst MIN6 cells are known to secrete insulin in response to glucose and this expression was therefore expected, it was important to confirm this in our cell line model, since glucose responsiveness, insulin expression and secretion have all been reported to be diminished with continued passage of MIN6 cells (Cheng, *et al.*, 2012b; Roderigo-Milne, *et al.*, 2002). Consistent with this, a decrease in the expression of Ins1 and Ins2 mRNA was observed from passage 40 to passage 46. The observed decline in Ins1 expression was greater than the decline in Ins2 which led to a decrease in the ratio of Ins1:Ins2 in the MIN6 cells. Roderigo-Milne *et al*. (2002) suggested that there may be differential regulation of these genes which leads to a shift in this ratio in some circumstances. It was also suggested that Ins1 mRNA expression was both diminished more than Ins2 mRNA expression by repeated passage, - consistent with the results in section 5.3, and also more responsive to glucose stimulation and cell-cell contacts than Ins2. Incubation of MIN6 cells in 20 mM glucose led to a decrease in the ratio of Ins1:Ins2 at passage 40 compared to the mRNA expression ratio observed in control MIN6 cells of the same passage cultured alongside in 5.5 mM glucose. Whilst the connection between this insulin expression ratio and insulin secretion and glucose responsiveness is not conclusive, a similar shift to that observed in the current study was reported by Roderigo-Milne *et al*. (2002) with continued passage when insulin secretion and glucose responsiveness are known to decline. Therefore a similar mechanism could underlie this shift in ratio – a loss of glucose responsiveness and insulin secretion with prolonged exposure to high glucose. This shift in insulin mRNA expression ratio was no longer apparent at passage 46, when the insulin expression had declined for both Ins1 and Ins2. Based on the expression of these genes and the physiological

impairments reported in high passage MIN6 cells, all experiments were performed over the passage range 40 - 45 to limit the decline in insulin expression.

The efficient metabolism of dicarbonyls in MIN6 cells is emphasised further in experiments with exogenous methylglyoxal. Approximately one third of a bolus dose of 500 µM MG had been metabolised by MIN6 cells *in vitro* within 30 min. The cellular methylglyoxal increased 2-fold. This also highlights the limitation of studies which use high exogenous doses of MG to treat cells. It is rapidly metabolised and consequently the physiological effects are difficult to judge, especially of concentrations to which cells would not be exposed endogenously. Incubation of MIN6 cells *in vitro* with the cell permeable inhibitor of glyoxalase 1, $BrBzGSHCp_2$ indicated that the potency and cytotoxicity of this cell permeable Glo1 inhibitor was less than previously reported in other cell types, potentially due to differences in esterase activity, necessary to cleave the $BrBzGSHCp_2$ rendering the active form. It has previously been shown that 1 µM is sufficient to increase dicarbonyl levels in the endothelial cell line HMEC-1 and that 10 µM is cytotoxic to HL60 cells, decreasing viability to below 10% (Dobler, *et al.*, 2006; Thornalley, *et al.*, 1996). In MIN6 cells 10 µM $BrBzGSHCp_2$ was necessary to elicit increases in dicarbonyl levels and the GC_{50} was 27.3 ± 0.9 µM.

Incubation of MIN6 cells *in vitro* with 10 µM $BrBzGSHCp_2$ for 48 h resulted in an increase in the cellular content of methylglyoxal only when incubations of low and high glucose were combined. Incubation of MIN6 cells *in vitro* with 10 µM $BrBzGSHCp_2$ for 48 h also resulted in *ca.* a 2-fold increase in cellular GSH and GSSG content, when compared to the content in control MIN6 cells incubated alongside. The increase in cellular GSSG may be due to inhibition of glutathione reductase by $BrBzGSHCp_2$. However, the concurrent increase in GSH means that it is more likely that this treatment is increasing GSH synthesis or impairing glutathione export from MIN6 cells. Increased GSH content of cells will increase the *in situ* activity of Glo1 and thereby provide resistance to decreases in the *in situ* activity of Glo1 and increases in methylglyoxal concentration.

The expression of Glo1 and the insulin genes were also altered following treatment with $BrBzGSHCp_2$. Ins1 expression increased when cells were treated with $BrBzGSHCp_2$, indicative of a potential increase in insulin production and secretion capacity, whilst the combination of high glucose and $BrBzGSHCp_2$ led to a decrease in Glo1 expression compared to the expression in control untreated MIN6

cells in low glucose. However, it could not be determined whether these changes were actually due to the increases in dicarbonyls observed with this treatment, or whether they were due to other disturbances in cell metabolism related to the changes in glutathione and potential inhibition of glutathione reductase.

8.2.2. The effect of glycation of ECM collagen IV on MIN6 cells *in vitro*

Glycation of ECM proteins by methylglyoxal and effect on cell function has been investigated previously by this group and others: detachment of human HMEC-1 and aortal endothelial cells from collagen IV modified minimally by methylglyoxal; peripheral neurone detachment from laminin and fibronectin modified minimally by methylglyoxal; fibrosarcoma HT1080 and osteosarcoma MG63 cell detachment from collagen I with mild methylglyoxal modification; and detachment of mesangial cells from collagen IV modified by methylglyoxal (Dobler, *et al.*, 2006; Duran-Jimenez, *et al.*, 2009; Paul and Bailey, 1999; Pozzi, *et al.*, 2009). ECM proteins typically have a long half-life, and this, combined with their important physiological function has long made them an interesting target of glycation research. Other research has focussed on the interactions between pancreatic beta cells and components of the basement membrane (Iino, *et al.*, 2004; Nikolova, *et al.*, 2006; Weber, *et al.*, 2008). Basement membrane proteins are known to be essential to pancreatic beta cell function – isolated primary islets can only survive in culture with the addition of ECM proteins in their culture environment. The beneficial effects on beta cell physiology have been demonstrated in beta cell lines. However, whilst these studies have indicated the importance of ECM and basement membrane proteins to pancreatic beta cells, the effect of glycation of collagen IV or other basement membrane proteins on the adhesion and function of beta cells has not been investigated.

Incubation of type IV collagen in culture plates overnight led to the adhesion of 33% of this collagen – washing the wells with Triton X-100 was necessary to remove adhered collagen IV. Collagen coated plates were incubated with methylglyoxal for 24 h at 37 °C which was sufficient to modify the collagen. The concentrations of methylglyoxal herein are comparable to the concentrations observed in physiological systems and the increases typically observed in diabetes. Since plates were washed following incubation of collagen with methylglyoxal, any

remaining methylglyoxal is adhered to collagen and therefore not free in solution to directly enter and affect MIN6 cells. Previous studies have characterised this glycation of collagen IV and shown that incubation of collagen IV with MG results in an increase in MG-H1 adduct residue formation on collagen with specific modifications occurring on the arginine motifs of the integrin binding sites (Dobler, *et al.*, 2006).

Coating of culture plates with collagen IV increased cell adhesion. This is in agreement with previous studies investigating the effect of ECM proteins on adhesion in the beta cell line MIN6 *in vitro* (Iino, *et al.*, 2004; Weber, *et al.*, 2008). In addition, culture of primary islets necessitates the presence of ECM proteins to prevent anoikis. The benefits of collagen IV to cultured MIN6 cells, both in this study and reported in the literature, is consistent with the effects seen in primary tissue, although adherence and survival of MIN6 is possible without collagen. These effects were due to the specific interactions between MIN6 cells and collagen IV via integrin binding sites since adhesion was blocked by pre-incubation of cells with both the peptide RGD and an anti-Itgb1 antibody.

Plated collagen IV was glycated by incubation with methylglyoxal and the interactions of MIN6 cells with MG-glycated collagen IV were investigated. It was hypothesised that the increase in MG-H1 adduct residue formation on the integrin binding sites of collagen IV would block the binding sites and be detrimental to cell adhesion – as has been previously reported in both endothelial cells and in fibrosarcoma HT1080 and osteosarcoma MG63 cell lines (Dobler, *et al.*, 2006; Paul and Bailey, 1999). However, herein the addition of increasing concentrations of methylglyoxal increased the proportion of adhered MIN6 cells *in vitro*. This appeared to be due not to an increase in the number of cells directly attached to the glycated collagen IV substrate, but rather, due to an increase in clustering of MIN6 cells that were not attached. Therefore, although there was an increase in adhesion measured by cell counting, this is likely due to an increase in cell-cell contacts, in spite of an actual decrease in the number of cells directly attached to the plate. This is consistent with experimental observations that cells cultured on MG-modified collagen IV appeared looser and in clusters when viewed under a microscope and less appeared to be directly attached to the culture plate. This potentially indicates an experimental limitation of this adhesive beta cell line which is known to form clusters and pseudo-islets in culture. The same effect of MG-glycated collagen IV

on MIN6 cells was observed with both human and mouse collagen IV. The increase in adhesion when collagen IV was modified by methylglyoxal was unexpected. Additionally, it is unlikely that this was actually due to an increase in the interactions between cells and the basement membrane protein collagen IV. Therefore, these cell-extracellular matrix interactions were investigated at the single cell level by use of AFM-FS to determine the energy required to separate individual MIN6 cells from collagen and MG-glycated collagen. These experiments showed a substantial decrease in the total energy required to separate a single MIN6 cell from collagen IV both when the collagen was glycated with MG and when cells were pre-incubated with the integrin blocking peptide RGD. The maximum unbinding force also decreased when collagen was modified by methylglyoxal. These results indicate that MG-glycation of collagen IV is detrimental to adhesion of the cell line MIN6 *in vitro*. The specific integrin interaction of MIN6 cells with collagen IV is blocked by formation of MG-H1 adduct residues, and consequently the energy required to detach cells from the basement membrane protein is vastly decreased. This is suggestive of an increase in cell detachment and anoikis if similar effects are observed with beta cells *in vivo*. In addition, if cells remain adhered, albeit loosely, perhaps through a decline in the number of functional attachment sites, this may impair communication between beta cells and the basement membrane and consequently ablate beta cell function.

Expression of genes associated with communication between beta cells, communication between beta cells and the basement membrane, the glyoxalase system and insulin were analysed to assess whether the plated collagen substrate affected these aspects of beta cell function. Glo1 mRNA expression was unaltered by plating on uncoated, collagen IV or MG-glycated collagen IV coated plates.

The mRNA expression of Ins2 in MIN6 cells was not significantly different between the three culture conditions, whereas the expression of Ins1 increased in MIN6 cells cultured on collagen, compared to those in uncoated wells. However, this increase was small. Previous studies have shown beneficial effects of collagen IV on insulin gene expression and secretion. Nikolova *et al*. (2006) demonstrated that both Ins1 and Ins2 mRNA expression increased when MIN6 cells were cultured on collagen IV, compared to expression in control cells on uncoated plates. However, the control uncoated plates used were non-tissue culture-treated and the authors do not state the effect of using non-tissue culture plates for culture on

adhesion or other cellular effects of MIN6 cells *in vitro*. In addition, their experiments were performed with incubations of 3 - 4 days and the exact culture period is not stated. It is not therefore known whether the experimental protocol is comparable to expect similar changes in insulin gene expression. The beneficial effect of collagen IV and another basement membrane protein, laminin, was also demonstrated by Weber *et al*. (2008). They established that when MIN6 cells were cultured in a three-dimensional poly(ethylene glycol) hydrogel the presence of basement membrane proteins markedly increased the measured GSIS. However, insulin gene expression was not reported in this study. Earlier work by Kaido *et al*. (2004) demonstrated in human adult beta cells that the beneficial effect of collagen IV on insulin secretion was specific and occurred through the integrin heterodimer $\alpha_1\beta_1$. Whilst these studies have demonstrated the favourable effects of collagen IV on insulin gene expression and more noticeably on insulin secretion, the effects of glycation of collagen IV on insulin gene expression or secretion has not been reported. This project has demonstrated that there is no significant effect of MG-glycation of collagen IV on insulin gene expression in cultured MIN6 cells.

Culture of MIN6 cells for three days on collagen IV glycated by methylglyoxal resulted in a decrease in the mRNA expression of Itgb1 compared to expression in cells cultured on control collagen IV alone. Methylglyoxal has been shown to modify arginine motifs of the integrin binding sites on type IV collagen, and thereby block the interaction with the cellular integrin receptors. The subsequent down-regulation of Itgb1 suggests negative feedback, down-regulating Itgb1 when receptors have no substrate with which to bind. However, the existence of such a mechanism would need to be investigated further at the protein level to determine whether this decrease in mRNA expression actually translates into a decrease in the active protein within the cells.

E-cadherin is involved in communication between beta cells within the islets of Langerhans. It is a developmental gene and its expression declines within beta cells when the organ is fully developed and there is sufficient cell-cell adhesion. It has been described as an adhesive molecule involved in the maintenance of viability and an increase in apoptosis has been reported in E-cadherin negative beta cells (Parnaud, *et al.*, 2011). Additionally, down-regulation of E-cadherin using RNAi has previously been shown to decrease GSIS in confluent MIN6 cells (Jaques, *et al.*, 2008). Therefore the decrease in E-cadherin mRNA expression in MIN6 cells

cultured *in vitro* on MG-glycated collagen IV could be implicated in impaired GSIS, potentially via a loss of beta cell to beta cell communication. Impairment in GSIS is often observed in beta cell dysfunction in the pathogenesis of diabetes. Alternatively, the decrease in E-cadherin may result in an increase in cell apoptosis, and consequently a decrease in beta cell mass if these effects are also observed *in vivo* and the decline in mRNA expression is severe enough. However, since E-cadherin expression is also known to decrease when the islets are fully formed and sufficient cell-cell contacts have been made, this decrease in E-cadherin could be a consequence of the cell clustering observed when MIN6 cells were cultured on MG-glycated collagen IV.

Cx36 is involved in communication between pancreatic beta cells. It is necessary for the control of insulin biosynthesis and secretion from beta cells as well as for survival under cell stress (Cigliola, *et al.*, 2013). Alterations in Cx36 expression or in downstream signalling may be implicated in altered beta cell function and the pathogenesis of diabetes. The decrease in Cx36 expression observed in MIN6 cells cultured on MG-glycated human collagen may suggest impaired insulin secretion or even beta cell survival. It also suggests interplay between cell-cell and cell-extracellular matrix interactions, with impaired cell-extracellular matrix interactions resulting in attenuation of cell-cell communication through a decrease in both E-cadherin and Cx36 expression. However, this decrease in Cx36 expression could not be reliably reproduced in MIN6 cells cultured on MG-glycated mouse collagen IV, potentially due to the higher variability observed between replicates.

Studies with similar insulinoma cell lines, INS-1 and HIT-T15, treated with both exogenous methylglyoxal and AGEs to investigate dicarbonyl stress have been reported (Fiory, *et al.*, 2011; Puddu, *et al.*, 2012). The supraphysiological levels of methylglyoxal and AGE-modified protein used, however, suggest findings and related conclusions may have limited physiological relevance.

8.3. Studies with the HFD fed mouse model of insulin resistance and beta cell dysfunction: the effects of HFD and omega-3 fatty acid supplementation on the glyoxalase system and dicarbonyl metabolism

The HFD fed C57BL6 mouse is a well-studied model of insulin resistance and the development of diabetes. The induction of T2DM in mice by HFD was first reported in 1988 where it was shown to exhibit a genetic predisposition to develop the disease (Surwit, *et al.*, 1988). These mice had elevated fasting blood glucose and insulin levels and at the time it was suggested that this model would be relevant in advancing understanding of the pathophysiology of T2DM in humans. Since then, other studies have confirmed insulin resistance and impaired glucose tolerance in this animal model (Hancock, *et al.*, 2008; Kuda, *et al.*, 2009; Souza-Mello, *et al.*, 2010; Winzell and Ahrén, 2004). Data from the current study is consistent with these previous reports. Fasting plasma glucose and insulin concentrations increased markedly and glucose tolerance was impaired in mice fed a HFD. This was related to increased weight gain compared to control animals, as a result of an increase in food intake. Consequently, cholesterol, fatty acids and lipids measured in the plasma and liver also increased. In addition, it was shown that supplementing the HFD with LC-PUFA - omega-3 fatty acids - improved glucose homeostasis. Measurements of fasting insulin and glucose tolerance, hepatic steatosis and cholesterol were still significantly higher than in control chow fed mice but showed large improvements when compared to HFD fed mice, indicative of improved glucose tolerance and less insulin resistance when the HFD was supplemented with LC-PUFA. Plasma NEFA and triglyceride concentrations were also comparable with those observed in control chow fed mice. These findings are consistent with recent reports indicating that HFD supplementation with omega-3 fatty acids prevents some of the metabolic changes observed in insulin resistance (Jilkova, *et al.*, 2013; Kuda, *et al.*, 2009; Rossmeisl, *et al.*, 2009).

Analysis of gene expression from the pancreatic samples proved problematic. This was due to the heterogeneity of the pancreas and so whilst there was a high amount of measurable mRNA in the pancreas, the mRNA of genes of interest was difficult to detect and quantify, most likely due to the high amount of digestive enzymes and other proteins within the exocrine pancreas. Consequently, Ins2 and

Glo1 were below the limit of quantification in the pancreas. Analysis of Ins1 indicated no difference in expression in the pancreas of mice fed the three dietary regimes. This is despite an increase in the fasting insulin concentration in the plasma of HFD fed and HFD supplemented with omega-3 fatty acid fed mice. The changes in plasma concentration may also be explained at the protein level, without changes in the mRNA expression occurring – rather, changes in insulin secretion and in the regulation of protein translation.

It has been suggested that the concentration of inflammatory cytokines increases in the pancreas of HFD fed rats (Yan, *et al.*, 2012). However, herein data failed to show a change in ICAM-1 mRNA expression in the pancreas of HFD fed mice. This discrepancy may be due to the sample heterogeneity or to differences in the study protocol or species investigated – the study by Yan *et al*. (2012) was performed over 20 weeks in Wistar rats. In addition, Mathur *et al*. (2007) associated the inflammatory markers TNF-α and interleukin-1β (IL-1β) in the mouse pancreas with an increase in pancreas mass in obesity; a similar increase in pancreas mass was not observed in the current study. However, the study by Mathur *et al*. (2007) has limitations: - samples were pooled from all mice for analysis and control C57BL6J mice were compared to leptin deficient obese mice. Differences observed may therefore be due to strain differences or differences in leptin metabolism and not necessarily due to obesity or insulin resistance. Inflammation and ICAM-1 expression were not followed up further and remaining analysis instead focussed on the glyoxalase system and examining the effects of these dietary regimes on dicarbonyl stress.

Activities of the glyoxalase system enzymes and the D-lactate and total thiol content of the pancreas gave an indication as to the effect of diet-induced insulin resistance and diabetes on dicarbonyl metabolism by the glyoxalase system in the pancreas. Studies quantifying these analytes in the pancreas following these dietary treatments is lacking, indeed dicarbonyl stress in the pancreas has not been examined in either an *in vivo* or *in vitro* model. The current study showed that there were no alterations in the glyoxalase enzymatic activities or in the amount of D-lactate in the pancreas following these different diets. Therefore there are no alterations in methylglyoxal flux through the dicarbonyl system or in the activity of the enzymes responsible for this metabolism. Since there was no change in the metabolism of dicarbonyls in the pancreas, the steady state amount of dicarbonyls was measured in

the pancreas to indicate whether there were any changes in the cellular exposure to these reactive damaging metabolites. This indicated that there was an increase in methylglyoxal in the pancreas in both the HFD fed mice and the omega-3 fatty acid supplemented HFD fed mice. Glyoxal increased when the HFD was supplemented with omega-3 fatty acids, consistent with an increase in lipid peroxidation, but there was no increase in glyoxal in the HFD group compared to the levels observed in the control group. The decrease in 3-DG observed in the pancreas following HFD feeding is consistent with a decrease in glucose and fructose metabolism in the presence of high amounts of lipids. There were no changes in the amount of dicarbonyls in the plasma which implies that the changes observed in the pancreas are a result of altered pancreatic metabolism and not due to an increased flux coming from the plasma. This is consistent with the concentration of these analytes being higher in the pancreas than observed in the plasma.

The higher amount of methylglyoxal in the pancreas of HFD fed mice indicates that there would be an increase in glycation of protein by methylglyoxal. Consequently, glycation, oxidation and nitration adduct residues on cytosolic and extracellular matrix proteins within the pancreas and plasma proteins were measured to assess damage by methylglyoxal or other metabolites. These experiments indicated that there was a higher degree of glycation by methylglyoxal in the pancreas than in the plasma, as shown by the higher levels of MG-H1, MOLD and ornithine adducts, - consistent with the higher exposure of the pancreas to methylglyoxal. However, despite an increase in the methylglyoxal content of the pancreas in the HFD fed mice, there were no differences in the levels of these MG-glycation adducts within the pancreas, in either cytosolic or ECM protein, following the different dietary regimes. MOLD did however increase in the plasma, suggesting an increase in exposure to methylglyoxal resulted in this glycation. Other changes in the pancreas suggest a decrease in glycation by both glyoxal (CMA adduct residues) and 3-DG (3DG-H adduct residues) as well as oxidative stress (MetSO) following HFD feeding. This is contrary to expectations of an increase in glycation damage, especially given the higher methylglyoxal content, and also contrary to published reports of increased oxidative stress following HFD and in insulin resistance (Kondo, *et al.*, 2013; Matsuzawa-Nagata, *et al.*, 2008; Yan, *et al.*, 2012). Similarly, changes in glycation and oxidation adduct residues on ECM protein within the pancreas were small – an increase in CML was observed when HFD was

supplemented with omega-3 fatty acids, consistent with the increase in glyoxal in this group. This was in combination with both decreased FL and an increase in the CML/FL ratio, indicative of increased oxidative stress. However, there were no corresponding changes in MetSO, dityrosine or NFK and consequently no further indications of oxidative stress in the pancreatic ECM protein. Given the long half-life associated with ECM proteins, such as collagen IV, it was anticipated that increased glycation and oxidation would be observed. It is therefore hypothesised that these findings are due to an increase in protein turnover and clearance in the HFD stressed mice, with associated metabolic disturbances.

In the plasma there were both increases in MOLD formation and decreases in CEL formation following a HFD. These are both methylglyoxal derived adduct residues, and with MG-H1 adduct formation unaltered there is no significant overall change in methylglyoxal derived glycation adducts. The glyoxal derived hydroimidazolone, G-H1 was also lower in the plasma of mice fed a HFD supplemented with omega-3 fatty acid than in plasma of mice fed a HFD without supplementation. This is consistent with the lower plasma NEFA and triglyceride levels in this treatment group, and may occur as a result of less lipid peroxidation decreasing the glyoxal exposure of plasma proteins. The increase in FL adduct residues on plasma protein is indicative of an increase in early stage glycation by glucose when plasma glucose levels are increased in the diabetic state following a HFD. The ratio of CML to FL decreased as a result of the increased FL formation, indicating no alteration in the oxidative formation of CML from FL when higher amounts of FL were present. The increase in MetSO formation was however suggestive of an increase in oxidative stress in the plasma of mice fed a HFD.

Analysis of the free adducts of these markers in the pancreas indicated substantial decreases in a number of glycation markers following a HFD feeding regime including: the hydroimidazolones and other dicarbonyl glycation adducts – MG-H1, G-H1, 3DG-H and CMA; and the early stage glucose glycation adduct, FL. This was contrary to expectations of increased free adducts if an increase in protein turnover in the HFD fed mice accounts for the lack of increases in glycation adducts on pancreatic protein. Consequently, it is hypothesised that this increased protein turnover is in combination with increased clearance of damaged adducts from the pancreas during metabolic stress. In addition, the free amino acid concentration of both arginine and tryptophan were decreased indicative of a lower amino acid

bioavailability, perhaps due to the increased protein turnover suggested herein. Other measured amino acids were not significantly altered by these different diets.

In the plasma the free adduct concentrations of MG-H1, CMA, CML, 3DG-H and FL were lower following a HFD than following a diet consisting of control chow. This was in combination with a decrease in the free arginine concentration, but no significant alterations in other measured amino acids. In addition, the free adduct concentration of NFK increased in HFD, but not when the diet was supplemented with omega-3 fatty acids; this change is indicative of an increase in oxidative damage in the plasma of mice following a HFD. Supplementation of the HFD with omega-3 fatty acid goes some way to prevent this oxidative damage. Together these changes are consistent with the changes observed in the pancreas and are suggestive of a combination of increased protein turnover and increased renal clearance of damaged protein and damaged protein adducts following a HFD. It has previously been reported that despite autophagy being down-regulated in a number of insulin-sensitive tissues in the insulin resistant state, the activity in the pancreas, and in particular beta cells, is in fact increased and consequently an increase in protein turnover would therefore be expected (Chen and White, 2011; Ebato, *et al.*, 2008; Jung, *et al.*, 2008; Yoshizaki, 2012). However, measurement of these damage marker adducts in urine with indications of increases in glycation markers are necessary for this hypothesis to be conclusive.

Analysis of free citrulline in both the pancreas and plasma indicated no change in the free adducts. Free adducts in the pancreas were 69.5 ± 7.2, 70.5 ± 8.6 and 65.3 ± 11.1 pmol per mg wet weight in control, HFD fed and HFD supplemented with omega-3 fatty acid fed mice, respectively (n = 6 - 7). Free adducts in the plasma were 34.0 ± 4.2, 30.2 ± 6.6 and 31.5 ± 5.8 µM in control, HFD fed and HFD supplemented with omega-3 fatty acid fed mice, respectively (n = 8 - 9). This is contrary to recent reports of elevated systemic citrulline combined with a decrease in the arginine bioavailability in diet-induced obese mice (Sailer, *et al.*, 2013). These effects were tissue specific, with arginine and citrulline bioavailability unchanged in the intestine and kidney. The data herein showed decreased plasma and pancreas arginine following HFD and HFD supplemented with omega-3 fatty acids, respectively, indicative of disturbances in arginine metabolism following a HFD.

Immunostaining of collagen IV and insulin in the pancreas indicated that collagen IV is present within the islets of Langerhans and that this provides

structural integrity. No differences were observed in the localisation of these proteins in pancreatic sections from mice fed the different diets. Sections were also immunostained for both MG-H1 and insulin and MG-H1 and collagen IV in combination. This indicated that MG-H1 and insulin do not co-localise; whilst sections showed both MG-H1 and insulin staining, the MG-H1 appears to surround the islet and not occur within it. In addition, this immunostaining potentially shows a higher degree of MG-H1 staining in the pancreas sections from a HFD fed mouse than from a control chow fed mouse. This was again noted in the sections co-stained for MG-H1 and collagen IV; pancreas sections from HFD fed mice demonstrated more staining for MG-H1 than observed in sections from control chow fed mice. Furthermore, this staining is ECM localised – it displays similar localisation to observed for collagen IV. In HFD fed mice pancreas sections co-localisation of collagen IV and MG-H1 was observed, indicating that the MG-H1 adduct residues were likely adducts on collagen IV. These images show methylglyoxal-modification of ECM proteins within the pancreas and also indicate an increase in the MG-H1 residues, although this could not be confirmed by LC-MS/MS quantification. Staining of collagen IV displays an extensive and well-defined network in the pancreas; this is clearest in the sections from the control pancreas. This may be due to disruption of the collagen IV network by glycation following HFD, hence the corresponding increase in MG-H1 adduct immunostaining, or alternatively the increased lipid content following HFD may have interfered with this structure.

8.4. Other advances: quantification of GSH and related metabolites by LC-MS/MS

Application of LC-MS/MS for detection of metabolites gives high selectivity and sensitivity and has been used routinely for quantification analysis in a variety of matrices. Published estimates of GSH and GSSG vary due to differences in both sample preparation and assay methodology – values obtained by different investigators span two orders of magnitude (Rossi, *et al.*, 2002). Chromatographic methods have advantages over the spectrophotometric methods – they are more selective and measure and distinguish related compounds simultaneously, whereas

spectrophotometric assays, such as that used by Kaneko *et al*. (2009) measure total glutathione content.

As discussed by Rossi *et al*. (2002) and Roberts and Francetic (1993) consideration should be taken to sample preparation in order to reliably quantify the concentration of GSH and associated metabolites. Protein precipitation by acidification is usually the first step in preparation of samples for quantification of glutathione. This gives robust estimates of glutathione; the acid also inactivates γ-glutamyl transpeptidase, the enzyme responsible for the first step in the degradation of GSH (Roberts and Francetic, 1993). This enzyme is reported to be of a high level in the pancreas, kidney and liver and can lead to vast underestimates of glutathione in tissue samples. TCA was shown to be the most effective acid for the precipitation of protein, compared to perchloric and sulfosalicylic acids, since the loss of GSH from de-proteinised solutions was minimal (Rossi, *et al.*, 2002). In addition, the oxidation of thiol groups in acidified samples was shown to be minimal, although this did increase substantially if the de-proteinised samples were neutralised.

An LC-MS/MS method for the detection and quantification of GSH, GSSG and S-D-lactoylglutathione was developed. Spike recovery was assessed for all three analytes and indicated that this method is a reliable method of measuring these metabolites, with almost complete recovery. The concentrations of GSH and GSSG are within the physiological range and consistent with suggestions of a low concentration of GSSG when oxidation of GSH during sample preparation is avoided (Roberts and Francetic, 1993; Rossi, *et al.*, 2002). The assessment of intra-batch variability indicated that the method is robust and reproducible. In addition, calibration curves were reproducible, with slopes consistent when re-prepared for fresh analysis. The limitation of this method is that despite the LoD for S-D-lactoylglutathione being assessed as 1.1 pmol/10^6 cells, this analyte has been below the LoD in all samples tested and not detectable.

9. Conclusions and further work

9.1. Conclusions

This PhD project is composed of 3 parts:

(i) Characterisation of the glyoxalase system and dicarbonyl metabolism in a beta cell line model and investigation of the effects of high glucose and dicarbonyl stress on this system.

(ii) Investigation of the effect of MG-glycation of the ECM protein collagen IV on the functionality and adhesion of MIN6 cells *in vitro*.

(iii) Characterisation of dicarbonyl metabolism in the pancreas of diet induced insulin resistant C57BL6 male mice. The extent of damage to the proteome by glycation, oxidation and nitration is also assessed.

An LC-MS/MS assay was validated for the detection and quantification of GSH and related metabolites and had a LoD of 0.92, 1.46 and 0.54 pmol for GSH, GSSG and S-D-lactoylglutathione respectively. This method is shown to be robust and takes into account important aspects of sample preparation to ensure that quantification of analytes is reliable.

Results from the beta cell line model, MIN6, indicate that MIN6 cells cultured in high glucose have an increased nutrient consumption and that this in turn increases the glycolytic flux. There is a consequential increase in the flux of formation of D-lactate, indicative of higher MG production and higher flux through the glyoxalase system but the proportion of flux from glycolysis was not affected by culture in high glucose. The cellular content of MG, glyoxal and 3-DG did not increase when MIN6 cells were incubated in high glucose. This indicates that although there is more MG production, as indicated by the D-lactate flux, this is largely within the capacity of the cells to metabolise it and therefore changes in MG were not detected in the MIN6 cells. This is despite the measured activity of the glyoxalase system not increasing when the cellular demands upon it have increased. Glycation, oxidation and nitration of MIN6 cellular proteins occurred *in vitro* but the amounts of these adduct residues on cellular proteins were not affected by the increase in glucose. Impaired adhesion to collagen IV was demonstrated following methylglyoxal-glycation of collagen. This was suggestive of altered beta cell

function through changes in the expression of genes involved in both cell-cell and cell-extracellular matrix interactions.

Observations from experimental diabetes suggest that whilst methylglyoxal does increase in the pancreas of HFD fed mice this is not associated with quantifiable changes in glycation adduct residues on protein. It is concluded that whilst an increase in MG-H1 formation does occur as a result of the higher methylglyoxal content of the pancreas, a combination of increased protein turnover in the pancreas and renal clearance of damaged proteins and free adducts results in no measurable increase in glycated or oxidised protein. The pancreas is therefore highly effective in removing damaged and dysfunctional proteins which would otherwise impose cell stress. Supplementation of the HFD with omega-3 fatty acids has not been observed to have any significant effect on the glycation status of the pancreas in this model, despite going some way to prevent insulin resistance and associated metabolic disturbances. Immunostaining images have also indicated that glycation damage observed within the pancreas is predominantly ECM directed.

In summary, the data generated from this *in vitro* model of beta cells and *in vivo* model of diabetes suggests there are indications of dicarbonyl stress within beta cells and the pancreas - increased flux of methylglyoxal formation in MIN6 cells *in vitro* and increase concentration of methylglyoxal in the pancreas in HFD fed mice *in vivo*. Increased pancreatic methylglyoxal in HFD-fed mice without increased methylglyoxal modified protein does not mean that the pancreas is resistant to protein glycation. Since glycation by methylglyoxal is non-enzymatic pancreatic proteins are likely being increasingly damaged and degraded. Consequential decreases in protein concentration or compensatory gene expression may increasingly drive the pancreas into a state of increased protein turnover which eventually takes its toll as pancreatic dysfunction sets in. Clearance of damaged protein and an increased protein turnover are vital to maintenance of beta cell health. In times of continued stress, it is likely that this increased protein turnover will impact detrimentally on other aspects of beta cell function and contribute to the decline in beta cell function observed in T2DM. This study has also indicated that ECM proteins of the pancreas are particularly susceptible to glycation and that this could contribute to the demise of beta cell mass through cell-detachment stimulated cell apoptosis – anoikis.

A limitation of this study has been that the pancreas is a heterogeneous cell population and that the cells of interest, pancreatic beta cells, are only a small subset of this organ. However, this thesis has shown that glycation occurs within both cultured beta cells and in the pancreas, and that methylglyoxal does accumulate. The effect of protein glycation on beta cell function is limited by the high rate of protein turnover and clearance of damaged proteins from the system. Perhaps under more prolonged glycation stress, further impairments in beta cell function would be observed, especially with regards to their interactions with ECM proteins such as collagen IV.

9.2. Further work

In this thesis a method to quantify S-D-lactoylglutathione was developed. This analyte was, however, below the LoD in all samples tested. Further development of this assay on the more sensitive Xevo triple quadrupole mass spectrometer may enable detection and quantification of this analyte which would give a more complete picture as to dicarbonyl metabolism and the activity of the glyoxalase system in these cell systems.

The studies with MIN6 cells require follow-up with mature mammalian beta cells and pancreatic islets since transformed insulinoma cells can give misleading metabolic effects as models of beta cells.

Co-localisation of collagen IV and the methylglyoxal glycation adduct MG-H1 have been observed within the pancreas and the effects of this glycation indicated within an *in vitro* model of beta cells. It would be interesting to follow up these findings in a primary cell model and additionally investigate whether this glycation has a direct effect on insulin secretion or on E-cadherin or Cx36 protein level. The *in vivo* study suggested the pancreatic proteome may suffer increased glycation with related changes in protein turnover (and possible increased compensatory gene expression). Characterisation of the HFD fed mouse pancreatic dicarbonyl proteome, proteome dynamics and changes in gene transcription are now required. Finally, studies with Glo1 transgenic and Glo1deficient mice would reveal the link between dicarbonyl stress and the development of insulin resistance and glucotoxicity.

Appendix A: Primer sequences

Primer	Sequence (Sense, Antisense)
Glo1	5'- CCCAGCTGCTGCTCCGATCCAGACCCT -3' 5'- CCGCGATATCGTTCTTATCCTCA -3'
Ins1	5'- CAACCGTGTAAATGCCACTG -3' 5'- CCTGCTACGGATGGACTGTT -3'
Ins2	5'- CCATCAGCAAGCAGGAAGCCTATC -3' 5'- CCCCACACACCAGGTAGAGAGCG -3' (Nikolova, *et al.*, 2006)
Itgb1	5'- TTCAGACTTCCGCATTGGCTTTGG -3' 5'- TGGGCTGGTGCAGTTTTGTTCAC -3' (Ramirez, *et al.*, 2011)
E-cadherin	5'- AGCCATTGCCAAGTACATCC -3' 5'- AAAGACCGGCTGGGTAAACT -3'
Cx36	5'- GGAATGGACCATCTTGGAGA -3' 5'- TCGTACACCGTCTCCCCTAC -3'
ICAM-1	5'- TTCACACTGAATGCCAGCTC -3' 5'- GTCTGCTGAGAGCCCCTCTTG -3'
18S	Qiagen commercial stock. Sequence not known

References

Abdel-Wahab, Y.H., O'Harte, F.P., Boyd, A.C., Barnett, C.R. and Flatt, P.R. (1997). Glycation of insulin results in reduced biological activity in mice. *Acta Diabetologica* **34**(4), 265-270.

Abdel-Wahab, Y.H., O'Harte, F.P., Mooney, M.H., Barnett, C.R. and Flatt, P.R. (2002). Vitamin C supplementation decreases insulin glycation and improves glucose homeostasis in obese hyperglycemic (ob/ob) mice. *Metabolism* **51**(4), 514-517.

Abdel-Wahab, Y.H., O'Harte, F.P., Ratcliff, H., McClenaghan, N.H., Barnett, C.R. and Flatt, P.R. (1996). Glycation of insulin in the islets of Langerhans of normal and diabetic animals. *Diabetes* **45**(11), 1489-1496.

Abordo, E.A., Minhas, H.S. and Thornalley, P.J. (1999). Accumulation of alpha-oxoaldehydes during oxidative stress: a role in cytotoxicity. *Biochemical Pharmacology* **58**(4), 641-648.

Adeva, M.M., Calviño, J., Souto, G. and Donapetry, C. (2012). Insulin resistance and the metabolism of branched-chain amino acids in humans. *Amino Acids* **43**(1), 171-181.

Agalou, S., Karachalias, N., Thornalley, P.J., Tucker, B. and Dawnay, A.B. (2002). Estimation of α-oxoaldehyes formed from the degradation of glycolytic intermediates and glucose fragmentation in blood plasma of human subjects with uraemia. *International Congress Series* **1245,** 181-182.

Ahmed, M.U., Thorpe, S.R. and Baynes, J.W. (1986). Identification of N epsilon-carboxymethyllysine as a degradation product of fructoselysine in glycated protein. *Journal of Biological Chemistry* **261**(11), 4889-4894.

Ahmed, N., Argirov, O.K., Minhas, H.S., Cordeiro, C.A. and Thornalley, P.J. (2002). Assay of advanced glycation endproducts (AGEs): surveying AGEs by chromatographic assay with derivatization by 6-aminoquinolyl-N-hydroxysuccinimidyl-carbamate and application to Nepsilon-carboxymethyl-lysine- and Nepsilon-(1-carboxyethyl)lysine-modified albumin. *Biochemical Journal* **364**(Part 1), 1-14.

Ahmed, N., Babaei-Jadidi, R., Howell, S.K., Beisswenger, P.J. and Thornalley, P.J. (2005a). Degradation products of proteins damaged by glycation, oxidation and nitration in clinical type 1 diabetes. *Diabetologia* **48,** 1590-1603.

Ahmed, N., Mirshekar-Syahkal, B., Kennish, L., Karachalias, N., Babaei-Jadidi, R. and Thornalley, P.J. (2005b). Assay of advanced glycation endproducts in selected beverages and food by liquid chromatography with tandem mass spectrometric detection. *Molecular Nutrition and Food Research* **49**(7), 691-699.

Ahmed, N. and Thornalley, P.J. (2007). Advanced glycation endproducts: what is their relevance to diabetic complications? *Diabetes Obesity and Metabolism* **9**(3), 233-245.

Ahnfelt-Rønne, J., Hecksher-Sørensen, J., Schäffer, L. and Madsen, O.D. (2012). A new view of the beta cell. *Diabetologia* **55**(9), 2316-2318.

Allen, D.W., Schroeder, W.A. and Balog, J. (1958). Observations on the Chromatographic Heterogeneity of Normal Adult and Fetal Human Hemoglobin: a Study of the Effects of Crystallization and Chromatography on the Heterogeneity and Isoleucine Content. *Journal of the American Chemical Society* **80**(7), 1628-1634.

Allen, R.E., Lo, T.W.C. and Thornalley, P.J. (1993a). Purification and characterisation of glyoxalase II from human red blood cells. *European Journal of Biochemistry* **213,** 1261-1267.

Allen, R.E., Lo, T.W.C. and Thornalley, P.J. (1993b). A Simplified Method for the Purification of Human Red Blood Cell Glyoxalase. I. Characteristics, Immunoblotting, and Inhibitor Studies. *Journal of Protein Chemistry* **12**(2), 111-119.

American Diabetes Association. (2004). Diagnosis and Classification of Diabetes Mellitus. *Diabetes Care* **27 Supplement 1,** S5-S10.

American Diabetes Association. (2011). Standards of Medical Care in Diabetes - 2011. *Diabetes Care* **34 Supplement 1,** S11-S61.

American Diabetes Association. (2012). Diagnosis and Classification of Diabetes Mellitus. *Diabetes Care* **35 Supplement 1,** S64-S71.

American Diabetes Association. (2013). Standards of Medical Care in Diabetes - 2013. *Diabetes Care* **36 Supplement 1,** S11-S66.

Andrali, S.S., Sampley, M.L., Vanderford, N.L. and Ozcan, S. (2008). Glucose regulation of insulin gene expression in pancreatic beta-cells. *Biochemical Journal* **415**(1), 1-10.

Asfari, M., Janjic, D., Meda, P., Li, G., Halban, P.A. and Wollheim, C.B. (1992). Establishment of 2-mercaptoethanol-dependent differentiated insulin-secreting cell lines. *Endocrinology* **130**(1), 167-178.

Asplin, C.M., Paquette, T.L. and Palmer, J.P. (1981). In vivo inhibition of glucagon secretion by paracrine beta cell activity in man. *Journal of Clinical Investigation* **68**(1), 314-318.

Atkinson, M.A. and Maclaren, N.K. (1994). The pathogenesis of insulin-dependent diabetes mellitus. *New England Journal of Medicine* **331**(21), 1428-1436.

Baba, S.P., Barski, O.A., Ahmed, Y., O'Toole, T.E., Conklin, D.J., Bhatnagar, A. and Srivastava, S. (2009). Reductive metabolism of AGE precursors: a

metabolic route for preventing AGE accumulation in cardiovascular tissue. *Diabetes* **58**(11), 2486-2497.

Back, S.H., Kang, S.W., Han, J. and Chung, H.T. (2012). Endoplasmic reticulum stress in the β-cell pathogenesis of type 2 diabetes. *Experimental Diabetes Research* **2012,** 618396.

Ball, J.C. and Vander Jagt, D.L. (1979). Purification of S-2-Hydroxyacylglutathione Hydrolase (Glyoxalase II) from Rat Erythrocytes. *Analytical Biochemistry* **98**, 472-477.

Barnett, A.H., Eff, C., Leslie, R.D. and Pyke, D.A. (1981). Diabetes in identical twins. A study of 200 pairs. *Diabetologia* **20**(2), 87-93.

Bartlett, G.J., Porter, C.T., Borkakoti, N. and Thornton, J.M. (2002). Analysis of catalytic residues in enzyme active sites. *Journal of Molecular Biology* **324**(1), 105-121.

Beisswenger, P.J., Howell, S.K., O'Dell, R.M., Wood, M.E., Touchette, A.D. and Szwergold, B.S. (2001). alpha-Dicarbonyls increase in the postprandial period and reflect the degree of hyperglycemia. *Diabetes Care* **24**(4), 726-732.

Beisswenger, P.J., Howell, S.K., Touchette, A.D., Lal, S. and Szwergold, B.S. (1999). Metformin reduces systemic methylglyoxal levels in type 2 diabetes. *Diabetes* **48,** 198-202.

Bender, K. and Grzeschik, K.H. (1976). Possible assignment of the glyoxalase I (GLO) gene to chromosome 6 using man-mouse somatic cell hybrids. *Human Genetics* **31**(3), 341-345.

Benedict, S.R. (1909). A reagent for the detection of reducing sugars. *Journal of Biological Chemsitry* **5,** 485-487.

Bensellam, M., Laybutt, D.R. and Jonas, J.C. (2012). The molecular mechanisms of pancreatic β-cell glucotoxicity: recent findings and future research directions. *Molecular and Cellular Endocrinology* **364**(1-2), 1-27.

Bensley, R.R. (1911). Studies on the pancreas of the guinea pig. *American Journal of Anatomy* **12,** 297-388.

Bergman, M., Dankner, R., Roth, J. and Narayan, K.M. (2013). Are current diagnostic guidelines delaying early detection of dysglycemic states? Time for new approaches. *Endocrine* **44**(1), 66-69.

Berlanga, J., Cibrian, D., Guillen, I., Freyre, F., Alba, J.S., Lopez-Saura, P., Merino, N., Aldama, A., Quintela, A.M., Triana, M.E., Montequin, J.F., Ajamieh, H., Urquiza, D., Ahmed, N. and Thornalley, P.J. (2005). Methylglyoxal administration induces diabetes-like microvascular changes and perturbs the healing process of cutaneous wounds. *Clinical Science* **109,** 83-95.

Berner, A.K., Brouwers, O., Pringle, R., Klaassen, I., Colhoun, L., McVicar, C., Brockbank, S., Curry, J.W., Miyata, T., Brownlee, M., Schlingemann, R.O., Schalkwijk, C. and Stitt, A.W. (2012). Protection against methylglyoxal-derived AGEs by regulation of glyoxalase 1 prevents retinal neuroglial and vasodegenerative pathology. *Diabetologia* **55**(3), 845-854.

Bertholet, R., Finot, P.-A. and Hirsbrunner, P. (1977). *Preparation of ε-(γ-glutamyl)-lysine*. United States of America Patent 4052372.

Best, L., Miley, H.E., Brown, P.D. and Cook, L.J. (1999). Methylglyoxal causes swelling and activation of a volume-sensitive anion conductance in rat pancreatic beta-cells. *Journal of Membrane Biology* **167**(1), 65-71.

Bierhaus, A., Konrade, I., Haag, G.-M., Humpert, P.M., Morcos, M., Hammes, H.-P., Tew, K. and Nawroth, P.P. (2005). The receptor RAGE regulates glyoxalase-1 transcription, expression and activity. *Diabetologia* **48,** A90.

Birkenmeier, G., Stegemann, C., Hoffmann, R., Günther, R., Huse, K. and Birkemeyer, C. (2010). Posttranslational modification of human glyoxalase 1 indicates redox-dependent regulation. *PLoS One* **5**(4), e10399.

Bliss, M. (1993). The history of insulin. *Diabetes Care* **16 Supplement 3,** 4-7.

Bonner-Weir, S., Li, W.-C., Ouziel-Yahalom, L., Guo, L., Weir, G.C. and Sharma, A. (2010). Beta-cell growth and regeneration: replication is only part of the story. *Diabetes* **59,** 2340-2348.

Bookchin, R.M. and Gallop, P.M. (1968). Structure of hemoglobin AIc: nature of the N-terminal beta chain blocking group. *Biochemical and Biophysical Research Communications* **32**(1), 86-93.

Bradford, M.M. (1976). A rapid and sensitive method for the quantitation of microgram quantities of protein utilizing the principle of protein-dye binding. *Analytical Biochemistry* **72,** 248-254.

Brambilla, G., Sciabà, L., Faggin, P., Finollo, R., Bassi, A.M., Ferro, M. and Marinari, U.M. (1985). Methylglyoxal-induced DNA-protein cross-links and cytotoxicity in Chinese hamster ovary cells. *Carcinogenesis* **6**(5), 683-686.

Briscoe, C.P., Peat, A.J., McKeown, S.C., Corbett, D.F., Goetz, A.S., Littleton, T.R., McCoy, D.C., Kenakin, T.P., Andrews, J.L., Ammala, C., Fornwald, J.A., Ignar, D.M. and Jenkinson, S. (2006). Pharmacological regulation of insulin secretion in MIN6 cells through the fatty acid receptor GPR40: identification of agonist and antagonist small molecules. *British Journal of Pharmacology* **148**(5), 619-628.

Brouwers, O., Niessen, P.M., Ferreira, I., Miyata, T., Scheffer, P.G., Teerlink, T., Schrauwen, P., Brownlee, M., Stehouwer, C.D. and Schalkwijk, C.G. (2011). Overexpression of glyoxalase-I reduces hyperglycemia-induced levels of advanced

glycation end products and oxidative stress in diabetic rats. *Journal of Biological Chemistry* **286**(2), 1374-1380.

Brownlee, M. (2005). The pathobiology of diabetic complications: a unifying mechanism. *Diabetes* **54**(6), 1615-1625.

Bunn, H.F., Gabbay, K.H. and Gallop, P.M. (1978). The glycosylation of hemoglobin: relevance to diabetes mellitus. *Science* **200**(4337), 21-27.

Bunn, H.F., Haney, D.N., Kamin, S., Gabbay, K.H. and Gallop, P.M. (1976). The biosynthesis of human hemoglobin A1c. Slow glycosylation of hemoglobin in vivo. *Journal of Clinical Investigation* **57**(6), 1652-1659.

Burbelo, P.D., Martin, G.R. and Yamada, Y. (1988). Alpha 1(IV) and alpha 2(IV) collagen genes are regulated by a bidirectional promoter and a shared enhancer. *Proceedings of the National Academy of Sciences of the United States of America* **85**(24), 9679-9682.

Bush, P.E. and Norton, S.J. (1985). S-(nitrocarbobenzoxy)glutathiones: potent competitive inhibitors of mammalian glyoxalase II. *Journal of Medicinal Chemistry* **28**(6), 828-830.

Butler, A.E., Janson, J., Bonner-Weir, S., Ritzel, R., Rizza, R.A. and Butler, P.C. (2003). Beta-cell deficit and increased beta-cell apoptosis in humans with type 2 diabetes. *Diabetes* **52,** 102-110.

Cameron, J.D., Skubitz, A.P. and Furcht, L.T. (1991). Type IV collagen and corneal epithelial adhesion and migration. Effects of type IV collagen fragments and synthetic peptides on rabbit corneal epithelial cell adhesion and migration in vitro. *Investigative Ophthalmology & Visual Science* **32**(10), 2766-2773.

Cerami, A. (1986). Aging of proteins and nucleic acids: what is the role of glucose? *Trends in Biochemical Sciences* **11**(8), 311-314.

Chang-Chen, K.J., Mullur, R. and Bernal-Mizrachi, E. (2008). Beta-cell failure as a complication of diabetes. *Reviews in Endocrine and Metabolic Disorders* **9**(4), 329-343.

Chen, H.Y. and White, E. (2011). Role of autophagy in cancer prevention. *Cancer Prevention Research* **4**(7), 973-983.

Chen, J., Hui, S.T., Couto, F.M., Mungrue, I.N., Davis, D.B., Attie, A.D., Lusis, A.J., Davis, R.A. and Shalev, A. (2008). Thioredoxin-interacting protein deficiency induces Akt/Bcl-xL signaling and pancreatic beta-cell mass and protects against diabetes. *The FASEB Journal* **22,** 3581-3594.

Cheng, J.Y., Whitelock, J. and Poole-Warren, L. (2012a). Syndecan-4 is associated with beta-cells in the pancreas and the MIN6 beta-cell line. *Histochemistry and Cell Biology* **138**(6), 933-944.

Cheng, K., Delghingaro-Augusto, V., Nolan, C.J., Turner, N., Hallahan, N., Andrikopoulos, S. and Gunton, J.E. (2012b). High passage MIN6 cells have impaired insulin secretion with impaired glucose and lipid oxidation. *PLoS One* **7**(7), e40868.

Chetyrkin, S., Mathis, M., Pedchenko, V., Sanchez, O.A., McDonald, W.H., Hachey, D.L., Madu, H., Stec, D., Hudson, B. and Voziyan, P. (2011). Glucose autoxidation induces functional damage to proteins via modification of critical arginine residues. *Biochemistry* **50**(27), 6102-6112.

Chow, J.P., Simionescu, D.T., Warner, H., Wang, B., Patnaik, S.S., Liao, J. and Simionescu, A. (2013). Mitigation of diabetes-related complications in implanted collagen and elastin scaffolds using matrix-binding polyphenol. *Biomaterials* **34**(3), 685-695.

Cigliola, V., Chellakudam, V., Arabieter, W. and Meda, P. (2013). Connexins and beta-cell functions. *Diabetes Research and Clinical Practice* **99,** 250-259.

Clelland, J.D. and Thornalley, P.J. (1991). S-2-Hydroxyacylglutathione derivatives: enzymatic preparation, purification and characterisation. *Journal of the Chemical Society, Perkin Transactions 1*, 3009-3015.

Cohen, R.M., Franco, R.S., Khera, P.K., Smith, E.P., Lindsell, C.J., Ciraolo, P.J., Palascak, M.B. and Joiner, C.H. (2008). Red cell life span heterogeneity in hematologically normal people is sufficient to alter HbA1c. *Blood* **112**(10), 4284-4291.

Collard, F., Vertommen, D., Fortpied, J., Duester, G. and Van Schaftingen, E. (2007). Identification of 3-deoxyglucosone dehydrogenase as aldehyde dehydrogenase 1A1 (retinaldehyde dehydrogenase 1). *Biochimie* **89**(3), 369-373.

Collins, S.C., Hoppa, M.B., Walker, J.N., Amisten, S., Abdulkader, F., Bengtsson, M., Fearnside, J., Ramracheya, R., Toye, A.A., Zhang, Q., Clark, A., Gauguier, D. and Rorsman, P. (2010). Progression of diet-induced diabetes in C57BL6J mice involves functional dissociation of Ca2(+) channels from secretory vesicles. *Diabetes* **59**(5), 1192-1201.

Cook, L.J., Davies, J., Yates, A.P., Elliott, A.C., Lovell, J., Joule, J.A., Pemberton, P., Thornalley, P.J. and Best, L. (1998). Effects of methylglyoxal on rat pancreatic beta-cells. *Biochemical Pharmacology* **55**(9), 1361-1367.

Cooperberg, B.A. and Cryer, P.E. (2010). Insulin reciprocally regulates glucagon secretion in humans. *Diabetes* **59**(11), 2936-2940.

Corkey, B.E. (2012). Banting lecture 2011: hyperinsulinemia: cause or consequence? *Diabetes* **61**(1), 4-13.

Dakin, H.D. and Dudley, H.W. (1913). On glyoxalase. *Journal of Biological Chemistry* **14,** 423-431.

Dandona, P., Aljada, A. and Bandyopadhyay, A. (2004). Inflammation: the link between insulin resistance, obesity and diabetes. *Trends in Immunology* **25**(1), 4-7.

Delpierre, G., Rider, M.H., Collard, F., Stroobant, V., Vanstapel, F., Santos, H. and Van Schaftingen, E. (2000). Identification, cloning, and heterologous expression of a mammalian fructosamine-3-kinase. *Diabetes* **49**(10), 1627-1634.

Dhar, A., Dhar, I., Jiang, B., Desai, K.M. and Wu, L. (2011). Chronic methylglyoxal infusion by minipump causes pancreatic beta-cell dysfunction and induces type 2 diabetes in Sprague-Dawley rats. *Diabetes* **60,** 899-908.

Dobler, D., Ahmed, N., Song, L., Eboigbodin, K.E. and Thornalley, P.J. (2006). Increased dicarbonyl metabolism in endothelial cells in hyperglycaemia induces anoikis and impairs angiogenesis by RGD and GFOGER motif modification. *Diabetes* **55,** 1961-1969.

Dohan, F.C. and Lukens, F.D. (1948). Experimental diabetes produced by the administration of glucose. *Endocrinology* **42**(4), 244-262.

Dolhofer, R. and Wieland, O.H. (1979). Preparation and biological properties of glycosylated insulin. *FEBS Letters* **100**(1), 133-136.

Dor, Y., Brown, J., Martinez, O.I. and Melton, D.A. (2004). Adult pancreatic beta-cells are formed by self-duplication rather than by stem-cell differentiation. *Nature* **429,** 41-46.

Dunn, J.A., Ahmed, M.U., Murtiashaw, M.H., Richardson, J.M., Walla, M.D., Thorpe, S.R. and Baynes, J.W. (1990). Reaction of ascorbate with lysine and protein under autoxidizing conditions: formation of N epsilon-(carboxymethyl)lysine by reaction between lysine and products of autoxidation of ascorbate. *Biochemistry* **29**(49), 10964-10970.

Dunn, J.A., McCance, D.R., Thorpe, S.R., Lyons, T.J. and Baynes, J.W. (1991). Age-dependent accumulation of N epsilon-(carboxymethyl)lysine and N epsilon-(carboxymethyl)hydroxylysine in human skin collagen. *Biochemistry* **30**(5), 1205-1210.

Dunn, J.A., Patrick, J.S., Thorpe, S.R. and Baynes, J.W. (1989). Oxidation of glycated proteins: age-dependent accumulation of N epsilon-(carboxymethyl)lysine in lens proteins. *Biochemistry* **28**(24), 9464-9468.

Duran-Jimenez, B., Dobler, D., Moffatt, S., Rabbani, N., Streuli, C.H., Thornalley, P.J., Tomlinson, D.R. and Gardiner, N.J. (2009). Advanced glycation end products in extracellular matrix proteins contribute to the failure of sensory nerve regeneration in diabetes. *Diabetes* **58**(12), 2893-2903.

Dyer, D.G., Dunn, J.A., Thorpe, S.R., Bailie, K.E., Lyons, T.J., McCance, D.R. and Baynes, J.W. (1993). Accumulation of Maillard reaction products in skin collagen in diabetes and aging. *Journal of Clinical Investigation* **91**(6), 2463-2469.

Ebato, C., Uchida, T., Arakawa, M., Komatsu, M., Ueno, T., Komiya, K., Azuma, K., Hirose, T., Tanaka, K., Kominami, E., Kawamori, R., Fujitani, Y. and Watada, H. (2008). Autophagy is important in islet homeostasis and compensatory increase of beta cell mass in response to high-fat diet. *Cell Metabolism* **8**(4), 325-332.

Eberhard, D., Kragl, M. and Lammert, E. (2010). 'Giving and taking': endothelial and beta-cells in the islets of Langerhans. *Trends in Endocrinology and Metabolism* **21**(8), 457-463.

Eberhard, D. and Lammert, E. (2009). The pancreatic beta-cell in the islet and organ community. *Current Opinion in Genetics and Development* **19**(5), 469-475.

Efrat, S. (1997). Making sense of glucose sensing. *Nature Genetics* **17,** 249-250.

Efrat, S., Linde, S., Kofod, H., Spector, D., Delannoy, M., Grant, S., Hanahan, D. and Baekkeskov, S. (1988). Beta-cell lines derived from transgenic mice expressing a hybrid insulin gene-oncogene. *Proceedings of the National Academy of Sciences of the United States of America* **85**(23), 9037-9041.

Fiory, F., Lombardi, A., Miele, C., Giudicelli, J., Beguinot, F. and Van Obberghen, E. (2011). Methylglyoxal impairs insulin signalling and insulin action on glucose-induced insulin secretion in the pancreatic beta cell line INS-1E. *Diabetologia* **54,** 2941-2952.

Flax, H., Matthews, D.R., Levy, J.C., Coppack, S.W. and Turner, R.C. (1991). No glucotoxicity after 53 hours of 6.0 mmol/l hyperglycaemia in normal man. *Diabetologia* **34**(8), 570-575.

Florez, J.C. (2008). Newly identified loci highlight beta cell dysfunction as a key cause of type 2 diabetes: where are the insulin resistance genes? *Diabetologia* **51**(7), 1100-1110.

Folch, J., Lees, M. and Sloane Stanley, G.H. (1957). A simple method for the isolation and purification of total lipides from animal tissues. *Journal of Biological Chemistry* **226,** 497-509.

Franco, O.H., Steyerberg, E.W., Hu, F.B., Mackenbach, J. and Nusselder, W. (2007). Associations of diabetes mellitus with total life expectancy with and without cardiovascular disease. *Archives of Internal Medicine* **167,** 1145-1151.

Franklin, I., Gromada, J., Gjinovci, A., Theander, S. and Wollheim, C.B. (2005). Beta-cell secretory products activate alpha-cell ATP-dependent potassium channels to inhibit glucagon release. *Diabetes* **54**(6), 1808-1815.

Frisch, S.M. and Francis, H. (1994). Disruption of epithelial cell-matrix interactions induces apoptosis. *Journal of Cell Biology* **124**(4), 619-626.

Fujitani, Y., Kawamori, R. and Watada, H. (2009). The role of autophagy in pancreatic beta-cell and diabetes. *Autophagy* **5**(2), 280-282.

Gallet, X., Charloteaux, B., Thomas, A. and Brasseur, R. (2000). A fast method to predict protein interaction sites from sequences. *Journal of Molecular Biology* **302**(4), 917-926.

Gautam, D., Han, S.J., Hamdan, F.F., Jeon, J., Li, B., Li, J.H., Cui, Y., Mears, D., Lu, H., Deng, C., Heard, T. and Wess, J. (2006). A critical role for beta cell M3 muscarinic acetylcholine receptors in regulating insulin release and blood glucose homeostasis in vivo. *Cell Metabolism* **3**(6), 449-461.

Grankvist, N., Amable, L., Honkanen, R.E., Sjöholm, A. and Ortsäter, H. (2012). Serine/threonine protein phosphatase 5 regulates glucose homeostasis in vivo and apoptosis signalling in mouse pancreatic islets and clonal MIN6 cells. *Diabetologia* **55**(7), 2005-2015.

Grune, T., Reinheckel, T. and Davies, K.J. (1996). Degradation of oxidized proteins in K562 human hematopoietic cells by proteasome. *Journal of Biological Chemistry* **271**(26), 15504-15509.

Guariguata, L. (2012). By the numbers: New estimates from the IDF Diabetes Atlas Update for 2012. *Diabetes Research and Clinical Practice* **98,** 524-525.

Haffner, S.M. (2006). The metabolic syndrome: inflammation, diabetes mellitus, and cardiovascular disease. *The American Journal of Cardiology* **97**(2A), 3A-11A.

Halban, P.A., Praz, G.A. and Wollheim, C.B. (1983). Abnormal glucose metabolism accompanies failure of glucose to stimulate insulin release from a rat pancreatic cell line (RINm5F). *The Biochemical Journal* **212**(2), 439-443.

Hales, C.N. and Barker, D.J.P. (1992). Type 2 (non-insulin-dependent) diabetes mellitus: the thrifty phenotype hypothesis. *Diabetologia* **35,** 595-601.

Hamada, Y., Nakamura, J., Fujisawa, H., Yago, H., Nakashima, E., Koh, N. and Hotta, N. (1997). Effects of glycemic control on plasma 3-deoxyglucosone levels in NIDDM patients. *Diabetes Care* **20,** 1466-1469.

Hancock, C.R., Han, D.H., Chen, M., Terada, S., Yasuda, T., Wright, D.C. and Holloszy, J.O. (2008). High-fat diets cause insulin resistance despite an increase in muscle mitochondria. *Proceedings of the National Academy of Sciences of the United States of America* **105**(22), 7815-7820.

Harmon, J.S., Stein, R. and Robertson, R.P. (2005). Oxidative stress-mediated, post-translational loss of MafA protein as a contributing mechanism to loss of insulin gene expression in glucotoxic beta cells. *Journal of Biological Chemistry* **280**(12), 11107-11113.

Hauge-Evans, A.C., Squires, P.E., Persaud, S.J. and Jones, P.M. (1999). Pancreatic beta-cell-to-beta-cell interactions are required for integrated responses to nutrient stimuli. Enhanced calcium and insulin secretory responses of MIN6 pseudoislets. *Diabetes* **48,** 1402-1408.

Hay, C.W. and Docherty, K. (2006). Comparative analysis of insulin gene promoters: implications for diabetes research. *Diabetes* **55**(12), 3201-3213.

Hegab, Z., Gibbons, S., Neyses, L. and Mamas, M.A. (2012). Role of advanced glycation end products in cardiovascular disease. *World Journal of Cardiology* **4**(4), 90-102.

Henquin, J.C., Cerasi, E., Efendic, S., Steiner, D.F. and Boitard, C. (2008). Pancreatic beta-cell mass or beta-cell function? That is the question! *Diabetes Obesity and Metabolism* **10 Supplement 4,** 1-4.

Hernebring, M., Brolén, G., Aguilaniu, H., Semb, H. and Nyström, T. (2006). Elimination of damaged proteins during differentiation of embryonic stem cells. *Proceedings of the National Academy of Sciences of the United States of America* **103**(20), 7700-7705.

Hodge, J.E. and Rist, C.E. (1953). The Amadori Rearrangement under New Conditions and its Significance for Non-enzymatic Browning Reactions. *Journal of the American Chemical Society* **75**(2), 316-322.

Hopcroft, D.W., Mason, D.R. and Scott, R.S. (1985). Structure-function relationships in pancreatic islets:support for intraislet modulation of insulin secretion. *Endocrinology* **117,** 2073-2080.

Hopkins, F.G. and Morgan, E.J. (1945). On the distribution of glyoxalase and glutathione. *Biochemical Journal* **39,** 320-324.

Hoppa, M.B., Collins, S., Ramracheya, R., Hodson, L., Amisten, S., Zhang, Q., Johnson, P., Ashcroft, F.M. and Rorsman, P. (2009). Chronic palmitate exposure inhibits insulin secretion by dissociation of Ca(2+) channels from secretory granules. *Cell Metabolism* **10**(6), 455-465.

Hudson, B.G., Tryggvason, K., Sundaramoorthy, M. and Neilson, E.G. (2003). Alport's syndrome, Goodpasture's syndrome, and type IV collagen. *New England Journal of Medicine* **348**(25), 2543-2556.

Huypens, P., Ling, Z., Pipeleers, D. and Schuit, F. (2000). Glucagon receptors on human islet cells contribute to glucose competence of insulin release. *Diabetologia* **43**(8), 1012-1019.

Iino, S., Abeyama, K., Kawahara, K., Yamakuchi, M., Hashiguchi, T., Matsukita, S., Yonezawa, S., Taniguchi, S., Nakata, M., Takao, S., Aikou, T. and Maruyama, I. (2004). The antimetastatic role of thrombomodulin expression in islet cell-derived tumors and its diagnostic value. *Clinical Cancer Research* **10**(18 Part 1), 6179-6188.

In't Veld, P., De Munck, N., Van Belle, K., Buelens, N., Ling, Z., Weets, I., Haentjens, P., Pipeleers-Marichal, M., Gorus, F. and Pipeleers, D. (2010). Beta-

cell replication is increased in donor organs from young patients after prolonged life support. *Diabetes* **59,** 1702-1708.

International Diabetes Federation. (2011). *IDF Diabetes Atlas, 5th Edition*. [Online]. (http://www.idf.org/diabetesatlas). Brussels, Belgium: International Diabetes Federation.

International Diabetes Federation. (2012). *IDF Diabetes Atlas, 5th Edition Update*. [Online]. (http://www.idf.org/diabetesatlas/5e/Update2012). Brussels, Belgium: International Diabetes Federation.

International Expert Committee. (2009). International Expert Committee Report on the Role of A1C Assay in the Diagnosis of Diabetes. *Diabetes Care* **32**(7), 1327-1334.

Itoh, Y., Kawamata, Y., Harada, M., Kobayashi, M., Fujii, R., Fukusumi, S., Ogi, K., Hosoya, M., Tanaka, Y., Uejima, H., Tanaka, H., Maruyama, M., Satoh, R., Okubo, S., Kizawa, H., Komatsu, H., Matsumura, F., Noguchi, Y., Shinohara, T., Hinuma, S., Fujisawa, Y. and Fujino, M. (2003). Free fatty acids regulate insulin secretion from pancreatic beta cells through GPR40. *Nature* **422**(6928), 173-176.

Jain, R. and Lammert, E. (2009). Cell-cell interactions in the endocrine pancreas. *Diabetes, Obesity and Metabolism* **11,** 159-167.

Jaques, F., Jousset, H., Tomas, A., Prost, A.-L., Wollheim, C.B., Irminger, J.-C., Demaurex, N. and Halban, P.A. (2008). Dual Effect of Cell-Cell Contact Disruption on Cytosolic Calcium and Insulin Secretion. *Endocrinology* **149**(5), 2494-2505.

Jia, X., Olson, D.J.H., Ross, A.R.S. and Wu, L. (2006). Structural and functional changes in human insulin induced by methylglyoxal. *FASEB Journal* **20,** E871-E879.

Jilkova, Z.M., Hensler, M., Medrikova, D., Janovska, P., Horakova, O., Rossmeisl, M., Flachs, P., Sell, H., Eckel, J. and Kopecky, J. (2013). Adipose tissue-related proteins locally associated with resolution of inflammation in obese mice. *International Journal of Obesity,* Online ahead of print. DOI: 10.1038/ijo.2013.1108.

Johnson, J.H., Newgard, C.B., Milburn, J.L., Lodish, H.F. and Thorens, B. (1990a). The high K_M Glucose Transporter of Islets of Langerhans is Functionally Similar to the Low Affinity Transporter of Liver and Has an Identical Primary Sequence. *Journal of Biological Chemistry* **265**(12), 6548-6551.

Johnson, J.H., Ogawa, A., Chen, L., Orci, L., Newgard, C.B., Alam, T. and Unger, R.H. (1990b). Underexpression of beta Cell High K_M Glucose Transporters in Noninsulin-Dependent Diabetes. *Science* **250,** 546-549.

Jonas, J.C., Bensellam, M., Duprez, J., Elouil, H., Guiot, Y. and Pascal, S.M.A. (2009). Glucose regulation of islet stress responses and beta-cell failure in type 2 diabetes. *Diabetes, Obesity and Metabolism* **11,** 65-81.

Jung, H., Joo, J., Jeon, Y., Lee, J., In, J., Kim, D., Kang, E., Kim, Y., Lim, Y., Kang, J. and Choi, J. (2011). Advanced glycation end products downregulate glucokinase in mice. *Diabetes Metabolism Research and Reviews* **27,** 557-563.

Jung, H.S., Chung, K.W., Won Kim, J., Kim, J., Komatsu, M., Tanaka, K., Nguyen, Y.H., Kang, T.M., Yoon, K.H., Kim, J.W., Jeong, Y.T., Han, M.S., Lee, M.K., Kim, K.W., Shin, J. and Lee, M.S. (2008). Loss of autophagy diminishes pancreatic beta cell mass and function with resultant hyperglycemia. *Cell Metabolism* **8**(4), 318-324.

Kaido, T., Yebra, M., Cirulli, V. and Montgomery, A.M. (2004). Regulation of human beta-cell adhesion, motility, and insulin secretion by collagen IV and its receptor alpha1beta1. *Journal of Biological Chemistry* **279**(51), 53762-53769.

Kaneko, Y., Kimura, T., Taniguchi, S., Souma, M., Kojima, Y., Kimura, Y., Kimura, H. and Niki, I. (2009). Glucose-induced production of hydrogen sulfide may protect the pancreatic beta-cells from apoptotic cell death by high glucose. *FEBS Letters* **583**(2), 377-382.

Kanno, T., Gopel, S.O., Rorsman, P. and Wakui, M. (2002). Cellular function in multicellular system for hormone-secretion: electrophysiological aspect of studies on alpha-, beta- and delta-cells of the pancreatic islet. *Neuroscience Research* **42**(2), 79-90.

Karachalias, N., Babaei-Jadidi, R., Rabbani, N. and Thornalley, P.J. (2010). Increased protein damage in renal glomeruli, retina, nerve, plasma and urine and its prevention by thiamine and benfotiamine therapy in a rat model of diabetes. *Diabetologia* **53**(7), 1506-1516.

Karjalainen, J., Knip, M., Hyöty, H., Leinikki, P., Ilonen, J., Käär, M.L. and Akerblom, H.K. (1988). Relationship between serum insulin autoantibodies, islet cell antibodies and Coxsackie-B4 and mumps virus-specific antibodies at the clinical manifestation of type 1 (insulin-dependent) diabetes. *Diabetologia* **31**(3), 146-152.

Kefalides, N.A. (1966). A collagen of unusual composition and a glycoprotein isolated from canine glomerular basement membrane. *Biochemical and Biophysical Research Communication* **22**(1), 26-32.

Kelly, C., Guo, H., McCluskey, J.T., Flatt, P.R. and McClenaghan, N.H. (2010). Comparison of insulin release from MIN6 Pseudoislets and pancreatic islets of Langerhans reveals importance of homotypic cell interactions. *Pancreas* **39,** 1016-1023.

Khoshnoodi, J., Pedchenko, V. and Hudson, B.G. (2008). Mammalian collagen IV. *Microscopy Research and Technique* **71**(5), 357-370.

Kilpatrick, E., Bloomgarden, Z. and Zimmet, P. (2009). Is haemoglobin A_{1c} a step forward for diagnosing diabetes? *British Medical Journal.* **339,** 1288-1290.

Kim, J.K., Kim, Y.J., Fillmore, J.J., Chen, Y., Moore, I., Lee, J., Yuan, M., Li, Z.W., Karin, M., Perret, P., Shoelson, S.E. and Shulman, G.I. (2001). Prevention of fat-induced insulin resistance by salicylate. *Journal of Clinical Investigation* **108**(3), 437-446.

Kim, M.J., Kim, D.W., Lee, B.R., Shin, M.J., Kim, Y.N., Eom, S.A., Park, B.J., Cho, Y.S., Han, K.H., Park, J., Hwang, H.S., Eum, W.S. and Choi, S.Y. (2013). Transduced Tat-glyoxalase protein attenuates streptozotocin-induced diabetes in a mouse model. *Biochemical and Biophysical Research Communications* **430**(1), 294-300.

Kim, N.S., Sekine, S., Kiuchi, N. and Kato, S. (1995). cDNA cloning and characterization of human glyoxalase I isoforms from HT-1080 cells. *Journal of Biochemistry* **117**(2), 359-361.

Kitiphongspattana, K., Khan, T.A., Ishii-Schrade, K., Roe, M.W., Philipson, L.H. and Gaskins, H.R. (2007). Protective role for nitric oxide during the endoplasmic reticulum stress response in pancreatic beta-cells. *American Journal of Physiology - Endocrinology and Metabolism* **292**(6), E1543-E1554.

Kleinman, H.K., Luckenbill-Edds, L., Cannon, F.W. and Sephel, G.C. (1987). Use of extracellular matrix components for cell culture. *Analytical Biochemistry* **166**(1), 1-13.

Knecht, K.J., Dunn, J.A., McFarland, K.F., McCance, D.R., Lyons, T.J., Thorpe, S.R. and Baynes, J.W. (1991). Effect of diabetes and aging on carboxymethyllysine levels in human urine. *Diabetes* **40**(2), 190-196.

Kondo, H., Mori, S., Takino, H., Kijima, H., Yamasaki, H., Ozaki, M., Tetsuya, I., Urata, Y., Abe, T., Sera, Y., Yamakawa, K., Kawasaki, E., Yamaguchi, Y., Kondo, T. and Eguchi, K. (2000). Attenuation of expression of gamma-glutamylcysteine synthetase by ribozyme transfection enhance insulin secretion by pancreatic beta cell line, MIN6. *Biochemical and Biophysical Research Communications* **278**(1), 236-240.

Kondo, K., Ishigaki, Y., Gao, J., Yamada, T., Imai, J., Sawada, S., Muto, A., Oka, Y., Igarashi, K. and Katagiri, H. (2013). Bach1 deficiency protects pancreatic β-cells from oxidative stress injury. *American Journal of Physiology - Endocrinology and Metabolism* **305**(5), E641-648.

Kondoh, Y., Kawase, M. and Ohmori, S. (1992). D-lactate concentrations in blood, urine and sweat before and after exercise. *European Journal of Applied Physiology and Occupational Physiology* **65**(1), 88-93.

Konstantinova, I., Nikolova, G., Ohara-Imaizumi, M., Meda, P., Kucera, T., Zarbalis, K., Wurst, W., Nagamatsu, S. and Lammert, E. (2007). EphA-Ephrin-

A-mediated beta cell communication regulates insulin secretion from pancreatic islets. *Cell* **129**(2), 359-370.

Kosower, N.S., Kosower, E.M. and Wertheim, B. (1969). Diamide, a new reagent for the intracellular oxidation of glutathione to the disulfide. *Biochemical and Biophysical Research Communications* **37,** 593-596.

Kragl, M. and Lammert, E. (2010). Chapter 10: Basement Membrane in Pancreatic Islet Function. In: Islam, M.S. *The Islets of Langerhans: Advances in Experimental Medicine and Biology*, vol. 654, 217-234: Springer Science.

Kuda, O., Jelenik, T., Jilkova, Z., Flachs, P., Rossmeisl, M., Hensler, M., Kazdova, L., Ogston, N., Baranowski, M., Gorski, J., Janovska, P., Kus, V., Polak, J., Mohamed-Ali, V., Burcelin, R., Cinti, S., Bryhn, M. and Kopecky, J. (2009). n-3 fatty acids and rosiglitazone improve insulin sensitivity through additive stimulatory effects on muscle glycogen synthesis in mice fed a high-fat diet. *Diabetologia* **52**(5), 941-951.

Kuhla, B., Lüth, H.J., Haferburg, D., Boeck, K., Arendt, T. and Münch, G. (2005). Methylglyoxal, glyoxal, and their detoxification in Alzheimer's disease. *Annals of the New York Academy of Sciences* **1043,** 211-216.

Kulkarni, R.N., Brüning, J.C., Winnay, J.N., Postic, C., Magnuson, M.A. and Kahn, C.R. (1999). Tissue-specific knockout of the insulin receptor in pancreatic beta cells creates an insulin secretory defect similar to that in type 2 diabetes. *Cell* **96**(3), 329-339.

Kuroda, A., Rauch, T.A., Todorov, I., Ku, H.T., Al-Abdullah, I.H., Kandeel, F., Mullen, Y., Pfeifer, G.P. and Ferreri, K. (2009). Insulin gene expression is regulated by DNA methylation. *PLoS One* **4**(9), e6953.

Kurz, A., Rabbani, N., Walter, M., Bonin, M., Thornalley, P., Auburger, G. and Gispert, S. (2011). Alpha-synuclein deficiency leads to increased glyoxalase I expression and glycation stress. *Cell and Molecular Life Sciences* **68,** 721-733.

Kwak, M.K., Wakabayashi, N., Itoh, K., Motohashi, H., Yamamoto, M. and Kensler, T.W. (2003). Modulation of gene expression by cancer chemopreventive dithiolethiones through the Keap1-Nrf2 pathway. Identification of novel gene clusters for cell survival. *Journal of Biological Chemistry* **278**(10), 8135-8145.

Kühn, K. (1994). Basement Membrane (Type IV) Collagen. *Matrix Biology* **14,** 439-445.

Lal, S., Randall, W.C., Taylor, A.H., Kappler, F., Walker, M., Brown, T.R. and Szwergold, B.S. (1997). Fructose-3-phosphate production and polyol pathway metabolism in diabetic rat hearts. *Metabolism* **46**(11), 1333-1338.

Lapolla, A., Tessari, P., Poli, T., Valerio, A., Duner, E., Iori, E., Fedele, D. and Crepaldi, G. (1988). Reduced in vivo biological activity of in vitro glycosylated insulin. *Diabetes* **37**(6), 787-791.

Larsen, K., Aronsson, A.C., Marmstål, E. and Mannervik, B. (1985). Immunological comparison of glyoxalase I from yeast and mammals and quantitative determination of the enzyme in human tissues by radioimmunoassay. *Comparative Biochemistry and Physiology B* **82**(4), 625-638.

Leahy, J.L., Cooper, H.E. and Weir, G.C. (1987). Impaired insulin secretion associated with near normoglycemia. Study in normal rats with 96-h in vivo glucose infusions. *Diabetes* **36**(4), 459-464.

Lejeune, D., Delsaux, N., Charloteaux, B., Thomas, A. and Brasseur, R. (2005). Protein-nucleic acid recognition: statistical analysis of atomic interactions and influence of DNA structure. *Proteins* **61**(2), 258-271.

Leroux, L., Desbois, P., Lamotte, L., Duvillié, B., Cordonnier, N., Jackerott, M., Jami, J., Bucchini, D. and Joshi, R.L. (2001). Compensatory responses in mice carrying a null mutation for Ins1 or Ins2. *Diabetes* **50**(Supplement 1), S150-S153.

Li, H., Nakamura, S., Miyazaki, S., Morita, T., Suzuki, M., Pischetsrieder, M. and Niwa, T. (2006). N2-carboxyethyl-2'-deoxyguanosine, a DNA glycation marker, in kidneys and aortas of diabetic and uremic patients. *Kidney International* **69**(2), 388-392.

Liang, Y., Bai, G., Doliba, N., Buettger, C., Wang, L., Berner, D.K. and Matschinsky, F.M. (1996). Glucose metabolism and insulin release in mouse beta HC9 cells, as model for wild-type pancreatic beta-cells. *American Journal of Physiology - Endocrinology and Metabolism* **270**(5 Part 1), E846-E857.

Liardon, R., De Weck-Gaudard, D., Philippossian, G. and Finot, P.A. (1987). Identification of N.epsilon.-carboxymethyllysine:a new Maillard reaction product in rat urine. *Journal of Agricultural and Food Chemistry* **35**(3), 427-431.

Lieuw-A-Fa, M.L., van Hinsbergh, V.W., Teerlink, T., Barto, R., Twisk, J., Stehouwer, C.D. and Schalkwijk, C.G. (2004). Increased levels of N(epsilon)-(carboxymethyl)lysine and N(epsilon)-(carboxyethyl)lysine in type 1 diabetic patients with impaired renal function: correlation with markers of endothelial dysfunction. *Nephrology, Dialysis, Transplantation* **19**(3), 631-636.

Limphong, P., McKinney, R.M., Adams, N.E., Bennett, B., Makaroff, C.A., Gunasekera, T. and Crowder, M.W. (2009). Human glyoxalase II contains an Fe(II)Zn(II) center but is active as a mononuclear Zn(II) enzyme. *Biochemistry* **48**(23), 5426-5434.

Lindstad, R.I. and McKinley-McKee, J.S. (1993). Methylglyoxal and the polyol pathway: three-carbon compunds are substrates for sheep liver sorbitol dehydrogenase. *Federation of the Societies of Biochemistry and Molecular Biology* **330**, 31-35.

Lis, H. and Sharon, N. (1993). Protein glycosylation. Structural and functional aspects. *European Journal of Biochemistry* **218**(1), 1-27.

Liu, Y.Q., Tornheim, K. and Leahy, J.L. (1998). Shared biochemical properties of glucotoxicity and lipotoxicity in islets decrease citrate synthase activity and increase phosphofructokinase activity. *Diabetes* **47**(12), 1889-1893.

Lo, T.W. and Thornalley, P.J. (1992). Inhibition of proliferation of human leukaemia 60 cells by diethyl esters of glyoxalase inhibitors in vitro. *Biochemical Pharmacology* **44**(12), 2357-2363.

Lo, T.W., Westwood, M.E., McLellan, A.C., Selwood, T. and Thornalley, P.J. (1994). Binding and modification of proteins by methylglyoxal under physiological conditions. A kinetic and mechanistic study with N alpha-acetylarginine, N alpha-acetylcysteine, and N alpha-acetyllysine, and bovine serum albumin. *Journal of Biological Chemistry* **269**(51), 32299-32305.

Lu, J., Xie, G. and Jia, W. (2013). Insulin resistance and the metabolism of branched-chain amino acids. *Frontiers of Medicine* **7**(1), 53-59.

Lüth, H.J., Ogunlade, V., Kuhla, B., Kientsch-Engel, R., Stahl, P., Webster, J., Arendt, T. and Münch, G. (2005). Age- and stage-dependent accumulation of advanced glycation end products in intracellular deposits in normal and Alzheimer's disease brains. *Cerebral Cortex* **15**(2), 211-220.

Ma, R.C.W. and Chan, J.C.N. (2009). Diabetes: incidence of childhood type 1 diabetes: a worrying trend. *Nature Reviews Endocrinology* **5**(10), 529-530.

MacLeod, A.K., McMahon, M., Plummer, S.M., Higgins, L.G., Penning, T.M., Igarashi, K. and Hayes, J.D. (2009). Characterization of the cancer chemopreventive NRF2-dependent gene battery in human keratinocytes: demonstration that the KEAP1-NRF2 pathway, and not the BACH1-NRF2 pathway, controls cytoprotection against electrophiles as well as redox-cycling compounds. *Carcinogenesis* **30**(9), 1571-1580.

Maedler, K., Schumann, D.M., Schulthess, F., Oberholzer, J., Bosco, D., Berney, T. and Donath, M.Y. (2006). Aging correlates with decreased beta-cell proliferative capacity and enhanced sensitivity to apoptosis: a potential role for Fas and pancreatic duodenal homeobox-1. *Diabetes* **55,** 2455-2462.

Maillard, L.C. (1912). Action des acides amines sur les sucres: formation des melanoidines par voie methodique. *Comptes Rendus de l'Academie des Sciences* **154,** 66-68.

Masiello, P., Broca, C., Gross, R., Roye, M., Manteghetti, M., Hillaire-Buys, D., Novelli, M. and Ribes, G. (1998). Experimental NIDDM: development of a new model in adult rats administered streptozotocin and nicotinamide. *Diabetes* **47**(2), 224-229.

Masterjohn, C., Mah, E., Guo, Y., Koo, S.I. and Bruno, R.S. (2012). γ-Tocopherol abolishes postprandial increases in plasma methylglyoxal following an

oral dose of glucose in healthy, college-aged men. *Journal of Nutritional Biochemistry* **23**(3), 292-298.

Matafome, P., Sena, C. and Seiça, R. (2013). Methylglyoxal, obesity, and diabetes. *Endocrine* **43**(3), 472-484.

Mathews, A.E. and Mathews, C.E. (2012). Inherited β-cell dysfunction in lean individuals with type 2 diabetes. *Diabetes* **61**(7), 1659-1660.

Mathur, A., Marine, M., Lu, D., Swartz-Basile, D.A., Saxena, R., Zyromski, N.J. and Pitt, H.A. (2007). Nonalcoholic fatty pancreas disease. *HPB (Oxford)* **9**(4), 312-318.

Matschinsky, F.M. (1990). Glucokinase as glucose sensor and metabolic signal generator in pancreatic beta-cells and hepatocytes. *Diabetes* **39**(6), 647-652.

Matsuzawa-Nagata, N., Takamura, T., Ando, H., Nakamura, S., Kurita, S., Misu, H., Ota, T., Yokoyama, M., Honda, M., Miyamoto, K. and Kaneko, S. (2008). Increased oxidative stress precedes the onset of high-fat diet-induced insulin resistance and obesity. *Metabolism* **57**(8), 1071-1077.

Matthews, D.R., Hosker, J.P., Rudenski, A.S., Naylor, B.A., Treacher, D.F. and Turner, R.C. (1985). Homeostasis model assessment: insulin resistance and beta-cell function from fasting plasma glucose and insulin concentrations in man. *Diabetologia* **28**(7), 412-419.

Matveyenko, A.V. and Butler, P.C. (2006). ß-cell deficit due to increased apoptosis in the human islet amyloid polypeptide transgenic (HIP) rat recapitulates the metabolic defects present in type 2 diabetes. *Diabetes* **55,** 2106-2114.

McCarthy, M.I. (2010). Genomics, Type 2 Diabetes, and Obesity. *The New England Journal of Medicine* **363,** 2339-2350.

McCarthy, M.I., Rorsman, P. and Gloyn, A.L. (2013). TCF7L2 and diabetes: a tale of two tissues, and of two species. *Cell Metabolism* **17**(2), 157-159.

McCluskey, J.T., Hamid, M., Guo-Parke, H., McClenaghan, N.H., Gomis, R. and Flatt, P.R. (2011). Development and functional characterization of insulin-releasing human pancreatic beta cell lines produced by electrofusion. *Journal of Biological Chemistry* **286**(25), 21982-21992.

McLellan, A.C., Phillips, S.A. and Thornalley, P.J. (1992). Fluorimetric Assay of D-lactate. *Analytical Biochemistry* **206,** 12-16.

McLellan, A.C. and Thornalley, P.J. (1992). Synthesis and chromatography of 1,2-diamino-4,5-dimethoxybenzene, 6,7-dimethoxy-2-methylquinoxaline and 6,7-dimethoxy-2,3-dimethylquinoxaline for use in a liquid chromatography fluorimetric assay for methylglyoxal. *Analytica Chimica Acta* **263,** 137-142.

McLellan, A.C., Thornalley, P.J., Benn, J. and Sonksen, P.H. (1994). Glyoxalase system in clinical diabetes mellitus and correlation with diabetic complications. *Clinical Science* **87,** 21-29.

Meier, J.J., Breuer, T.G., Bonadonna, R.C., Tannapfel, A., Uhl, W., Schmidt, W.E., Schrader, H. and Menge, B.A. (2012). Pancreatic diabetes manifests when beta cell area declines by approximately 65% in humans. *Diabetologia* **55**(5), 1346-1354.

Meijer, A.J. and Codogno, P. (2008). Autophagy: a sweet process in diabetes. *Cell Metabolism* **8**(4), 275-276.

Meister, A. (1983). Selective modification of glutathione metabolism. *Science* **220,** 472-477.

Minna, J.D., Bruns, G.A., Krinsky, A.H., Lalley, P.A., Francke, U. and Gerald, P.S. (1978). Assignment of a Mus musculus gene for triosephosphate isomerase to chromosome 6 and for glyoxalase-I to chromosome 17 using somatic cell hybrids. *Somatic Cell Genetics* **4**(2), 241-252.

Miyazaki, J., Araki, K., Yamato, E., Ikegami, H., Asano, T., Shibasaki, Y., Oka, Y. and Yamamura, K. (1990). Establishment of a pancreatic beta cell line that retains glucose-inducible insulin secretion: special reference to expression of glucose transporter isoforms. *Endocrinology* **127**(1), 126-132.

Modak, M.A., Parab, P.B. and Ghaskadbi, S.S. (2009). Pancreatic islets are very poor in rectifying oxidative DNA damage. *Pancreas* **38**(1), 23-29.

Monder, C. (1967). Alpha-keto aldehyde dehydrogenase, an enzyme that catalyzes the enzymic oxidation of methylglyoxal to pyruvate. *Journal of Biological Chemistry* **242**(20), 4603-4609.

Morcos, M., Du, X., Pfisterer, F., Hutter, H., Sayed, A.A., Thornalley, P., Ahmed, N., Baynes, J., Thorpe, S., Kukudov, G., Schlotterer, A., Bozorgmehr, F., El Baki, R.A., Stern, D., Moehrlen, F., Ibrahim, Y., Oikonomou, D., Hamann, A., Becker, C., Zeier, M., Schwenger, V., Miftari, N., Humpert, P., Hammes, H.P., Buechler, M., Bierhaus, A., Brownlee, M. and Nawroth, P.P. (2008). Glyoxalase-1 prevents mitochondrial protein modification and enhances lifespan in Caenorhabditis elegans. *Aging Cell* **7**(2), 260-269.

Morioka, T., Asilmaz, E., Hu, J., Dishinger, J.F., Kurpad, A.J., Elias, C.F., Li, H., Elmquist, J.K., Kennedy, R.T. and Kulkarni, R.N. (2007). Disruption of leptin receptor expression in the pancreas directly affects beta cell growth and function in mice. *Journal of Clinical Investigation* **117**(10), 2860-2868.

Mosmann, T. (1983). Rapid Colorimetric Assay for Cellular Growth and Survival: Application to Proloferation and Cytotoxicity Assays. *Journal of Immunological Methods* **65,** 55-63.

Muoio, D.M. and Newgard, C.B. (2008). Molecular and metabolic mechanisms of insulin resistance and beta-cell failure in type 2 diabetes. *Nature Reviews Molecular Cell Biology* **9,** 193-205.

Murata-Kamiya, N., Kaji, H. and Kasai, H. (1999). Deficient nucleotide excision repair increases base-pair substitutions but decreases TGGC frameshifts induced by methylglyoxal in Escherichia coli. *Mutation Research* **442**(1), 19-28.

Murata-Kamiya, N. and Kamiya, H. (2001). Methylglyoxal, an endogenous aldehyde, crosslinks DNA polymerase and the substrate DNA. *Nucleic Acids Research* **29**(16), 3433-3438.

Murata-Kamiya, N., Kamiya, H., Kaji, H. and Kasai, H. (1998). Nucleotide excision repair proteins may be involved in the fixation of glyoxal-induced mutagenesis in Escherichia coli. *Biochemical and Biophysical Research Communications* **248**(2), 412-417.

Murata-Kamiya, N., Kamiya, H., Kaji, H. and Kasai, H. (2000a). Mutations induced by glyoxal and methylglyoxal in mammalian cells. *Nucleic Acids Symposium Series* **44**(1), 3-4.

Murata-Kamiya, N., Kamiya, H., Kaji, H. and Kasai, H. (2000b). Methylglyoxal induces G:C to C:G and G:C to T:A transversions in the supF gene on a shuttle vector plasmid replicated in mammalian cells. *Mutation Research* **468**(2), 173-182.

Narayan, K.M., Boyle, J.P., Thompson, T.J., Gregg, E.W. and Williamson, D.F. (2007). Effect of BMI on lifetime risk for diabetes in the U.S. *Diabetes Care* **30**(6), 1562-1566.

Newgard, C.B., An, J., Bain, J.R., Muehlbauer, M.J., Stevens, R.D., Lien, L.F., Haqq, A.M., Shah, S.H., Arlotto, M., Slentz, C.A., Rochon, J., Gallup, D., Ilkayeva, O., Wenner, B.R., Yancy, W.S., Eisenson, H., Musante, G., Surwit, R.S., Millington, D.S., Butler, M.D. and Svetkey, L.P. (2009). A branched-chain amino acid-related metabolic signature that differentiates obese and lean humans and contributes to insulin resistance. *Cell Metabolism* **9**(4), 311-326.

Newsholme, P., Brennan, L., Rubi, B. and Maechler, P. (2005). New insights into amino acid metabolism, beta-cell function and diabetes. *Clinical Science* **108**(3), 185-194.

Nguidjoe, E., Sokolow, S., Bigabwa, S., Pachera, N., D'Amico, E., Allagnat, F., Vanderwinden, J.M., Sener, A., Manto, M., Depreter, M., Mast, J., Joanny, G., Montanya, E., Rahier, J., Cardozo, A.K., Eizirik, D.L., Schurmans, S. and Herchuelz, A. (2011). Heterozygous inactivation of the Na/Ca exchanger increases glucose-induced insulin release, β-cell proliferation, and mass. *Diabetes* **60**(8), 2076-2085.

Nicolay, J.P., Schneider, J., Niemoeller, O.M., Artunc, F., Portero-Otin, M., Haik Jr., G., Thornalley, P.J., Schleicher, E., Wieder, T. and Lang, F. (2006).

Stimulation of suicidal erythrocyte death by methylglyoxal. *Cellular Physiology and Biochemistry* **18,** 223-232.

Nikolova, G., Jabs, N., Konstantinova, I., Domogatskaya, A., Tryggvason, K., Sorokin, L., Fässler, R., Gu, G., Gerber, H.P., Ferrara, N., Melton, D.A. and Lammert, E. (2006). The vascular basement membrane: a niche for insulin gene expression and Beta cell proliferation. *Developmental Cell* **10**(3), 397-405.

Nishimura, C., Furue, M., Ito, T., Omori, Y. and Tanimoto, T. (1993). Quantitative determination of human aldose reductase by enzyme-linked immunosorbent assay. Immunoassay of human aldose reductase. *Biochemical Pharmacology* **46**(1), 21-28.

Nishinaka, T. and Yabe-Nishimura, C. (2005). Transcription factor Nrf2 regulates promoter activity of mouse aldose reductase (AKR1B3) gene. *Journal of Pharmacological Sciences* **97**(1), 43-51.

Nissen, R., Cardinale, G.J. and Udenfriend, S. (1978). Increased turnover of arterial collagen in hypertensive rats. *Proceedings of the National Academy of Sciences of the United States of America* **75**(1), 451-453.

Niwa, T. (2006). Mass spectrometry for the study of protein glycation in disease. *Mass Spectrometry Reviews* **25**(5), 713-723.

Nolan, C.J. and Prentki, M. (2008). The islet beta-cell: fuel responsive and vulnerable. *Trends in Endocrinology and Metabolism* **19**(8), 285-291.

Nolan, J.J. and Færch, K. (2012). Estimating insulin sensitivity and beta cell function: perspectives from the modern pandemics of obesity and type 2 diabetes. *Diabetologia* **55**(11), 2863-2867.

Nunemaker, C.S., Zhang, M. and Satin, L.S. (2004). Insulin feedback alters mitochondrial activity through an ATP-sensitive K+ channel-dependent pathway in mouse islets and beta-cells. *Diabetes* **53**(7), 1765-1772.

O'Harte, F.P., Højrup, P., Barnett, C.R. and Flatt, P.R. (1996). Identification of the site of glycation of human insulin. *Peptides* **17**(8), 1323-1330.

Ohmori, S. and Iwamoto, T. (1988). Sensitive determination of D-lactic acid in biological samples by high-performance liquid chromatography. *Journal of Chromatography* **431**(2), 239-247.

Okada, T., Liew, C.W., Hu, J., Hinault, C., Michael, M.D., Krtzfeldt, J., Yin, C., Holzenberger, M., Stoffel, M. and Kulkarni, R.N. (2007). Insulin receptors in beta-cells are critical for islet compensatory growth response to insulin resistance. *Proceedings of the National Academy of Sciences of the United States of America* **104**(21), 8977-8982.

Olsson, R. and Carlsson, P.-O. (2011). A low-oxygenated subpopulation of pancreatic islets constitutes a functional reserve of endocrine cells. *Diabetes* **60,** 2068-2075.

Oray, B. and Norton, S.J. (1980). Purification and characterization of mouse liver glyoxalase II. *Biochimica et Biophysica Acta* **611**(1), 168-173.

Orban, T., Bundy, B., Becker, D.J., DiMeglio, L.A., Gitelman, S.E., Goland, R., Gottlieb, P.A., Greenbaum, C.J., Marks, J.B., Monzavi, R., Moran, A., Raskin, P., Rodriguez, H., Russell, W.E., Schatz, D., Wherrett, D., Wilson, D.M., Krischer, J.P., Skyler, J.S. and Group, T.D.T.A.S. (2011). Co-stimulation modulation with abatacept in patients with recent-onset type 1 diabetes: a randomised, double-blind, placebo-controlled trial. *Lancet* **378**(9789), 412-419.

Otonkoski, T., Banerjee, M., Korsgren, O., Thornell, L.E. and Virtanen, I. (2008). Unique basement membrane structure of human pancreatic islets: implications for beta-cell growth and differentiation. *Diabetes Obesity and Metabolism* **10 Supplement 4,** 119-127.

Parnaud, G., Gonelle-Gispert, C., Morel, P., Giovannoni, L., Muller, Y.D., Meier, R., Borot, S., Berney, T. and Bosco, D. (2011). Cadherin Engagement Protects Human Beta-Cells from Apoptosis. *Endocrinology* **152**(12), 4601-4609.

Pascal, S.M., Veiga-da-Cunha, M., Gilon, P., Van Schaftingen, E. and Jonas, J.C. (2010). Effects of fructosamine-3-kinase deficiency on function and survival of mouse pancreatic islets after prolonged culture in high glucose or ribose concentrations. *American Journal of Physiology - Endocrinology and Metabolism* **298**(3), E586-E596.

Patterson, C.C., Dahlquist, G.G., Gyürüs, E., Green, A., Soltész, G. and Group, E.S. (2009). Incidence trends for childhood type 1 diabetes in Europe during 1989-2003 and predicted new cases 2005-20: a multicentre prospective registration study. *Lancet* **373**(9680), 2027-2033.

Paul, R.G. and Bailey, A.J. (1999). The effect of advanced glycation end-product formation upon cell-matrix interactions. *International Journal of Biochemistry & Cell Biology* **31**(6), 653-660.

Pedchenko, V.K., Chetyrkin, S.V., Chuang, P., Ham, A.J., Saleem, M.A., Mathieson, P.W., Hudson, B.G. and Voziyan, P.A. (2005). Mechanism of perturbation of integrin-mediated cell-matrix interactions by reactive carbonyl compounds and its implication for pathogenesis of diabetic nephropathy. *Diabetes* **54**(10), 2952-2960.

Perkins, B.A., Rabbani, N., Weston, A., Ficociello, L.H., Adaikalakoteswari, A., Niewczas, M., Warram, J., Krolewski, A.S. and Thornalley, P. (2012). Serum levels of advanced glycation endproducts and other markers of protein damage in early diabetic nephropathy in type 1 diabetes. *PLoS One* **7**(4), e35655.

Perl, S., Kushner, J.A., Buchholz, B.A., Meeker, A.K., Stein, G.M., Hsieh, M., Kirby, M., Pechhold, S., Liu, E.H., Harlan, D.M. and Tisdale, J.F. (2010). Significant human beta-cell turnover is limited to the first three decades of life as determined by *in vivo* thymidine analog incorporation and radiocarbon dating. *Journal of Clinical Endocrinology and Metabolism* **95 (10),** E234-E239.

Pescovitz, M.D., Greenbaum, C.J., Krause-Steinrauf, H., Becker, D.J., Gitelman, S.E., Goland, R., Gottlieb, P.A., Marks, J.B., McGee, P.F., Moran, A.M., Raskin, P., Rodriguez, H., Schatz, D.A., Wherrett, D., Wilson, D.M., Lachin, J.M., Skyler, J.S. and Group, T.D.T.A.-C.S. (2009). Rituximab, B-lymphocyte depletion, and preservation of beta-cell function. *The New England Journal of Medicine* **361**(22), 2143-2152.

Phillips, S.A., Mirrlees, D. and Thornalley, P.J. (1993). Modification of the glyoxalase system in streptozotocin-induced diabetic rats. Effect of the aldose reductase inhibitor Statil. *Biochemical Pharmacology* **46**(5), 805-811.

Phillips, S.A. and Thornalley, P. (1993). The formation of methylglyoxal from triose phosphates: Investigation using a specific assay for methylglyoxal. *European Journal of Biochemistry* **212,** 101-105.

Pi, J., Bai, Y., Zhang, Q., Wong, V., Floering, L.M., Daniel, K., Reece, J.M., Deeney, J.T., Andersen, M.E., Corkey, B.E. and Collins, S. (2007). Reactive oxygen species as a signal in glucose-stimulated insulin secretion. *Diabetes* **56**(7), 1783-1791.

Piercy, V., Toseland, C.D. and Turner, N.C. (1998). Potential benefit of inhibitors of advanced glycation end products in the progression of type II diabetes: a study with aminoguanidine in C57/BLKsJ diabetic mice. *Metabolism* **47**(12), 1477-1480.

Pinkse, G.G., Bouwman, W.P., Jiawan-Lalai, R., Terpstra, O.T., Bruijn, J.A. and de Heer, E. (2006). Integrin signaling via RGD peptides and anti-beta1 antibodies confers resistance to apoptosis in islets of Langerhans. *Diabetes* **55**(2), 312-317.

Poitout, V., Hagman, D., Stein, R., Artner, I., Robertson, R.P. and Harmon, J.S. (2006). Regulation of the insulin gene by glucose and fatty acids. *The Journal of Nutrition* **136**(4), 873-876.

Pozzi, A., Zent, R., Chetyrkin, S., Borza, C., Bulus, N., Chuang, P., Chen, D., Hudson, B. and Voziyan, P. (2009). Modification of collagen IV by glucose or methylglyoxal alters distinct mesangial cell functions. *Journal of the American Society of Nephrology* **20**(10), 2119-2125.

Puddu, A., Sanguineti, R., Durante, A. and Viviani, G.L. (2012). Pioglitazone attenuates the detrimental effects of advanced glycation end-products in the pancreatic beta cell line HIT-T15. *Regulatory Peptides* **177**(1-3), 79-84.

Pöschl, E., Pollner, R. and Kühn, K. (1988). The genes for the alpha 1(IV) and alpha 2(IV) chains of human basement membrane collagen type IV are arranged

head-to-head and separated by a bidirectional promoter of unique structure. *EMBO Journal* **7**(9), 2687-2695.

Queisser, M.A., Yao, D., Geisler, S., Hammes, H.-P., Lochnit, G., Schleicher, E.D., Brownlee, M. and Preissner, K.T. (2010). Hyperglycemia impairs proteosome function by methylglyoxal. *Diabetes* **59,** 670-678.

Rabbani, N., Godfrey, L., Xue, M., Shaheen, F., Geoffrion, M., Milne, R. and Thornalley, P.J. (2011). Glycation of LDL by methylglyoxal increases arterial atherogenicity: a possible contributor to increased risk of cardiovascular disease in diabetes. *Diabetes* **60**(7), 1973-1980.

Rabbani, N. and Thornalley, P.J. (2011). Glyoxalase in diabetes, obesity and related disorders. *Seminars in Cell and Developmental Biology* **22,** 309-317.

Rabbani, N. and Thornalley, P.J. (2012a). Methylglyoxal, glyoxalase 1 and the dicarbonyl proteome. *Amino Acids* **42**(4), 1133-1142.

Rabbani, N. and Thornalley, P.J. (2012b). Glycation research in amino acids: a place to call home. *Amino Acids* **42**(4), 1087-1096.

Rabbani, N. and Thornalley, P.J. (2012c). Dicarbonyls (Glyoxal, Methylglyoxal and 3-Deoxyglucosone). In: Niwa, T. *Uremic Toxins*. 1st, 177-192. Hoboken, New Jersey: John Wiley and Sons.

Racker, E. (1951). The mechanism of action of glyoxalase. *Journal of Biological Chemistry* **190,** 685-696.

Radvanyi, F., Christgau, S., Baekkeskov, S., Jolicoeur, C. and Hanahan, D. (1993). Pancreatic beta cells cultured from individual preneoplastic foci in a multistage tumorigenesis pathway: a potentially general technique for isolating physiologically representative cell lines. *Molecular and Cellular Biology* **13**(7), 4223-4232.

Rae, C., Board, P.G. and Kuchel, P.W. (1991). Glyoxalase 2 deficiency in the erythrocytes of a horse: 1H NMR studies of enzyme kinetics and transport of S-lactoylglutathione. *Archives of Biochemistry and Biophysics* **291**(2), 291-299.

Rahbar, S. (1968). An abnormal hemoglobin in red cells of diabetics. *Clinica Chimica Acta* **22**(2), 296-298.

Ramirez, N.E., Zhang, Z., Madamanchi, A., Boyd, K.L., O'Rear, L.D., Nashabi, A., Li, Z., Dupont, W.D., Zijlstra, A. and Zutter, M.M. (2011). The $\alpha_2\beta_1$ integrin is a metastasis suppressor in mouse models and human cancer. *Journal of Clinical Investigation* **121**(1), 226-237.

Reaven, G.M. (1988). Banting lecture 1988. Role of insulin resistance in human disease. *Diabetes* **37**(12), 1595-1607.

Rees, D.A. and Alcolado, J.C. (2005). Animal models of diabetes mellitus. *Diabetic Medicine* **22**(4), 359-370.

Reisman, S.A., Yeager, R.L., Yamamoto, M. and Klaassen, C.D. (2009). Increased Nrf2 activation in livers from Keap1-knockdown mice increases expression of cytoprotective genes that detoxify electrophiles more than those that detoxify reactive oxygen species. *Toxicological Sciences* **108**(1), 35-47.

Riboulet-Chavey, A., Pierron, A., Durand, I., Murdaca, J., Giudicelli, J. and Van Obberghen, E. (2006). Methylglyoxal impairs the insulin signaling pathways independently of the formation of intracellular reactive oxygen species. *Diabetes* **55,** 1289-1299.

Roberts, J.C. and Francetic, D.J. (1993). The importance of sample preparation and storage in glutathione analysis. *Analytical Biochemistry* **211**(2), 183-187.

Robertson, R.P., Harmon, J., Tran, P.O., Tanaka, Y. and Takahashi, H. (2003). Glucose toxicity in ß-cells: Type 2 Diabetes, good radicals gone bad, and the glutathione connection. *Diabetes* **52,** 581-587.

Robertson, R.P. and Harmon, J.S. (2006). Diabetes, glucose toxicity, and oxidative stress: A case of double jeopardy for the pancreatic islet beta cell. *Free Radical Biology and Medicine* **41**(2), 177-184.

Roderigo-Milne, H., Hauge-Evans, A.C., Persaud, S.J. and Jones, P.M. (2002). Differential expression of insulin genes 1 and 2 in MIN6 cells and pseudoislets. *Biochemical and Biophysical Research Communications* **296**(3), 589-595.

Rogers, G.J., Hodgkin, M.N. and Squires, P.E. (2007). E-cadherin and cell adhesion: a role in architecture and function in the pancreatic islet. *Cellular Physiology and Biochemistry* **19**, 987-994.

Rorsman, P. and Braun, M. (2013). Regulation of insulin secretion in human pancreatic islets. *Annual Review of Physiology* **75,** 155-179.

Rosca, M.G., Monnier, V.M., Szweda, L.I. and Weiss, M.F. (2002). Alterations in renal mitochondrial respiration in response to the reactive oxoaldehyde methylglyoxal. *American Journal of Physiology. Renal Physiology* **283**(1), F52-F59.

Rosengren, A.H., Braun, M., Mahdi, T., Andersson, S.A., Travers, M.E., Shigeto, M., Zhang, E., Almgren, P., Ladenvall, C., Axelsson, A.S., Edlund, A., Pedersen, M.G., Jonsson, A., Ramracheya, R., Tang, Y., Walker, J.N., Barrett, A., Johnson, P.R., Lyssenko, V., McCarthy, M.I., Groop, L., Salehi, A., Gloyn, A.L., Renström, E., Rorsman, P. and Eliasson, L. (2012). Reduced insulin exocytosis in human pancreatic β-cells with gene variants linked to type 2 diabetes. *Diabetes* **61**(7), 1726-1733.

Rossi, R., Milzani, A., Dalle-Donne, I., Giustarini, D., Lusini, L., Colombo, R. and Di Simplicio, P. (2002). Blood glutathione disulfide: in vivo factor or in vitro artifact? *Clinical Chemistry* **48**(5), 742-753.

Rossini, A.A., Like, A.A., Chick, W.L., Appel, M.C. and Cahill, G.F. (1977). Studies of streptozotocin-induced insulitis and diabetes. *Proceedings of the National Academy of Sciences of the United States of America* **74**(6), 2485-2489.

Rossmeisl, M., Jelenik, T., Jilkova, Z., Slamova, K., Kus, V., Hensler, M., Medrikova, D., Povysil, C., Flachs, P., Mohamed-Ali, V., Bryhn, M., Berge, K., Holmeide, A.K. and Kopecky, J. (2009). Prevention and reversal of obesity and glucose intolerance in mice by DHA derivatives. *Obesity* **17**(5), 1023-1031.

Rossmeisl, M., Jilkova, Z.M., Kuda, O., Jelenik, T., Medrikova, D., Stankova, B., Kristinsson, B., Haraldsson, G.G., Svensen, H., Stoknes, I., Sjövall, P., Magnusson, Y., Balvers, M.G., Verhoeckx, K.C., Tvrzicka, E., Bryhn, M. and Kopecky, J. (2012). Metabolic effects of n-3 PUFA as phospholipids are superior to triglycerides in mice fed a high-fat diet: possible role of endocannabinoids. *PLoS One* **7**(6), e38834.

Sailer, M., Dahlhoff, C., Giesbertz, P., Eidens, M.K., de Wit, N., Rubio-Aliaga, I., Boekschoten, M.V., Müller, M. and Daniel, H. (2013). Increased plasma citrulline in mice marks diet-induced obesity and may predict the development of the metabolic syndrome. *PLoS One* **8**(5), e63950.

Sakai, K., Matsumoto, K., Nishikawa, T., Suefuji, M., Nakamaru, K., Hirashima, Y., Kawashima, J., Shirotani, T., Ichinose, K., Brownlee, M. and Araki, E. (2003). Mitochondrial reactive oxygen species reduce insulin secretion by pancreatic beta-cells. *Biochemical and Biophysical Research Communications* **300**(1), 216-222.

Sakamoto, H., Mashima, T., Sato, S., Hashimoto, Y., Yamori, T. and Tsuruo, T. (2001). Selective activation of apoptosis program by S-p-bromobenzylglutathione cyclopentyl diester in glyoxalase I-overexpressing human lung cancer cells. *Clinical Cancer Research* **7**(8), 2513-2518.

Salpeter, S.J., Khalaileh, A., Weinberg-Corem, N., Ziv, O., Glaser, B. and Dor, Y. (2013). Systemic Regulation of the Age-Related Decline of Pancreatic β-Cell Replication. *Diabetes* **62**(8), 2843-2848.

Samols, E., Marri, G. and Marks, V. (1966). Interrelationship of glucagon, insulin and glucose. The insulinogenic effect of glucagon. *Diabetes* **15**(12), 855-866.

Santerre, R.F., Cook, R.A., Crisel, R.M., Sharp, J.D., Schmidt, R.J., Williams, D.C. and Wilson, C.P. (1981). Insulin synthesis in a clonal cell line of simian virus 40-transformed hamster pancreatic beta cells. *Proceedings of the National Academy of Sciences of the United States of America* **78**(7), 4339-4343.

Schleicher, E.D., Wagner, E. and Nerlich, A.G. (1997). Increased accumulation of the glycoxidation product N(epsilon)-(carboxymethyl)lysine in human tissues in diabetes and aging. *Journal of Clinical Investigation* **99**(3), 457-468.

Sejersen, H. and Rattan, S.I. (2009). Dicarbonyl-induced accelerated aging in vitro in human skin fibroblasts. *Biogerontology* **10**(2), 203-211.

Sell, D.R. and Monnier, V.M. (2004). Conversion of arginine into ornithine by advanced glycation in senescent human collagen and lens crystallins. *Journal of Biological Chemistry* **279**(52), 54173-54184.

Serre-Beinier, V., Le Gurun, S., Belluardo, N., Trovato-Salinaro, A., Charollais, A., Haefliger, J.-A., Condorelli, D.F. and Meda, P. (2000). Cx36 preferentially connects beta-cells within pancreatic islets. *Diabetes* **49** 727-734.

Sharon, N. (1988). Nomenclature of glycoproteins, glycopeptides and peptidoglycans (recommendations 1985). *Pure and Applied Chemistry* **60**(9), 1389-1394.

Shaw, J.E., Sicree, R.A. and Zimmet, P.Z. (2010). Global estimates of the prevalence of diabetes for 2010 and 2030. *Diabetes Research and Clinical Practice* **87** 4-14.

She, P., Van Horn, C., Reid, T., Hutson, S.M., Cooney, R.N. and Lynch, C.J. (2007). Obesity-related elevations in plasma leucine are associated with alterations in enzymes involved in branched-chain amino acid metabolism. *American Journal of Physiology - Endocrinology and Metabolism* **293**(6), E1552-E1563.

Sherwin, R.S., Kramer, K.J., Tobin, J.D., Insel, P.A., Liljenquist, J.E., Berman, M. and Andres, R. (1974). A model of the kinetics of insulin in man. *Journal of Clinical Investigation* **53**(5), 1481-1492.

Shiao, M.S., Liao, B.Y., Long, M. and Yu, H.T. (2008). Adaptive evolution of the insulin two-gene system in mouse. *Genetics* **178**(3), 1683-1691.

Shinohara, M., Thornalley, P.J., Giardino, I., Beisswenger, P., Thorpe, S.R., Onorato, J. and Brownlee, M. (1998). Overexpression of glyoxalase-I in bovine endothelial cells inhibits intracellular advanced glycation endproduct formation and prevents hyperglycaemia-induced increases in macromolecular endocytosis. *Journal of Clinical Investigation* **101** 1142-1147.

Shirakawa, J., Togashi, Y., Sakamoto, E., Kaji, M., Tajima, K., Orime, K., Inoue, H., Kubota, N., Kadowaki, T. and Terauchi, Y. (2013). Glucokinase Activation Ameliorates ER Stress-Induced Apoptosis in Pancreatic β-Cells. *Diabetes* **62**(10), 3448-3458.

Simons, M. and Horowitz, A. (2001). Syndecan-4-mediated signalling. *Cell Signal* **13**(12), 855-862.

Skelin, M., Rupnik, M. and Cencic, A. (2010). Pancreatic beta cell lines and their applications in diabetes mellitus research. *Alternatives to Animal Experimentation* **27 Part 2,** 105-113.

Smith, P.R. and Thornalley, P.J. (1992). Mechanism of the degradation of non-enzymatically glycated proteins under physiological conditions. Studies with the model fructosamine, N epsilon-(1-deoxy-D-fructos-1-yl)hippuryl-lysine. *European Journal of Biochemistry* **210**(3), 729-739.

Souza-Mello, V., Gregório, B.M., Cardoso-de-Lemos, F.S., de Carvalho, L., Aguila, M.B. and Mandarim-de-Lacerda, C.A. (2010). Comparative effects of telmisartan, sitagliptin and metformin alone or in combination on obesity, insulin resistance, and liver and pancreas remodelling in C57BL/6 mice fed on a very high-fat diet. *Clinical Science* **119**(6), 239-250.

Spanakis, E., Milord, E. and Gragnoli, C. (2008). AVPR2 variants and mutations in nephrogenic diabetes insipidus: review and missense mutation significance. *Journal of Cellular Physiology* **217,** 605-617.

Stendahl, J.C., Kaufman, D.B. and Stupp, S.I. (2009). Extracellular Matrix in Pancreatic Islets: Relevance to Scaffold Design and Transplantation. *Cell Transplantation* **18,** 1-12.

Strober, W. (2001). Trypan blue exclusion test of cell viability. *Current Protocols in Immunology* **Appendix 3,** Appendix 3B.

Støy, J., Edghill, E.L., Flanagan, S.E., Ye, H., Paz, V.P., Pluzhnikov, A., Below, J.E., Hayes, M.G., Cox, N.J., Lipkind, G.M., Lipton, R.B., Greeley, S.A., Patch, A.M., Ellard, S., Steiner, D.F., Hattersley, A.T., Philipson, L.H., Bell, G.I. and Group, N.D.I.C. (2007). Insulin gene mutations as a cause of permanent neonatal diabetes. *Proceedings of the National Academy of Sciences of the United States of America* **104**(38), 15040-15044.

Sugimoto, K., Nishizawa, Y., Horiuchi, S. and Yagihashi, S. (1997). Localization in human diabetic peripheral nerve of N(epsilon)-carboxymethyllysine-protein adducts, an advanced glycation endproduct. *Diabetologia* **40**(12), 1380-1387.

Sugita, H. and Takahama, K. (1983). Red cell glyoxalase II type in a Japanese population. *Jinrui Idengaku Zasshi - The Japanese Journal of Human Genetics* **28**(3), 201-203.

Surwit, R.S., Kuhn, C.M., Cochrane, C., McCubbin, J.A. and Feinglos, M.N. (1988). Diet-induced type II diabetes in C57BL/6J mice. *Diabetes* **37**(9), 1163-1167.

Szkudelski, T. (2001). The mechanism of alloxan and streptozotocin action in B cells of the rat pancreas. *Physiological Research* **50**(6), 537-546.

Szkudelski, T. (2012). Streptozotocin-nicotinamide-induced diabetes in the rat. Characteristics of the experimental model. *Experimental Biology and Medicine (Maywood)* **237**(5), 481-490.

Szoke, E., Shrayyef, M.Z., Messing, S., Woerle, H.J., Van Haeften, T.W., Meyer, C., Mitrakou, A., Pimenta, W. and Gerich, J.E. (2008). Effect of Aging

on Glucose Homeostasis. Accelerated deterioration of beta-cell function in individuals with impaired glucose tolerance. *Diabetes Care* **31,** 539-543.

Tajiri, Y., Möller, C. and Grill, V. (1997). Long-term effects of aminoguanidine on insulin release and biosynthesis: evidence that the formation of advanced glycosylation end products inhibits B cell function. *Endocrinology* **138**(1), 273-280.

Takahashi, K. (1977). The reactions of phenylglyoxal and related reagents with amino acids. *The Journal of Biochemistry* **81,** 395-402.

Tan, H. and Whitney, J.B. (1993). Genomic rearrangement of the alpha-globin gene complex during mammalian evolution. *Biochemical Genetics* **31**(11-12), 473-484.

Tan, Y., Ichikawa, T., Li, J., Si, Q., Yang, H., Chen, X., Goldblatt, C.S., Meyer, C.J., Li, X., Cai, L. and Cui, T. (2011). Diabetic downregulation of Nrf2 activity via ERK contributes to oxidative stress-induced insulin resistance in cardiac cells in vitro and in vivo. *Diabetes* **60**(2), 625-633.

Tanaka, Y., Gleason, C.E., Tran, P.O., Harmon, J.S. and Robertson, R.P. (1999). Prevention of glucose toxicity in HIT-T15 cells and Zucker diabetic fatty rats by antioxidants. *Proceedings of the National Academy of Sciences of the United States of America* **96**(19), 10857-10862.

Taniguchi, C.M., Emanuelli, B. and Kahn, C.R. (2006). Critical nodes in signalling pathways: insights into insulin action. *Nature Reviews Molecular Cell Biology* **7,** 85-96.

Taylor, R. (2006). The role of islet-cell function in the onset and progression of type-2 diabetes. *US Endocrine Disease,* 53-55.

The Expert Committee on the Diagnosis and Classification of Diabetes Mellitus. (1997). Report of the Expert Committee on the Diagnosis and Classification of Diabetes Mellitus. *Diabetes Care* **20**(7), 1183-1197.

The Lancet. (2008). The global challenges of diabetes. *Lancet* **371 9626,** 1723.

Thimmulappa, R.K., Mai, K.H., Srisuma, S., Kensler, T.W., Yamamoto, M. and Biswal, S. (2002). Identification of Nrf2-regulated genes induced by the chemopreventive agent sulforaphane by oligonucleotide microarray. *Cancer Research* **62**(18), 5196-5203.

Thornalley, P. (2008). Protein and nucleotide damage by glyoxal and methylglyoxal in physiological systems - role in ageing and disease. *Drug Metabolism and Drug Interactions* **23,** 125-150.

Thornalley, P.J. (1988). Modification of the glyoxalase system in human red blood cells by glucose *in vitro*. *Biochemical Journal* **254,** 751-755.

Thornalley, P.J. (1990). The glyoxalase system: new developments towards functional characterization of a metabolic pathway fundamental to biological life. *Biochemical Journal* **269,** 1-11.

Thornalley, P.J. (1993). The glyoxalase system in health and disease. *Molecular Aspects of Medicine* **14**(4), 287-371.

Thornalley, P.J. (1994). Methylglyoxal, glyoxalases and the development of diabetic complications. *Amino Acids* **6,** 15-23.

Thornalley, P.J. (2003a). Glyoxalase 1 - structure, function and a critical role in the enzymatic defence against glycation. *Biochemical Society Transactions* **31 part 6,** 1343-1348.

Thornalley, P.J. (2003b). Use of aminoguanidine (Pimagedine) to prevent the formation of advanced glycation end products. *Archives of Biochemistry and Biophysics* **419,** 31-40.

Thornalley, P.J. (2005). Dicarbonyl intermediates in the Maillard reaction. *Annals New York Academy of Sciences* **1043,** 111-117.

Thornalley, P.J. (2007). Dietary AGEs and ALEs and risk to human health by their interaction with the receptor for advanced glycation endproducts (RAGE)--an introduction. *Molecular Nutrition and Food Research* **51**(9), 1107-1110.

Thornalley, P.J., Battah, S., Ahmed, N., Karachalias, N., Agalou, S., Babaei-Jadidi, R. and Dawnay, A. (2003). Quantitative screening of advanced glycation endproducts in cellular and extracellular proteins by tandem mass spectrometry. *Biochemical Journal* **375,** 581-592.

Thornalley, P.J., Edwards, L.G., Kang, Y., Wyatt, C., Davies, N., Ladan, M.J. and Double, J. (1996). Antitumour activity of S-p-bromobenzylglutathione Cyclopentyl Diester *in Vitro* and *in Vivo*. Inhibition of glyoxalase I and induction of apoptosis. *Biochemical Pharmacology* **51,** 1365-1372.

Thornalley, P.J., Hooper, N.I., Jennings, P.E., Florkowski, C.M., Jones, A.F., Lunec, J. and Barnett, A.H. (1989). The human red blood cell glyoxalase system in diabetes mellitus. *Diabetes Research and Clinical Practice* **7,** 115-120.

Thornalley, P.J., Langborg, A. and Minhas, H.S. (1999). Formation of glyoxal, methylglyoxal and 3-deoxyglucosone in the glycation of proteins by glucose. *Biochemical Journal* **344,** 109-116.

Thornalley, P.J. and Rabbani, N. (2013). Detection of oxidized and glycated proteins in clinical samples using mass spectrometry - A user's perspective. *Biochimica et Biophysica Acta.* Online ahead of print. DOI: 10.1016/j.bbagen.2013.03.025.

Thornalley, P.J. and Tisdale, M.J. (1988). Inhibition of proliferation of human promyelocytic leukaemia HL60 cells by S-D-lactoylglutathione in vitro. *Leukemia Research* **12**(11-12), 897-904.

Thornalley, P.J., Waris, S., Fleming, T., Santarius, T., Larkin, S.J., Winklhofer-Roob, B.M., Stratton, M.R. and Rabbani, N. (2010). Imidazopurinones are markers of physiological genomic damage linked to DNA instability and glyoxalase 1-associated tumour multidrug resistance. *Nucleic Acids Research* **38**(16), 5432-5442.

Thornalley, P.J., Yurek-George, A. and Argirov, O.K. (2000). Kinetics and mechanism of the reaction of aminoguanidine with the α-oxoaldehydes glyoxal, methylglyoxal, and 3-deoxyglucosone under physiological conditions. *Biochemical Pharmacology* **60**(1), 55-65.

Tillmar, L., Carlsson, C. and Welsh, N. (2002). Control of insulin mRNA stability in rat pancreatic islets. Regulatory role of a 3'-untranslated region pyrimidine-rich sequence. *Journal of Biological Chemistry* **277**(2), 1099-1106.

Tinto, N., Zagari, A., Capuano, M., De Simone, A., Capobianco, V., Daniele, G., Giugliano, M., Spadaro, R., Franzese, A. and Sacchetti, L. (2008). Glucokinase gene mutations: Structural and Genotype-Phenotype analyses in MODY children from South Italy. *PLoS ONE* **3,** e1870.

Tom, A. and Nair, K.S. (2006). Assessment of branched-chain amino Acid status and potential for biomarkers. *Journal of Nutrition* **136**(Supplement 1), 324S-330S.

Turk, Z. (2010). Glycotoxines, carbonyl stress and relevance to diabetes and its complications. *Physiological Research* **59**(2), 147-156.

UKPDS. (1995). UKPDS Study 16. Overview of 6 years' therapy of type II diabetes: a progressive disease. *Diabetes* **44**(11), 1249-1258.

UKPDS. (1998). Intensive blood-glucose control with sulphonylureas or insulin compared with conventional treatment and risk of complications in patients with type 2 diabetes (UKPDS 33). *Lancet* **352**(9131), 837-853.

Ulrich, P. and Cerami, A. (2001). Protein glycation, Diabetes, and Aging. *Recent Progress in Hormone Research* **56,** 1-21.

van Raalte, D.H. and Diamant, M. (2011). Glucolipotoxicity and beta cells in type 2 diabetes mellitus: target for durable therapy? *Diabetes Research and Clinical Practice* **93 Supplement 1,** S37-S46.

Vander Jagt, D.L., Robinson, B., Taylor, K.K. and Hunsaker, L.A. (1992). Reduction of Trioses by NADPH-dependent Aldo-Keto Reductases. *The Journal of Biological Chemistry* **267,** 4364-4369.

Vander Mierde, D., Scheuner, D., Quintens, R., Patel, R., Song, B., Tsukamoto, K., Beullens, M., Kaufman, R.J., Bollen, M. and Schuit, F.C. (2007). Glucose

activates a protein phosphatase-1-mediated signaling pathway to enhance overall translation in pancreatic beta-cells. *Endocrinology* **148**(2), 609-617.

Vasu, S., McClenaghan, N.H., McCluskey, J.T. and Flatt, P.R. (2013). Effects of lipotoxicity on a novel insulin-secreting human pancreatic β-cell line, 1.1B4. *Biological Chemistry* **394**(7), 909-918.

Verzijl, N., DeGroot, J., Thorpe, S.R., Bank, R.A., Shaw, J.N., Lyons, T.J., Bijlsma, J.W., Lafeber, F.P., Baynes, J.W. and TeKoppele, J.M. (2000). Effect of collagen turnover on the accumulation of advanced glycation end products. *Journal of Biological Chemistry* **275**(50), 39027-39031.

Vince, R. and Daluge, S. (1971). Glyoxalase inhibitors. A possible approach to anticancer agents. *Journal of Medicinal Chemistry* **14**(1), 35-37.

Vince, R., Daluge, S. and Wadd, W.B. (1971). Studies on the inhibition of glyoxalase I by S-substituted glutathiones. *Journal of Medicinal Chemistry* **14**(5), pp. 402-404.

Voight, B.F. Scott, L.J. Steinthorsdottir, V. Morris, A.P. Dina, C. Welch, R.P. Zeggini, E. Huth, C. Aulchenko, Y.S. Thorleifsson, G. McCulloch, L.J. Ferreira, T. Grallert, H. Amin, N. Wu, G. Willer, C.J. Raychaudhuri, S. McCarroll, S.A. Langenberg, C. Hofmann, O.M. Dupuis, J. Qi, L. Segrè, A.V. van Hoek, M. Navarro, P. Ardlie, K. Balkau, B. Benediktsson, R. Bennett, A.J. Blagieva, R. Boerwinkle, E. Bonnycastle, L.L. Bengtsson Boström, K. Bravenboer, B. Bumpstead, S. Burtt, N.P. Charpentier, G. Chines, P.S. Cornelis, M. Couper, D.J. Crawford, G. Doney, A.S. Elliott, K.S. Elliott, A.L. Erdos, M.R. Fox, C.S. Franklin, C.S. Ganser, M. Gieger, C. Grarup, N. Green, T. Griffin, S. Groves, C.J. Guiducci, C. Hadjadj, S. Hassanali, N. Herder, C. Isomaa, B. Jackson, A.U. Johnson, P.R. Jørgensen, T. Kao, W.H. Klopp, N. Kong, A. Kraft, P. Kuusisto, J. Lauritzen, T. Li, M. Lieverse, A. Lindgren, C.M. Lyssenko, V. Marre, M. Meitinger, T. Midthjell, K. Morken, M.A. Narisu, N. Nilsson, P. Owen, K.R. Payne, F. Perry, J.R. Petersen, A.K. Platou, C. Proença, C. Prokopenko, I. Rathmann, W. Rayner, N.W. Robertson, N.R. Rocheleau, G. Roden, M. Sampson, M.J. Saxena, R. Shields, B.M. Shrader, P. Sigurdsson, G. Sparsø, T. Strassburger, K. Stringham, H.M. Sun, Q. Swift, A.J. Thorand, B. Tichet, J. Tuomi, T. van Dam, R.M. van Haeften, T.W. van Herpt, T. van Vliet-Ostaptchouk, J.V. Walters, G.B. Weedon, M.N. Wijmenga, C. Witteman, J. Bergman, R.N. Cauchi, S. Collins, F.S. Gloyn, A.L. Gyllensten, U. Hansen, T. Hide, W.A. Hitman, G.A. Hofman, A. Hunter, D.J. Hveem, K. Laakso, M. Mohlke, K.L. Morris, A.D. Palmer, C.N. Pramstaller, P.P. Rudan, I. Sijbrands, E. Stein, L.D. Tuomilehto, J. Uitterlinden, A. Walker, M. Wareham, N.J. Watanabe, R.M. Abecasis, G.R. Boehm, B.O. Campbell, H. Daly, M.J. Hattersley, A.T. Hu, F.B. Meigs, J.B. Pankow, J.S. Pedersen, O. Wichmann, H.E. Barroso, I. Florez, J.C. Frayling, T.M. Groop, L. Sladek, R. Thorsteinsdottir, U. Wilson, J.F. Illig, T. Froguel, P. van Duijn, C.M. Stefansson, K. Altshuler, D. Boehnke, M. McCarthy, M.I. investigators, M. and Consortium, G. (2010). Twelve type 2 diabetes susceptibility loci identified through large-scale association analysis. *Nature Genetics* **42**(7), 579-589.

Vozzi, C., Ullrich, S., Charollais, A., Philippe, J., Orci, L. and Meda, P. (1995). Adequate Connexin-mediated coupling is required for proper insulin production. *The Journal of Cell Biology* **131 Part 1,** 1561-1572.

Wang, R.N. and Rosenberg, L. (1999). Maintenance of beta-cell function and survival following islet isolation requires re-establishment of the islet-matrix relationship. *Journal of Endocrinology* **163**(2), 181-190.

Weber, L.M., Hayda, K.N. and Anseth, K.S. (2008). Cell-Matrix Interactions improve beta-cell survival and insulin secretion in three-dimensional culture. *Tissue Engineering: Part A* **14 number 12,** 1959-1968.

Weir, G.C. and Bonner-Weir, S. (2004). Five stages of evolving beta-cell dysfunction during progression to diabetes. *Diabetes* **53 Supplement 3,** S16-S21.

Weir, G.C. and Bonner-Weir, S. (2011). Sleeping islets and the relationship between beta-cell mass and function. *Diabetes* **60,** 2018-2019.

Welsh, M., Nielsen, D.A., MacKrell, A.J. and Steiner, D.F. (1985). Control of insulin gene expression in pancreatic beta-cells and in an insulin-producing cell line, RIN-5F cells. II. Regulation of insulin mRNA stability. *Journal of Biological Chemsitry* **260**(25), 13590-13594.

Wentworth, B.M., Schaefer, I.M., Villa-Komaroff, L. and Chirgwin, J.M. (1986). Characterization of the two nonallelic genes encoding mouse preproinsulin. *Journal of Molecular Evolution* **23**(4), 305-312.

Wicksteed, B., Herbert, T.P., Alarcon, C., Lingohr, M.K., Moss, L.G. and Rhodes, C.J. (2001). Cooperativity between the preproinsulin mRNA untranslated regions is necessary for glucose-stimulated translation. *Journal of Biological Chemistry* **276**(25), 22553-22558.

Winzell, M.S. and Ahrén, B. (2004). The high-fat diet-fed mouse: a model for studying mechanisms and treatment of impaired glucose tolerance and type 2 diabetes. *Diabetes* **53 Supplement 3,** S215-S219.

Wolfsdorf, J., Craig, M.E., Daneman, D., Dunger, D., Edge, J., Lee, W., Rosenbloom, A., Sperling, M. and Hanas, R. (2009). Diabetic ketoacidosis in children and adolescents with diabetes. *Pediatric Diabetes* **10 Supplement S12,** 118-133.

Xian, X., Gopal, S. and Couchman, J.R. (2010). Syndecans as receptors and organizers of the extracellular matrix. *Cell and Tissue Research* **339**(1), 31-46.

Xue, M., Rabbani, N., Momiji, H., Imbasi, P., Anwar, M.M., Kitteringham, N., Park, B.K., Souma, T., Moriguchi, T., Yamamoto, M. and Thornalley, P.J. (2012). Transcriptional control of glyoxalase 1 by Nrf2 provides a stress-responsive defence against dicarbonyl glycation. *Biochemical Journal* **443**(1), 213-222.

Xue, M., Rabbani, N. and Thornalley, P.J. (2011). Glyoxalase in ageing. *Seminars in Cell and Developmental Biology* **22 (3)** 293-301.

Yamagata, K., Nammo, T., Moriwaki, M., Ihara, A., Iizuka, K., Yang, Q., Satoh, T., Li, M., Uenaka, R., Okita, K., Iwahashi, H., Zhu, Q., Cao, Y., Imagawa, A., Tochino, Y., Hanafusa, T., Miyagawa, J. and Matsuzawa, Y. (2002). Overexpression of dominant-negative mutant hepatocyte nuclear fctor-1 alpha in pancreatic beta-cells causes abnormal islet architecture with decreased expression of E-cadherin, reduced beta-cell proliferation, and diabetes. *Diabetes* **51**(1), 114-123.

Yamaguchi, M., Nakamura, N., Nakano, K., Kitagawa, Y., Shigeta, H., Hasegawa, G., Ienaga, K., Nakamura, K., Nakazawa, Y., Fukui, I., Obayashi, H. and Kondo, M. (1998). Immunochemical quantification of crossline as a fluorescent advanced glycation endproduct in erythrocyte membrane proteins from diabetic patients with or without retinopathy. *Diabetic Medicine* **15**(6), 458-462.

Yamaoka, M., Maeda, N., Nakamura, S., Mori, T., Inoue, K., Matsuda, K., Sekimoto, R., Kashine, S., Nakagawa, Y., Tsushima, Y., Fujishima, Y., Komura, N., Hirata, A., Nishizawa, H., Matsuzawa, Y., Matsubara, K., Funahashi, T. and Shimomura, I. (2013). Gene expression levels of S100 protein family in blood cells are associated with insulin resistance and inflammation (Peripheral blood S100 mRNAs and metabolic syndrome). *Biochemical and Biophysical Research Communications* **433**(4), 450-455.

Yan, M.X., Ren, H.B., Kou, Y., Meng, M. and Li, Y.Q. (2012). Involvement of nuclear factor kappa B in high-fat diet-related pancreatic fibrosis in rats. *Gut and Liver* **6**(3), 381-387.

Yang, K., Feng, C., Lip, H., Bruce, W.R. and O'Brien, P.J. (2011). Cytotoxic molecular mechanisms and cytoprotection by enzymic metabolism or autoxidation for glyceraldehyde, hydroxypyruvate and glycolaldehyde. *Chemico-Biological Interactions* **191**(1-3), 315-321.

Yki-Järvinen, H. (1992). Glucose toxicity. *Endocrine Reviews* **13**(3), 415-431.

Yoshizaki, T. (2012). Autophagy in Insulin Resistance. *Anti-Aging Medicine* **9**(6), 180-184.

Zhang, J., Li, C., Shi, T., Chen, K., Shen, X. and Jiang, H. (2009). Lys169 of human glucokinase is a determinant for glucose phosphorylation: implication for the atomic mechanism of glucokinase catalysis. *PLoS ONE* **4,** e6304.

Zhao, Z., Zhao, C., Zhang, X.H., Zheng, F., Cai, W., Vlassara, H. and Ma, Z.A. (2009). Advanced glycation end products inhibit glucose-stimulated insulin secretion through nitric oxide-dependent inhibition of cytochrome c oxidase and adenosine triphosphate synthesis. *Endocrinology* **150**(6), 2569-2576.

Zimmet, P., Alberti, K.G.M.M. and Shaw, J. (2001). Global and societal implications of the diabetes epidemic. *Nature* **414,** 782-787.